

F. Fischmann

MSc Thesis Report

Assessing the effect of reservoir operation
on seasonal flooding of the Masaka
wetland, Rwanda

Assessing the effect of reservoir operation on seasonal flooding of the Masaka wetland, Rwanda

By

F. Fischmann

in partial fulfilment of the requirements for the degree of

Master of Science
in Civil Engineering

at the Delft University of Technology,
to be defended publicly on Wednesday December 19, 2018 at 14:00 PM.

Supervisor:	Dr. M. Hrachowitz	
Thesis committee:	Prof.dr.ir. P.H.A.J.M. van Gelder, Dr. J. Wenninger, L. Hoogduin	TU Delft TU Delft / IHE Delft Royal HaskoningDHV

An electronic version of this thesis is available at <http://repository.tudelft.nl/>.

Cover image credits: Anne Floor Timan / Royal HaskoningDHV

Executive Summary

Due to a combination of climate, topography and human interventions, flooding is a recurring phenomenon in Rwanda. This is particularly relevant in low-lying areas adjacent to major rivers, such as the Masaka wetland located in the southern edge of Kigali. However, the expected commissioning of the Shyorongi reservoir within the scope of the Nyabarongo II Multipurpose Development Project may have significant effects on flood peaks and durations in this location. Therefore, this study aimed to investigate the potential effects of different reservoir operation policies on the seasonal discharge regime of the Nyabarongo river and its consequences to flooding in the Masaka wetland.

Two families of reservoir operation rules were tested: one aiming to maximise hydropower output, and the other focussing on the mitigation of flood peaks by limiting releases to a prescribed maximum value. For each family, varying electricity generation targets and reservoir release thresholds were tested, respectively. A total of 50 scenarios were simulated for the 1981-2018 period and compared to the baseline (no-reservoir) scenario. The effectiveness of each policy was assessed in terms of the estimated reduction in both flood peaks and durations in the Masaka wetland.

On specific years such as 2018, operation emphasising hydropower production had the secondary result of reducing peak discharges by up to 20%. However, over most simulated years, reductions were found to be insignificant. This type of operation also had generally negligible effects on flood durations. In contrast, it was observed that reservoir operation with the specific goal of flood mitigation may consistently result in 20% to 25% reductions of seasonal peak discharges. Over the entire simulated period, the best-performing scenarios consisted of those with prescribed maximum releases of 75 to 100 m³s⁻¹. However, performance was found to depend, to a large extent, on the varying inflow hydrographs for each year.

Therefore, the availability of a seasonal outlook on discharges may guide the definition of optimal release criteria for each year. Additionally, reservoir rules that account for the pronounced seasonal variability in inflows may allow for significant reductions on both flood peaks and durations in comparison to the policies hereby simulated. Therefore, it is recommended that such optimisation be carried out for the Shyorongi reservoir. However, due to the limited storage capacity of this reservoir and low overbank discharge thresholds in the Masaka region, flood management in this location requires the adoption of complementary structural and non-structural measures according to the desired goals.

It is highlighted that several assumptions have been made concerning the conceptualisation of the catchment and characteristics of the Shyorongi dam and the Masaka wetland, as detailed in the body of the report. Additionally, the estimation of parameters for hydrological models and extreme value distribution functions inherently involves uncertainties. Therefore, the results and associated elucidations hereby presented should be interpreted in the context of a considerable amount of propagated uncertainty, and should not be adopted for design purposes.

"From everyone who has been given much, much will be demanded; and from the one who has been entrusted with much, much more will be asked"

– Luke 12:48

Contents

Acronyms and Abbreviations.....	viii
List of Figures	ix
List of Tables.....	xiv
1 Introduction	1
1.1 Background	1
1.1.1 Previous investigations on the hydrology of Rwanda	1
1.1.2 Reservoir effects on river discharges and flooding.....	4
1.2 Problem statement	8
1.2.1 The increasing relevance of the Masaka wetland.....	8
1.2.2 A changing landscape for seasonal flooding in the Masaka wetland.....	9
1.3 Research outline	11
1.3.1 Research question.....	11
1.3.2 Hypotheses	11
1.3.3 Report structure.....	11
2 Study area.....	12
2.1 Masaka wetland and the Kanzenze station.....	12
2.2 The catchment.....	14
2.2.1 Climate	14
2.2.2 Soil types.....	19
2.2.3 Land cover.....	22
2.2.4 Hydrology	24
2.2.5 Erosion	24
2.2.6 Reservoir development.....	26
2.3 System conceptualisation	27
3 Data	30
3.1 Hydrometric data	31
3.2 Precipitation and potential evaporation.....	36
3.3 Reservoir characteristics	40
3.4 Data processing	42
3.4.1 Validation of observed discharges against long-term catchment water balance.....	42
3.4.2 Estimation of discharges at the Akanyaru river outlet.....	44
4 Methods.....	49
4.1 Catchment and reservoir simulations.....	49
4.1.1 Hydrological modelling: generation of discharge time series at key catchment locations	49

4.1.2 Reservoir modelling for different scenarios	66
4.1.3 Coupled rainfall-runoff and reservoir modelling.....	67
4.2 Estimation of flood peak probability distribution	69
4.2.1 Peak selection	69
4.2.2 Estimation of return periods	71
4.3 Estimation of flood durations	78
5 Results and discussion.....	79
5.1 The relative contribution of the Akanyaru catchment to flooding and the potential for reservoir regulation	79
5.2 A seasonal hydrograph example: the flood of 2018	85
5.3 Peak discharges.....	90
5.4 Flood durations.....	96
5.5 Considerations on uncertainty propagation and key assumptions.....	102
6 Conclusions	105
References.....	107

Acronyms and Abbreviations

cdf	Cumulative distribution function
cf	Capacity factor
ci	Confidence interval
EDCL	Energy Development Corporation Limited
ENSO	El Niño–Southern Oscillation
ESDAC	European Soil Data Centre
EVD	Extreme value distribution
GEV	Generalised Extreme Value (distribution)
GIS	Geographical Information System
GoR	Government of Rwanda
ITCZ	Inter Tropical Convergence Zone
JRC	Joint Research Centre
Meteo Rwanda	Rwanda Meteorology Agency
NMDP	Nyabarongo II Multipurpose Development Project
NSE	Nash–Sutcliffe model efficiency coefficient
pdf	Probability density function
POT	Peaks-Over-Threshold
REMA	Rwanda Environment Management Authority
RHDHV	Royal HaskoningDHV
RIWSP	Rwanda Integrated Water Security Program
SOP	Standard operating policy
SSR	Sum of squared residuals

List of Figures

Figure 1: The potential effect of reservoir operation on the distribution of downstream discharges and associated water levels and flood damage (Loucks and Van Beek, 2017). K_r in this context corresponds to the reservoir storage capacity.	5
Figure 2: Feasible zone for reservoir operation (Loucks and Van Beek, 2017).....	5
Figure 3: Conceptualisation of seasonal flood hydrograph in unregulated conditions and after regulation by storage and control reservoirs (FAO, 2005).....	6
Figure 4: A general example of the influence of a reservoir on the frequency distribution of downstream discharges. Discontinuity in reservoir scenario corresponds to dam failure, which was outside the scope of this study. Adapted from Mei (2013).....	7
Figure 5: Potential effects of reservoir regulation on flooding behaviour. Top plot: for areas where the bankfull discharge is relatively high in comparison to the regulated hydrograph, the reduction in peak discharges may result in the cassation of flooding altogether on typical years. Bottom plot: in areas where overbank flow occurs for relatively low discharges, the same reservoir regulation may result in increased flooding durations. The latter behaviour is hypothesised to occur in the Masaka wetland.....	10
Figure 6: Study area with features of interest and elevation.	13
Figure 7: Illustration of the typical annual distribution of rainfall and discharge for the Kanzenze station and its catchment. The discharge data consists of the available reference time series (described in section 3.1.1). Rainfall data source: CHIRPS (described in section 3.1.2). The hydrograph for 2018 consists of simulated data for the baseline scenario of the calibrated rainfall-runoff model described in section 4.1.1.	15
Figure 8: Mean annual precipitation (for the 1981~2017 period) in the Kanzenze station catchment. Major subcatchments correspond to the Ruliba station catchment (North) and Akanyaru river catchment (South). Data source: CHIRPS (Funk et al., 2015).....	17
Figure 9: Estimated evaporation in January 2000 for grid cells overlapping with the Kanzenze station catchment. Major subcatchments correspond to the Ruliba station catchment (North) and Akanyaru river catchment (South). Data source: GLDAS (Rodell et al., 2004).	18
Figure 10: Root-zone soil texture in the Kanzenze station catchment. Major subcatchments correspond to the Ruliba station catchment (North) and Akanyaru river catchment (South). Shown for the purpose of contextualisation only. Data source: Leenaars et al. (2018).....	20
Figure 11: Soil types in the Kanzenze station catchment. Major subcatchments correspond to the Ruliba station catchment (North) and Akanyaru river catchment (South). Shown for the purpose of contextualisation only. Data source: JRC/ESDAC (Panagos et al., 2012, Dewitte et al., 2013).	21
Figure 12: Land cover in the Kanzenze station catchment. Major subcatchments correspond to the Ruliba station catchment (North) and Akanyaru river catchment (South). Data source: Hydroscape (RIWSP, 2012e).....	22
Figure 13: Land cover in the main subcatchments adopted in this study. Adapted from Pandey (2014).	23
Figure 14: Slope in the Kanzenze station catchment: the occurrence of high slopes is commonly associated with accelerated erosion in Rwanda. Major subcatchments correspond to the Ruliba station catchment (North) and Akanyaru river catchment (South). Derived from HydroSHEDS hydrologically conditioned elevation data (Lehner et al., 2011).....	25
Figure 15: High turbidity and active bank erosion in the vicinities of the Masaka wetland. From RHDHV (2017b).	26
Figure 16: Key subcatchment division adopted in the current study.	28

Figure 17: System conceptualisation implemented for the estimation of discharges at the Kanzenze station based on three contributing areas.	29
Figure 18: Raw gauge height data available at the Rwanda Water Portal (RWFA, 2018) for the stations Ruliba and Kanzenze as of August 2018. The terminology adopted in this source is: <i>H</i> : “historical” data; <i>HO</i> : “observers” data; <i>HFV</i> : “field visit” data (i.e. rating curve points); <i>HT</i> : “telemetry” data. A period with reported extreme floods (November 2000) is highlighted.....	32
Figure 19: Available discharge time series for Kanzenze and Ruliba stations, estimated by the RIWSP. The shaded area corresponds to the period adopted for calibration of the rainfall-runoff models of the Ruliba station and Akanyaru river catchments.....	33
Figure 20: Available rating curve points and fitted rating curves for the Kanzenze station. The points consist of available “field visit” measurements of gauge height and corresponding discharge, coloured according to the year of collection. The lines for the periods 1955-1977 and 1986-2012 are based on coefficients adopted in RIWSP (2012d). A tentative rating curve based on post-2012 records was not employed but is plotted to illustrate the likely inadequacy of employing previous rating curves for the estimation of discharges from recent gauge height records.....	34
Figure 21: Discontinuity in rating curve reflected in gauge height distribution (Vrijling and Van Gelder, 2002). The plots correspond, in clockwise order from the top left, to the probability distribution of gauge heights, the rating curve and the probability distribution of discharges.....	35
Figure 22: Gauge height observations at the Kanzenze station (horizontal axis) and estimated flood extent for the corresponding dates (vertical axis). Each plot corresponds to one year, and observations are color-coded by the month of the year in which they were taken.	36
Figure 23: The generation of CHIRPS rainfall estimates (le Coz, 2018).	38
Figure 24: Comparison of potential evapotranspiration time series before and after application of CDF matching and standard deviation of 30-day rolling means. The dotted line represents the beginning of the period for which V2.1 data was adopted.....	39
Figure 25: Illustration of CDF matching procedure for potential evaporation time series for the Kanzenze station catchment for GLDAS versions 2.0 (pre-2011) and 2.1 (post-2011).....	39
Figure 26: Comparison of area-aggregated daily mean potential evaporation for the Ruliba catchment and sample time series of monthly pan evaporation for the Kigali Airport meteorological station on daily time...40	40
Figure 27: Cumulative yearly discharge volumes and corresponding catchment water balance estimates for Ruliba and Kanzenze stations. Plots on the same row share the same y axis scale.....	43
Figure 28: Examples of seasonal hydrographs for the Kanzenze and Ruliba stations.	44
Figure 29: Optimisation of the linear reservoir coefficient for the river segment between Ruliba and Kanzenze stations. For varying values of <i>K</i> (linear reservoir coefficient), the obtained spearman correlation coefficient and number of days on which estimated discharges were negative are shown in the top and bottom plot, respectively.....	45
Figure 30: Analysis of observed discharges for years with full records for stations Kanzenze and Ruliba. The discharge of the Akanyaru river is approximated by the difference in discharge at the Kanzenze and Ruliba stations, after the latter is routed in a linear reservoir to simulate temporary storage in floodplains between the two stations.....	47
Figure 31: Representation of implemented methodology.....	50
Figure 32: Perceptual model of hydrological processes in the Migina catchment (Munyaneza, 2014).	51
Figure 33: Conceptual rainfall-runoff model applied to the Ruliba station and Akanyaru river catchments...53	53
Figure 34: Relationship between the relative storage level in the unsaturated reservoir to the coefficient <i>c</i> for varying β values (equation 11)	59

Figure 35: Performance (Nash-Sutcliffe Efficiency) sensitivity to varying values of the calibration parameters for model runs with NSE ≥ 0 for the Ruliba station catchment. Rows correspond, from top to bottom, to plots of the Hillslope, Wetland and Groundwater modules, and to the global parameter T_{lag}60

Figure 36: Illustration of parameter selection for the rainfall-runoff model of the Ruliba station catchment. The selected parametrisation yielded a compromise between performance measured by the logNSE and NSE indicators.61

Figure 37: Simulated discharges at the Ruliba station for the calibration period, split into runoff components and compared against reference discharges. The main rainy season (Itumba) is highlighted on each year.62

Figure 38: Simulated discharges at the Akanyaru river outlet for the calibration period, split into runoff components and compared against reference discharges. The main rainy season (Itumba) is highlighted on each year.63

Figure 39: Time series of the calibrated Akanyaru model output and available gauge height observations at the Gihinga station.64

Figure 40: Observed gauge height at the Gihinga station and (a) raw incremental discharge between Ruliba and Kanzenze station and (b) Akanyaru model output after regionalisation by the area of the Gihinga station. In both cases discharges have been scaled by the area of the Gihinga station catchment.....65

Figure 41: Time series and flow duration curves for reference data and model simulation for the Kanzenze station for the corresponding dates.65

Figure 42: Illustration of the implemented standard operating policy assuming a reservoir operated with the primary goal of hydropower generation (storage corresponds to active storage volume at the beginning of a given time step).....68

Figure 43: Illustration of the implemented standard operating policy assuming a reservoir operated with the primary goal of minimising downstream peak discharges. Q_{flood} corresponds to the prescribed maximum reservoir release for each scenario.69

Figure 44: Autocorrelation function for simulated discharges at the Kanzenze station, and selected maximum correlation and corresponding lag time value, adopted as minimum peak width70

Figure 45: Simulated discharge time series and identified peaks over threshold (POT) for the no-reservoir scenario. Annual maxima plotted for comparison.72

Figure 46: Sum of squared residuals for candidate extreme value distribution functions for all simulated scenarios. No_Res: no-reservoir scenario. “Hydro” and “FloodPrev” labels correspond to hydropower and flood mitigation scenarios, followed by the assumed capacity factor and target maximum downstream releases, respectively.....73

Figure 47: Diagnostic plots for Gumbel distribution fitted to the selected peaks of the simulated time series for the no-reservoir scenario.....74

Figure 48 Density plot for entire discharge time series and annual peaks (no-reservoir scenario). A and B correspond to the values of the location and scale parameters of the Gumbel distribution that was fitted to both samples.....75

Figure 49: Distribution of MLE estimates for Gumbel parameters in 10^5 bootstrap samples of peak discharges for the no-reservoir scenario.....76

Figure 50: Return level plots with the respective 95% confidence interval of each parameter of Gumbel distribution. Plots share the same horizontal and vertical axes scales.....76

Figure 51: Return level plot for peak discharges generated in the no-reservoir scenario. Confidence bound indicates the range of estimates obtained with the parametrisation of the Gumbel function with 95% confidence for the scale and location parameters.....77

Figure 52: Return level plot for peak discharges generated in the no-reservoir scenario. Area illustrates the range in predicted peak discharges by different distribution functions fitted to the reference data. The exceedance probabilities estimated by the fitted generalised logistic distribution largely coincides with those of the Gumbel distribution, which was therefore highlighted.78

Figure 53: Output of semi-distributed model discretised by discharge components from the Nyabarongo and Akanyaru rivers for the 1981-1990 period. Reference discharge records at the Kanzenze station are plotted for comparison.80

Figure 54: Contributions to total discharge at the Kanzenze station from the Nyabarongo river (above) and Akanyaru river (below) for the entire simulation period.81

Figure 55: Relative (percentual) contributions to total discharge at the Kanzenze station from the Nyabarongo and Akanyaru rivers for the entire simulation period. The dotted line indicates the expected proportion in discharges based on the relative catchment sizes.82

Figure 56: Comparison of contributions from the Akanyaru and Nyabarongo rivers to simulated daily discharges in the no-reservoir scenario, for the entire simulated period (left) and during the Itumba season (right).83

Figure 57: Cross correlation between area-aggregated rainfall time series (red; left vertical axis) and simulated discharge components (blue; right vertical axis) of the Nyabarongo and Akanyaru rivers for the no-reservoir scenario.83

Figure 58: Hypothetical boundary scenarios for discharge regulation in the two main subcatchments of the Ruliba station catchment, from top to bottom: total regulation of the Akanyaru river, total regulation of the Nyabarongo river, total regulation of both rivers. Total regulation in this context is implemented by replacing simulated daily discharges by their long-term means.85

Figure 59: Simulated 2018 seasonal hydrograph for all flood mitigation and hydropower scenarios (top and bottom, respectively). The baseline scenario is overlaid on both plots for comparison. The Akanyaru river discharge component is constant for all scenarios. The discharges from the Nyabarongo river catchment for each scenario are given by the distance between the grey area and the respective lines.86

Figure 60: Comparison of simulated seasonal hydrographs at the Kanzenze station (top) and respective reservoir storage evolution (bottom) for flood mitigation scenarios in 2017 and 2018. The curves highlighted in red correspond to a policy with a target maximum downstream release of $120 \text{ m}^3\text{s}^{-1}$. The black curve indicates the baseline (no reservoir) scenario. For the year 2017, scenarios with high target maximum releases coincide with this curve.87

Figure 61: Comparison of simulated reservoir behaviour for the hydropower scenario for different prescribed maximum reservoir releases in 2017 and 2018. Releases and spills are the two components of total reservoir outflows.88

Figure 62: Comparison of simulated seasonal hydrographs at the Kanzenze station and respective reservoir storage evolution for hydropower scenarios in 2017 and 2018. The black curve indicates the baseline (no reservoir) scenario. The curves highlighted in red correspond to a policy with an assumed capacity factor of 0.40.89

Figure 63: Comparison of simulated reservoir behaviour for the hydropower scenario for different assumed capacity factors in 2017 and 2018. Releases and spills are the two components of total reservoir outflows.90

Figure 64: Simplified illustration of implemented policy for hydropower reservoir operation (left) and likely practical operation (right). The implemented policy triggers a positive feedback loop where increased storage leads to higher heads, which drive lower releases and hence further increases in storage (and vice-versa for decreasing storage). In contrast, practical reservoir operation can be expected to involve, to some extent, of a negative feedback loop with a self-balancing component with the goal of preventing fast filling or depletion of storage.91

Figure 65: Estimated percentage reductions in the maximum seasonal peak discharge magnitudes (in relation to the no-reservoir scenario) for all simulated scenarios, for the years 1981 to 1999.	92
Figure 66: Estimated percentage reductions in the maximum seasonal peak discharge magnitudes (in relation to the no-reservoir scenario) for all simulated scenarios, for the years 1999 to 2018.	93
Figure 67: Gumbel probability density function fitted to the peak discharges simulated for each scenario...	94
Figure 68: Gumbel cumulative distribution function fitted to the peak discharges simulated for each scenario.	94
Figure 69: Values of the location and scale parameters of the Gumbel distribution fitted to the peaks simulated for all scenarios.	95
Figure 70: Return level plots of peak discharges at the Kanzenze station for all simulated scenarios. For consistency purposes, all curves correspond to the estimates associated with the Gumbel distribution fitted to each scenario. Please refer to Figure 76 for an illustration of the range in return levels estimated by different functions fitted to each scenario.	96
Figure 71: Range of maximum annual flood durations per scenario type: no-reservoir (baseline) scenario shown in black.	96
Figure 72: Estimated percentage changes in the maximum yearly flood durations (in relation to the no-reservoir scenario) for all simulated scenarios, for the years 1981 to 1999.	98
Figure 73: Estimated percentage changes in the maximum yearly flood durations (in relation to the no-reservoir scenario) for all simulated scenarios, for the years 1999 to 2018.	99
Figure 74: Maximum flood durations and respective peak discharges per year, per simulated scenario. For certain scenarios in certain years, no peaks over threshold were identified and hence no corresponding points exist. Flood durations for the year 2018 have been trimmed to the end of the simulation period and may be underestimated for certain scenarios where flooding would have exceeded this date (see top plot of Figure 59).	101
Figure 75: Non-exhaustive illustration of sources of uncertainty in the data and methods adopted in the current study.	103
Figure 76: Illustration of range in predicted return levels for alternative distribution functions fitted to peak discharges simulated in each scenario. Plotted range includes functions with a difference in performance measured by SSR of less than 0.001. Areas are coloured by scenario family: No reservoir (green), hydropower (blue) and flood mitigation (red). Values on the title of subplots correspond to the assumed capacity factor (for hydropower scenarios) or target maximum release in m^3s^{-1} (for flood mitigation scenarios).	104

List of Tables

Table 1: Scope of main consulted scientific studies on the Hydrology of Rwanda.	3
Table 2: Seasons in Rwanda.....	14
Table 3: Overview of available time series data sources.	30
Table 4: Hydrometric stations selected for the study.	31
Table 5: Parameter value selection for the hydrological models of the Ruliba station and Akanyaru river outlet models.....	58
Table 6: Overview of estimated Shyorongi reservoir influences on riverine flooding at the Masaka wetland according to scenario family and criterion of assessment.....	105

Abstract

Fluvial flooding is a recurring phenomenon in Rwanda due to a combination of climate, topography and human interventions. This poses a hazard to human lives and infrastructure, particularly in low-lying areas adjacent to major rivers. An example of such areas is the Masaka wetland, located in the southern edge of the capital Kigali along the Nyabarongo river. As the city expands into the vicinities of this location, there is growing concern regarding infrastructure damage and human losses associated with extreme discharges. Simultaneously, potential for agricultural development, for which flood duration is a critical factor, has also been identified. Hence, there is a need for increasing the available knowledge on the seasonal pattern of discharges at this location.

However, significant changes in this behaviour may occur as a result of reservoir commissioning in the Nyabarongo river catchment. In particular, the Shyorongi reservoir in the scope of the Nyabarongo II Multipurpose Development Project will regulate approximately 47% of the catchment of the Masaka wetland. Hence, its operation may result in significant shifts on seasonal discharges and associated flooding in this location, which consisted of the main topic of investigation in this research.

For this purpose, time series of inflows to the reservoir, as well as contributions from non-regulated areas, have been generated by separately-calibrated lumped rainfall-runoff models based on the FlexTOPO framework, the period from January 1981 to August 2018. The operation of the reservoir was approximated by a standard operating policy. Two operational scenario families were devised: one maximising hydropower generation and one prioritising the reduction in peak discharges by limiting releases to a pre-defined threshold. For each scenario family, different parametrisations (target electricity output and maximum release, respectively) were tested, comprising a total of 50 scenarios. The resulting discharge time series of each scenario was compared to the baseline (no-reservoir) scenario according to two criteria: reductions in flood durations and reductions flood peaks. While flood durations were assessed on a relative basis, the effect on flood peaks was quantified by the expected shifts in the exceedance probability curve. This was estimated by a partial duration series (i.e. Peaks-Over-Threshold) approach, which was implemented to estimate peak seasonal discharges associated with return periods ranging from 2 to 500 years.

On specific years such as 2018, operation emphasising hydropower production had the secondary result of reducing peak discharges by up to 20%. However, over the majority of the simulated period, reductions were found to be insignificant, as reflected in the limited shifts in the fitted probability distributions. This type of operation also had generally insignificant effects on flood durations, regardless of the electricity output (and associated release) target.

In contrast, it was observed that reservoir operation with the specific goal of flood mitigation may consistently result in 20% to 25% reductions of seasonal peak discharges. However, this performance was found to depend, to a large extent, on the specified reservoir releases in comparison to inflow hydrographs, which vary over different years. Therefore, the availability of a seasonal outlook on discharges may guide the definition of optimal release rules for each year. Additionally, reservoir rules that account for the pronounced seasonal variability in inflows may allow for significant reductions on both flood peaks and durations in comparison to the policies hereby simulated, and it is recommended that such optimisation be carried out for the Shyorongi reservoir.

On relatively wet years, a trade-off was observed between the minimisation of flood peaks and of flood durations at the Masaka wetland. This is linked to the increment in discharge at the tail of the hydrograph caused by reservoir emptying, which may trigger the exceedance of the relatively low bankfull discharge threshold at this location. However, the simplified implemented operation rules adopted in this study have a limited capacity to represent practical reservoir operation. Therefore, there may be considerable potential for the optimisation of reservoir operation to improve performance in both flood mitigation and hydropower generation scenarios. However, due to the limited storage capacity of this reservoir, flood management in the Masaka wetland requires the adoption of complementary structural and non-structural measures according to the desired targets.

It is highlighted that several assumptions have been made concerning the conceptualisation of the catchment and characteristics of the Shyorongi dam and the Masaka wetland, as detailed in the body of the report. Additionally, the estimation of parameters for hydrological models and extreme value distribution functions inherently involves uncertainties. Therefore, the results and associated interpretations hereby presented should be interpreted in the context of a considerable amount of propagated uncertainty, and should not be adopted for design purposes.

Acknowledgements

Throughout my life to this day, I have had the privilege of belonging to a family which stimulates learning and personal development, and that has been willing and able to support – in all spheres – my endeavours. Therefore, I am deeply grateful for the different efforts made by my mother, father, siblings, grandparents and stepparents, which have allowed me to achieve this level of education.

My period in Delft was one of great learning, which was accompanied by challenges. Hence, I am deeply thankful to my girlfriend Tatiana, who offered companionship, understanding, support and the necessary criticism throughout this journey. During my studies, I have also been surrounded by exceptionally talented, inspiring and receptive peers at the Water Management faculty, many of whom I now consider friends for life. I am also grateful to the housemates I had on my first two years of study, with whom I share some of my most beautiful memories of Delft.

While this particular work is formally authored by me, it is more than fair to say that it would not have been possible without the efforts of key people involved in it. Firstly, I would like to acknowledge the insights and advice provided by my supervisor Dr. Markus Hrachowitz, which have been essential, for instance, in defining a scope that is both relevant and feasible. I am also grateful towards all committee members, who have had key roles throughout this study. In particular, I thank Dr. Jochen Wenninger for the guidance on the sometimes-challenging world of the hydrology of Rwanda, Prof. Pieter van Gelder for essential insights of the statistical aspects of this work, and Lars Hoogduin for the trust and support on behalf of Royal HaskoningDHV. A fifth person who also deserves my greatest acknowledgements is Bram Evers from Royal HaskoningDHV, who made himself available throughout this study and provided invaluable advice during the elaboration of this report.

This thesis has also been made possible due to the dedication of individuals and organisations who committed voluntarily to providing essential advice and information. In particular, I acknowledge the collaborators from the Rwanda Energy Group (REG), the Ministry of Agriculture (MINAGRI), the Rwanda Water and Forestry Authority (RWFA) and Water4Growth programme, Karisimbi Business Partners, the Global Disaster Alerting Coordination System (GDACS) and the Centre for Ecology & Hydrology (CEH NORA), among others. I also express my gratitude towards Marc Manyifika for pointing me to key hydrological data and previous studies carried out in Rwanda at the start of this study.

A final acknowledgement is made to the community behind the development of open-source Python packages extensively deployed in this project: pandas (McKinney, 2010), NumPy (Oliphant, 2006), matplotlib (Hunter, 2007) and SciPy (Jones et al., 2001).

1 Introduction

1.1 Background

Rwanda is a landlocked country with an area of 26.338 km² and a population exceeding 12 million inhabitants as of 2017 (UN DESA, 2018). It is located in the East African Great Lakes Region, between the latitudes 1°S and 3°S and longitudes 28°E and 31°S. Due to a combination of climate, topography and different types of human interventions, floods are a recurring phenomenon in the country, with several events recorded in the past decades (MIDIMAR, 2015).

Such events are linked to the loss of lives, damage to transport and water supply infrastructure as well as to food shortages due to crop damage (Munyaneza et al., 2011a). In 2008, 2.4% of the country's population was exposed to floods (RIWSP, 2012b). Losses in 2012 have been estimated to amount to approximately 1.4% of the country's GDP (REMA, 2013). In 2018, flooding and landslides arising from extreme rainfall have caused more than 200 deaths (Quackenbush, 2018), the destruction of over 10.000 houses (Okiror, 2018) and road damages amounting to US\$28.000.000 (Kanamugire, 2018).

Low-lying areas adjacent to rivers are particularly susceptible to flooding. In particular, the Masaka wetland, located in the southern edge of the capital Kigali, has been subject to growing attention due to risks to surrounding infrastructure and the potential for agricultural development. This has led to a demand for an improved understanding of the seasonal variability of discharges in the adjacent Nyabarongo river. However, the implementation of the Shyorongi reservoir in the context of the Nyabarongo II Multipurpose Development Project has the potential of significantly altering this discharge regime. Therefore, this research has been set to assess the potential effect of this reservoir on the seasonal hydrograph of this river and associated flooding in the Masaka wetland.

Sub-items 1.1.1 and 1.1.2, respectively, provide an overview of the existing knowledge concerning the hydrology of Rwanda and the expected effects of reservoir regulation on river discharges, which have guided the selection of hypotheses and methods for this study. Section 1.2 provides further details on the motivation for the current research briefly described above.

1.1.1 Previous investigations on the hydrology of Rwanda

Existing information on the hydrology of Rwanda generally stems from three kinds of sources:

- a. Scientific investigations (theses, dissertations and journal articles) (e.g. Abimbola, 2014, Munyaneza, 2014, Pandey, 2014, Bugingo, 2017),
- b. Studies carried out by international organisations and programmes (KOICA, 2008, e.g. RIWSP, 2012a, RIWSP, 2012b) or by private firms (e.g. LTS, 2012a, WECA Ltd., 2014, FutureWater and eLeaf, 2017) and
- c. Official policies and plans, which are often based on the previous two (e.g. MINAGRI, 2010, MIDIMAR, 2015, MININFRA, 2015, MINIRENA and RNRA, 2015).

Abimbola et al. (2017) employed a **regionalisation** approach to estimate four discharge quantiles and a flow index based on the nine catchments for which most reliable discharge data was available as reported in RIWSP (2012a) (to be detailed in section 3.1). 18 descriptors of catchment physiography, climate, hydrology and land cover were employed for multiple regression. The predictors of discharges with a 5% exceedance probability – the quantile of the highest interest for the current study – were found to be: mean annual precipitation and potential evaporation, catchment area, and the percentage of grassland, forest and salt hardpan cover of the total catchment area. This provides an indication that land cover may have a significant influence on flooding in the context of Rwanda. However, when using a log-transformed regression model, mean annual precipitation and drainage density were the only significant explanatory variables for discharges with high return periods.

Different modelling approaches have been adopted for the **estimation of discharge time series** in Rwanda. Munyaneza et al. (2011b) experimented with the rational method an area reduction factor in the 260 km² Migina catchment. Sendama (2015) tested different gridded precipitation products as forcing data for the HBV-light model, while Van Griensven et al. (2008) and Ndekezi (2010) adopted the SWAT model. HEC-HMS software has also been used in several previous studies (Munyaneza, 2014, Munyaneza et al., 2014, SHER Ingénieurs-Conseils S.A., 2014, Manyifika, 2015, Rukundo and Dogan, 2016). EDCL (2016) adopted the lumped NAM (Nielsen and Hansen, 1973) model for 15 subcatchments of the Kanzenze station catchment.

Several regional or global **gridded products** have also been tested and used in studies related to water resources in Rwanda. Bugingo (2017) compared the PERSIANN-CDR and African Flood and Drought Monitor (AFDM) products with ground measurements of rainfall and discharge, respectively. Dinku et al. (2007) has linked the accuracy of RS-based rainfall products to factors such as elevation and, but also showed that such influences vary across locations. Most existing literature either focusses on the assessment of remote sensing products for the prediction of drought events and water resources assessment (Pandey, 2014, Bugingo, 2017) or flooding in specific sub-catchments (Sendama, 2015, Munyaneza, 2014, Musoni, 2009, Umutoni et al., 2016) or in urban areas (Manyifika, 2015). The scope of previous scientific studies that are particularly relevant to the current research is summarised in Table 1.

In spite of the considerable impact of flooding, regions of Rwanda also experience issues of water scarcity and erosion, and recent studies have often focussed on topics such as environmental flows and land conservation (LTS, 2012a) as well as water availability and allocation (MINIRENA and RNRA, 2015). The country expects to develop a National Water Security Plan, of which water storage will be a main component (RNRA, 2016). A key required measure identified in the Rwanda National Water Resources Master Plan (MINIRENA and RNRA, 2015) is the assessment of interventions in the natural hydrological cycle, including flow regime changes which are the focus of this study.

Key knowledge gaps

Based on the studies described above, some knowledge gaps have been identified to which the current study aims to contribute. The first of them consists of the limited understanding of hydrological drivers of flooding in the specific context of the Masaka area, as described by Water4Growth and MINIRENA (2018). Second, none of the consulted literature has explicitly accounted for the potential effect of reservoir regulation on observed or simulated discharges; this research proposes a method for doing so in the context of Rwanda. A third gap consists of the estimation of daily discharges in Rwandan catchments for the period between 1990 and 2012 based on global gridded forcing data. This is particularly relevant at the ungauged outlet of the Akanyaru river catchment, since the studies comprising this area have been limited to providing water balances on a monthly or yearly time scale.

Table 1: Scope of main consulted scientific studies on the Hydrology of Rwanda.

Source	Main topic	Geographic area		
		Nyabarongo river basin	Akanyaru river basin	Other
Abimbola (2014); Abimbola et al. (2017)	Regionalisation of flow duration curves	✓	✓	
Munyaneza et al. (2011a)	Flood and drought management	✓	✓	
Pandey (2014)	General water resources assessment; catchment characterisation and water balance	✓	✓	
Bugingo (2017)	Performance assessment of PERSIANN-CDR (Ashouri et al., 2015) products against ground data in Rwanda	✓		
Sendama (2015)	Rainfall-runoff modelling based on remote-sensing forcing products	✓ (2009-2013)		
Munyaneza et al. (2010), Munyaneza et al. (2011b), Munyaneza et al. (2012), Munyaneza et al. (2014), Munyaneza (2014)	- Trend detection - Tracer hydrology - Rainfall-runoff modelling			
Umutoni et al. (2016)	Rainfall-runoff modelling based on remote-sensing forcing products			Migina catchment ¹
Van den Berg and Bolt (2010)	Fieldwork on discharge, groundwater levels, rainfall and evaporation			
Manyifika (2015)	Rainfall-runoff modelling based on remote-sensing forcing products; fieldwork; flood routing			Nyabugogo catchment ²
Musoni (2009)	Runoff coefficient estimation			

1 - The Migina catchment is a 147 km² subcatchment of Akanyaru river, indicated in Figure 6

2 - The Nyabugogo catchment is a subcatchment of the Kanzenze catchment, as shall be detailed in further sections

1.1.2 Reservoir effects on river discharges and flooding

Reservoirs are known to cause changes of varying extents in downstream discharge regimes. In fact, they are often built with this precise goal: dams are the most frequent means implemented by humans to prevent flooding (Mei, 2013). Figure 1 below illustrates the theoretical effect of reservoir regulation on the probability distribution of discharges (plot c), which is directly related to the probability distribution of water levels by the rating curve (plot b). Hence, if a function relating water levels to damage (plot a) exists, for any given probability of exceedance, a discharge and the corresponding damage can be estimated (plot d). In this context, the expected annual damage can be estimated by the integration of the estimated damage for each discharge over the probability interval $[0,1]$. The buffering capacity of reservoirs allows for a reduction in the probabilities of exceedance of given discharges associated with flooding, and hence of the expected annual damage (shown in dark blue).

A key goal of the current study can be described as providing the probability of exceedance of discharges at the Masaka wetland – function (c) in Figure 1 below – for different reservoir regulation scenarios. This may assist in the estimation of the changes in expected flood damage in the region as a result of the operation of the Shyorongi reservoir, and hence the need for supplementary actions for flood risk management.

A basic representation of the possibilities for reservoir operation is illustrated in Figure 2. The operation of a reservoir can be illustrated, in a simplified manner, as the releases associated with a given storage and inflows for a given time step. The regulation caused by a reservoir is a function of (a) its storage capacity and (b) its operating rules (Loucks and Van Beek, 2017). A larger storage capacity increases the area of the zone of feasible release, and the operating rules define, for a given storage and inflow volume at a given moment, the corresponding release. Operating rules affect discharges according to the primary goal of a reservoir.

Storage reservoirs are commissioned with the goal of enhancing water availability in low-discharge periods. Therefore, their operation broadly consists of maximising the stored volume at any given moment. Hydropower reservoirs can be included in this category, as higher stored volumes imply both greater security in drier periods and higher heads. In this particular type of reservoir, water is generally released according to electricity demand with a daily cycle (Mei, 2013), but weekly and seasonal cycles may also occur (Deane et al., 2010).

In contrast, dams built with the specific goal flood prevention, or **control reservoirs**, generally aim at limiting the downstream discharge – and associated water level – to a given threshold, often the one associated with bankfull conditions (Mei, 2013). For a given inflow hydrograph, the reservoir imposes a constant downstream release by changing its storage over time. The conceptualised effect of both types of reservoir on the seasonal hydrograph of a hypothetical river is contrasted with the non-regulated regime (which corresponds to the reservoir inflows) in Figure 3.

In both scenarios of operation, reservoirs tend to reduce the frequency of low flows, but also of discharges with low probability of exceedance, effectively confining the range of flows into a narrower interval than in unregulated conditions (Mei et al., 2016). A general illustration of this effect is presented in Figure 4. The increase in the frequency of very high peak discharges is associated with dam failure, which has not simulated in this study due to limitations in data availability.

In general terms, a reservoir can have two distinct effects on discharges (Mei, 2013), namely:

- a. to successfully prevent or reduce the frequency and intensity of downstream flooding, or
- b. to fail and aggravate flooding. This may in turn be broadly classified into (Baecher et al., 1980):
 - overtopping;
 - breaching, piping or seepage;
 - other miscellaneous causes, such as poor construction, earthquake effects and inadequate maintenance.

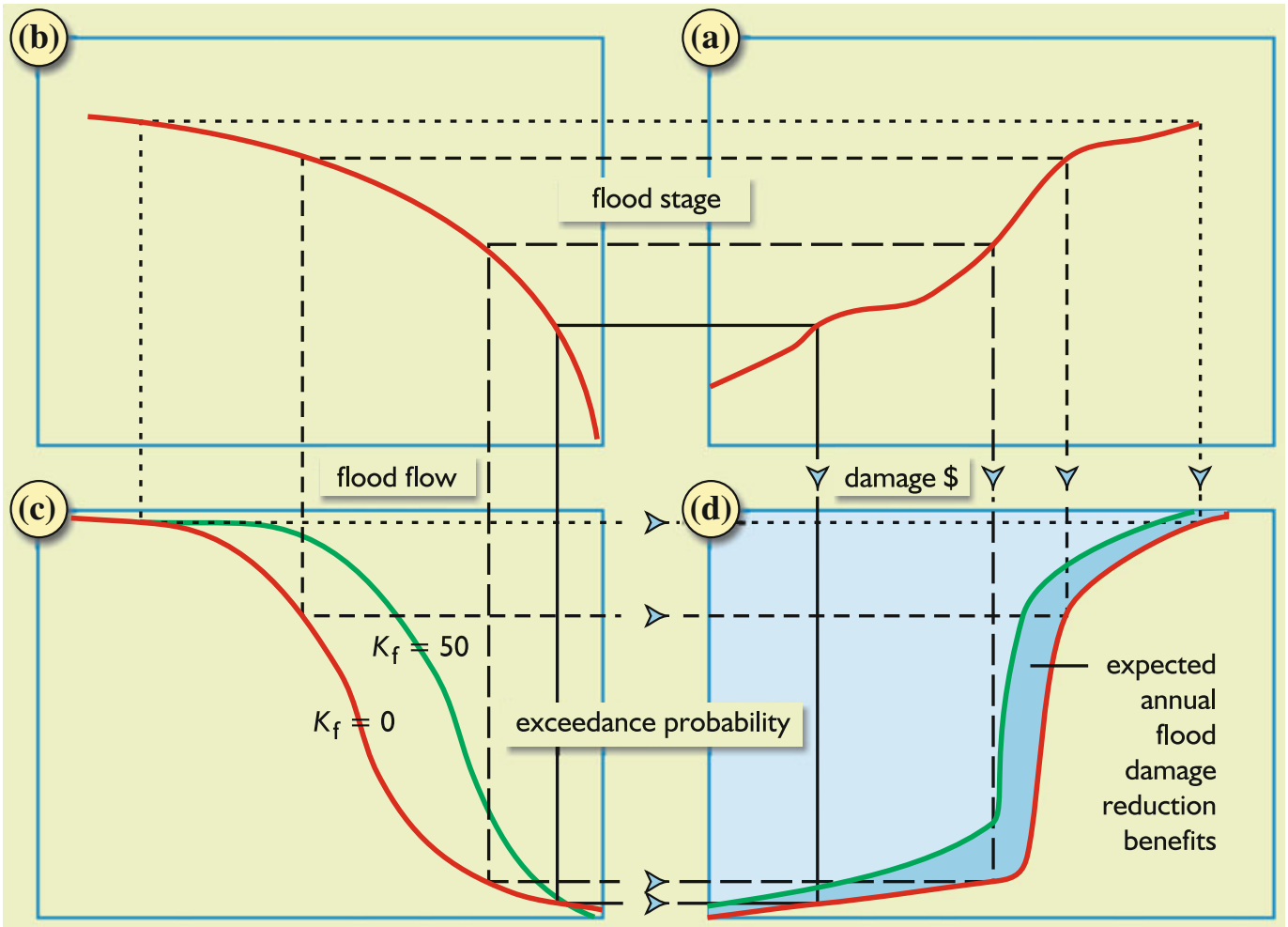


Figure 1: The potential effect of reservoir operation on the distribution of downstream discharges and associated water levels and flood damage (Loucks and Van Beek, 2017). K_f in this context corresponds to the reservoir storage capacity.

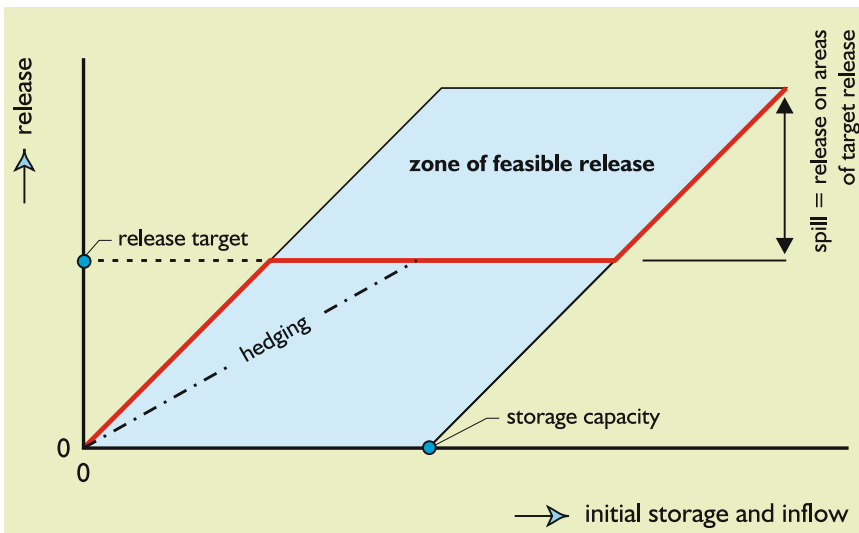


Figure 2: Feasible zone for reservoir operation (Loucks and Van Beek, 2017).

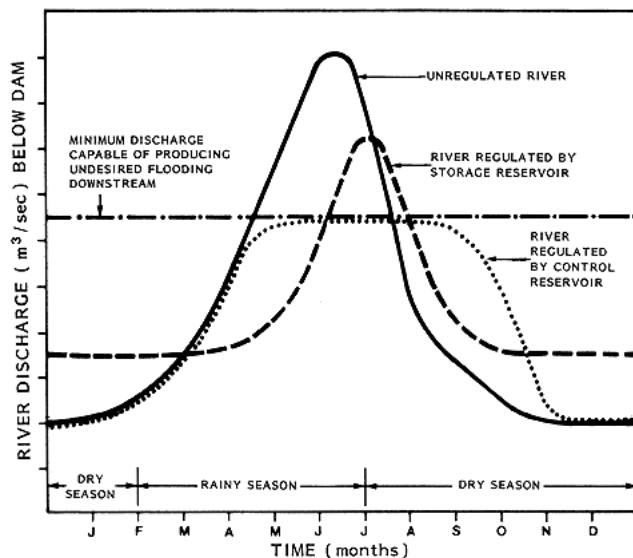


Figure 3: Conceptualisation of seasonal flood hydrograph in unregulated conditions and after regulation by storage and control reservoirs (FAO, 2005).

It is highlighted that Figure 3 provides an idealised representation of control reservoir behaviour, with the underlying assumption that its capacity is large enough to fully store the excess volume generated by the difference in discharges during the period for which inflows exceed releases – approximately mid-April to late July in that representation. This assumption does not necessarily hold for all reservoirs, including the Shyorongi reservoir, as shall be shown. In the context of the Nyabarongo catchment, the discharge regime, topography and low river banks mean that implementing reservoirs that would confine the occurrence of floods to high return periods is, if not technically challenging, economically unfavourable.

An important observation by Mei (2013) is that the effect of a given reservoir (the Feitsui Reservoir in that case) on flooding behaviour decreases as one moves downstream and away from the dam – both in the cases of normal operation and dam failure. This can be associated with the “dilution” of the regulated flow by discharges generated in non-regulated downstream catchments (Mei, 2013). In the context of the current study, this effect may in principle be expected to be considerable. As previously mentioned, the area of the catchment regulated by the Shyorongi reservoir corresponds to approximately 47 % of the total catchment of Masaka wetland (refer to Figure 4 in section 2.1). Therefore, contributions from the remaining 53% of the area – with little or no regulation – can be expected to comprise significant proportion of the discharge.

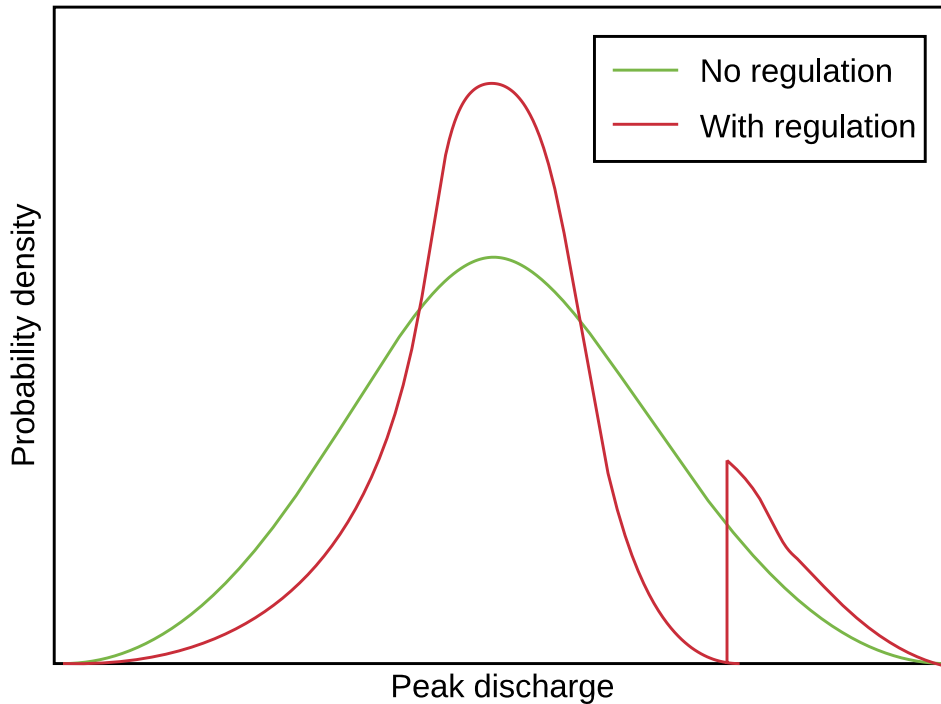


Figure 4: A general example of the influence of a reservoir on the frequency distribution of downstream discharges. Discontinuity in reservoir scenario corresponds to dam failure, which was outside the scope of this study. Adapted from Mei (2013).

According to Mei (2013) two main approaches exist for the quantification of reservoir effects on downstream discharges. The first consists of a **measurement-based method**, and involves the comparison of discharge time series of two periods – prior to and after the implementation of a reservoir – in order to identify eventual break points in patterns around the period of dam commissioning. This was adopted by Mei et al. (2016) for 38 rivers in the USA. The authors verified that dam commissioning has led to significant decreases in flooding magnitude for all but one of the investigated catchments. This effect was noticeable for both regular floods and extreme events.

The second approach for the estimation of dam effects on flooding is a **model-based method**, which is generally implemented when discharge observations are insufficient or lacking either before or after reservoir commissioning. This involves building and calibrating a model aimed to reproduce the variable of interest (i.e. water levels or discharges) based on forcing data, and simulating scenarios with and without dam regulation. This approach was adopted by Mei (2013) in a study case of the Tanshui river under typhoon conditions. In that study, a coupled hydrological and hydrodynamic model was devised and calibrated based on flood records. Design storms were generated from the analysis of ground rainfall records, and the flooding behaviour was compared for scenarios with and without dam commissioning.

The measurement-based method is a data-intensive approach, as ideally 30 years of observations are required before and after dam commissioning (Mei, 2013). There are additional challenges involved in the task of isolating “natural” changes in flooding behaviour from those associated with human interventions, as catchments with longer records tend to also be those a higher degree of anthropogenic interferences beyond dam construction (Mei et al., 2018). This limitation in data is evident in Rwanda, where reliable discharge records are generally constrained to limited periods of time and include gaps (to be detailed in section 3.1). Additionally, since the Shyorongi dam has not yet been commissioned, no discharge records exist for the period after implementation. These two considerations have motivated the adoption of a model-based method for this study.

Reservoirs have been included in previous hydrological exercises at the scale of the Nile river basin (NBI, 2012) – on that occasion, the Global Lakes and Wetlands Database (GLWD - Lehner and Döll, 2004) was

adopted. However, the relatively small scale of existing reservoirs within the Nyabarongo river catchment has resulted in their neglect in regional and global-scale studies. None of the local studies mentioned in the previous section has been found to explicitly account for this influence.

1.2 Problem statement

1.2.1 The increasing relevance of the Masaka wetland

Due to its low-lying position, the Masaka wetland has historically been subject to seasonal flooding associated to water level fluctuations in the Nyabarongo¹ river, which has limited the occupation of this location (Agriterra, 2017). However, this area has received increasing attention in recent years due to factors including the following:

Increasing exposure of inhabitants and infrastructure to flooding

Expansion in the city of Kigali has taken place predominantly in the Eastern and Southern parts of the city, towards the Nyabarongo river (Nkurunziza, 2018). The Masaka area, which encompasses the Masaka wetland and adjoining areas, is identified in the Kigali City Master Plan (City of Kigali, 2013) as a key location for urban expansion over the coming decades. The floods of 2018 in the Masaka wetland have triggered concerns and an express intention by the Government of Rwanda to “protect the wetland environment and, at the same time, protect existing infrastructures in the area” (Water4Growth and MINIRENA, 2018).

Interest in developing agriculture in the area

The looming issue of land scarcity – a major driver of poverty in Rwanda (REMA, 2009) – has also triggered a government strategy to stimulate agriculture expansion in wetlands along major rivers of the country (RHDHV, 2017a) – an activity that dates back to the middle of the 20th century (MINAGRI, 2010). More specifically, the goal to reduce dependence on imported sugar and the relative tolerance of sugarcane to limited periods of flooding have led to an effort to expand the cultivation of this crop into marshlands along the Nyabarongo river. However, flooding consists of a hazard to agricultural activities in these areas. For example, a large flood event has been reported to have taken place in the Masaka area in November 2000, causing losses of approximately 195 ha of sugarcane (Agriterra, 2017).

It is known that the extent to which plants are damaged by floods depends on factors such as flooding depth, duration and water flow (Hidaka and Karim, 2007). Therefore, it is important to understand the current and future risk of flooding in the area in order to select coping measures that reflect the tolerable expected damage.

Increased flood frequency and severity

To some extent, there is a positive feedback loop between flood occurrence and the construction of protection infrastructure for the reclamation of floodplains for agricultural development in Rwanda. For example, in order to prevent flooding, the Bugesera Agricultural Development Support Project (PADAB) project involved the construction of high embankments on the right margin of the Nyabarongo river opposite to the Masaka wetland, reducing of the floodplain width by up to 80% (RHDHV, 2017a).

¹ According to some sources, the Akagera river is formed by the confluence of the Nyabarongo and Akanyaru rivers upstream of the Masaka wetland. However, the river stretch at the Masaka wetland is commonly referred to as the Nyabarongo river, and this choice has been adopted for this study. However, the term “Nyabarongo river catchment” in the context of the current study corresponds to the area drained by this river upstream of the Akanyaru river outlet, which corresponds approximately to the catchment of the Ruliba station (see Figure 6). Hence, the terms “Nyabarongo river catchment” and “Ruliba station catchment” are used interchangeably in this report.

Simultaneously, due to interventions such as the above, recent years have witnessed increased water levels with some areas of the Masaka wetland having been reported to be flooded throughout the year (Agriterra, 2017). The formation of a small lake in the location has also been reported (Water4Growth and MINIRENA, 2018). This has increased crop damage, leading to a general growth in poverty in the Masaka area (Agriterra, 2017).

Need for allowing the flood regime to be maintained

As in other regions of the world, occasional flooding originating from the Nyabarongo river has the beneficial effect of bringing fertile sediments to the floodplains (Bayley, 1995). It is also known that the soils underlying wetlands in Rwanda generally have a high peat content, and their excessive drainage triggers oxidation and associated CO₂ emissions, as well as loss of stability (REMA, 2018). These characteristics mean that excessive intervention in the local system might not only be undesirable from an economic perspective but also from an environmental one.

1.2.2 A changing landscape for seasonal flooding in the Masaka wetland

The scenario described above motivates the need to understand the sources of flooding in this area and to assess the demand for appropriate structural and non-structural measures for the management of this risk. Reaching an optimal compromise between maximising flood protection and minimising system intervention requires that the future discharge regime be sufficiently well understood.

At the same time, given the fast pace of interventions in the catchment of the area, an assessment of flood risk based solely on historical data is likely to provide misleading results. The Nyabarongo II Multipurpose Development Project has as one of its goals the reduction of flood risk in downstream areas. One of its key components is the Shyorongi dam, which will drain a catchment of 6.489 km² or approximately 47 % of the area drained by the Nyabarongo river at the upstream boundary of the Masaka wetland. Therefore, its operation may in principle have a significant impact on the flooding regime at this location. However, such influence can be expected to be tied to the operation policy of this reservoir.

The quantification of the potential influence of the Shyorongi II reservoir on seasonal flooding of the Masaka wetland consisted of the primary goal of this investigation. The reservoir will drain a fraction of the Masaka wetland catchment and hence a fraction of its discharge, while the remainder of the discharge can be expected to remain virtually unaltered (detailed in section 2.3). Hence, it is critical to discretise the runoff at the Masaka wetland into these two components in order to understand the potential effect of regulation of one of them – see hypothesis A.

A second step consisted of defining qualitative and quantitative criteria for assessing the potential effect of reservoir operation on the flooding regime. While human life losses and infrastructure damage are most directly linked to the magnitude of peak discharges, certain types of crops (e.g. sugarcane) are resistant to flooding for limited periods of time; hence flood duration is the critical factor in this case. Hence, this study aimed to investigate potential shifts in both flood peaks and flood durations.

As described in section 1.1.2, reservoirs are generally associated with – intentionally or not – reducing the frequency of extreme values immediately downstream of the release point, while increasing the frequency of discharges around a certain intermediate value. In the context of hydropower, this value can be expected to be the discharge required to meet a pre-defined generation target. At the time of elaboration of this study, this target – and hence the associated release – is unknown. If the sum of this release and the component from the unregulated catchments exceeds the channel capacity at the Masaka wetland, one can expect an increase in flooding frequency. In contrast, if the discharge required for hydropower is relatively low and the regulation capacity of the reservoir is sufficiently high, the reservoir may play a significant role in concentrating the regulated component of the discharge at Masaka around a relatively low value, hence reducing flooding frequency – see hypothesis B.

Reservoirs may also be operated with the primary goal of preventing downstream discharges from exceeding a certain threshold. This is achieved by minimising the stored volume in order to provide buffering during periods of high discharges as the reservoir fills. When inflows decrease, the reservoir releases the stored volume in order to prepare for the following rainy season. When the storage capacity of

the reservoir in relation to the hydrographs to be regulated is sufficiently high, a considerable reduction in the magnitudes of flood peaks can be expected – see hypothesis C.

In contrast with flood magnitude and/or frequency, flood duration may increase with reservoir operation. The volume stored over a rainy season is gradually released after it. This causes downstream discharges to remain higher than they would have been in a scenario without regulation (i.e. the hydrograph is flattened and extended). For a certain period of time, this incremental discharge can be expected to cause flooding in areas where, under non-regulated conditions, bankfull discharge would be exceeded. Hence, flooding duration in these areas may increase. In the current study, this proposition was translated into hypothesis D. However, due to the high uncertainty involved in the estimation of flood durations in this location, no quantitative criteria for this effect were defined. Figure 5 illustrates, in a summarised manner, the possible expected effects of reservoir regulation on flood peaks and durations described above.

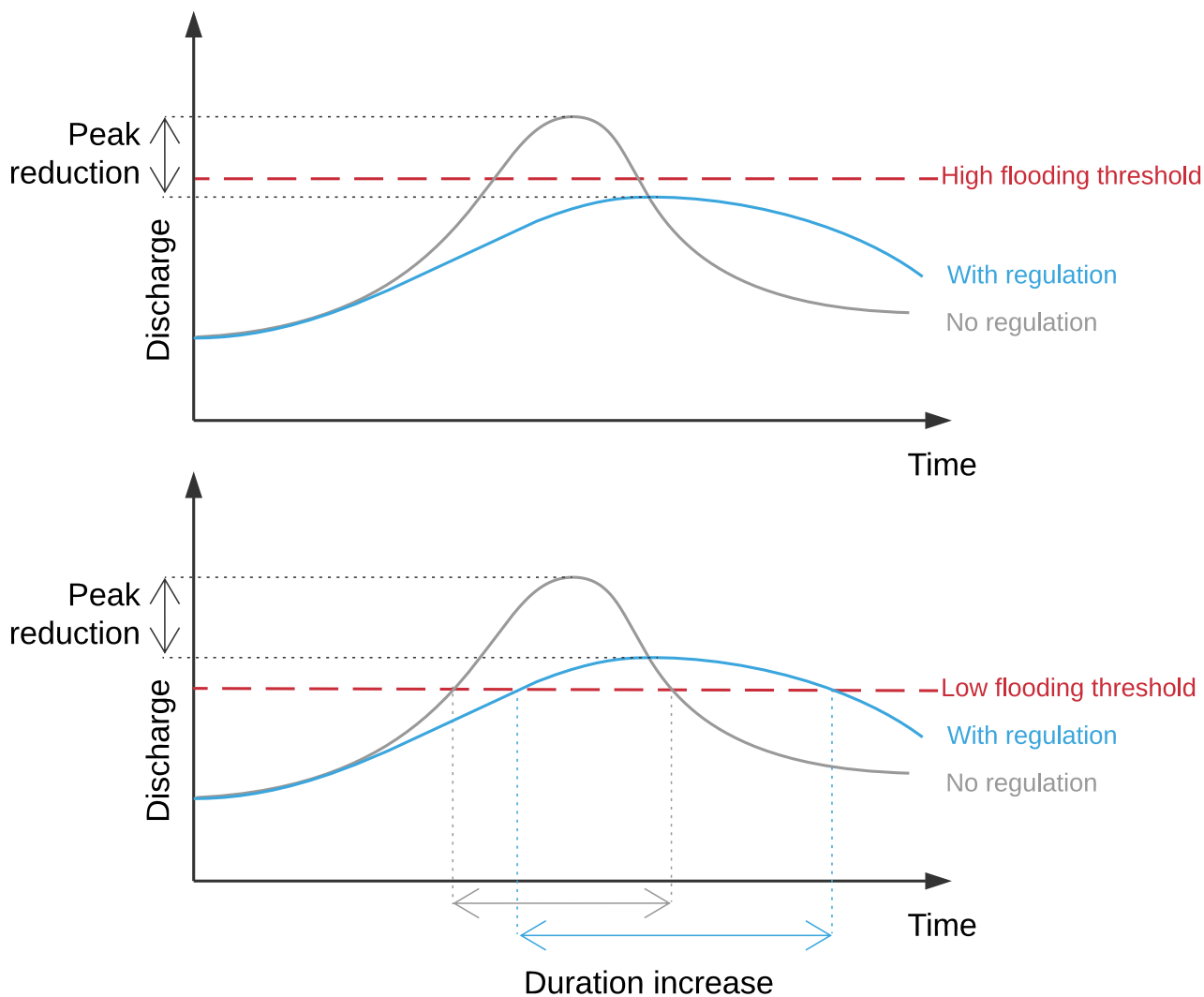


Figure 5: Potential effects of reservoir regulation on flooding behaviour. Top plot: for areas where the bankfull discharge is relatively high in comparison to the regulated hydrograph, the reduction in peak discharges may result in the cassation of flooding altogether on typical years. Bottom plot: in areas where overbank flow occurs for relatively low discharges, the same reservoir regulation may result in increased flooding durations. The latter behaviour is hypothesised to occur in the Masaka wetland.

1.3 Research outline

Considering the context outlined in the previous section, the research has been set as follows.

1.3.1 Research question

The question to be answered by this study was:

What is the expected influence of the Shyorongi multipurpose reservoir on seasonal flooding in the Masaka wetland?

1.3.2 Hypotheses

Based on the aforementioned research question, the study was set to test the following hypotheses:

- A. Discharge from the mostly-unregulated Akanyaru river is a significant driver of flooding in the Masaka wetland.
- B. If operated with the strict goal of hydropower generation, the Shyorongi reservoir may shift the distribution of peak seasonal discharges such that the discharge currently associated with a 2-year return period will have a return period of 10 years or higher.
- C. If operated with the strict goal of flood mitigation, the Shyorongi reservoir may shift the distribution of peak seasonal discharges such that the discharge currently associated with a 2-year return period will have a return period of 10 years or higher.
- D. The Shyorongi reservoir has the potential to increase the duration of seasonal floods in the Masaka wetland

1.3.3 Report structure

The remainder of this report is structured as follows: chapter 2 provides a description of the Masaka wetland and the Kanzenze station located immediately upstream, as well as key characteristics of its catchment. Section 2.3 describes and illustrates how the knowledge of the catchment, the goals of the current research and data availability guided the system representation adopted throughout this study. Chapter 4 details the procedures undertaken for the examination of the defined hypotheses. These broadly consisted of the generation of daily discharge time series for several reservoir operating scenarios by means of a rainfall-runoff model coupled with a simplified reservoir model (described in section 4.1), and the estimation of return periods for peak discharges based on the fitting of frequency distributions to the respective model outputs (section 4.2). Chapter 5 describes the results obtained along with interpretations, and chapter 6 offers conclusions in light of the hypotheses defined above.

2 Study area

Figure 6 provides an overview of the Masaka wetland, as well as the planned location of the Shyorongi reservoir and the stations and catchments of interest to this study. The Kanzenze gauging station has been adopted as a suitable proxy for discharges at the Masaka wetland due to its proximity to the location and relatively long record of available discharges. Consequently, catchment of this station was adopted as the system boundary for this study. Considering the goal of estimating the effect of the Shyorongi dam on downstream discharges, it was necessary to simulate its inflows. For this purpose, records from the Ruliba station were adopted and scaled as described in section 4.1.1.5.

2.1 Masaka wetland and the Kanzenze station

It is generally acknowledged that the hilly topography and intense seasonal rainfall are the main sources of flooding in the Akagera river basin. In particular, flooding in the Masaka wetland has been reported to be affected by (Agriterra, 2017):

- **Flash floods** after intense rainfall events associated with runoff from local streams discharging directly into the wetland;
- **Fluvial floods** associated with the Nyabarongo river, which reaches high water levels and overflows on a seasonal basis. Fluvial flooding is defined by Thiemig (2014) as “a temporary condition in which (mostly after heavy rains) the water level of a river rises and spills out of its natural course, inundating land that is usually dry”.

The Masaka wetland is located in the Kicukiro district of the city of Kigali, approximately 20 km downstream of the point where the Akanyaru river joins the Nyabarongo river. Considering the trend of urban expansion into the area surrounding the Masaka wetland, an increase in the frequency of flash flooding – as has already been observed in other areas of Kigali (MINIRENA and RNRA, 2015) – can be expected. However, the temporal and spatial scales of the processes behind flash flooding are distinct from those of fluvial flooding, and generally have different requirements for data and methods. Additionally, there is no basis to infer that flash flooding will be directly affected by the operation of the Shyorongi reservoir. Hence, the scope of the current study has been limited to exploring fluvial floods, and specifically the discharges associated with them.

Local residents have reported that the flooding period generally begins in April, with fields beginning to dry in the end of May. However, it has also been reported that areas currently covered by papyrus are permanently wet, with lower water levels during the dry season (Agriterra, 2017). A survey commissioned by RHDHV (2017b) generated detailed cross-section and discharge profile data for near-bankfull conditions in a section of the Nyabarongo river adjacent to the Masaka wetland. At this location, a discharge of $112.5 \text{ m}^3\text{s}^{-1}$ was found to correspond to a cross-section area of 132.2 m^2 and a water level approximately 0.4 m below the floodplain elevation. Assuming no significant changes in mean water velocity and in cross-section width with an increase of 0.4 m in water level, a bankfull discharge of $127.5 \text{ m}^3\text{s}^{-1}$ or $1.102 \times 10^7 \text{ m}^3\text{day}^{-1}$ has been estimated.

A second source of approximate bankfull discharge values for this area consists of the discontinuities between section I and II of the Kanzenze station rating curves established by (RIWSP, 2012d) – to be detailed in section 3.1 – which correspond to discharge values of approximately 140 and $155 \text{ m}^3\text{s}^{-1}$ for the periods before and after 1986, respectively. However, considering that the Kanzenze station is located upstream of the Masaka wetland (see Figure 6), the bankfull discharge at that location cannot be expected to match precisely the value in the Masaka wetland. However, these values provide a broad validation of the approximate magnitude of discharges associated with floods in the area.

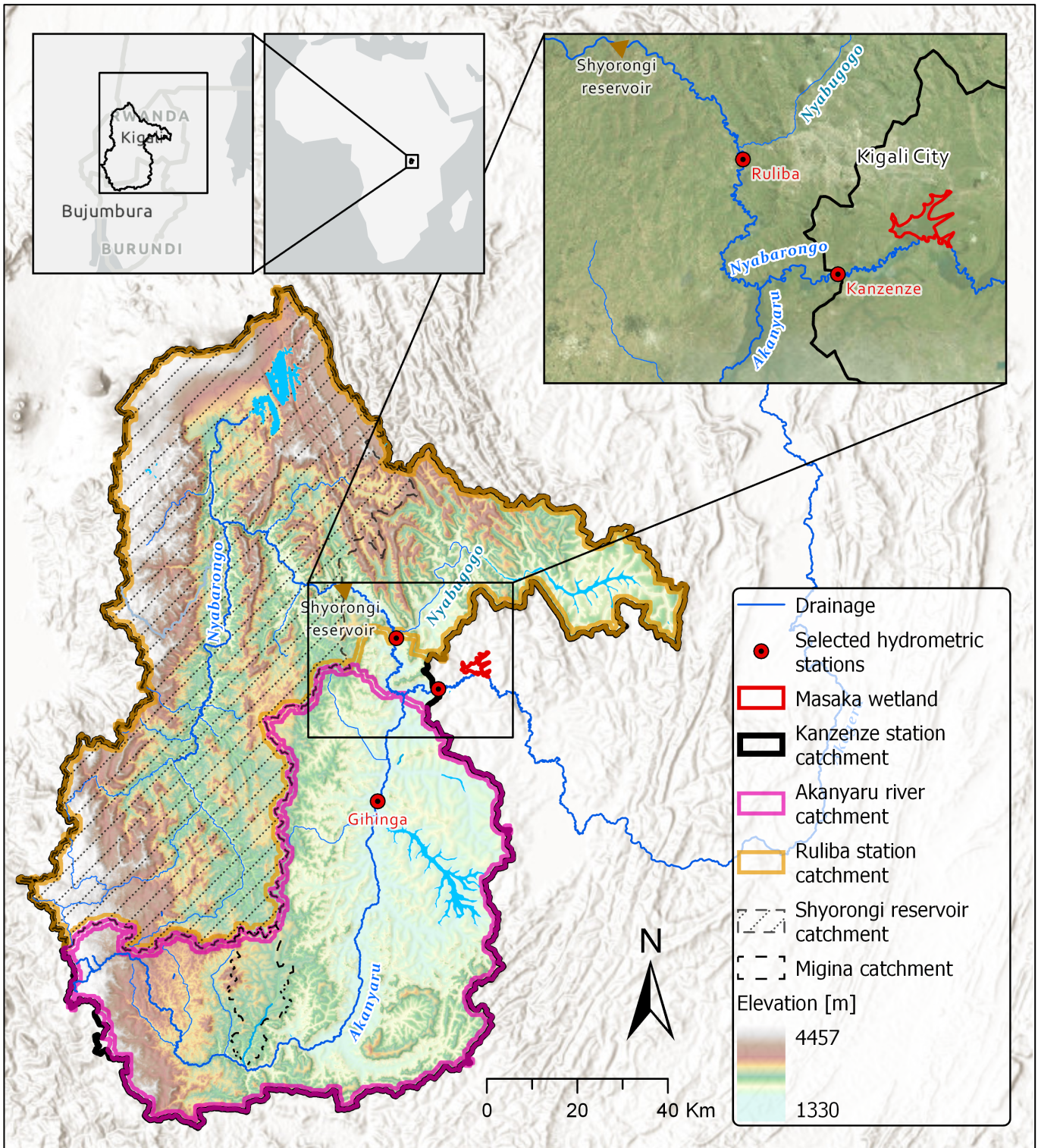


Figure 6: Study area with features of interest and elevation.

Therefore, the value of $127.5 \text{ m}^3\text{s}^{-1}$ has been adopted throughout this study as the threshold discharge above which flooding is expected to occur in the Masaka wetland. However, it is highlighted that:

- Observed differences in cross-section, slope and levee height along the Masaka wetland mean different bankfull discharge values exist even within the area (RHDHV, 2017b).
- A more accurate estimate of the discharge corresponding to overflow in the Masaka wetland in current conditions depends on a detailed hydraulic simulation in the area.

- c. Due to the active morphodynamics and human interventions in the location, this value is not necessarily representative of conditions in previous decades.

2.2 The catchment

2.2.1 Climate

The climate of Rwanda is equatorial, influenced by factors such as topography, land cover, local atmospheric circulation and the existence of large water bodies in the region (Muhire and Ahmed, 2014). In particular, the movement of the Inter Tropical Convergence Zone (ITCZ) drives a **bimodal rainfall pattern** in the country (Ilunga and Muhire, 2010, Wagesho and Claire, 2016). Table 2 illustrates the wet and dry periods resulting from this oscillation, and the respective names by which they are commonly known in Rwanda. This seasonal rainfall behaviour is reflected in discharge variability, as illustrated in Figure 7.

Table 2: Seasons in Rwanda.

Season	Dry/Wet	Start	End
Umuhindo	Wet (short)	Sep	Nov
Urugaryi	Dry	Dec	Feb
Itumba	Wet (long)	Mar	May
Icyi	Dry	Jun	Aug

Source: Ndekezi (2010)

Additionally, the El Niño–Southern Oscillation (ENSO) cycle drives **interannual variability** in rainfall (Wagesho and Claire, 2016). El Niño years have caused extensive flooding and associated crop damage, as reported for example for 1997-1998 (Munyaneza et al., 2011a, Wagesho and Claire, 2016) and 2015-2016 (RHDHV, 2017a).

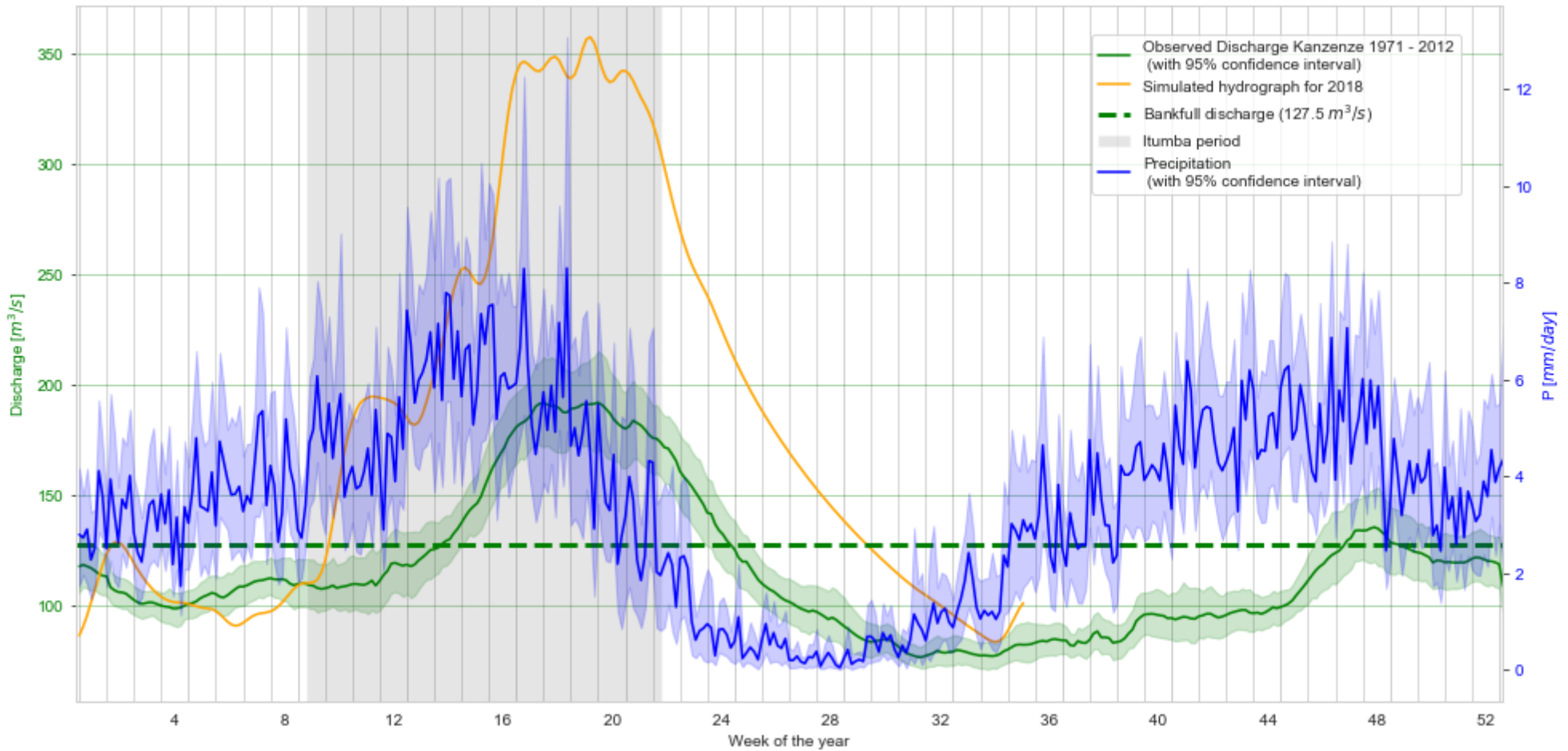


Figure 7: Illustration of the typical annual distribution of rainfall and discharge for the Kanzenze station and its catchment. The discharge data consists of the available reference time series (described in section 3.1). Rainfall data source: CHIRPS (described in section 3.2). The hydrograph for 2018 consists of simulated data for the baseline scenario of the calibrated rainfall-runoff model described in section 4.1.1.

Despite its relatively small area extent, Rwanda also experiences considerable variability in the **spatial distribution of rainfall**, with annual mean depths ranging from 750 mm in the north-eastern region to 2200 mm in locations in the southwest (MINAGRI, 2010). Within the Kanzenze catchment, this range consists of approximately 840 to 1650 mm, respectively, as shown in Figure 8. This variability has been attributed to its complex topography and the water bodies in the Great Lakes Region (Munyaneza, 2014) as well as anthropic activities (Wagesho and Claire, 2016).

Muhire and Ahmed (2014) carried out a study of **precipitation trends** in Rwanda, focussing on the number of rainy days and total rainfall depth for different time scales, based on ground observations. Considerable heterogeneity was observed in the signal and magnitude of changes in rainfall depth, both spatially and across months of the year. Within the Itumba period, while most stations showed a trend of increasing rainfall depths in March and April, 90% of the stations presented lower rainfall in the month of May. It should be noted, however, that the fraction of stations with statistically significant trends was limited to approximately 10%, 20% and below 5%, respectively, for each month. It is also highlighted that the magnitude of observed changes did not exceed 2 mm/month for any given month. Munyaneza (2014) identified virtually no trends at the 5% significance level over four different time periods for 10 stations. Eventual past trends in precipitation patterns have not been considered significant when compared to the region's characteristic inter-annual variability (REMA, 2015), and it has been acknowledged that there is high uncertainty on the expected effect of climate change on rainfall in Rwanda (MINIRENA and RNRA, 2015).

The **spatial and temporal variability in evaporation** is less pronounced than that of precipitation. Figure 9 illustrates this distribution by means of a sample of monthly estimate of evaporation for pixels of the GLDAS product overlapping the Kanzenze catchment. It is visible that the regions with higher altitudes (and lower temperatures) on the West of the catchment experience lower evaporation than the lower, warmer areas in the East.

Subcatchment-scale estimates of annual evaporation depths based on water balance were adopted in the National Water Resources Master Plan (MINIRENA and RNRA, 2015). For subcatchments of the region of interest in the current study, the reported values range from 851 mm for the Mukungwa river catchment in the Northwest of the country to 990 mm in the Akanyaru catchment². However, temperature observations between 1971 and 2006 showed increasing trends at the 5% significance level for nearly all stations, and temperature was found to be negatively correlated with streamflow (Munyaneza, 2014). Hence, a trend of increasing catchment evaporation may be expected as a result of climate change.

² Referred to as NMUK and NAKN, respectively, on that source.

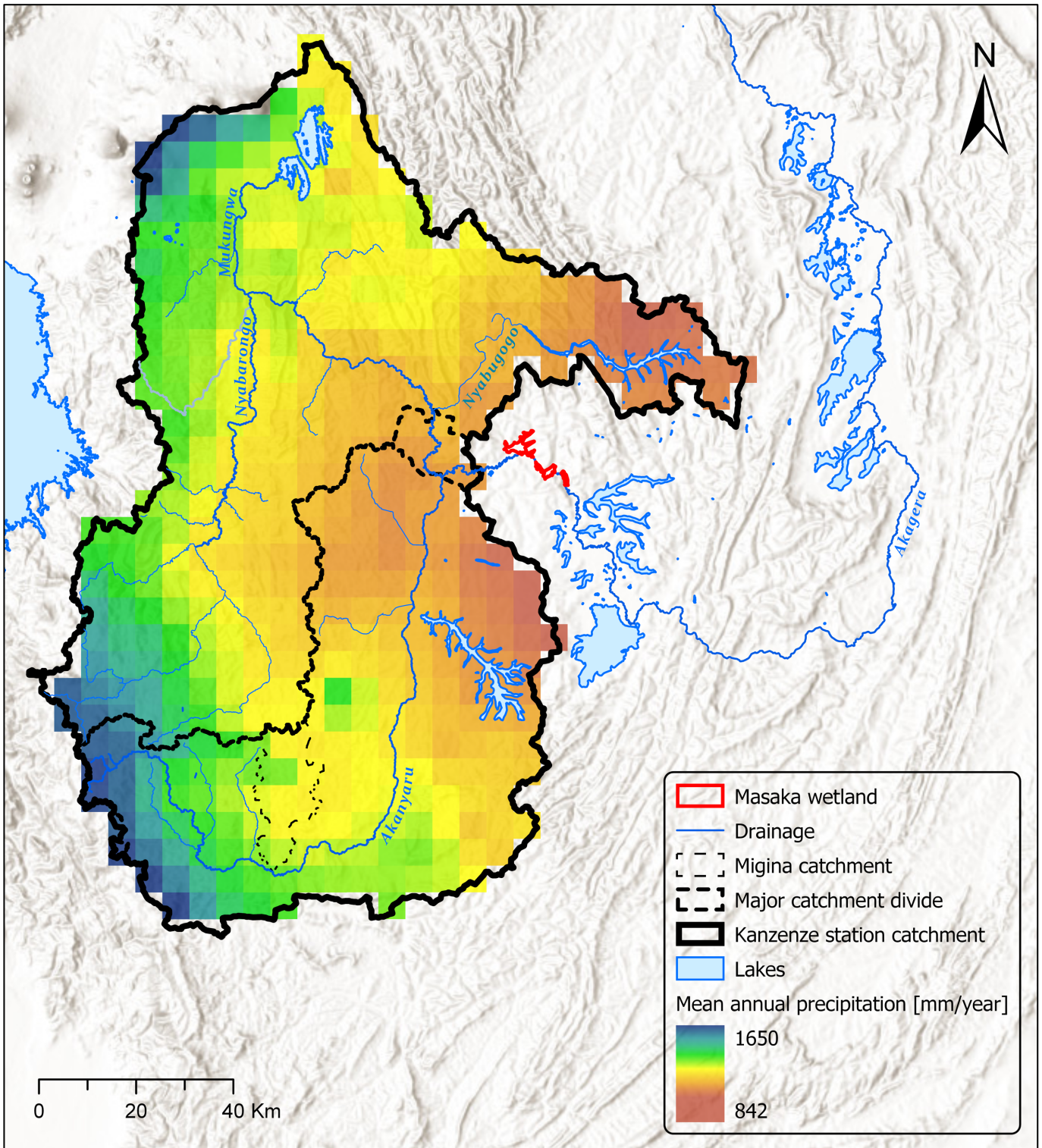


Figure 8: Mean annual precipitation (for the 1981~2017 period) in the Kanzenze station catchment. Major subcatchments correspond to the Ruliba station catchment (North) and Akanyaru river catchment (South). Data source: CHIRPS (Funk et al., 2015).

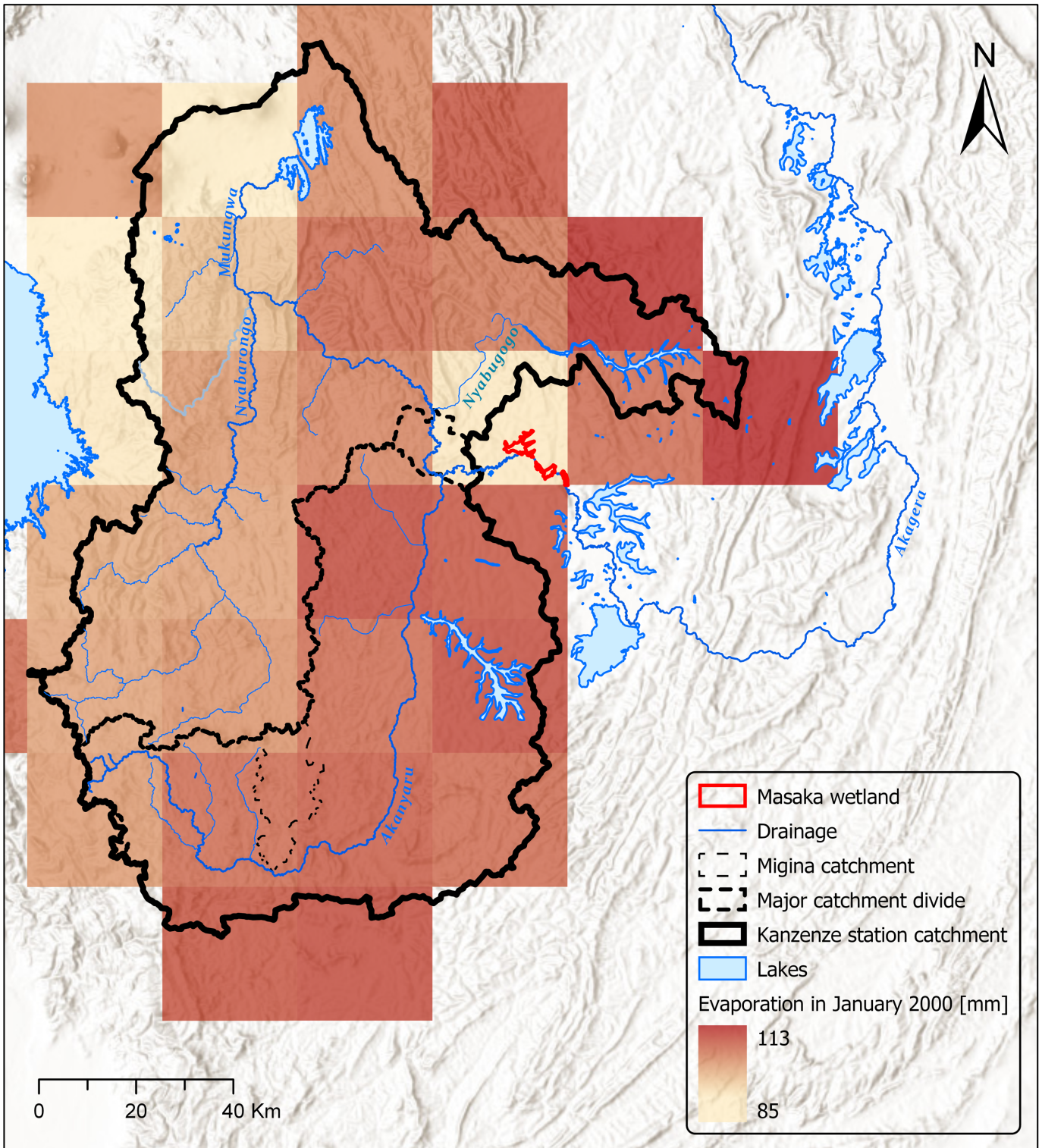


Figure 9: Estimated evaporation in January 2000 for grid cells overlapping with the Kanzenze station catchment. Major subcatchments correspond to the Ruliba station catchment (North) and Akanyaru river catchment (South). Data source: GLDAS (Rodell et al., 2004).

2.2.2 Soil types

This section provides an overview of the distribution of soil types in the country for the purpose of providing further contextualisation. Figure 10 illustrates the estimated distribution of root-zone soil textures in the Kanzenze station catchment as estimated by Leenaars et al. (2018). Fine-textured soils occur over most of the Akanyaru river catchment, as well as the Nyabugogo river catchment and in the headwaters of the Nyabarongo river. Higher fractions of sand and silt occur in the remainder of the catchment.

Acrisols and Ferrasols comprise a significant proportion of the Kanzenze station catchment, as illustrated in Figure 11. These soils are contained within a group known as “red earth” soils, which consists of highly weathered soils common in tropical and subtropical areas with high rainfall and temperature (Yu, 1997).

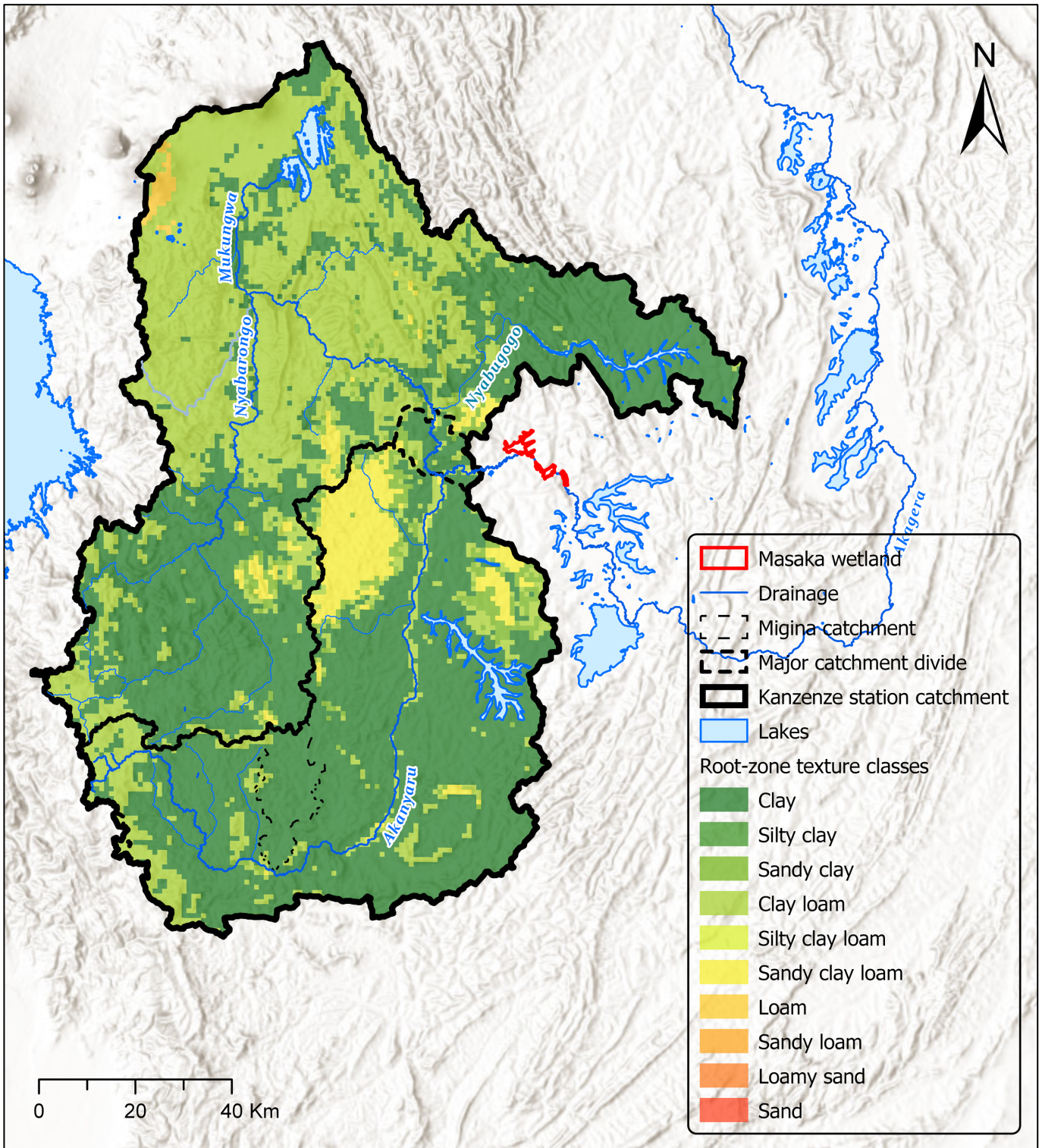


Figure 10: Root-zone soil texture in the Kanzenze station catchment. Major subcatchments correspond to the Ruliba station catchment (North) and Akanyaru river catchment (South). Shown for the purpose of contextualisation only. Data source: Leenaars et al. (2018).

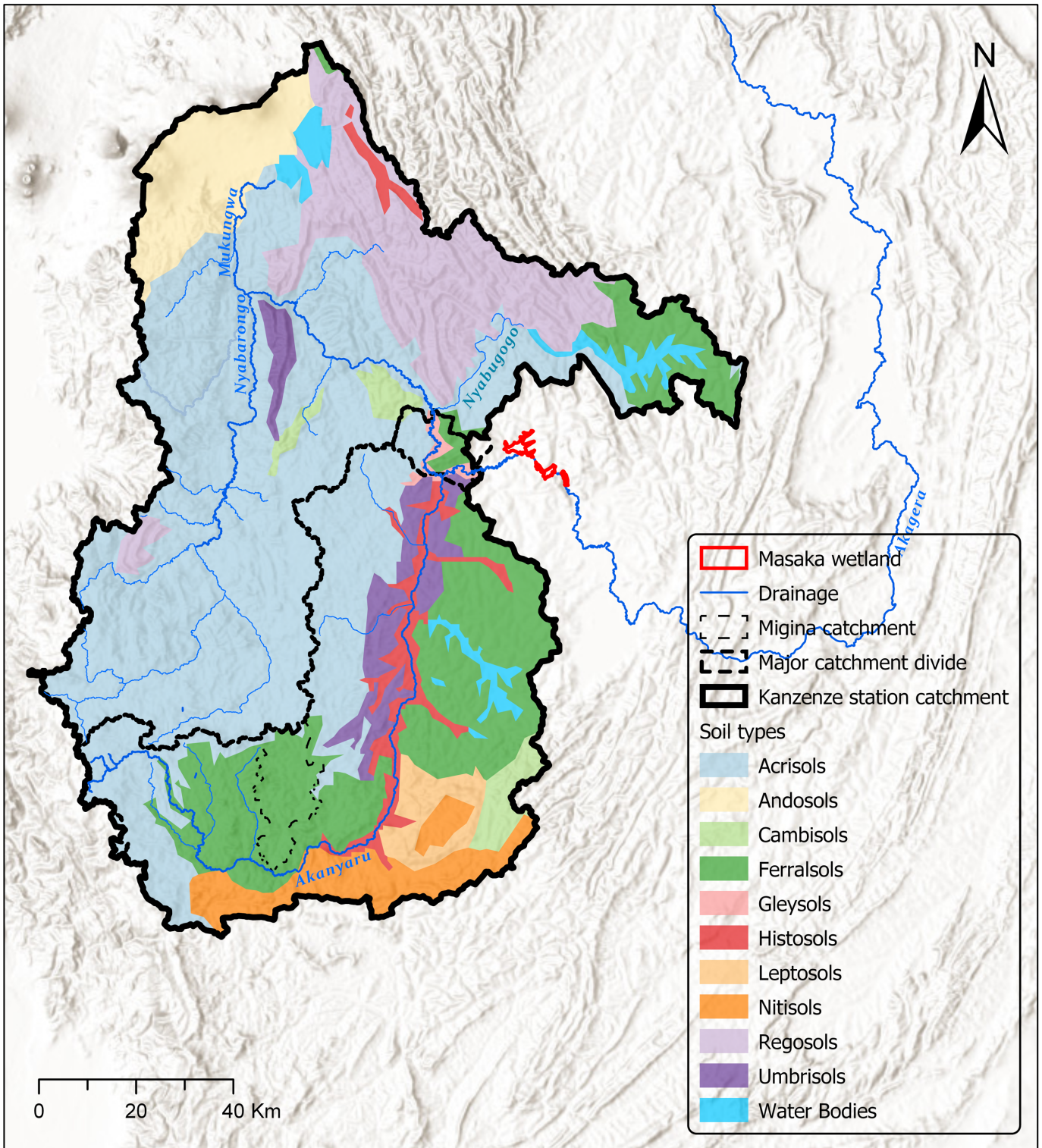


Figure 11: Soil types in the Kanzenze station catchment. Major subcatchments correspond to the Ruliba station catchment (North) and Akanyaru river catchment (South). Shown for the purpose of contextualisation only. Data source: JRC/ESDAC (Panagos et al., 2012, Dewitte et al., 2013).

2.2.3 Land cover

Land cover in the Kanzenze catchment follows the general pattern of Rwanda, being dominated by agriculture and grasslands. Figure 12 illustrates the main land cover types adopted in the context of the RIWSP, which were based on data from Mayaux et al. (2003).

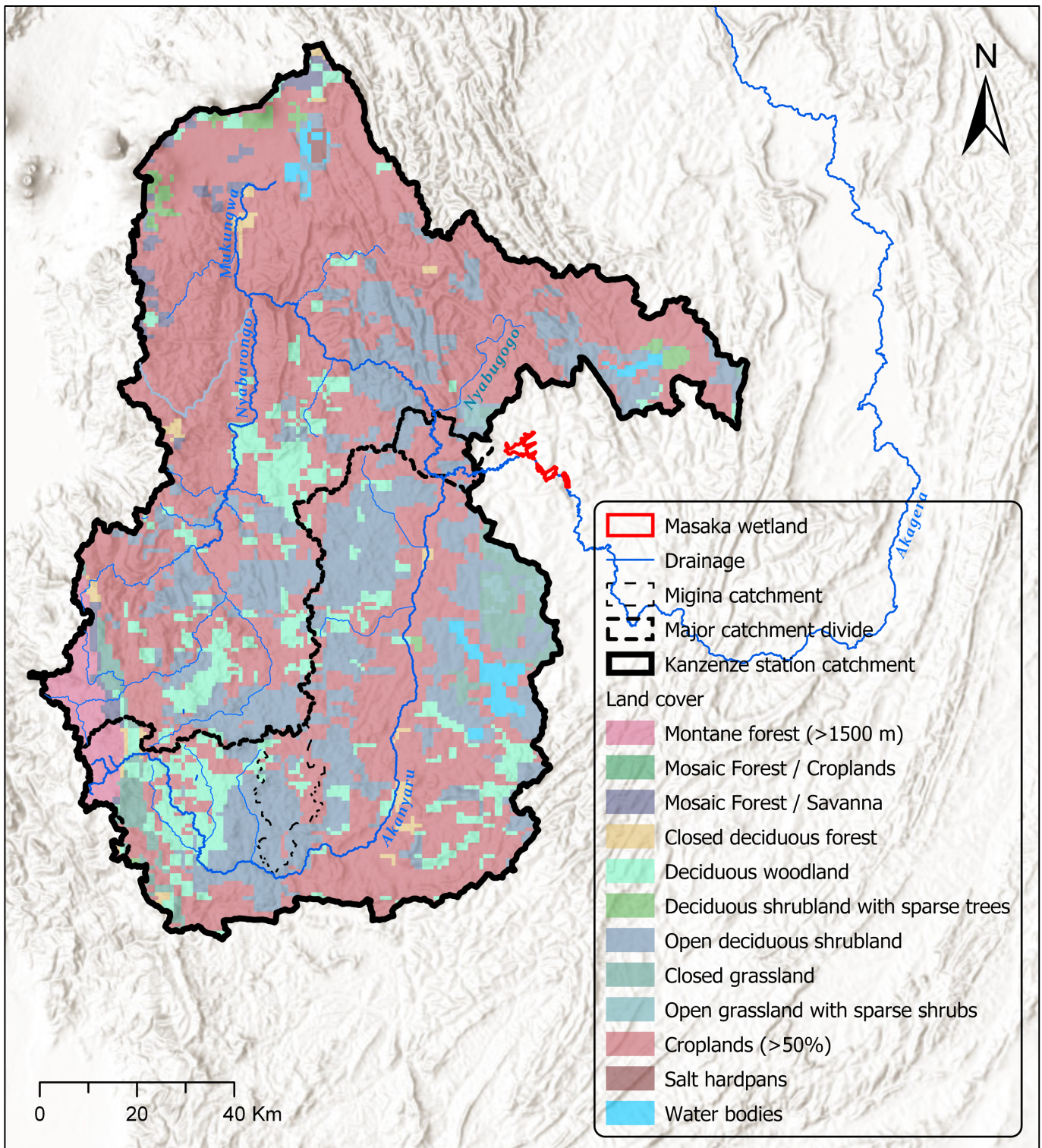


Figure 12: Land cover in the Kanzenze station catchment. Major subcatchments correspond to the Ruliba station catchment (North) and Akanyaru river catchment (South). Data source: Hydroscape (RIWSP, 2012e).

Figure 13 illustrates the mean land cover percentage of the Kanzenze station catchment by selected land use types according to reclassification performed by Pandey (2014) on the same data, as well as the values for the Ruliba station subcatchment and the incremental catchment between the Kanzenze station and the Ruliba station, 70% of which consists of the Akanyaru river catchment.

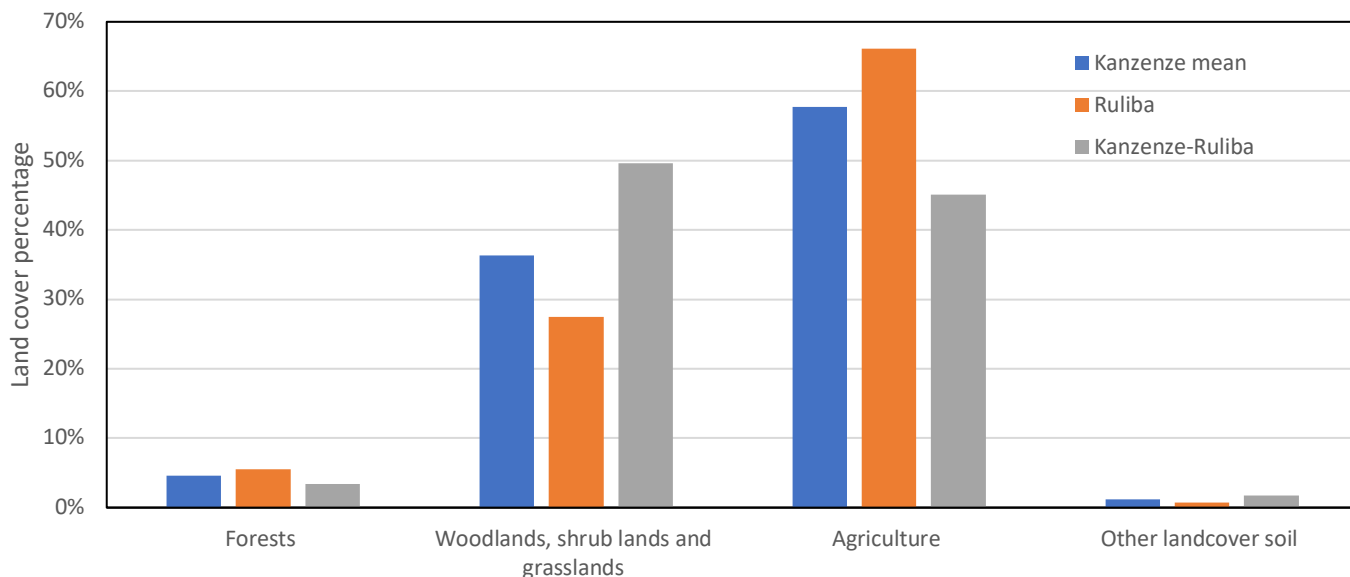


Figure 13: Land cover in the main subcatchments adopted in this study. Adapted from Pandey (2014).

It has been estimated that between 1990 and 2016, the areas of forest and grassland cover in Rwanda have decreased by 64.5% and 32.1%, respectively, while cropland and built-up areas have increased by 135.3% and 304.3% (Karamage et al., 2017). According to the same study, this factor has been estimated to result in a mean increase in annual runoff depth of 2.33 mm.year⁻¹ (0.38%) across the country, with some districts with high deforestation having experienced increases above 3.8 mm.year⁻¹. On a long-term basis, this effect has been dominant over possible shifts in precipitation (Karamage et al., 2017). On a larger scale, reduced vegetation cover has been reported to have led to increased runoff and lower water retention in subcatchments of the Akagera river (LTS, 2012a).

At the same time, Munyaneza (2014) identified a decreasing trend in mean discharge at the Kanzenze station during the Itumba period³. Change points were identified mostly in the 1980s and 1990s, which coincides with a period of intensification of irrigated agriculture and urbanisation (Munyaneza, 2014). However, it was also observed that political events in this period might have significantly compromised the quality of the collected data (Munyaneza, 2014).

A change in land use with particular implications for discharge regimes in Rwanda consists of the suppression of riverine wetlands. Rwanda contains 860 marshlands covering 278,536 ha – over 10% of the country’s territory. However, as of 2010, 53% of marshland areas in Rwanda were under cropping and an additional 6% was fallow agricultural area (REMA, 2015). Wetlands perform a significant role in catchment hydrology – as described in the next section, and hence their suppression may cause considerable impacts.

³ Mann-Kendall test at 5% significance level

2.2.4 Hydrology

As illustrated in Figure 6, the Kanzenze station catchment contains two major subcatchments: those of the Ruliba station (in this report also referred to as the Nyabarongo river catchment) and of the Akanyaru river. The Nyabarongo river catchment comprises an area of approximately 8.550 km² (RIWSP, 2012e) and contains the most significant regulated water bodies in the Kanzenze catchment (Lake Ruhondo, Lake Burera, Nyabarongo I reservoir). However, while lakes Burera and Ruhondo are deeper than 50 m (MINAGRI, 2010), their variation in elevation is generally restricted to a few meters (EDCL, 2018).

The Akanyaru river basin comprises 5.334 km², and its major natural water bodies consist of Lake Cyohoha South and Lake Cyohoha North. The majority of the length of the Akanyaru river is surrounded by wetlands (RIWSP, 2012b), which may provide significant temporary storage during the wet seasons.

Seasonal flooding in Rwanda is associated with the **fast routing of rainfall generated on hillslopes** to receiving streams and lakes, particularly between March and May (MINAGRI, 2010, Munyaneza et al., 2011a). Although there is a general lack of data concerning the characterisation and monitoring of groundwater in Rwanda (MINAGRI, 2010), **groundwater recharge** is also described to occur predominantly or exclusively during the wet seasons, with declining storages in the dry summer months. This has been described on the scale of a 147 km² catchment (Migina) based on observations by Munyaneza (2014) and on a larger scale based on seasonal catchment water balance by Pandey (2014).

In spite of the relatively fine soil textures, all the subcatchments within the Kanzenze catchment have been described as having “relatively high **infiltration** rates” (MINIRENA and RNRA, 2015). This has also been the conclusion based on field observations in the small-scale Migina catchment (Van den Berg and Bolt, 2010), where **infiltration excess overland flow** was reported not to play a major role. The same study has inferred that discharges are dominated by **baseflow** – also observed on a larger scale for the Akagera river basin (Sutcliffe and Parks, 1999), and that preferential flow paths exist in the valleys as a result of soil layers with remarkably different conductivities.

As mentioned in section 2.2.3, wetlands cover a relatively large areal extent in Rwanda, and more generally in the Akagera river basin, and have been reported to have a significant impact on catchment-scale hydrological processes. They are reported to enhance aquifer recharge and act as reservoirs on a catchment scale, attenuating peak discharges and maintaining baseflows in dry periods (MINAGRI, 2010), as well as retaining nutrients and sediments and levelling out temporal variations in their concentrations, which has been observed for instance in the Ngonzo wetland in Tanzania (LTS, 2012b). On a larger scale, the timing of discharges of the Akagera river has been reported to be delayed in comparison to other tributaries of Lake Victoria due to temporary storage in the extensive marshlands and lakes across the basin (Sutcliffe and Parks, 1999).

2.2.5 Erosion

Accelerated erosion rates are widely recognised as a significant issue in Rwanda. It has been estimated that 49% of the area of the Akagera river basin located within Rwanda – about 1 million hectares – faces a high erosion risk, and a further 28% faces moderate erosion risk (LTS, 2012a). A key driver of this threat consists of the high slopes in several regions of the country, as illustrated in Figure 14 – 70% of the country’s area consists of slopes above 10% (Abimbola et al., 2017). This factor has been compounded by agriculture and mining activities and associated soil exposure, in combination with intense rainfall events (MINIRENA and RNRA, 2015), and has led to increased turbidity in water bodies in the Nyabarongo river catchment (Nhapi et al., 2011).

High sediment concentrations can also be linked to accelerated changes in river cross-section by means of deposition or scour (due to increased stream power). Active bank erosion and meandering behaviour of the Nyabarongo river in the vicinities of the Masaka wetland has been previously identified (RHDHV, 2017b) and is depicted in Figure 15. The relevance of this factor to the current study is discussed in section 3.1. This process is also linked to flooding, as sedimentation has been regarded as a trigger for the majority of floods in the country (WECA Ltd., 2014) due to reductions in the conveyance capacity of streams (LTS, 2012a). There is also wide recognition of the risk of accelerated depletion of the live storage capacity in

existing and planned reservoirs in Rwanda due to sediment accumulation (MINIRENA and RNRA, 2015, NCEA, 2015, Mushuti and Narcisse, 2018, EDCL, 2016).

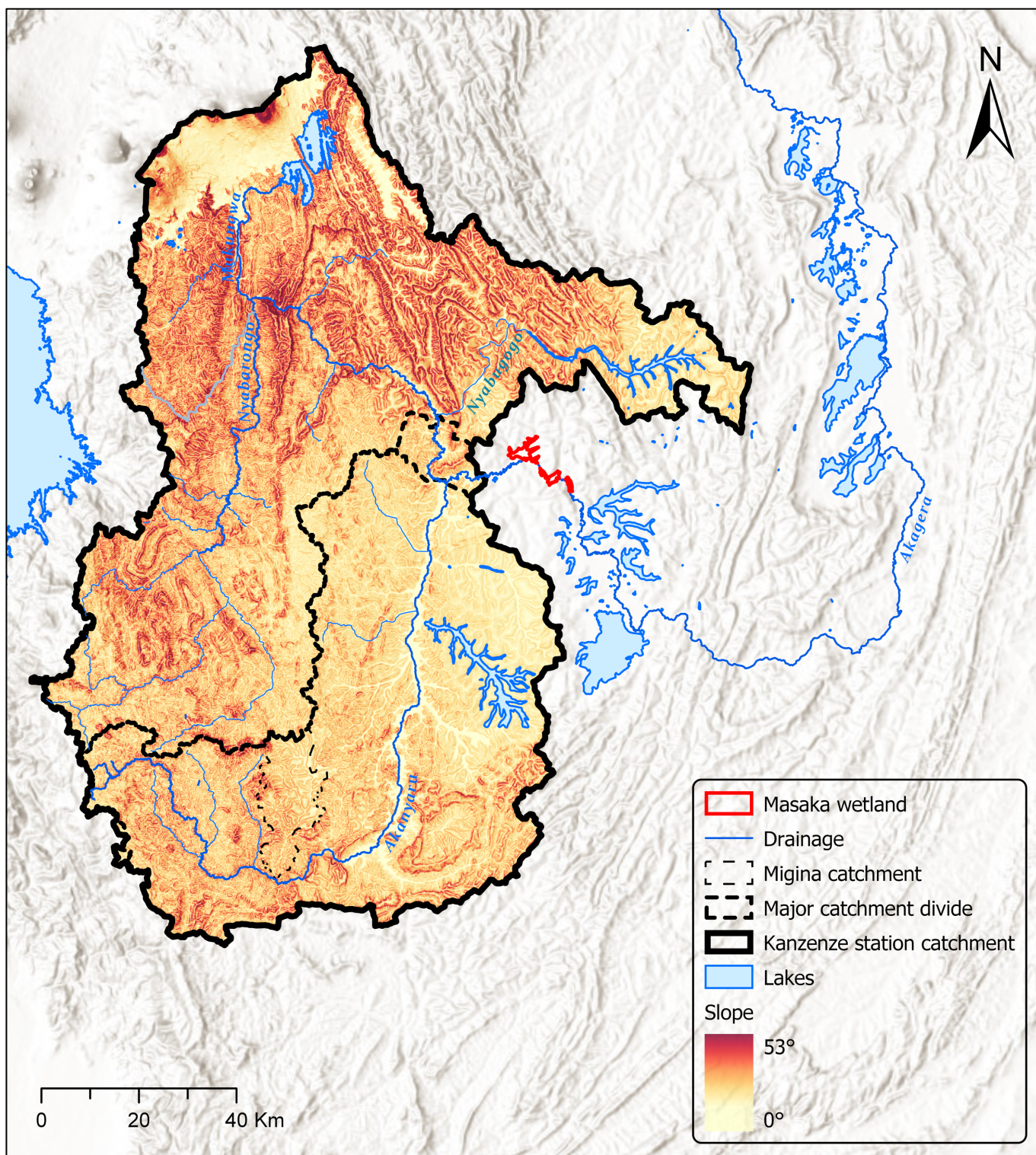


Figure 14: Slope in the Kanzenze station catchment: the occurrence of high slopes is commonly associated with accelerated erosion in Rwanda. Major subcatchments correspond to the Ruliba station catchment (North) and Akanyaru river catchment (South). Derived from HydroSHEDS hydrologically conditioned elevation data (Lehner et al., 2011).



Figure 15: High turbidity and active bank erosion in the vicinities of the Masaka wetland. From RHDHV (2017b).

2.2.6 Reservoir development

Increasing the availability and stability energy supply in Rwanda is seen as an essential factor for the country's economic growth and social development as the country aims to achieve universal access to electricity by 2024 with an installed capacity of 512 MW (REMA, 2015). Achieving this goal will require a considerable expansion is foreseen for the coming decades (REG, 2018, RDB, 2018). Locally available renewable sources, such as hydropower, are attributed particular importance due to their relatively low cost and the additional advantage of reducing vulnerability to oscillation in oil prices (MININFRA et al., 2012, AfDB, 2013) and imports from neighbouring countries. Additionally, hydropower is regarded as a key element to reduce dependence on wood for energy and hence halt deforestation (GoR and Water4Growth, 2017).

This scenario has also led to the commissioning of several – mostly small-scale – hydropower plants in recent years. Between 2009 and 2016, the hydropower-based energy availability in Rwanda nearly quadrupled, reaching 99 MW (Endev and EDCL, 2016). In 2016, 40 private additional projects (totalling 85 MW) were at different planning and implementation stages throughout the country. The installed energy generation capacity is currently 210.9 MW (RDB, 2018), with hydropower corresponding to 48% of this figure (Mushuti and Narcisse, 2018). However, most of the major planned developments are located outside the area of interest of this study, such as the hydropower plants Regional Rusumo Falls (Rwanda, Burundi and Tanzania) and Ruzizi III (Rwanda, Burundi and DRC) as well as the multipurpose dams Muvumba and Warufu.

While the majority of dams in Rwanda are intended for hydropower generation and irrigation purposes (ICOLD, 2018), the National Water Resources Plan (MINIRENA and RNRA, 2015) also recommends that “*strategic reserves in the Mukungwa basin and in the Upper Nyabarongo should be developed and kept*” with the goal of increasing resilience to water scarcity. Measures such as multipurpose dams have also been proposed as coping strategies in the context of increasing uncertainty in precipitation patterns and reduced wetland cover and associated services (Kabalisa, 2016).

The Shyorongi dam and the Nyabarongo II development

Among the several existing and proposed reservoir developments in Rwanda, the current study has focussed on the Shyorongi dam. This choice has been motivated by the fact that its position and estimated storage capacity lead to the inference that it will have the greatest potential effect on flooding in the Masaka wetland. The Shyorongi Dam will be located approximately 50 km upstream of the Masaka wetland, as illustrated in Figure 6, and is a part of the Nyabarongo II Multipurpose Development Project (NMDP), which will also include irrigation and water treatment infrastructure. The information on this project, as presented and implemented on this study, derives mostly from the hydrological feasibility study (EDCL, 2016) that has been kindly provided on request by the Rwandan Energy Development Corporation Limited (EDCL) for this research⁴. The purposes envisaged for the NMDP are:

- a. Hydropower generation;
- b. Drinking water supply for areas of Kigali and Bugesera;
- c. Downstream flood prevention;
- d. Marshland reclamation;
- e. Irrigation.

The NMDP is expected to mitigate the inherent hazard associated with downstream flooding (MININFRA, 2018) and enable the cultivation of a substantial amount of land (ICOLD, 2018). The potential of the Shyorongi dam site for hydropower generation was first identified in a study by the Korea International Cooperation Agency (KOICA, 2008). Its installed capacity is expected to be 43.5 MW (MININFRA, 2018), and its construction is planned for the period 2019-2024 (MININFRA, 2018).

However, the multiple purposes of the Nyabarongo II development may translate into competing operation objectives for the Shyorongi reservoir. For example, irrigation and drinking water supply generally entails that reservoirs be kept at the maximum possible capacity (storage reservoirs), while flood mitigation requires that lower storage volumes be maintained in order to maximize available storage capacity incoming flood waves (control reservoirs), as discussed in section 1.1.2. This has motivated the choice of testing operational scenarios with different goals in this study.

2.3 System conceptualisation

Considering the goal of estimating discharges at the Masaka wetland under the operation of the Shyorongi reservoir and the configuration of rivers and gauging stations in Rwanda, a conceptual representation of the system was adopted for the simulation exercise, as illustrated in Figure 16 and Figure 17. The Nyabarongo river at the Masaka wetland receives contributions from two major sources: the Akanyaru river and the Ruliba station catchment. The Shyorongi dam will be located along the Nyabarongo river and will regulate most of its catchment, as shown in Figure 6. However, the section of the Nyabarongo river between the dam and the Masaka wetland also receives significant contributions. These consist mostly of the discharges from the Nyabugogo river, whose catchment comprises approximately 89% of this area. Therefore, in this study this incremental area is referred to, in a simplified manner, as the Nyabugogo river catchment. The Nemba hydrometric station is located near the outlet of the Nyabugogo river and could in principle be used to estimate discharges from this specific area. However, a shifting control at this cross-section has rendered its rating curve and associated discharge estimates unusable (RIWSP, 2012c).

The Ruliba station is located a relatively short distance upstream from the outlet of the Akanyaru river. However, the section of the Nyabarongo river between these two points is characterised by low slopes and surrounded by floodplains of considerable dimensions. This factor is hypothesized to explain a lag between hydrograph peaks observed in the Ruliba and the Kanzenze station, to be further detailed in section 3.4.2.

⁴ The information was provided in the condition of confidentiality and hence key figures have been omitted from this report, without prejudice to interpretation.

The Akanyaru river has a lower data availability; the only station with reliable gauge height time series and rating curve being Butare-Ngozi Road (70010) which, however, drains a small percentage of the catchment. The Gihinga station (265701) is located relatively close to the Akanyaru river outlet and has a long record of gauge heights, but no rating curve points and hence no discharge records exist for this location.

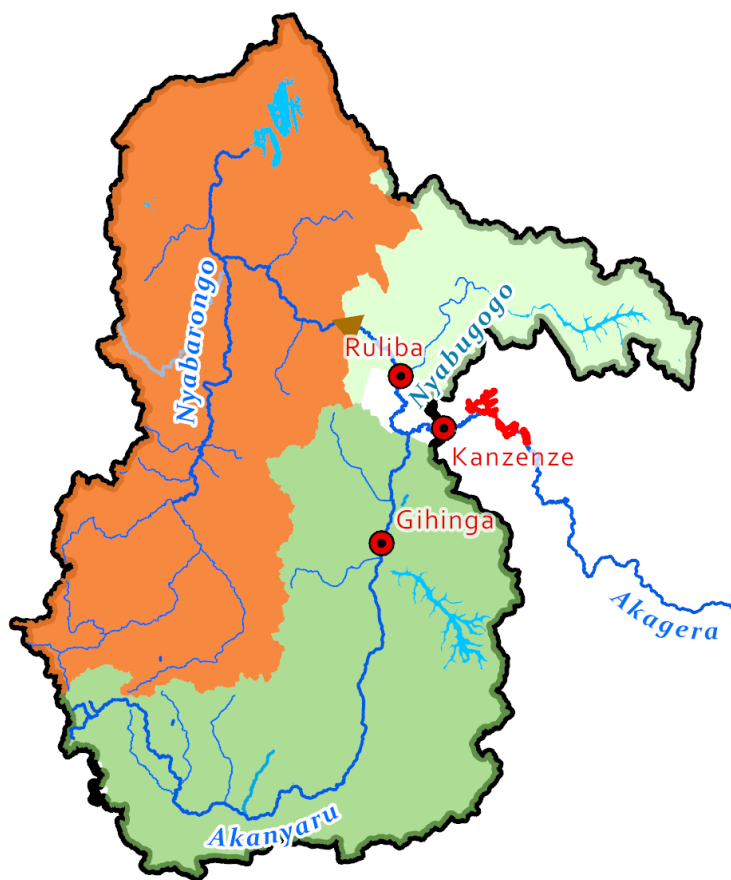


Figure 16: Key subcatchment division adopted in the current study.

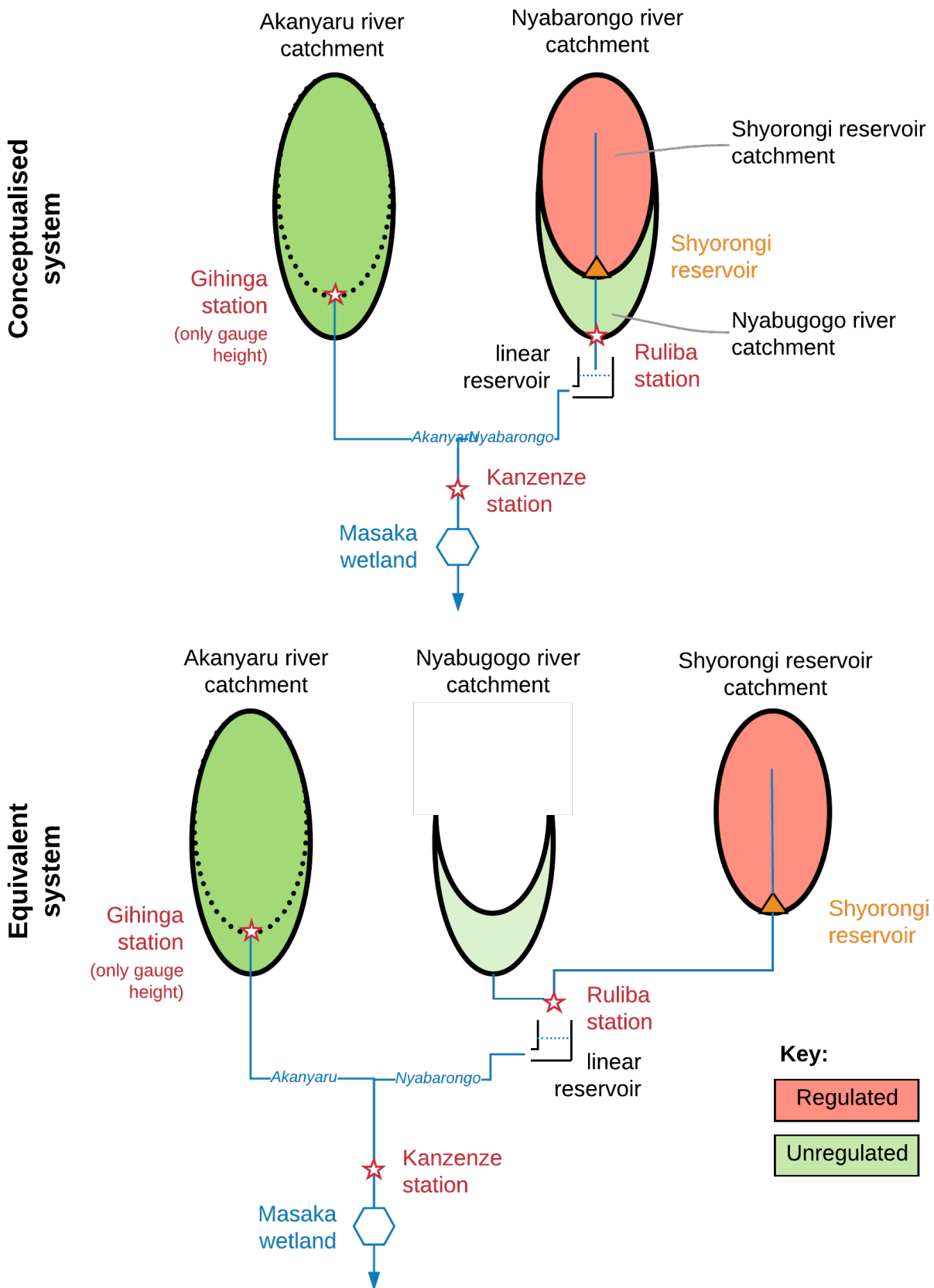


Figure 17: System conceptualisation implemented for the estimation of discharges at the Kanzenze station based on three contributing areas.

3 Data

The main data requirements of current study comprised:

- Reference discharge data for the calibration of the hydrological models, described in section 3.1
- Precipitation and potential evaporation data for the calibration of rainfall-runoff models and generation of discharge time series, described in section 3.2
- Actual evapotranspiration estimates for the validation of observed discharges against long-term catchment water balance, described in section 3.2
- Reservoir characteristics for the simulation of the operation of the Shyorongi reservoir, described in section 3.3

Sources for the aforementioned data known to be available for Rwanda are summarised in Table 3, where the sources selected for this study are indicated.

Table 3: Overview of available time series data sources.

Data type	Selected	Source	Spatial resolution	Temporal resolution	Temporal availability	Remarks
Discharge	✓	RIWSP (2012e)	N/A	Daily	Varies per station; see section 3.1	Estimates generated after thorough processing to discard unreliable time series and rating curves
		GRDC (2018)	N/A	Monthly	Varies per station	Only Kanzenze and Ruliba stations
Gauge heights + rating curve points	✓ (Gihinga station only)	Rwanda Water Portal (RWFA, 2018)	N/A	Daily; hourly ¹	Varies per station	Provided “as-is”; includes gaps; undocumented datum shifts; trends
Pan evaporation		Meteo Rwanda	Point	Monthly	Varies per station	Not available
Potential evaporation	✓	GLDAS (Rodell et al., 2004)	0.25°	3-hourly	01/01/1948 – near present ²	
Actual evapotranspiration	✓					
Precipitation	✓	CHIRPS (Funk et al., 2015)	0.05°	Daily	01/01/1981 – 31/08/2018	
		Meteo Rwanda	Point	Varies per station	Varies per station	Not available

1 – Selected stations have recently been fitted with telemetry transmission of gauge heights

2 – Considering versions 2.0 and 2.1

3.1 Hydrometric data

Rwanda has had a relatively dense hydrometric and meteorological network in the past. The largest amount of records dates to the period between 1960's and the end of the 1980's, and before 1994 nearly 200 meteorological stations had been installed in Rwanda (MINAGRI, 2010). However, the events of 1994 have resulted on the loss of a considerable part of the hydrometric and meteorological network and historical climatic and hydrometric records, only part of which has been restored (MINAGRI, 2010, Munyaneza, 2014). Hydrometric observations were largely discontinued in the early 2000's: as of 2010 only 6 climatic stations and 4 stage gauging stations were operational (MINAGRI, 2010). It is recognised that data concerning water resources in Rwanda is often unreliable or fragmented across institutions, requiring extensive quality control (MINAGRI, 2010, GoR and Water4Growth, 2017). This scenario has been linked to bureaucracy and insufficient budgets and associated insufficient maintenance, leading to gaps and errors in data availability (RIWSP, 2012b).

However, data collection has regained momentum in recent years: as of 2016, 24 meteorological stations and 11 rain gauges were operational in Rwanda, as well as 36 hydrometric stations within the section of the country in the Nile basin (NBI, 2016). The stations for which data was adopted in the current study are summarised in Table 4.

Table 4: Hydrometric stations selected for the study.

Name	Code	Catchment area [km ²]	Observations
Kanzenze	259501	13.930	
Ruliba	270001	8.336	Also referred to as Kigali station
Gihinga	265701	4.248	No rating curve available

A particularly comprehensive qualitative and quantitative assessment of the hydrometric data availability of Rwanda was carried out in the context of the Rwanda Integrated Water Security Program (RIWSP)⁵. This included an analysis of the institutions involved in the collection and storage of such data (RIWSP, 2012b), descriptions of the general state of each discharge station (RIWSP, 2012d), further analysis and derivation of rating curves for the stations where data availability and reliability allowed so (RIWSP, 2012a) and the subsequent estimation of discharge time series for the stations and periods in which data was assumed to be sufficiently reliable (RIWSP, 2012c). The programme also involved the generation of a Geographical Information System (GIS) with an emphasis on water resources management: the Hydroscape (RIWSP, 2012e). This work was complemented by an assessment of the hydrological data collection and storage system of Rwanda as of 2014 (WECA Ltd., 2014) which included site visits to each station.

A particular challenge concerning hydrometric records in Rwanda concerns the use rating curves. To the best of the author's knowledge, no official rating curves have been adopted in the country. The Rwanda Water Portal (RWFA, 2018) – the country's main source of hydrometric information – provides historical measurements of gauge height and corresponding discharges for selected stations. However, different sources (KOICA, 2008, RIWSP, 2012d) have derived different rating curve coefficients based on these values, mostly based on measurements taken before the 1990's (Munyaneza, 2014). The need for rating curves based on updated measurements was stressed in RIWSP (2012c), and WECA Ltd. (2014) reported ongoing efforts with this goal.

Figure 18 illustrates the gauge height time series and rating curve points available at the Rwanda Water Portal for the Ruliba and Kanzenze stations as of the elaboration of this study. It is indeed visible that new field measurements of water depth and discharge became available in 2014 and in 2017. However, it was also reported that considerable error may have been introduced due to limitations in the equipment and

⁵ [http://dpanther.fiu.edu/dpService/glowsProjectServices/project/RIWSP%20\(Rwanda\)](http://dpanther.fiu.edu/dpService/glowsProjectServices/project/RIWSP%20(Rwanda))

methods implemented to derive corresponding discharges (chiefly ADCPs and current meters/propellers) (WECA Ltd., 2014). Additionally, the amount of measurements taken since 2012 (8 for the each station) is still below the minimum amount of 12 recommended by the WMO (2010a).

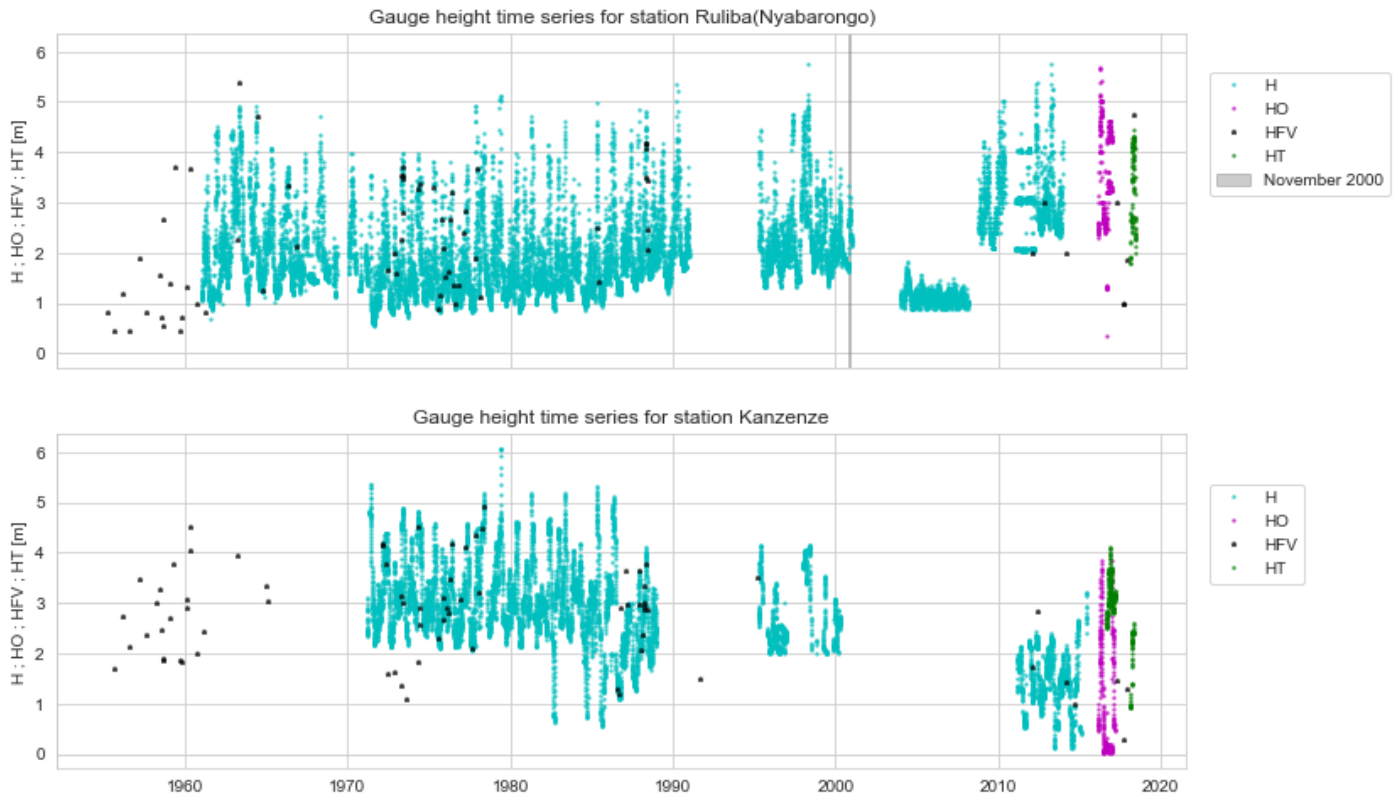


Figure 18: Raw gauge height data available at the Rwanda Water Portal (RWFA, 2018) for the stations Ruliba and Kanzenze as of August 2018. The terminology adopted in this source is: *H*: “historical” data; *HO*: “observers” data; *HFV*: “field visit” data (i.e. rating curve points); *HT*: “telemetry” data. A period with reported extreme floods (November 2000) is highlighted.

In certain locations and under certain conditions (e.g. floods), sediment may account for a significant percentage of the discharge, and result in scouring in the cross-section (WMO, 2010b). Intense sedimentation has also been reported for several stations (WECA Ltd., 2014), which may be linked to the accelerated erosion rates in the country described in section 2.2. Indeed, the accelerated morphodynamics and anthropic interventions in the area have been visible in field investigations in the Nyabarongo river in the vicinities of the Masaka wetland, where visible bank erosion has been reported (RHDHV, 2017b). Such changes may trigger the need for adjusting the datum of a gauging station (WMO, 2010b), or may be large to a point where the cross-section has totally different characteristics and therefore a new rating curve is required (WMO, 2010a).

A further observation derived from Figure 18 concerns the existence of apparent (undocumented) shifts in the datum adopted for gauge height records. For example, starting in 2011, a shift in recorded gauge height values for the Kanzenze station in the order of 1.0 m has been observed. The fact that it persists over several years is typical of a datum error (WMO, 2010a), which has been identified in RIWSP (2012a) as the most likely cause for the shift in readings. Both cross-section changes and datum shifts are likely causes for the visible changes in the rating curve of the Kanzenze station, as shown in Figure 20.

This factor, compounded with the aforementioned lack of recent rating curve observations in recent periods, has motivated the choice of restricting the adopted hydrometric data to the discharge time series product generated in the context of RIWSP, which is illustrated in Figure 19. Although estimates of discharges from gauge height readings after 1990 were generated, the applicability of rating curves based on points recorded over 20 years ago has been questioned (RIWSP, 2012c). This has led to the decision to restrict data use to the period where reliability is highest – the period of most frequent collection of rating curve

points. At the same time, limitations in the temporal availability of precipitation data (see Table 3) have also limited the selection of corresponding discharge time series. This resulted in the period of 01/02/1981 to 30/06/1986 having been selected as reference discharges for the model calibration described in section 4.1.1.

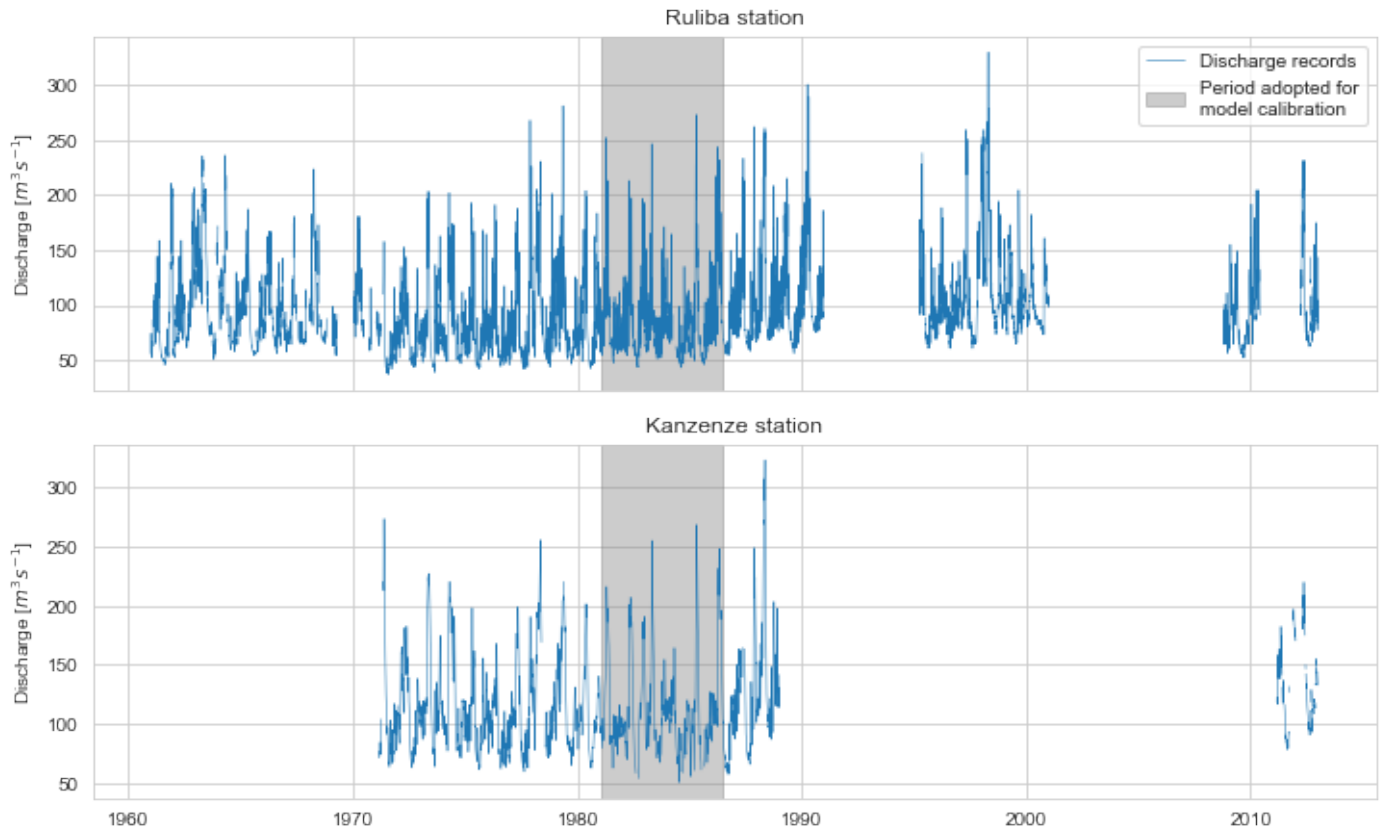


Figure 19: Available discharge time series for Kanzenze and Ruliba stations, estimated by the RIWSP. The shaded area corresponds to the period adopted for calibration of the rainfall-runoff models of the Ruliba station and Akanyaru river catchments.

Preliminary investigations have also indicated that the Kanzenze bridge (located at the location of the Kanzenze station) acts as a downstream control of discharge, at least during the wet season (RHDHV, 2017b). Therefore, the area immediately upstream of the bridge may act as a buffer and the magnitude of discharges into the Masaka wetland may be smaller than the discharges simulated by the model. This can be expected to result in smaller flooding frequencies in the Masaka wetland than would otherwise take place if the bridge control was not in place. Conversely, higher flooding frequencies can be expected in the area immediately upstream of the bridge.

Additionally, during extreme events, overbank conveyance may consist of a significant part of the total discharge (WMO, 2010b). Discharge measurements during flood conditions are particularly important (WMO, 2010a); however it has been recognised that local conditions (e.g. dense papyrus vegetation in the floodplain) often make it virtually unfeasible for such measurements to be taken. Some stations were also reported to lack staff gauges visible in the high water periods, making readings are scarcer during floods (WECA Ltd., 2014), and it is known that considerable distortions may exist in the peak discharge records at the Kanzenze station (Water4Growth and MINIRENA, 2018).

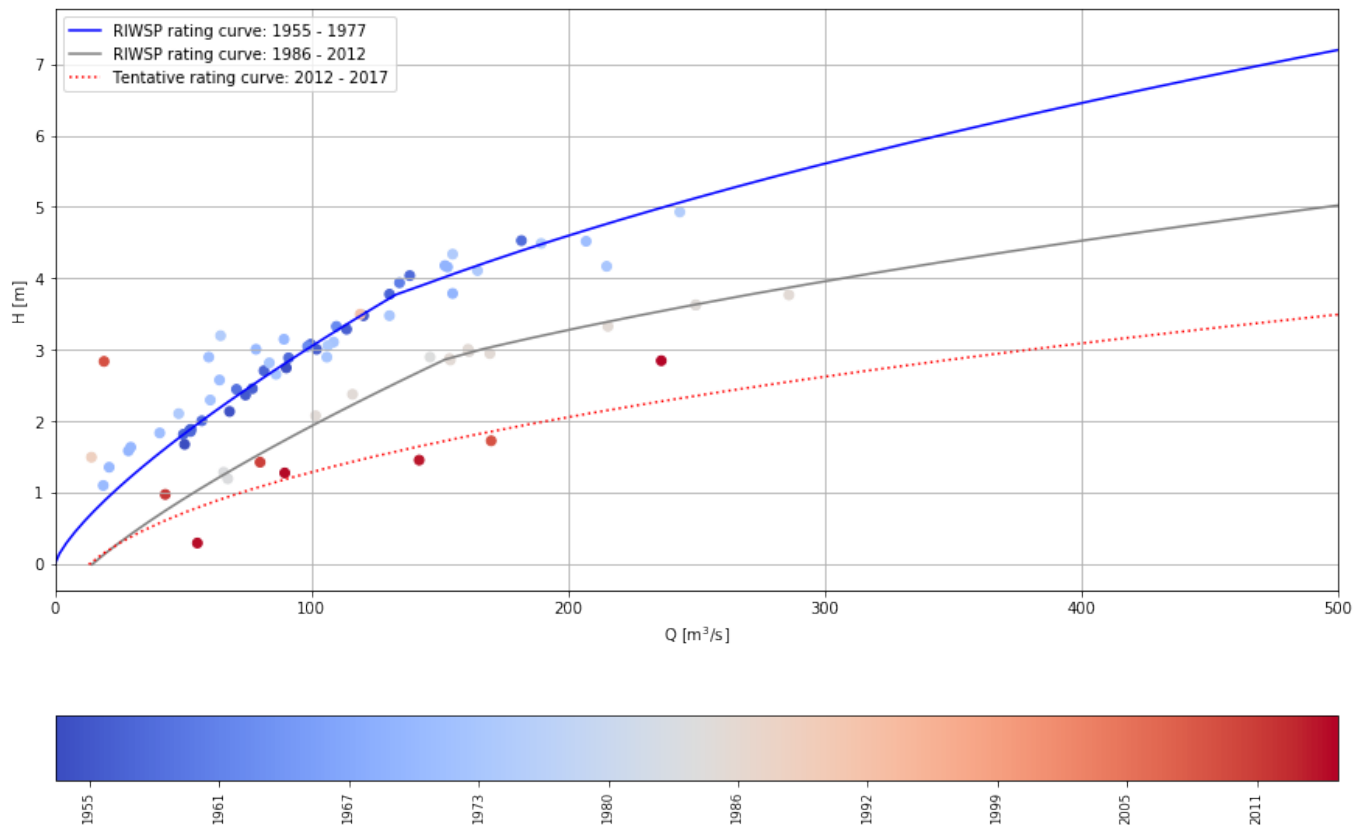


Figure 20: Available rating curve points and fitted rating curves for the Kanzenze station. The points consist of available “field visit” measurements of gauge height and corresponding discharge, coloured according to the year of collection. The lines for the periods 1955-1977 and 1986-2012 are based on coefficients adopted in RIWSP (2012d). A tentative rating curve based on post-2012 records was not employed but is plotted to illustrate the likely inadequacy of employing previous rating curves for the estimation of discharges from recent gauge height records.

While in flooding studies the main variable of interest consists of water levels, this study has restrained its focus on the estimation and analysis of discharges. This is justified by the fact that rating curves often have discontinuities at the gauge height corresponding to bankfull discharge – which has observed to be the case for the Kanzenze gauging station, for which two rating curve sections have been identified (RIWSP, 2012d). The effect of this factor is that a continuous frequency distribution of discharges may generate a discontinuous distribution of gauge heights, as illustrated in Figure 21, which adds complexity to describing it by means of a distribution function. A second consideration is that, as described above, the lack of rating curve points in recent years means that inferring water levels from discharges incurs in substantial uncertainty propagation. Finally, the complex hydraulic behaviour of the of the Masaka wetland and vicinities demands the application of a hydraulic model for the accurate estimation of water depths. The development of a hydraulic model was outside the scope of the current study, which was limited to estimating boundary conditions for such a model; i.e. upstream discharge time series.

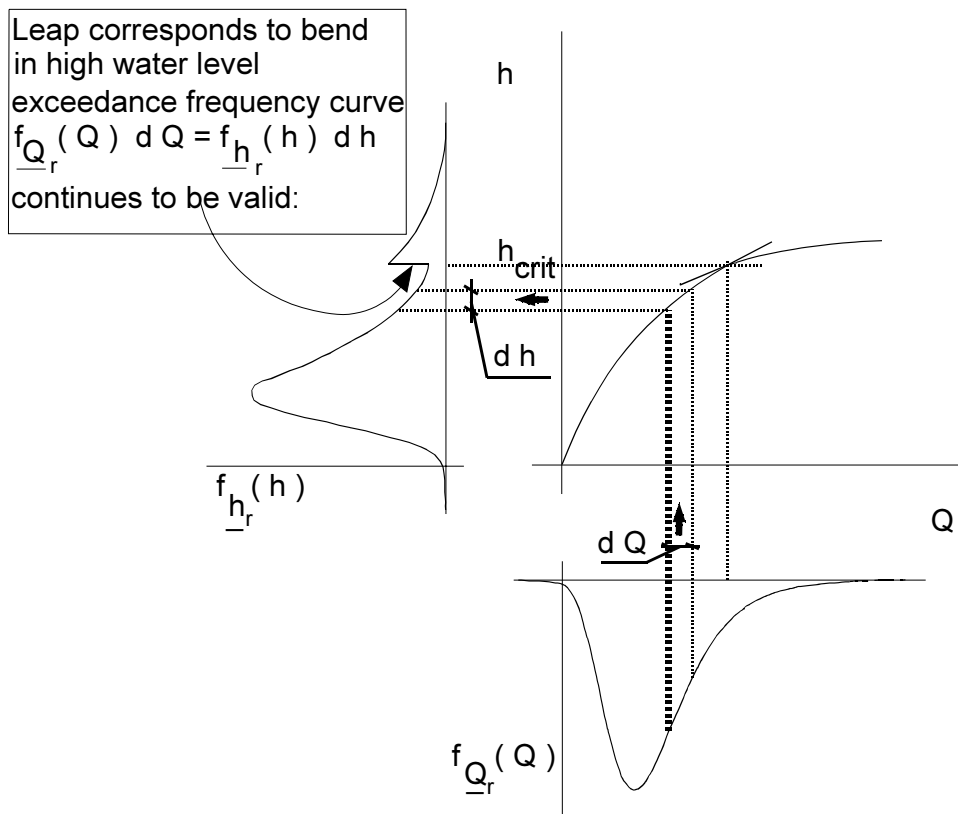


Figure 21: Discontinuity in rating curve reflected in gauge height distribution (Vrijling and Van Gelder, 2002). The plots correspond, in clockwise order from the top left, to the probability distribution of gauge heights, the rating curve and the probability distribution of discharges.

In order to provide an additional approximate source of validation for the gauge height time series available at the Rwanda Water Portal for the Kanzenze station at recent years, an attempt was made to establish a relationship between these records and flood magnitude in a reach of the Akagera river corresponding approximately to the Masaka wetland. Although the precise function relating these two variables is unknown, the relationship can be assumed to be monotonic – i.e. that higher water levels correspond to a greater flood magnitude. Flood magnitude records were retrieved from the Global Flood Detection System (GFDS) (Groeve et al., 2015), available from 2011. As illustrated in Figure 22, the expected monotonic relationship between the two variables was not verified. This could be traced to factors such as:

- a. Errors in the observed gauge height time series (e.g. datum shifts, reading errors);
- b. The limited capacity of the GFDS product to detect flooding in this particular area;
- c. Discrepancies between water levels observed in the Kanzenze station and in the downstream Masaka area due to the control of the Kanzenze bridge during high discharges, as mentioned above.

Considering factor a and the aforementioned uncertainties in the rating curve for recent years, this study has refrained from attempting to estimate discharges for recent years.

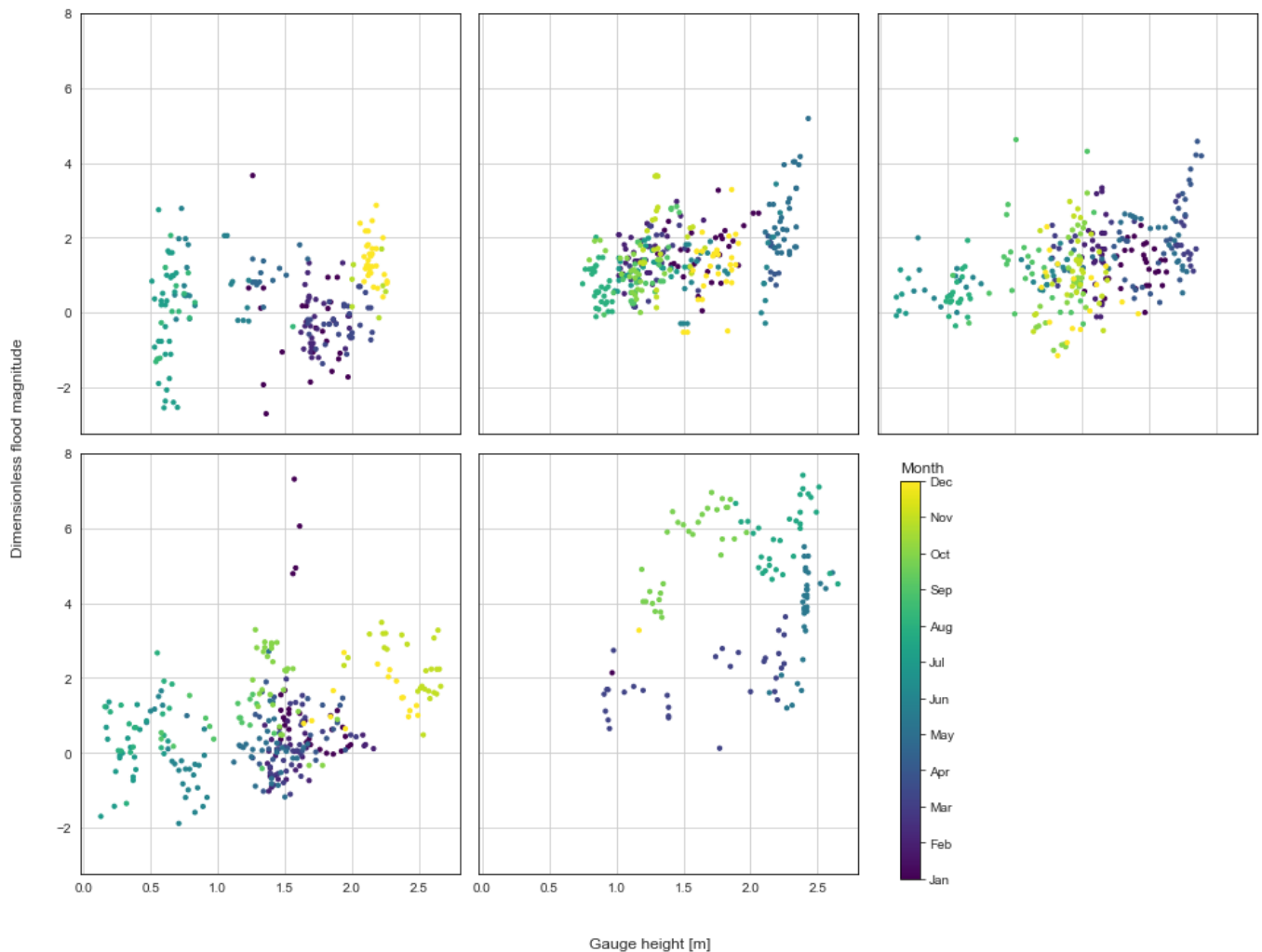


Figure 22: Gauge height observations at the Kanzenze station (horizontal axis) and estimated flood extent for the corresponding dates (vertical axis). Each plot corresponds to one year, and observations are color-coded by the month of the year in which they were taken.

3.2 Precipitation and potential evaporation

Precipitation and evaporation data collection in Rwanda currently complies with the standards set by the World Meteorological Organization (WMO) (WECA Ltd., 2014). However, similarly to hydrometric data, rainfall records are significantly scarcer for the period beginning in 1993, to an extent of having been neglected in previous studies (Muhire and Ahmed, 2014, Ilunga and Muhire, 2010). In addition to this factor, the temporal scale on which it is generally available (monthly in the case of pan evaporation) and difficulties in access have led recent studies (e.g. FutureWater and eLeaf, 2017) to opt for the use of readily-available data from regional and global-scale gridded products. The increasing importance of remote sensing-based information in light of the decline of ground observations in Rwanda matches the general description of Hrachowitz et al. (2013) for several regions of the world.

As cited in section 1.1.1, Sendama (2015) obtained reasonable model performances for simulating discharges at the Ruliba station by implementing the gridded precipitation products CMORPH (also used by Manyifika (2015)), TRMM (also adopted by Van Griensven et al. (2008) and Umutoni et al. (2016)) and RFE. However, the temporal availability of these data sources does not overlap with the period with most significant discharge records for the Kanzenze station.

A first selection criterion for a gridded rainfall product consisted of the available temporal resolution. Considering the goal of providing an input to a hydraulic model of the area, a daily or sub-daily scale is desirable. The adopted observed discharge data is available at a daily scale, and therefore this resolution

was adopted for the simulations in this study. Beck et al. (2017) provide an overview of the spatial and temporal coverage of available global and quasi-global daily-timescale datasets. Based on the datasets described in that study, a second selection criterion consisted of the temporal availability of the products, which should include the period before 1990 to allow for model calibration against discharges observed in that period. A third criterion involved spatial resolution, given the relatively small size of the Kanzenze station catchment and the known spatial variability in rainfall (see section 2.2.1).

The adoption of these three criteria has led to the choice of CHIRPS (Funk et al., 2015) as the source of rainfall timeseries for hydrological modelling. Data is available at a 0.05° grid (see relation to catchment size in Figure 8) at a daily time scale. CHIRPS is derived from the combination of a range of input data, as depicted in Figure 23, including satellite-based precipitation products, thermal infrared observations, ground observations and outputs of climate models. Further details on the algorithm are provided in Funk et al. (2014).

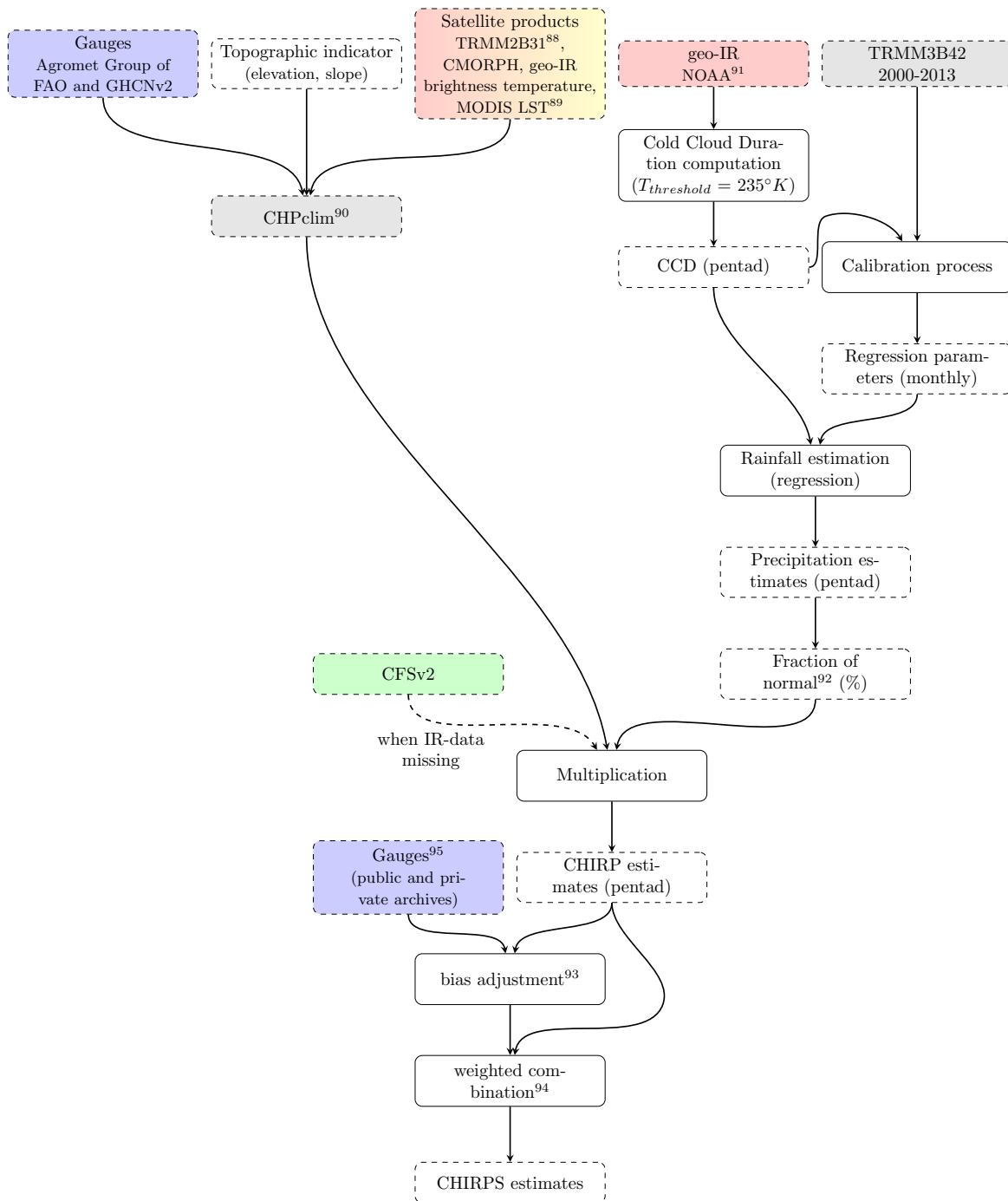


Figure 23: The generation of CHIRPS rainfall estimates (le Coz, 2018).

For the selection of the potential evaporation product, similar criteria were adopted, leading to the selection of the Global Land Data Assimilation System (GLDAS) Version 2 (Rodell et al., 2004), with highest spatial resolution being 0.25° (shown in Figure 9). This product is composed by a reprocessed 2.0 product spanning the period of 01/01/1948 to 31/12/2010 and a 2.1 product with outputs available since 01/01/2000. The precipitation product of GLDAS was exceptionally adopted for the assessment of observed discharges against the long-term catchment water balance described in section 3.4.1.

Given the span of the period to be incorporated into discharge estimation, both versions 2.0 and 2.1 of the GLDAS datasets have been used, which is an acceptable practice (Pham, 2018). The version 2.0 of the product was adopted until 31/12/2010, and complemented by the 2.1 product starting on 01/01/2011.

However, the different methods and sources adopted in the two versions translate into distinctions in their output, as illustrated in the blue lines in Figure 24.

In order to prevent eventual shift points in the output of the hydrological model due to differences in forcing, the time series adopted between 2011 and 2018 inclusive was adjusted by means of the quantile-based mapping method (CDF matching) (Panofsky et al., 1958), which has been applied in several occasions (Wang and Chen, 2014, Cayan et al., 2008, Li et al., 2010). This procedure and its result are illustrated for the Kanzenze catchment in Figure 25 and Figure 24, respectively.

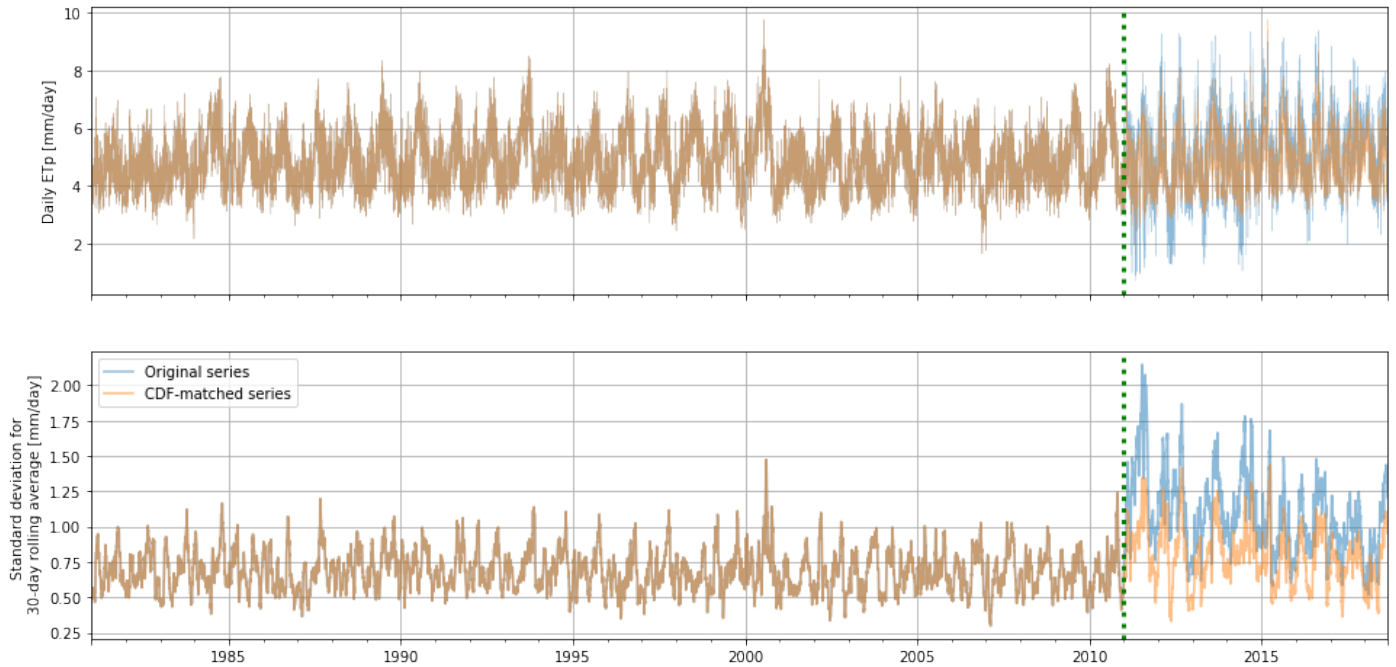


Figure 24: Comparison of potential evapotranspiration time series before and after application of CDF matching and standard deviation of 30-day rolling means. The dotted line represents the beginning of the period for which V2.1 data was adopted.

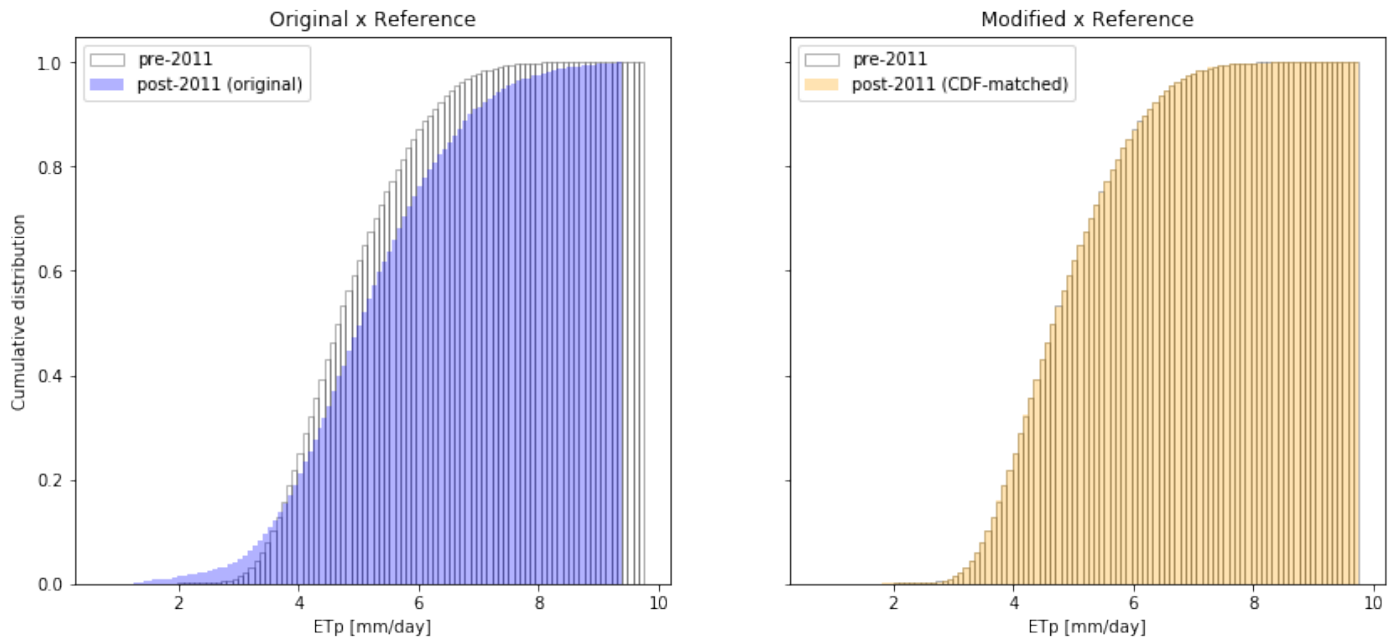


Figure 25: Illustration of CDF matching procedure for potential evaporation time series for the Kanzenze station catchment for GLDAS versions 2.0 (pre-2011) and 2.1 (post-2011).

The means of retrieval of catchment-lumped time series of precipitation and evaporation for the Ruliba station and Akanyaru river catchments consisted of a dedicated Google Earth Engine⁶ (Gorelick et al., 2017) script. For the case of evapotranspiration and potential evaporation, data provided at a 3-hour temporal resolution was resampled to daily means. For the latter, the output was also converted from $W m^{-2}$ to $mm day^{-1}$ assuming a constant water temperature of $20^{\circ}C$, and hence specific mass of $998.2 kg m^{-3}$ leading to $28.35 W m^{-2} = 1 mm day^{-1}$.

Figure 26 provides a comparison between a fraction of the catchment-lumped time series retrieved for the Ruliba station catchment and a sample of monthly pan evaporation at the Kigali Airport station to which the author had access. The period displayed corresponds to that selected for model calibration. It should be noted that the reference station is located immediately to the North of the Masaka area, outside the Ruliba station catchment, and therefore the magnitude of the values should not be expected to be representative of that area even after adjustment with pan coefficients. However, it indicates the reasonable capability of the chosen gridded potential evaporation product to reasonably reproduce the overall seasonal pattern for this variable.

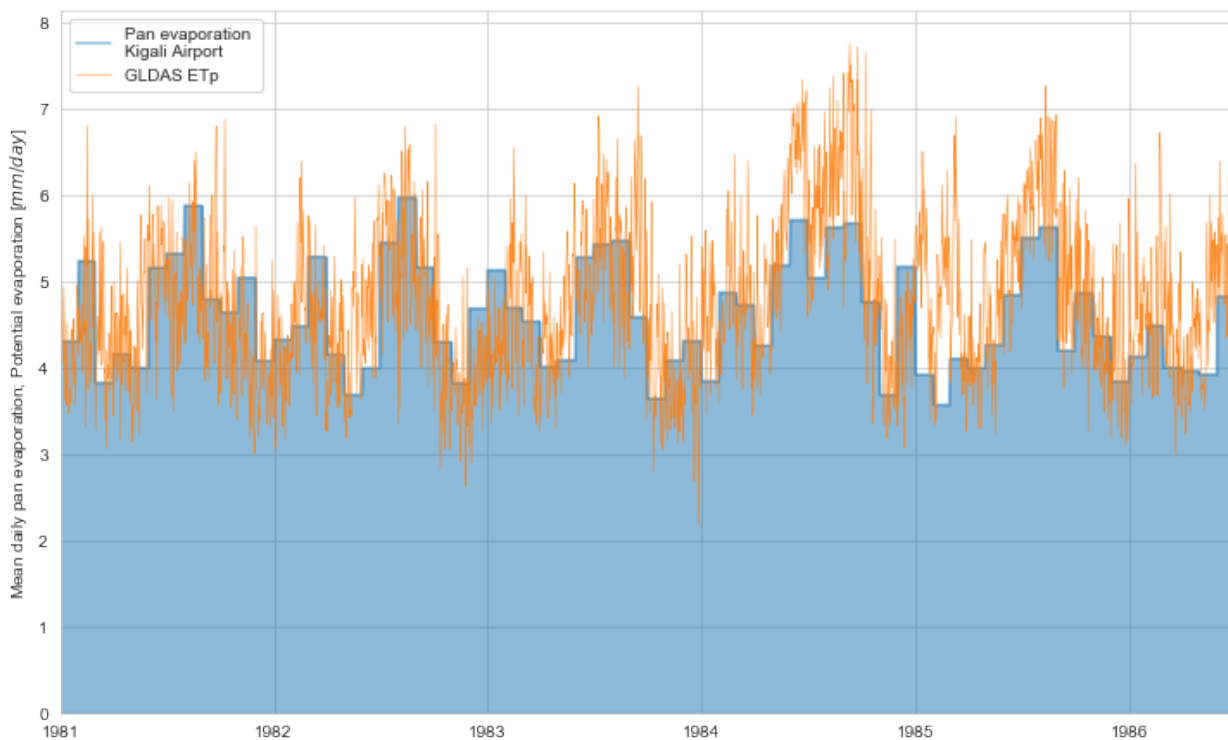


Figure 26: Comparison of area-aggregated daily mean potential evaporation for the Ruliba catchment and sample time series of monthly pan evaporation for the Kigali Airport meteorological station on daily time.

3.3 Reservoir characteristics

The Energy Development Corporation Limited (EDCL) has provided the Storage x Elevation and Storage x Area curves for the Shyorongi reservoir adopted in the occasion of its feasibility study (EDCL, 2016). The study estimated “failure percentages” associated with certain reservoir releases. While several failure possibilities exist for hydropower reservoirs (Oberrauch, 2017) and no definition was provided in the report,

⁶ ImageCollection IDs:

- CHIRPS: UCSB-CHG/CHIRPS/DAILY
- GLDAS V2.0: NASA/GLDAS/V20/NOAH/G025/T3H (PotEvap_tavg and Evap_tavg bands)
- GLDAS V2.1: NASA/GLDAS/V021/NOAH/G025/T3H (PotEvap_tavg and Evap_tavg bands)

these values were interpreted to refer to target releases for hydropower generation⁷. Accordingly, these discharges were taken as indicatives of the possible release target for reservoir operation, and served as initial guidelines for the scenarios adopted in this study, given that no further information on the expected reservoir operation was available.

⁷ This is coherent with higher failure rate reported for a discharge of $100 \text{ m}^3\text{s}^{-1}$ than for $80 \text{ m}^3\text{s}^{-1}$.

3.4 Data processing

3.4.1 Validation of observed discharges against long-term catchment water balance

Considering the aforementioned uncertainties in the reference discharge time series adopted for this study, a broad validation was carried out according to the procedure outlined in this section. The area-scaled water balance of a catchment for a given period dt can be described as:

$$\Delta S = P \cdot dt - Et \cdot dt - Q \cdot dt \quad (1)$$

Where ΔS [L] corresponds to the change in catchment-scale storage and P [L/T], Et [L/T] and Q [L/T] correspond, respectively, to the mean precipitation, evapotranspiration and discharge over the period. Therefore, the term $P \cdot dt$ corresponds to the total rainfall depth over the period, and the same logic applies to $Et \cdot dt$ and $Q \cdot dt$. On a long-term basis, changes in storage can be assumed to become negligible in comparison to the cumulative precipitation, evapotranspiration and discharge. Based on this assumption and rearranging and integrating equation 1, it is possible to estimate the long-term discharges as:

$$\int Q \cdot dt = \int P \cdot dt - \int Et \cdot dt \quad (2)$$

Equation 2 was implemented to generate estimates of yearly discharge volumes for the Ruliba and Kanzenze station catchments based on catchment-lumped estimated precipitation and evapotranspiration from GLDAS. These estimates were used for a broad verification of the adopted discharge datasets based on the cumulative annual discharges from ground observations for the corresponding years, as shown in Figure 27. For this procedure, only years with full records of ground observations were adopted, and hence not all years were suitable for comparison.

For the Ruliba station, most of the cumulative observed discharges are within a 20% margin of the corresponding water balance-based estimates. For the Kanzenze catchment, with three exceptions, ground observations appear to systematically underestimate flows in comparison to catchment water balance estimates. This might be partially justified by the reported limited ability of the station to record extreme discharges (Water4Growth and MINIRENA, 2018) and the uncertainty involved in the extrapolation of the rating curve under these conditions. However, it is also stressed that the adopted estimates of precipitation and evapotranspiration also carry underlying assumptions and errors that are propagated into the estimated yearly cumulative discharge volumes from the catchment water balance.

A further relevant illustration derived from this figure is that observed mean annual cumulative discharges from ground observations at the Ruliba station mostly range between 300 and 450 mm year⁻¹, while for the Kanzenze catchment this value is generally below 300 mm year⁻¹. This is consistent with the lower evaporative index for the Ruliba catchment than for the Kanzenze catchment derived by Abimbola (2014) from interpolated ground observations. Considering the former is one of the subcatchments of the latter, an inference can be made that the remaining subcatchments of the Kanzenze station (broadly the Akanyaru and the Nyabugogo river catchments – see Figure 17 for a schematisation) have runoff coefficients below those observed for the Ruliba station.

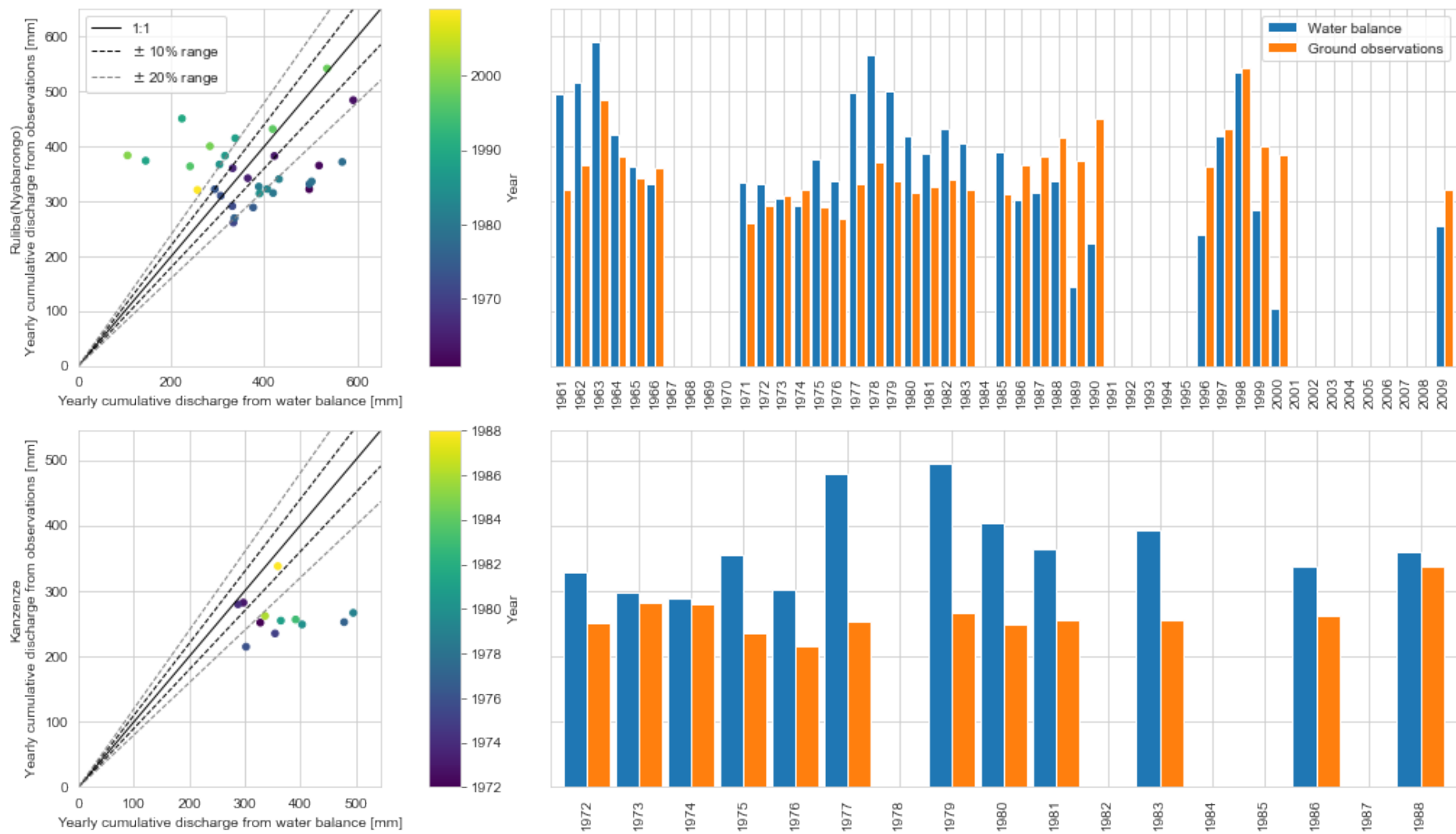


Figure 27: Cumulative yearly discharge volumes and corresponding catchment water balance estimates for Ruliba and Kanzenze stations. Plots on the same row share the same y axis scale.

3.4.2 Estimation of discharges at the Akanyaru river outlet

As illustrated in Figure 17, the Kanzenze gauging station catchment comprises both the Nyabarongo and the Akanyaru river catchments. Given the absence of hydrometric stations with rating curves in the lower reaches of the Akanyaru river, its discharge can alternatively be theoretically estimated by the difference in observed discharges at the Kanzenze station and at the section of the Nyabarongo river immediately upstream of the Akanyaru outlet, which corresponds approximately to the position of the Ruliba station. Therefore, as a first step, daily discharges at the outlet of the Nyabarongo river were estimated by regionalisation of the discharges at the Ruliba station considering catchment area as the only parameter.

However, the Ruliba and Kanzenze stations are separated by a river stretch of approximately 45 km length surrounded by wetlands. River gradients in the order of 0.02% have been reported in the vicinities of the region (RHDHV, 2017b). As discussed in section 2.2, wetlands are known to act as a significant water storage elements, across the Nile Basin (NBI, 2012, NBI, 2016), but also specifically in Rwanda (Nahayo et al.) and upstream of the Kanzenze station (Ndekezi, 2010). The Kanzenze bridge is also known to constrain discharges and hence the area immediately upstream acts as a temporary reservoir during peak flows. Temporary floodplain retention and the resulting hydrograph attenuation has been reported for a smaller catchment within Rwanda by Van den Berg and Bolt (2010). These phenomena are hypothesised to motivate the lag between the seasonal hydrographs of both stations and the periods when discharges in the Ruliba station exceed those at the downstream Kanzenze station, as illustrated in Figure 28.

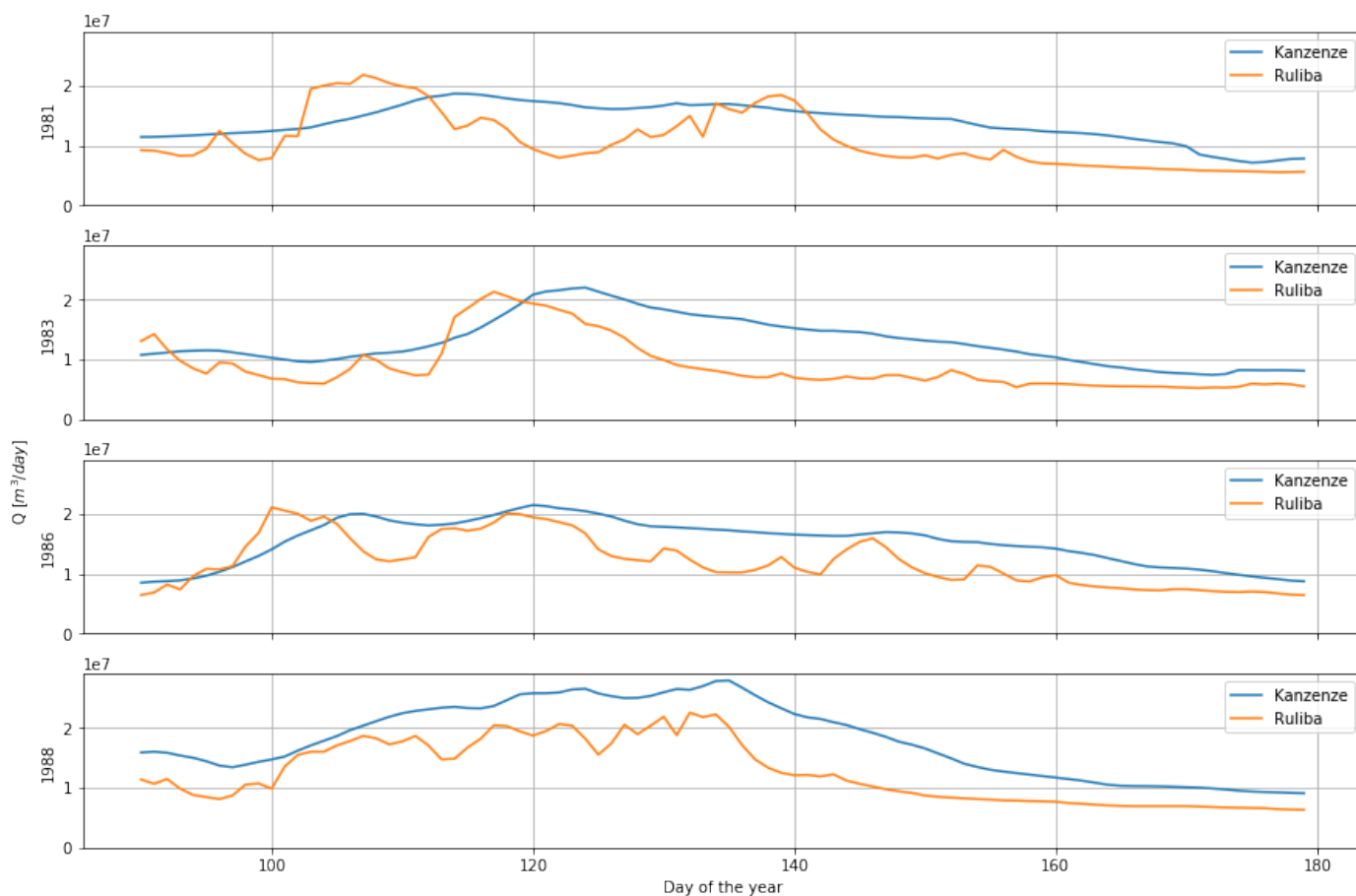


Figure 28: Examples of seasonal hydrographs for the Kanzenze and Ruliba stations.

With the goal of obtaining a compromise between simplicity and representability, and considering the limitations in available data and knowledge behind the processes taking place in the area, this buffering effect was approximated by the implementation of a linear reservoir downstream of the Ruliba station, defined by the formula below:

$$Q(t) \cdot dt = \frac{S(t)}{K} \quad (3)$$

Where Q is the discharge on a given day, S is a theoretical storage volume and K is a time scale coefficient. Evaporation and infiltration were assumed to be negligible. The time scale coefficient of the reservoir (K) was calibrated by comparing discharges at Kanzenze and at the Nyabarongo river outlet (after the reservoir routing) using two objective functions:

- The spearman correlation coefficient (to be maximised);
- The number of days in the series when estimated discharges at the Nyabarongo river outlet exceeded estimated discharges at the Kanzenze station (to be minimised).

Both objective functions yielded an optimum K value of 9 days, as illustrated in Figure 29.

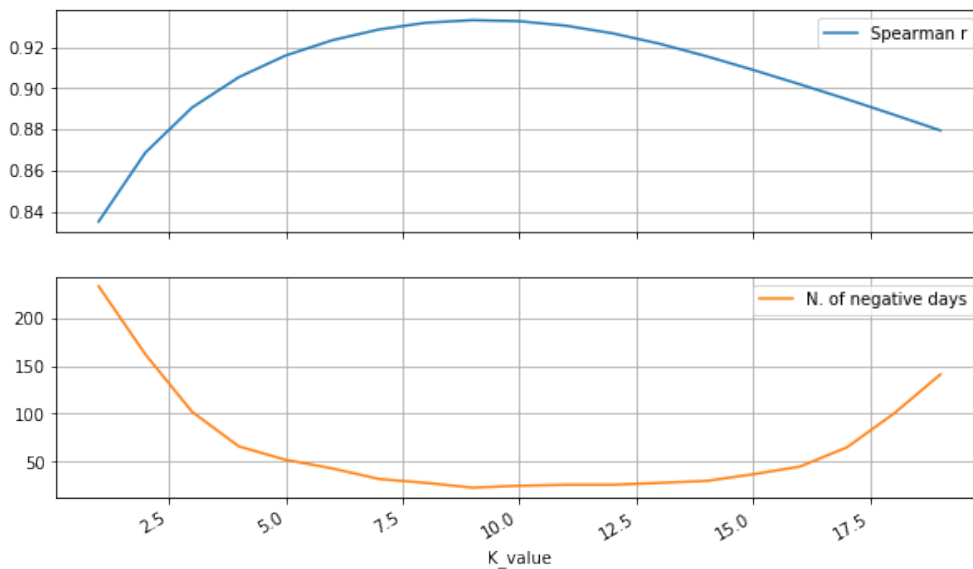


Figure 29: Optimisation of the linear reservoir coefficient for the river segment between Ruliba and Kanzenze stations. For varying values of K (linear reservoir coefficient), the obtained spearman correlation coefficient and number of days on which estimated discharges were negative are shown in the top and bottom plot, respectively.

The cumulative discharge volumes, daily discharges and differences in daily discharge between the Kanzenze and Ruliba stations after linear reservoir routing are depicted in Figure 30 for the four years for which full records exist for both stations.

According to the system description above (that the Kanzenze station receives contributions from the Ruliba station and Akanyaru river catchments), the third column corresponds to the estimated daily discharges at the Akanyaru river outlet, and the distance between the lines in the first column corresponds to the cumulative discharges of the Akanyaru river.

If the years depicted are assumed to be representative of the overall behaviour of the Kanzenze catchment, some preliminary conclusions can be drawn at this stage:

- On an annual basis, the discharge at the Kanzenze station is dominated by contributions from the Nyabarongo river catchment (from 74% to 85% of the annual volume in 1988 and 1986, respectively).
- While the seasonal flooding signal is identifiable in three out of four years, there appears to be a considerable amount of noise in the estimated discharges of the Akanyaru river. This can be attributed the uncertainty propagated from factors such as the discharge estimates at the Kanzenze and Ruliba stations, as well as the routing procedure described above. A particular example of this is the period in 1986 for which estimated discharges at the Nyabarongo river are greater upstream

of its confluence with the Akanyaru river (Ruliba station) than downstream (Kanzenze station), which indicates the limited capability of a linear reservoir to represent temporary storage in the area between the stations, as well as the possible existence of considerable errors in the discharge records at one or both stations.

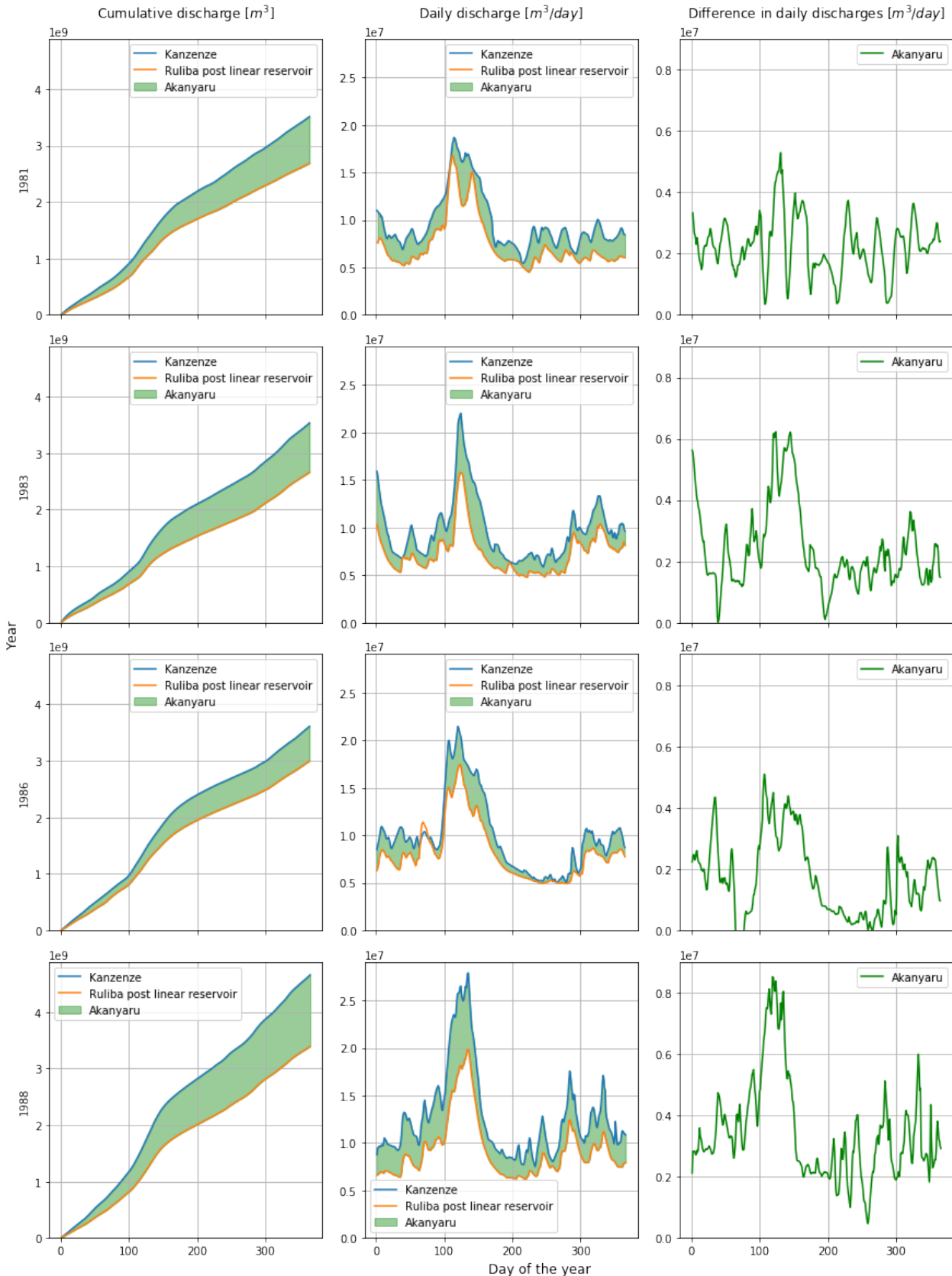


Figure 30: Analysis of observed discharges for years with full records for stations Kanzenze and Ruliba. The discharge of the Akanyaru river is approximated by the difference in discharge at the Kanzenze and Ruliba stations, after the latter is routed in a linear reservoir to simulate temporary storage in floodplains between the two stations.

In spite of the limitations mentioned above, the discharge time series for the Akanyaru river derived from this method provide an indication of its order or magnitude and seasonal behaviour. These are key components for the estimation of its contribution to seasonal flooding in the Masaka wetland. In order to generate a time series of discharges that (a) follows the trend and order of magnitude shown in the right column of Figure 30 but at the same time (b) is consistent with climatic forcing observed in the Akanyaru catchment and (c) has no gaps, a conceptual hydrological model for the Akanyaru river catchment was calibrated against the discharges generated at this step. There was no expectation that the model would accurately reproduce the estimated daily discharges illustrated on the right column of Figure 30 due to the aforementioned scatter and possible errors in this data. The purpose of the model was restricted to providing reasonable estimates of the contribution from the Akanyaru river to the discharges observed at the Kanzenze station, and hence at the Masaka wetland. Further discussion is provided in section 4.1.1.3.

4 Methods

4.1 Catchment and reservoir simulations

A schematisation of the steps involved in this research is presented in Figure 31, and descriptions are provided in the ensuing sections.

4.1.1 Hydrological modelling: generation of discharge time series at key catchment locations

The main purpose of this step was to generate time series of daily discharges without gaps spanning the 1981~2018b period in key locations according to the adopted system conceptualisation.

4.1.1.1 Perceptual model

A perceptual model for the hydrological functioning in the Nyabarongo and Akanyaru rivers, with an emphasis on processes that are most relevant for seasonal flooding, has been developed based on available descriptions based on fieldwork of previous studies on the topic (e.g. Van den Berg and Bolt, 2010, Munyaneza et al., 2010, Munyaneza et al., 2012), which was mostly carried out in the Migina catchment depicted in Figure 6. The availability of relatively detailed descriptions for this catchment motivated its adoption as a proxy for the behaviour at larger spatial scales (i.e. Akanyaru and Nyabarongo river catchments).

The seasonal rainfall pattern and short but intense rainfall events in Rwanda mean that the land surface has a low moisture content for most of the time. Therefore, transpiration is expected to comprise the majority of evapotranspiration, and interception is also relatively modest (Van den Berg and Bolt, 2010).

A total of 5 and 8 storm events were analysed by Munyaneza et al. (2012) for the Migina catchment and Cyihene-Kansi subcatchment, respectively. The observed runoff coefficients ranged between 31.5% and 44.4% for the Migina catchment and between 16.7% and 44.5% for the Cyihene-Kansi subcatchment. This observation, associated with tracer-based hydrograph separation, led to the conclusion that **a large fraction of the rainfall is transformed into subsurface flow (SSF)** in those catchments (Munyaneza et al., 2012). This can be linked to the relatively high infiltration capacities (208 to 1250 mm.h⁻¹) were reported for agricultural land in the Migina catchment, as well as a large specific storage capacity for the soil (60 to 70%), although such values tend to decrease over the rainy season (Van den Berg and Bolt, 2010). The hillslopes in the Migina catchment were reportedly affected by **infiltration-excess overland flow (IOF)** as observed by surface erosion marks, but this mechanism was deemed to have a secondary importance (Munyaneza, 2014).

Isotope analysis in the Migina catchment has indicated that that groundwater is likely recharged exclusively during the wet seasons (Munyaneza et al., 2012). The existence of an “important shallow subsurface water storage” was regarded by Munyaneza et al. (2012) as the factor enabling agriculture even during dry periods. **Shallow groundwater** depth was reported to range from 0.2 to 2 m in the valleys (Munyaneza et al., 2011b) to 4.1 m at the hilltops (Van den Berg and Bolt, 2010).

In the valleys, an impermeable layer separating deep and shallow groundwater was reported by Van den Berg and Bolt (2010). The same study observed that groundwater is increasingly influenced by streams as one moves closer to them. However, an analysis of the temperature of groundwater at different depths in the Migina catchment demonstrated that shallow rivers, being colder than shallow groundwater, are mostly fed by deep groundwater (Van den Berg and Bolt, 2010). The existence of two parallel groundwater systems was hypothesised: (a) a shallow one that originates mostly on valleys and lower hillslopes and (b) a deeper one that is fed by infiltration in plateaus and hillslopes and eventually seeps onto streams.

Based on the aforementioned descriptions, Munyaneza (2014), proposed a conceptualisation of the processes taking place at the Migina catchment, which is illustrated in Figure 32.

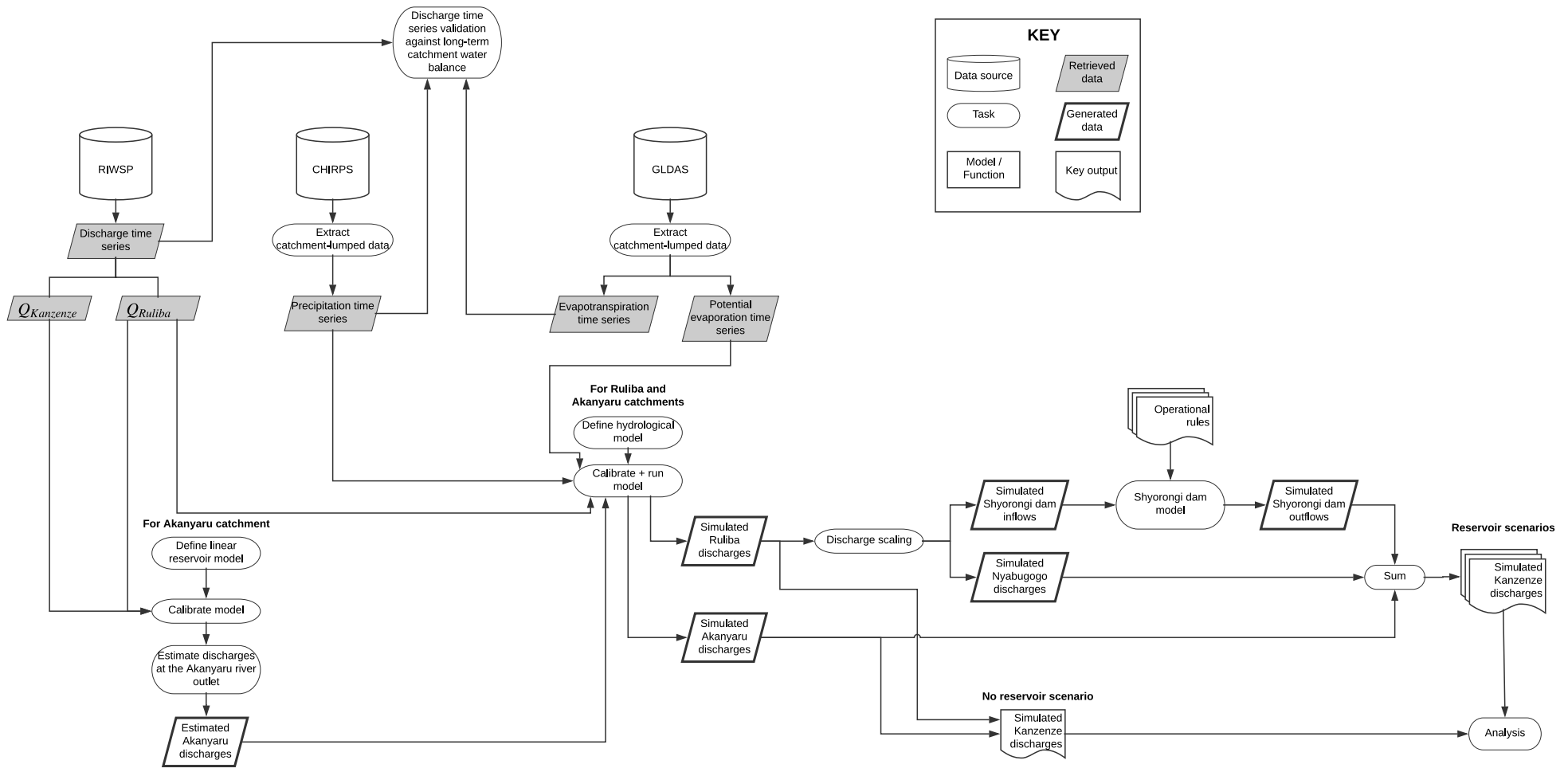


Figure 31: Representation of implemented methodology

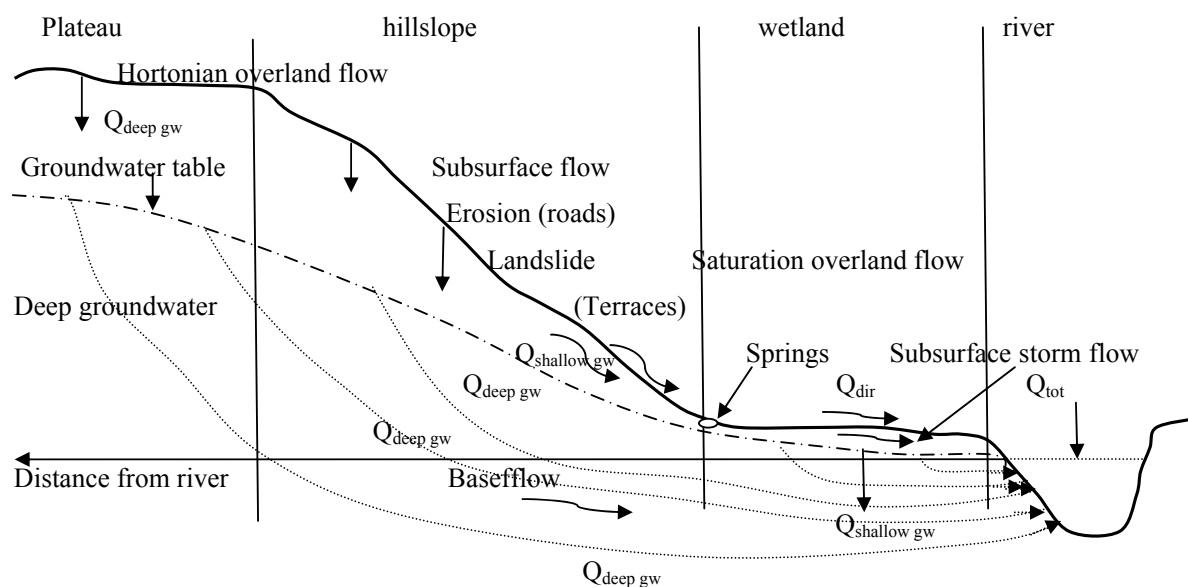


Figure 32: Perceptual model of hydrological processes in the Migina catchment (Munyaneza, 2014).

4.1.1.2 Conceptual model

The selection of the structure of the model for the current study is briefly described in the context of key factors outlined by Blöschl et al. (2013) and Hrachowitz et al. (2013):

- a. **A priori process perception:** The *a priori* process perception was guided by the descriptions provided for the Migina catchment, which were outlined in the previous section:
- b. **Field visits and reading of the landscape:** The current study did not involve field visits or the retrieval of field data. Therefore, the landscape perception was derived from the interpretation of satellite imagery and descriptions of previous studies involving field work in the Migina catchment (Van den Berg and Bolt, 2010) and in the vicinities of the Masaka wetland (RHDHV, 2017b).
- c. **Model structure of similar gauged catchments:** As outlined in section 1.1.1, several approaches have been deployed for rainfall-runoff modelling in Rwanda. While some studies implemented the distributed SWAT model, most authors selected a semi-distributed approach with models such as NAM and HBV-light.
- d. **Modelling purpose:** The purpose of modelling in this study – the simulation of seasonal hydrographs for flood estimation – was different from that of most of the previous large catchment-scale studies in Rwanda, which generally focussed on water resources availability. This is reflected, for example, on the need for adopting a daily time scale.
- e. **Data availability:** Constraints in data availability were a major factor determining the selection of a hydrological modelling approach in the context of the current study. As described in section 3, reference discharge estimates are limited to few stations across the country, and generally concentrated in the period before 1990. Adopting a model with a large number of parameters when the amount of observations is limited will trigger the possibility of equifinality and unnecessary complexity. Additionally, difficulties in access to and reported gaps in ground observations of climatic forcing data (precipitation and potential evaporation) have led to the choice of global gridded products for the estimation of these variables. The accuracy of these products can be expected to decrease with catchment size, and therefore the simulation was set at the largest possible spatial scale.

Based on the considerations above, an adapted version of the FlexTOPO framework (Savenije, 2010) was implemented for the current study. An attempt was made to obtain a compromise between the

representation of the processes as described in the previous section– the (deep) groundwater reservoir is assumed to be recharged exclusively in hillslope areas – while minimising the number of parameters. A graphical illustration of the model and an outline of its procedural implementation are provided in the ensuing sections.

Interception reservoir

The first bucket of the hillslope module consists of the interception reservoir, and has the maximum interception storage capacity ($S_{i,max}$) as its parameter. Rainfall (P) recharges the interception storage S_i (equation 4), and evaporation (E_i) depletes it (equation 9) at the rate of the potential evapotranspiration (Et_p) for the given day as long as enough storage is available (equation 8). If, on a given time step, the storage is exceeded, the exceeding rainfall depth becomes effective precipitation (P_e) (equation 5). If the amount of rainfall plus the storage at the beginning of a time step is smaller than the potential evapotranspiration rate, the evaporation from interception equals the available storage and the reservoir empties.

If $P \cdot dt > 0$:

$$S_i(t) = S_i(t - 1) + P(t) \cdot dt \quad (4)$$

$$P_e(t) \cdot dt = \begin{cases} S_i(t) - S_{i,max} & \text{if } S_i(t) > S_{i,max} \\ 0 & \text{otherwise} \end{cases} \quad (5)$$

$$S_i(t) = S_i(t) - P_e(t) \cdot dt \quad (6)$$

If $P \cdot dt = 0$:

$$P_e(t) \cdot dt = 0 \quad (7)$$

$$E_i \cdot dt = \min \begin{cases} Et_p(t) \cdot dt \\ S_i(t - 1) \end{cases} \quad (8)$$

$$S_i(t) = S_i(t - 1) - E_i(t) \cdot dt \quad (9)$$

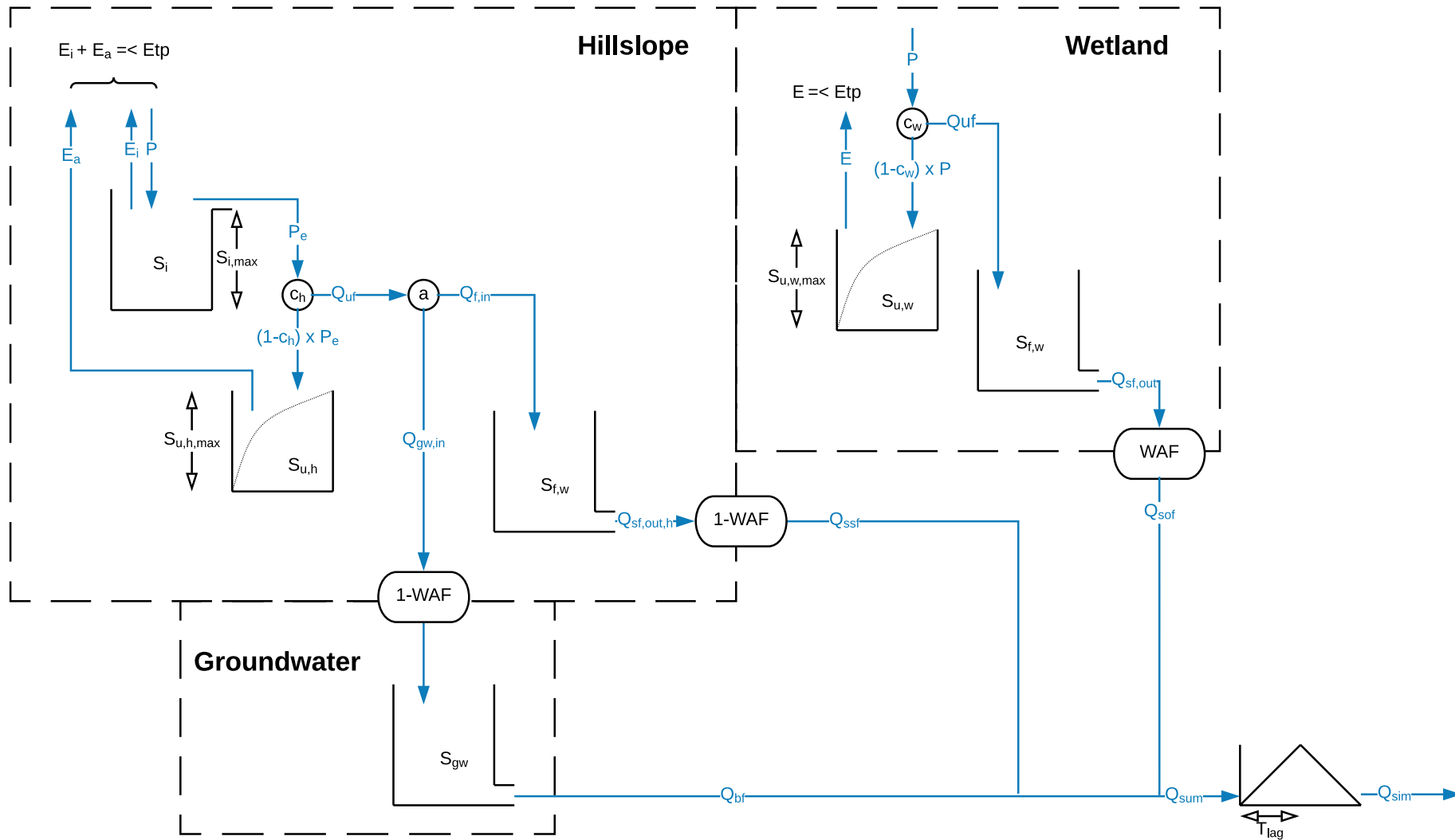


Figure 33: Conceptual rainfall-runoff model applied to the Ruliba station and Akanyaru river catchments.

Unsaturated reservoirs

The unsaturated reservoirs were implemented for hillslopes and wetlands with the goal of reproducing dynamics at the unsaturated portion of the soil. The unsaturated reservoir of each module is recharged by a fraction $(1-c_h)$ of the effective precipitation in the hillslope module:

$$S_{u,h}(t) = S_{u,h}(t-1) + (1-c_h) \cdot P_e \cdot dt \quad (10)$$

and by a fraction $(1-c_w)$ of the total precipitation in the wetland module:

$$S_{u,w}(t) = S_{u,w}(t-1) + (1-c_w) \cdot P \cdot dt \quad (11)$$

In both cases, the coefficient c is assumed to approach the value 1 as the reservoir approaches saturation following the formula:

$$c(t) = 1 - \left(1 - \frac{S_u(t)}{S_{u,max}}\right)^\beta \quad (12)$$

where c corresponds to c_h or c_w in the case of the hillslope and wetland modules, respectively, and similarly for S_u and $S_{u,max}$. Considering the lumped nature of the conceptual model, this coefficient is intended to represent the proportion of the hillslope or wetland area in saturated conditions.

After recharge, evapotranspiration losses are accounted for and removed. This flux is assumed to be proportional to the ratio between the storage at a given time step and the maximum storage capacity and to the available energy. In the case of the hillslope module, this amount is given by the remaining potential evaporation that has not been evaporated by the interception reservoir:

$$E_{a,h}(t) \cdot dt = \begin{cases} (ET_p(t) \cdot dt - E_i(t) \cdot dt) \cdot \frac{S_{u,h}(t)}{S_{u,h,max}} & \text{if } ET_p(t) \cdot dt > E_i(t) \cdot dt \\ 0 & \text{otherwise} \end{cases} \quad (13)$$

In the wetland module, this corresponds to the potential evaporation:

$$E_{a,w}(t) \cdot dt = ET_p(t) \cdot dt \cdot \frac{S_{u,h}(t)}{S_{u,h,max}} \quad (14)$$

The effective precipitation depth that did not recharge the unsaturated reservoir is given by:

$$Q_{uf}(t) \cdot dt = c_h(t) \cdot P_e(t) \cdot dt \quad (15)$$

in the case of the hillslope module and by:

$$Q_{uf}(t) = c_w \cdot P(t) \cdot dt \quad (16)$$

in the wetland module.

Fast-response reservoirs

Fast response reservoirs were implemented as linear reservoirs with relatively low time scale coefficients. They aim to reproduce the faster response mechanisms expected to occur in the hillslope (infiltration excess overland flow) and wetland (saturation excess overland flow) modules. In the wetland module, it is recharged by Q_{uf} :

$$S_{f,w}(t) = S_{f,w}(t - 1) + Q_{uf}(t) \cdot dt \quad (17)$$

The hillslope fast reservoir is recharged by $Q_{f,in}$:

$$S_{f,h}(t) = S_{f,h}(t - 1) + Q_{f,in}(t) \cdot dt \quad (18)$$

given by:

$$Q_{f,in}(t) \cdot dt = Q_{uf}(t) \cdot dt \cdot (1 - a) \quad (19)$$

where a is a pre-set parameter defining the partitioning of flow exceeding saturation between recharge of the fast reservoir ($Q_{f,in}$) and groundwater ($Q_{gw,in}$).

The releases of the fast reservoirs are given by the linear reservoir formula:

$$Q_{sf,out}(t) \cdot dt = \frac{S_f(t)}{K} \quad (20)$$

Where K is the time scale coefficient and $Q_{sf,out} = Q_{sf,out,h}$ for the hillslope module and $Q_{sf,out} = Q_{sf,out,w}$ for the wetland module.

Following the definition of a provided above, the groundwater recharge depth is given by:

$$Q_{gw,in}(t) \cdot dt = Q_{uf}(t) \cdot dt \cdot a \cdot (1 - WAF) \quad (21)$$

The multiplication by $(1-WAF)$ represents the conceptualisation that groundwater comprises the entire catchment area, and therefore a hypothetical 1 mm release from a hillslope module comprising 90% of the catchment area would result in a 0.9 mm recharge of the groundwater when averaged over the catchment. Following the same logic, the catchment-averaged outflows of the hillslope and wetland fast reservoirs are:

$$Q_{ssf}(t) \cdot dt = Q_{sf,out,h}(t) \cdot dt \cdot (1 - WAF) \quad (22)$$

$$Q_{sof}(t) \cdot dt = Q_{sf,out,w}(t) \cdot dt \cdot WAF \quad (23)$$

Groundwater reservoir

The groundwater reservoir is conceptualised as a linear reservoir. Hence, its outflow (the baseflow) is given similarly to equation 20:

$$Q_{bf}(t) \cdot dt = \frac{S_{gw}(t)}{K} \quad (24)$$

Convolution

The total discharge generated at a given time step is given by the sum of the components from the three modules:

$$Q_{sum}(t) \cdot dt = Q_{bf}(t) \cdot dt + Q_{ssf}(t) \cdot dt + Q_{sof}(t) \cdot dt \quad (25)$$

In order to account for the distribution of response times across the catchment, the time series of Q_{sum} is convoluted by a triangular function of width T_{lag} , yielding the simulated time series Q_{sim} :

$$Q_{sim}(t) \cdot dt = Q_{sum}(t) \cdot dt * f(T_{lag}) \quad (26)$$

4.1.1.3 Model calibration

Separate hydrological models for the Akanyaru river outlet and Ruliba station with the structure shown in Figure 33 were calibrated against observed (in the case of the Ruliba station) or estimated (in the case of the Akanyaru river; see section 3.4.2) discharges. The calibration followed a Monte Carlo procedure, where the model performance was assessed for random parameter combinations generated within specified ranges, as illustrated in Table 5. For the Ruliba station and Akanyaru river outlet model, 100.000 and 50.000 runs were performed, respectively.

Considering the limited amount of available information on the specific properties of the catchments, the prior ranges of values for all except one parameter were defined to relatively broad intervals within the respective valid ranges. In the absence of detailed country-wide information on parameters such as storage capacity and infiltration capacity, the values reported by Van den Berg and Bolt (2010) for the Migina subcatchment were used as broad indicators for parameter ranges, supported by values obtained for hydrological modelling of the same catchment by Munyaneza (2014).

An exception was made for the linear reservoir coefficient (K) of the groundwater module. For this parameter, the following procedure – adapted from McCuen (1998) – was adopted for each catchment:

1. Retrieve samples of consecutive observed daily discharges for periods in which recharge is assumed negligible.
2. For each day i of the sample starting on the second day:
 - 2.1. Estimate K with the formula:

$$K_i = \frac{(t_i - t_0)}{\ln(Q_{obs}(t_i)) - \ln(Q_{obs}(t_0))} \quad (27)$$

where t_0 and $Q_{obs}(t_0)$ are, respectively the first day of the sample and the respective observed discharge, and $Q_{obs}(t_i)$ is the discharge observed on the given day.

- 2.2. Retrieve the median value of the K values estimated for each day of the sample
- 2.3. Generate discharge estimates based on the mean K adopted above

2.4. Assess fit of estimated values to observed values with the root-mean-square deviation normalised by the range in observed values:

$$NMRSD = \frac{\frac{\sum_{i=1}^N (Q_{obs,i} - Q_{pred,i})^2}{N}}{\max(Q_{obs}) - \min(Q_{obs})} \quad (28)$$

Where $Q_{pred,i}$ is the predicted discharge on time step i , N is the number of time steps and $\max(Q_{obs})$ and $\min(Q_{obs})$ are the maximum and minimum observed discharges for the sample.

2.5. If $NMRSD < 0.2$, store the corresponding K value

3. Adopt the smallest and largest estimated K values as the boundaries of the prior range to be tested.

The calibrated values for the groundwater linear reservoir coefficient for both stations were relatively close to the upper limits of the respective prior ranges. This can be linked to the fact that some of the K values derived by the aforementioned procedure were based on time series separated from the last rainfall event by a relatively short amount of time. Therefore, one can expect the recession of the hydrograph in these series to contain a subsurface flow component, which reduces at a faster rate and therefore increases the derived K value.

Considerably higher values for the $S_{u,max}$ parameter were obtained for the Akanyaru river catchment than for the Ruliba station catchment in both the hillslope and wetland modules. According to equation 12, a higher value for $S_{u,max}$ implies a lower c value *ceteris paribus*. This in turn leads to a larger proportion of effective precipitation being retained at the unsaturated storage (given by $(1-c_h) * P_e \cdot dt$) and lower amounts being redirected to other buckets in the model. As a consequence, a higher proportion of the rainfall can be expected to evaporate over longer periods (i.e. a lower runoff coefficient). This observation agrees with the higher actual evaporation rates estimated by the GLDAS model for the Akanyaru river catchment (see Figure 9).

Table 5: Parameter value selection for the hydrological models of the Ruliba station and Akanyaru river outlet models

Module	Parameter	Unit	Valid range		Catchment	Prior range		Calibrated value
			Min.	Max		Min.	Max	
Groundwater	K	days	1	∞	Ruliba	13	185	175
					Akanyaru	20	180	150
Hillslope	$S_{i,max}$	mm	0	∞	Ruliba	5	10	9
					Akanyaru			6
	$S_{u,max}$	mm	0	∞	Ruliba	300	800	330
					Akanyaru			782
	β	-	0	∞	Ruliba	0.1	2.0	0.5
					Akanyaru			0.1
a	-	0	1	Ruliba	0.1	1.0	0.8	
				Akanyaru			0.5	
K	days	1	∞	Ruliba	1	*	10	
				Akanyaru			38	
Wetland	$S_{u,max}$	mm	0	∞	Ruliba	50	300	51
					Akanyaru			208
	β	-	0	∞	Ruliba	0.1	2.0	1.84
					Akanyaru			0.75
	K	days	1	∞	Ruliba	1	*	6
					Akanyaru			9
WAF	-	0	1	Ruliba	0.05	0.15	0.1	
				Akanyaru			0.05	
Global	T_{lag}	days	1	∞	Ruliba	1	10	2
					Akanyaru			1

* For each random parameter combination, the following constraint was enforced:
 $K_{Wetland} < 0.5 K_{Hillslope} < 0.5 K_{Groundwater}$

In contrast, lower values for the parameter β were obtained for the Akanyaru catchment for both the wetland and hillslope modules. β is also a parameter of the unsaturated storage reservoir, which drives the shape of the function linking the relative storage level in this reservoir to the value of the parameter c (i.e. equation 12).

The effect described above is illustrated in Figure 34. Lower values for the parameter β imply that, for a given storage level, the value of c will be lower ceteris paribus. A value of 0.1, as observed for the hillslope module of the Akanyaru catchment, indicates a relatively low sensitivity of c until the reservoir approaches saturation. This may be interpreted as the occurrence of a fairly uniform behaviour of the unsaturated reservoir across the catchment – i.e. a large proportion of the hillslopes achieving saturated conditions simultaneously. In contrast, a value of 1.84 as observed for the wetland module in the Ruliba catchment represents different regions of the catchment gradually achieving saturation as the reservoir fills.

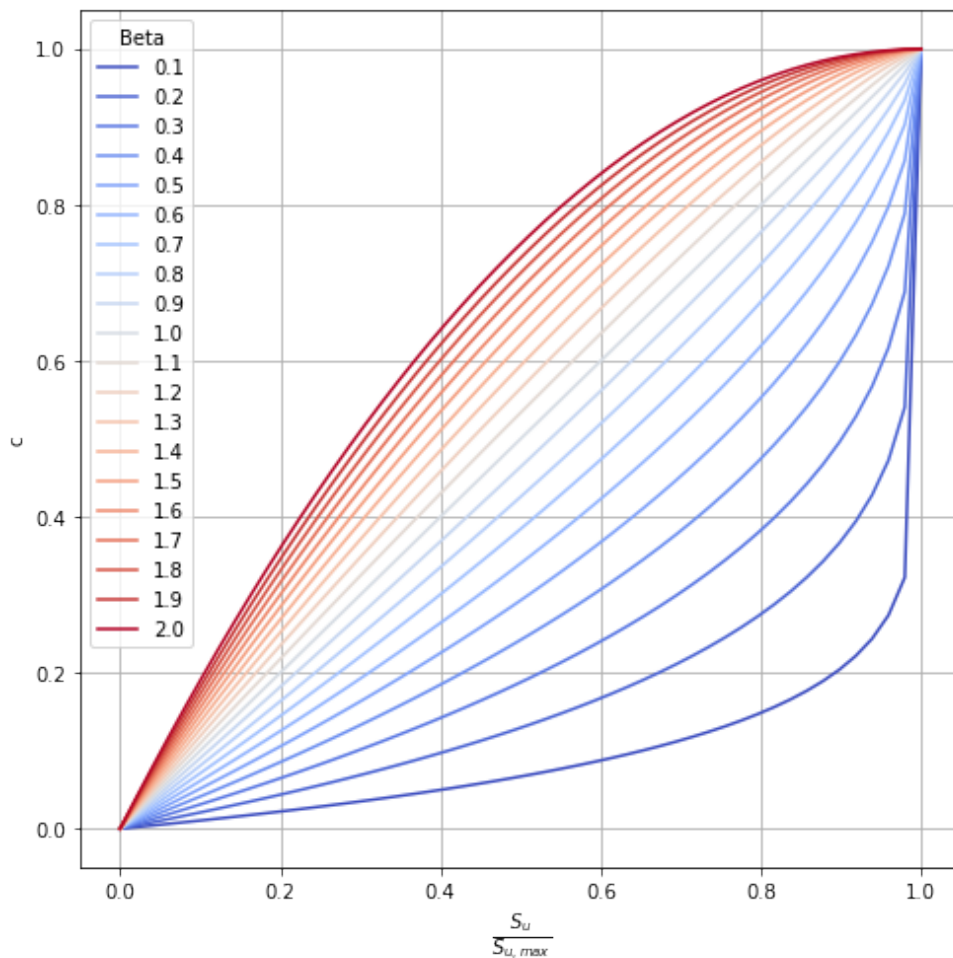


Figure 34: Relationship between the relative storage level in the unsaturated reservoir to the coefficient c for varying β values (equation 12)

The coefficient a drives the partitioning between groundwater recharge and subsurface flow. In the Akanyaru catchment, each component receives half of the discharge. In the Ruliba station catchment, the obtained value indicates that the subsurface flow component corresponds on average to a large proportion of the total discharge, which is in line with the field observations described in section 4.1.1.1.

However, it should be noted that while some general inferences have been presented above, conclusions regarding catchment behaviour based on the analysis of the calibrated parameter values alone are not possible in this context. This statement is supported by the observations that:

- a. The wetland area fraction (WAF) value was constrained to a maximum value of 0.15 and therefore the parametrisation of this module had a limited effect on overall discharge and model performance

- b. The reference discharge time series on which the models were calibrated contained considerable uncertainty – particularly on the case of the Akanyaru catchment as demonstrated in section 3.4.2. Due to this factor, even the optimal parameter set had a limited performance, and the uncertainty in estimated parameter values is too great for definitive comparisons of the two catchments to be made (as shall be discussed in the next sub-sections).

Ruliba station catchment

Figure 35 illustrates the sensitivity of the performance of the model, measured by the NSE, to varying values of each of the calibration parameters. As mentioned above, the limited sensitivity of the model performance to all parameters of the wetland module can be at least partially traced to the constraint imposed on the relative contribution of this module (i.e. the value of the Wetland Area Fraction parameter). In contrast, clear optima are identifiable for the parameters β and a of the hillslope module. These two parameters control the partition of rainfall into evapotranspiration, groundwater recharge and subsurface flow.

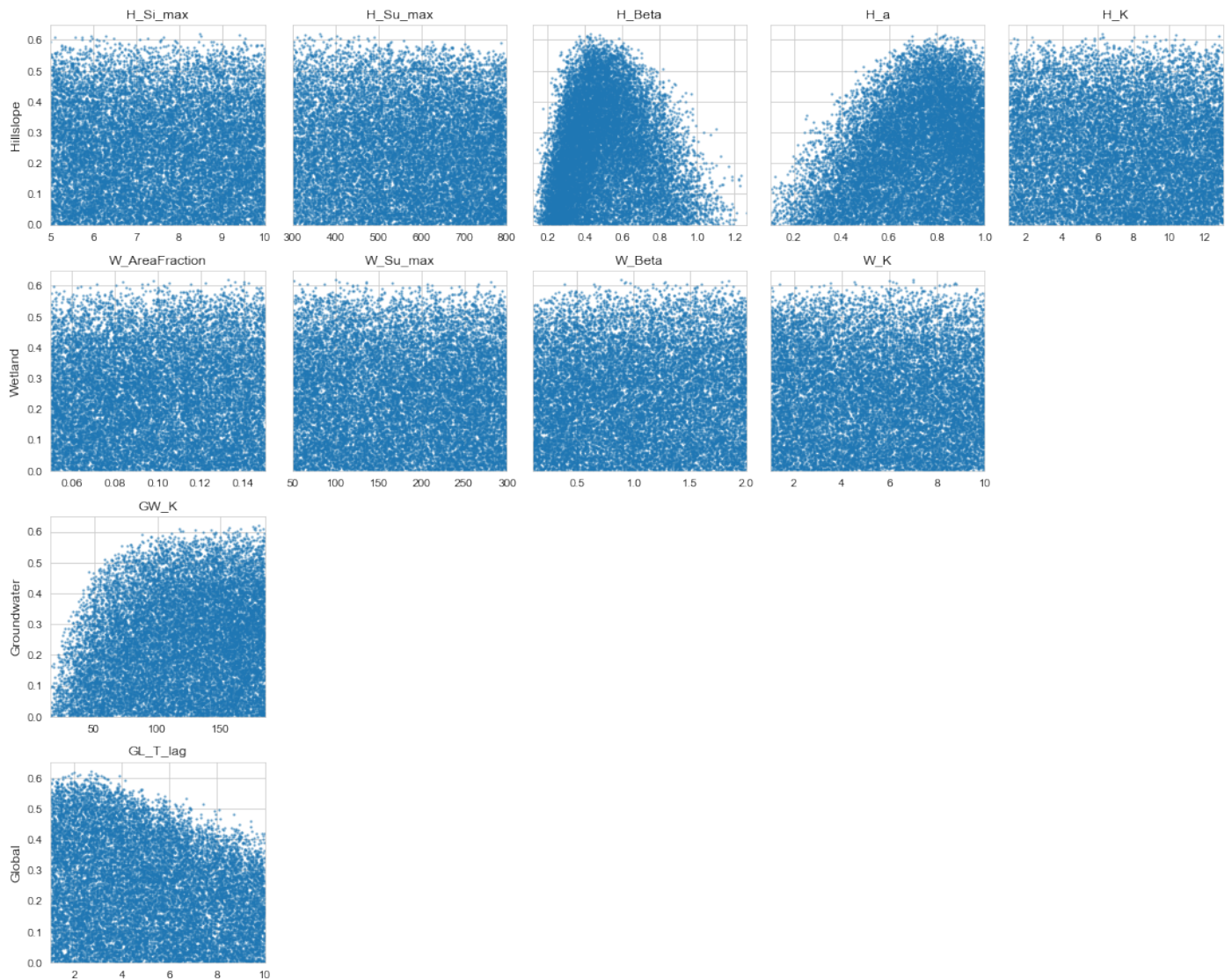


Figure 35: Performance (Nash-Sutcliffe Efficiency) sensitivity to varying values of the calibration parameters for model runs with $NSE \geq 0$ for the Ruliba station catchment. Rows correspond, from top to bottom, to plots of the Hillslope, Wetland and Groundwater modules, and to the global parameter T_{lag} .

The selected parameter combination corresponded to a compromise between the NSE and logNSE objective functions, as illustrated in Figure 36. The discharge time series simulated with this parametrisation

is shown in Figure 37. It is visible that baseflow comprises the majority of total runoff throughout the displayed period, which is consistent with the descriptions in section 4.1.1.1.

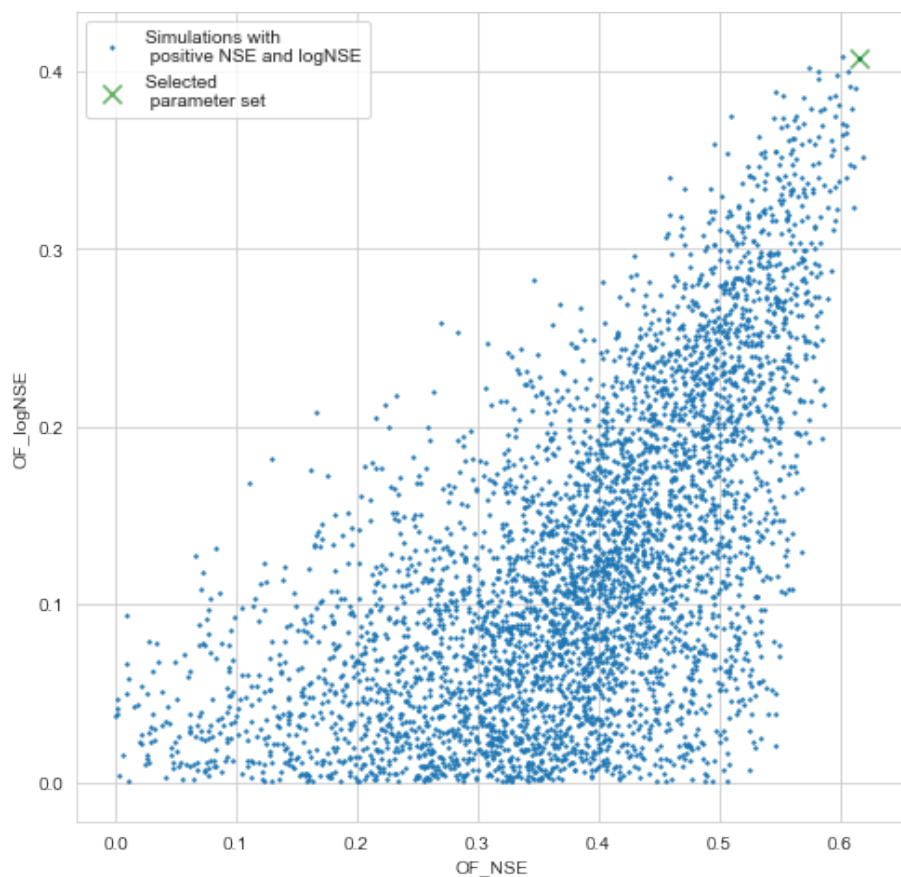


Figure 36: Illustration of parameter selection for the rainfall-runoff model of the Ruliba station catchment. The selected parametrisation yielded a compromise between performance measured by the logNSE and NSE indicators.

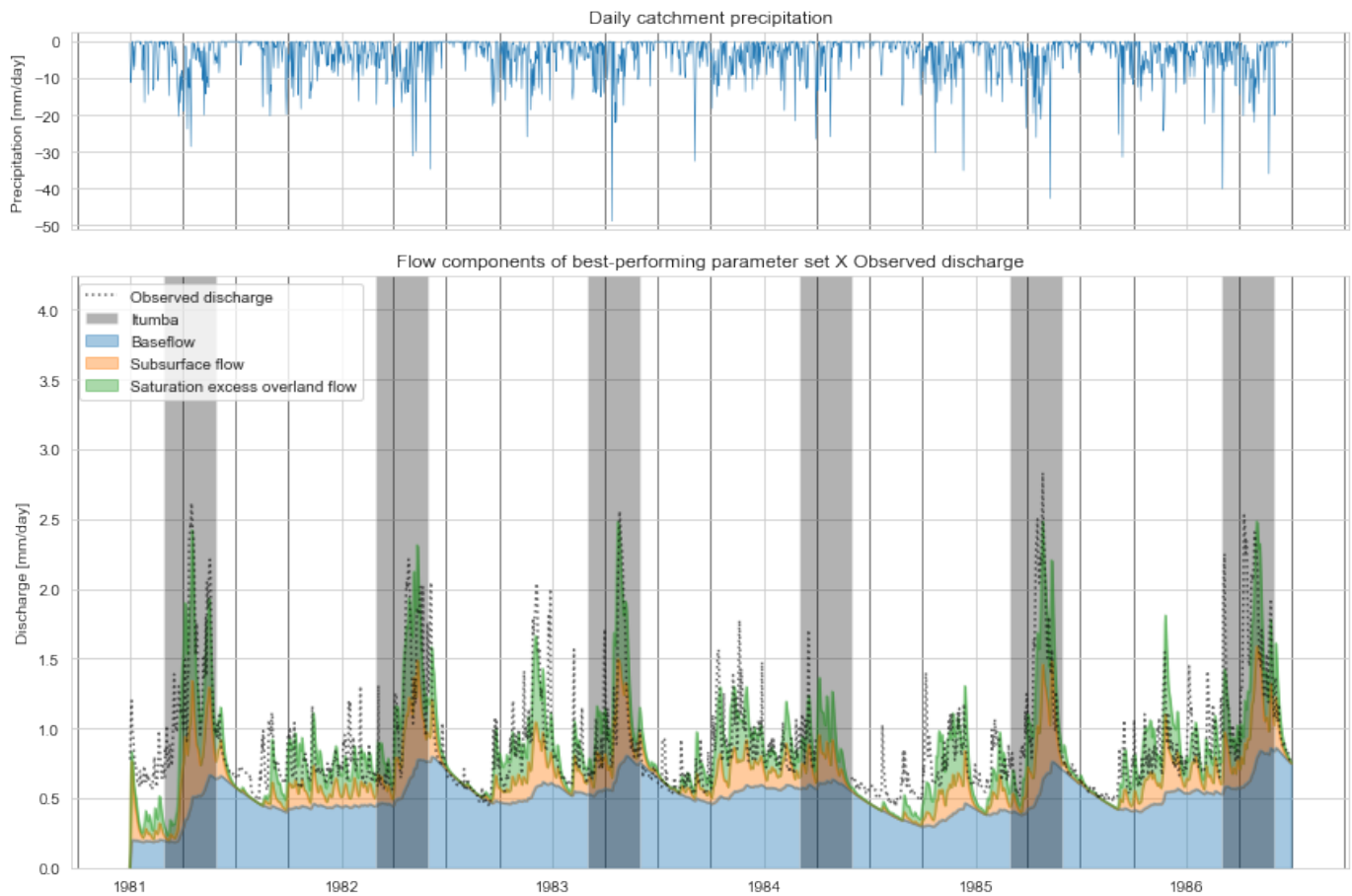


Figure 37: Simulated discharges at the Ruliba station for the calibration period, split into runoff components and compared against reference discharges. The main rainy season (Itumba) is highlighted on each year.

Akanyaru river catchment

The model for the Akanyaru river catchment has been calibrated against the discharge time series generated through the process described in section 3.4.2. As previously mentioned, it is relevant to remark that due to the considerable uncertainty propagated from the original discharge estimates at the Ruliba and Kanzenze stations and the adopted routing procedure, the model devised at this stage had the function of providing sound estimates of the seasonal fluctuation in discharges without the goal of precisely reproducing the discharges against which it was calibrated. Due to this factor, a low model performance was expected and observed. However, as visible in Figure 38, the model can be said to have met, to a reasonable extent, the goal of matching seasonal discharge oscillations in the Akanyaru river catchment.

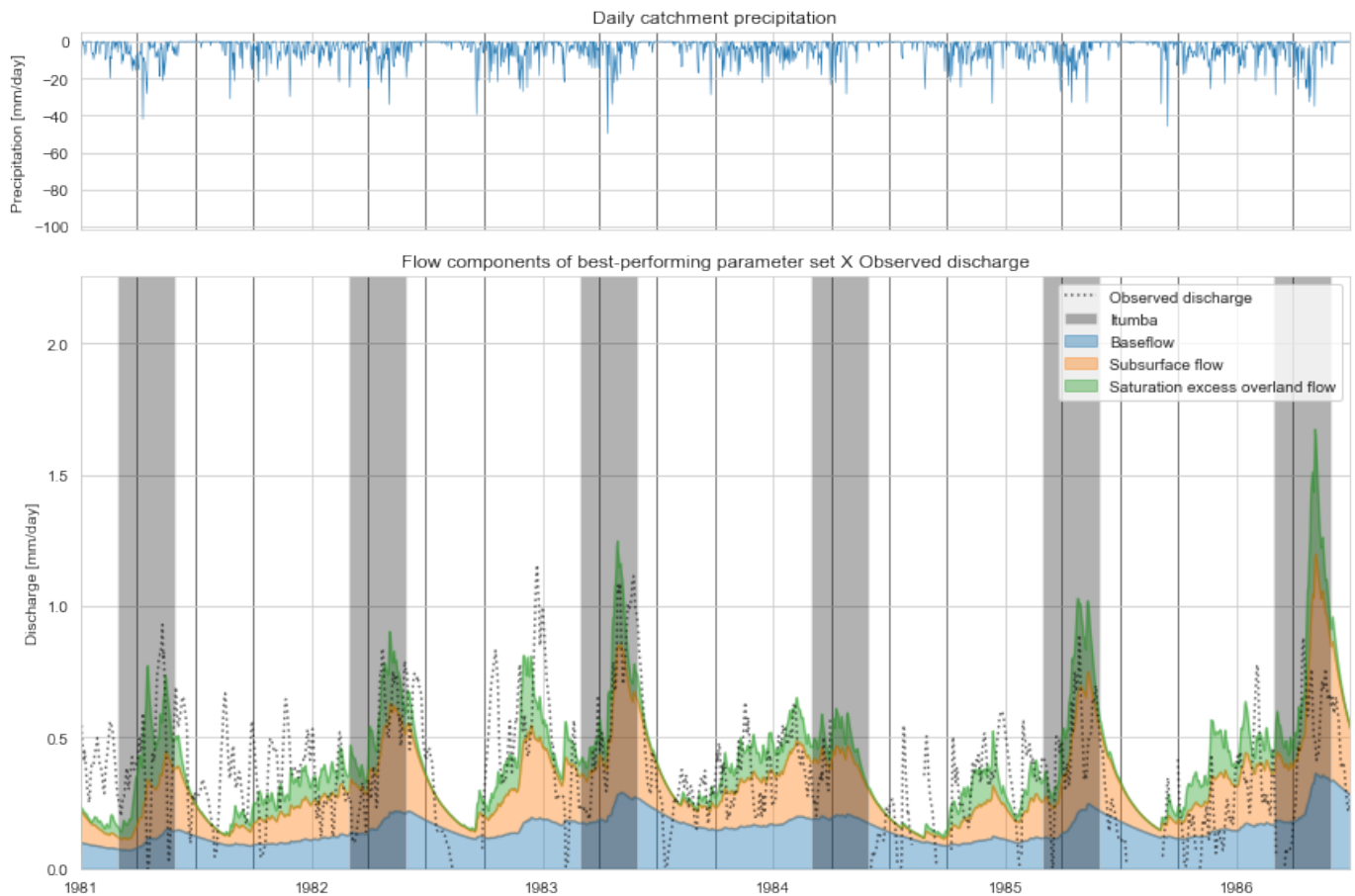


Figure 38: Simulated discharges at the Akanyaru river outlet for the calibration period, split into runoff components and compared against reference discharges. The main rainy season (Itumba) is highlighted on each year.

Due to the uncertainty in the data against which the model was calibrated, the verification of the model output was regarded as particularly relevant for the Akanyaru catchment. The lack of discharge observations in the vicinities of the Akanyaru river outlet led to the adoption of an empirical approach. This consisted in scaling the simulated discharges by the size of the Gihinga station catchment and comparing them with the available gauge height observations for the corresponding time steps. The different dimensions of the two time series [$L.T^{-1}$] for the model output and [L] for the observations without a defined relationship between them (i.e. rating curve) prevent an accurate comparison from being carried out. However, the two variables are expected to be monotonically related, and therefore to follow the same trends. As illustrated in Figure 39, in spite of short-term oscillations, this is verified on a seasonal basis. The observation that given discharge values correspond to higher water levels in the end of the series than in the beginning can be associated with cross-section changes, which has been observed for several stations in Rwanda (RIWSP, 2012a).

Figure 40 illustrates the apparent gains in performance obtained by the implementation of a hydrological model. The vertical axis on the left plot shows the discharges at the Akanyaru river outlet estimated according to the procedure described in section 3.4.2, scaled by the area of the Gihinga station catchment. This was the data against which the model was calibrated. The horizontal axis illustrates the gauge heights recorded at this station at the corresponding days. A distinction is made between gauge height points collected before 1990 and after 2010 due to the gap in observations and possible occurrence rating curve shift in this period, as discussed above. For this source of discharge data estimates, spearman correlations of 0.70 and 0.39 were observed for the pre-1990 and post-2010 period, respectively.

The right plot comprises the same data shown in Figure 39 in the dates for which gauge height observations are available – that is, the equivalent of the left plot with the discharge estimates replaced by

those of the calibrated model. Although the rating curve at this location is not known, a clear monotonic relationship between estimated discharges and observed gauge heights is visible. This is supported by the obtained spearman correlations: of 0.80 and 0.95 for the pre-1990 and post-2010 period, respectively. Some of the remaining scatter may be explained by the extensive floodplains between the station and the outlet of the Akanyaru river, which are likely to cause temporary storage similarly to what is hypothesised for the segment downstream of the Ruliba station.

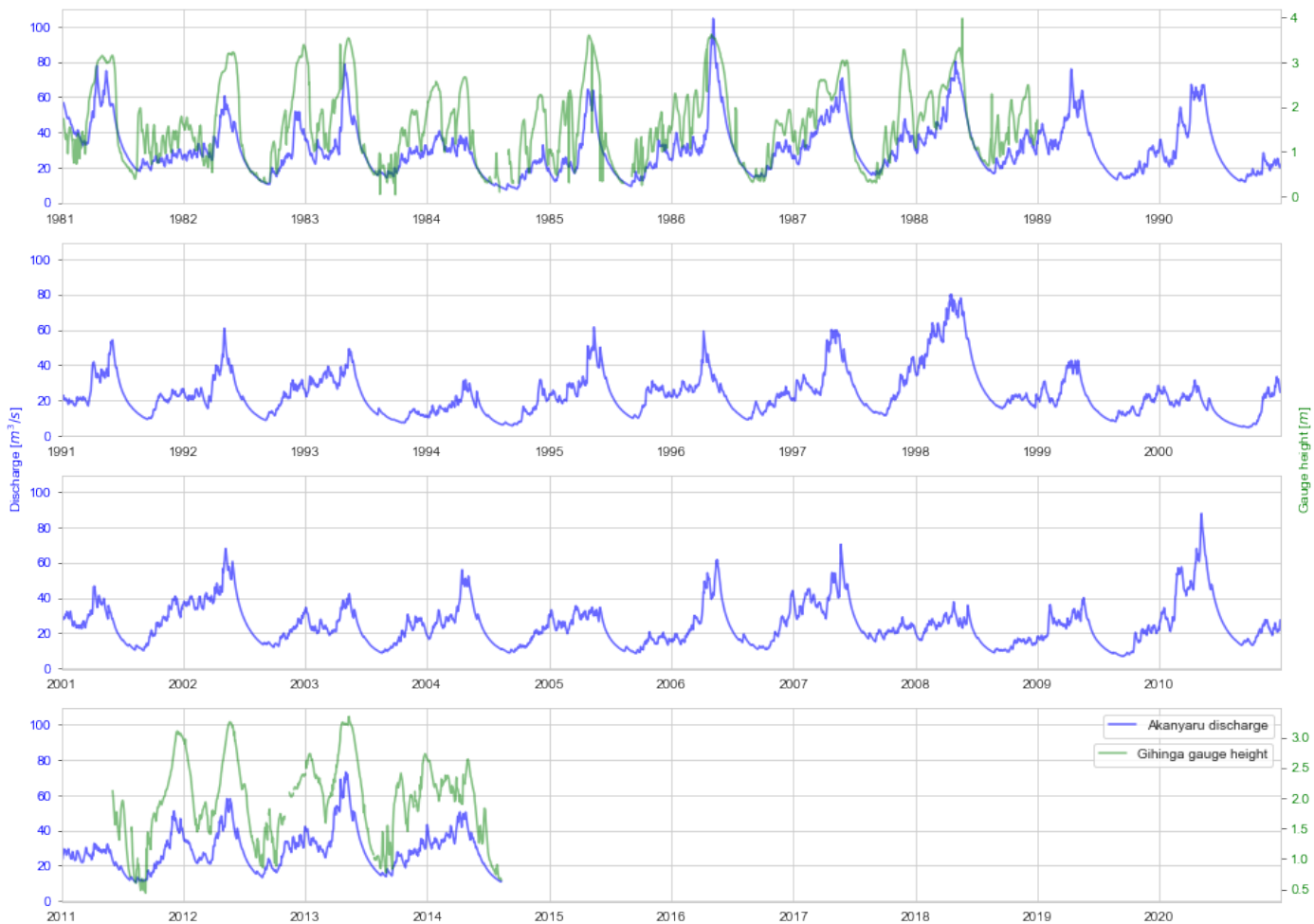


Figure 39: Time series of the calibrated Akanyaru model output and available gauge height observations at the Gihinga station.

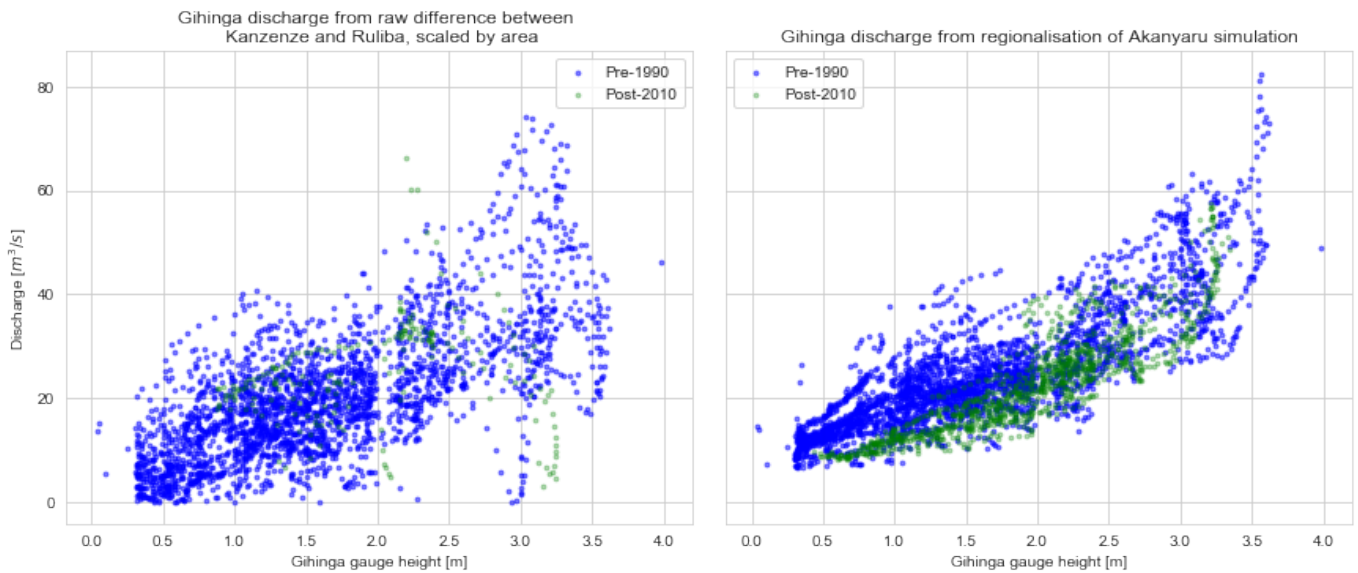


Figure 40: Observed gauge height at the Gihinga station and (a) raw incremental discharge between Ruliba and Kanzenze station and (b) Akanyaru model output after regionalisation by the area of the Gihinga station. In both cases discharges have been scaled by the area of the Gihinga station catchment.

4.1.1.4 Comparison with observed discharges at the Kanzenze station

After the estimation of discharge time series for the three contributing areas depicted in Figure 17, these were added up (i.e. a scenario without the Shyorongi reservoir) and compared to available discharge observations at the Kanzenze station⁸, illustrated in Figure 41. Based on visual interpretation, it can be inferred that the semi-distributed model provides a reasonable reproduction of the seasonal discharge behaviour at the location – further considerations on performance are given in chapter 5. However, a significant error is introduced in the empirical exceedance probabilities, particularly for discharges near the adopted bankfull threshold.

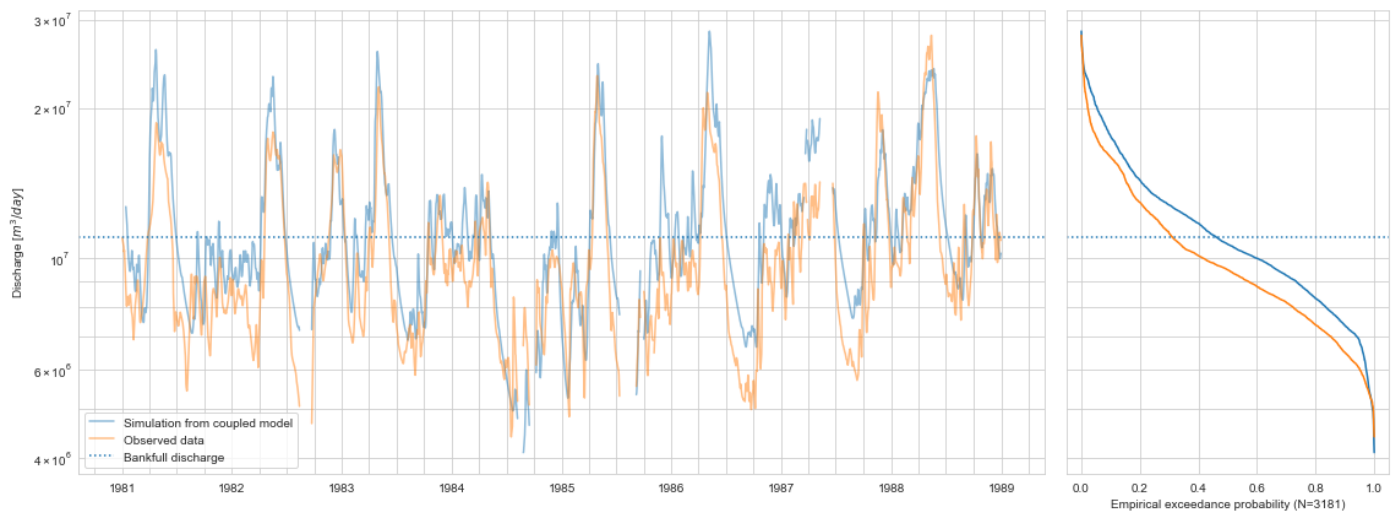


Figure 41: Time series and flow duration curves for reference data and model simulation for the Kanzenze station for the corresponding dates.

⁸ Model outputs corresponding to periods with no observations were removed from this analysis.

4.1.1.5 Estimation of Shyorongi reservoir inflows

As mentioned in section 1.1, Abimbola et al. (2017) provide a comprehensive study on the regionalisation of catchment signatures in Rwanda, with a considerable influence of precipitation on mean (specific) discharge for several stations. However, most previous studies have adopted an area-based regionalisation for discharges; e.g. Pandey (2014) obtained a correlation coefficient of 0.979 between catchment area and mean annual discharge for records of 7 stations in Rwanda.

The feasibility study of the Shyorongi reservoir (EDCL, 2016) established a linear function relating catchment area to the respective mean annual discharges of the Mwaka, Ruliba and Kanzenze stations:

$$Q_{annual} = 0.288 \times A + 411.7 \quad (29)$$

Where Q_{annual} is the mean annual discharge for a given catchment [$10^6 \text{ m}^3 \cdot \text{year}^{-1}$] and A is the catchment area [km^2]. This was employed to estimate a scaling factor between the mean annual inflows to the Shyorongi reservoir based on its catchment area and the mean annual discharge at the Ruliba station as:

$$\frac{Q_{in,Shyorongi,annual}}{Q_{Ruliba,annual}} = \frac{0.288 \times A_{Shyorongi} + 411.7}{2952} = 0.77261 \quad (30)$$

Where the units of the nominator and denominator are $10^6 \text{ m}^3 \cdot \text{year}^{-1}$. This relationship was assumed to hold for daily discharges, leading to the adoption of the following relationship for the estimation of daily inflows to the Shyorongi reservoir based on daily discharges at the Ruliba station:

$$Q_{in,Shyorongi,daily} = 0.77261 \cdot Q_{Ruliba,daily} \quad (31)$$

Based on the approximation that the discharges at the Ruliba station are composed by the sum of discharges from the Shyorongi reservoir catchment and the Nyabugogo river, one has:

$$Q_{Nyabugogo} = (1 - 0.77261) \cdot Q_{Ruliba,daily} \quad (32)$$

Formulas 31 and 32 were adopted for the partition of the simulated discharges at the Ruliba station between (regulated) inflows to the Shyorongi dam and (unregulated) discharges from the Nyabugogo river.

4.1.2 Reservoir modelling for different scenarios

The goal of this study comprised the analysis of the discharge behaviour at the Masaka wetland under different reservoir operational scenarios. For this purpose, the following scenario families were assessed:

- A. **No-reservoir** (i.e. baseline)
- B. Emphasis on **hydropower** generation assuming a capacity factor ranging from 0.2 to 0.6 (corresponding to a mean daily target electricity generation of 8.7 to 26.1 MW, respectively – see equations 33 and 34 below)
- C. **Flood mitigation** (i.e. reduction of downstream peak discharges) with limit releases ranging from $50 \text{ m}^3 \text{ s}^{-1}$ to $250 \text{ m}^3 \text{ s}^{-1}$

The capacity factor (cf) consists of “the ratio of the net electricity generated (E_{gen}), for the time considered, to the energy that could have been generated at continuous full-power operation during the same period (E_{pot})” (U.S. NRC, 2018), or:

$$cf = \frac{E_{gen}}{E_{pot}} \quad (33)$$

Therefore, the electricity output for a given period can be estimated by multiplying the installed capacity by an assumed capacity factor:

$$E_{gen} = cf \cdot E_{pot} \quad (34)$$

Since no specific information on the planned operation of the reservoir was available at the moment of the elaboration of this study, ranges of values were adopted within reasonable amounts. The purpose was to generate envelopes that reflect the largest range of results that can be expected under reasonable assumptions for the capacity factor and the target downstream release.

Key assumptions made for the simulation of the reservoir are:

- a. Constant active storage capacity over the entire simulated period
- b. Negligible water withdrawals for agriculture and urban water supply
- c. Constant target electricity generation (for the hydropower scenarios) or target maximum downstream release (for the flood mitigation scenarios)

Although there is extensive literature and scope for the development and implementation of optimised operating rules for reservoirs with the purpose of flood mitigation – e.g. (Votruba and Broža, 1989, Wurbs Ralph, 1993, Zhao et al., 2014) – this was outside the scope of the current study.

4.1.3 Coupled rainfall-runoff and reservoir modelling

After the estimation of discharge time series for the three contributing areas depicted in Figure 17, these were linked to a reservoir model. The following sub-sections describe the implementation of the different scenario families to be simulated.

4.1.3.1 SOP: Hydropower

A standard operating policy (SOP) was adopted for the simulation of the Shyorongi reservoir with the goal of maximising electricity generation. This was implemented as the following sequence, for each time step:

- i. Compute the reservoir active storage after accounting for inflows, direct precipitation and evaporation
- ii. Estimate the storage elevation based on the storage x head curve
- iii. Estimate the head based on the elevation
- iv. Estimate the discharge (D_{hydro}) required to meet the daily hydropower generation target (E)
- v. If:
 - a. the active storage is below the required discharge, release the active storage (reservoir emptying)
 - b. the active storage is above the required discharge: release the required discharge
- vi. For the latter case, if the stored volume after releasing the required amount for electricity generation is still greater than the total reservoir capacity, spill the excess volume until the reservoir is in full capacity.

These steps are illustrated in Figure 42. The total storage capacity of the reservoir was adopted from the feasibility study (see section 3.3), and the storage x head curve was derived by subtracting the elevation of the reservoir outlet from the elevations in the provided storage x elevation curve. Due to the limited availability of remaining data, the following key assumptions were made:

- a. The elevation of the reservoir outlet is approximately equal to the elevation of the bottom of the reservoir.

b. The overall efficiency in conversion of hydraulic energy into electrical energy is 85%.

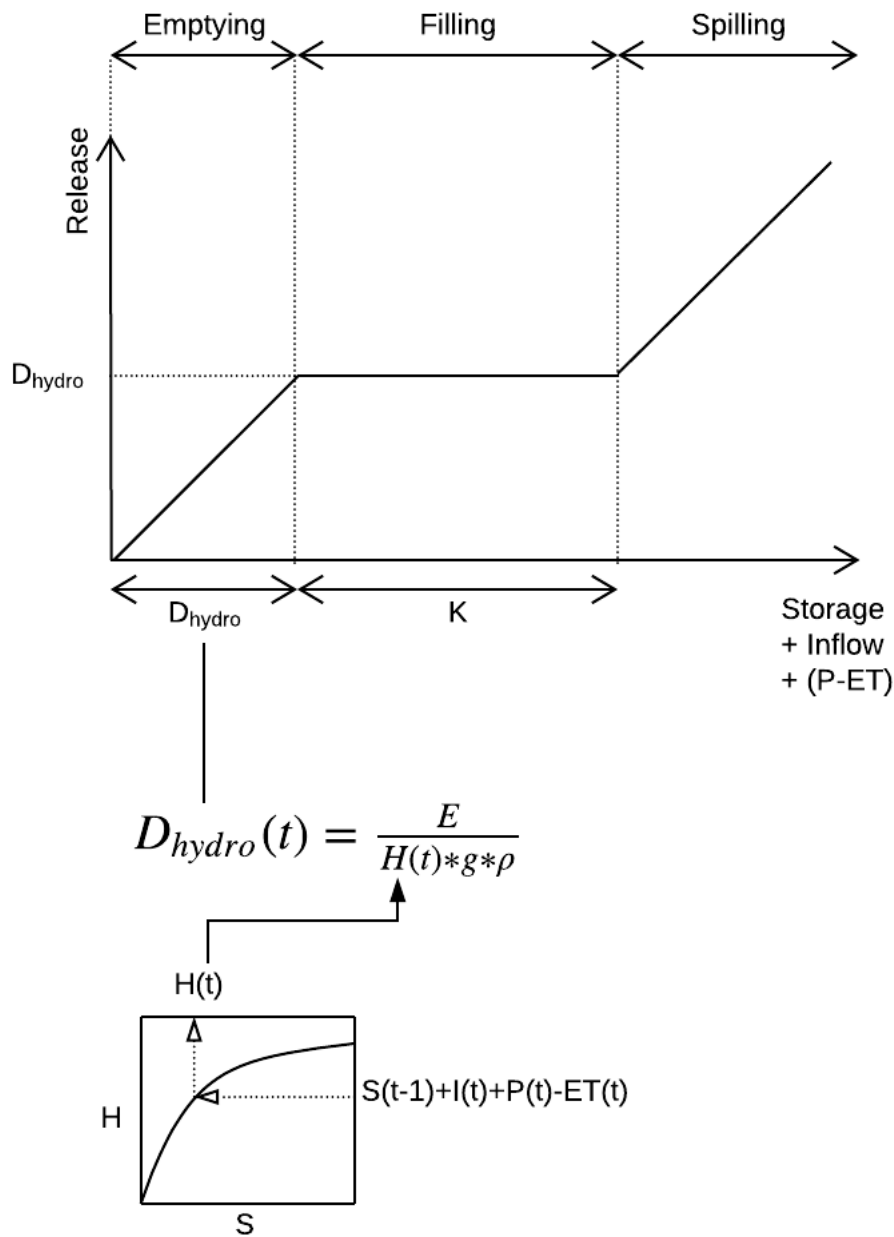


Figure 42: Illustration of the implemented standard operating policy assuming a reservoir operated with the primary goal of hydropower generation (storage corresponds to active storage volume at the beginning of a given time step).

4.1.3.2 Flood prevention

The flood prevention policy was implemented with the goal of reproducing the behaviour represented in Figure 3. It can be interpreted as a particular case of the SOP for the hydropower scenario family described above, where the release target is not a function of the head but instead a fixed value. In practice, the policy consists of emptying the reservoir at the end of each time step as long as the resulting released volume does not imply a discharge that exceeds the specified threshold (emptying phase). If emptying the reservoir

would cause a downstream discharge above this value, the volume corresponding to the maximum allowable discharge over a day is released and the exceeding volume is stored into the ensuing time step (filling phase). If the exceeding volume is greater than the available storage volume at the current time step, the available storage is filled and the remaining volume is spilled (spilling phase).

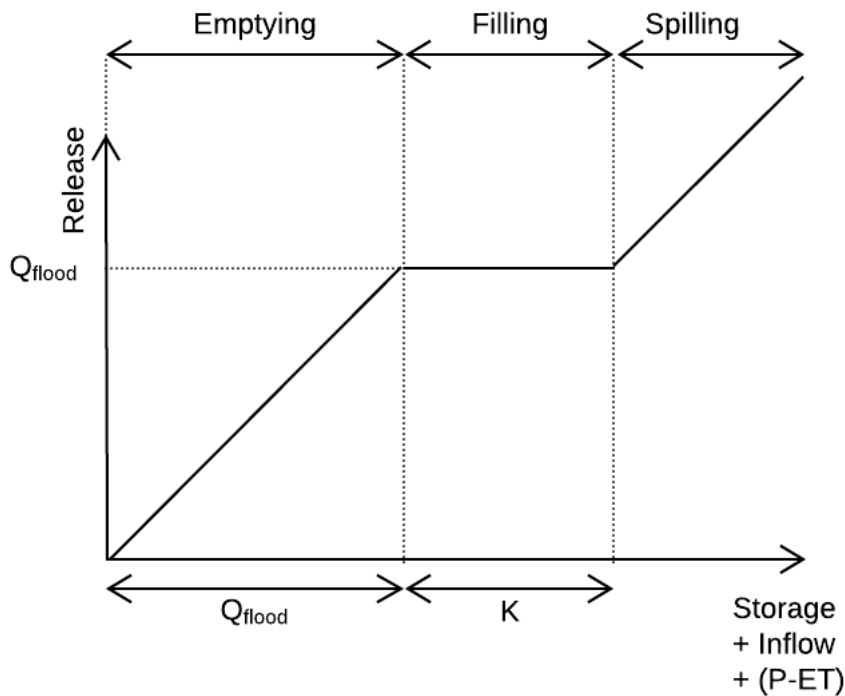


Figure 43: Illustration of the implemented standard operating policy assuming a reservoir operated with the primary goal of minimising downstream peak discharges. Q_{flood} corresponds to the prescribed maximum reservoir release for each scenario.

4.2 Estimation of flood peak probability distribution

In line with the objective and hypotheses of this study, the probability distributions of peak seasonal discharges were estimated. The same procedure was applied to the number of consecutive days with discharge estimated to exceed bankfull conditions in the Masaka wetland. For this purpose, the Peaks-Over-Threshold (POT) method (also referred to as partial duration series approach) was adopted. This choice was initially motivated by the possibility of enhancing the use of the generated discharge time series and reducing the confidence interval range in comparison to the Annual Maxima (AM) approach (Goda, 2010, Loucks and Van Beek, 2017, Coles, 2001).

An outline of the implemented procedure, adapted from Cunnane (1989), Coles (2001) and Goda (2010), follows in the coming sections. While specific results obtained for the no-reservoir scenario are presented for illustration purposes, the same steps were adopted for the peaks simulated for each scenario.

4.2.1 Peak selection

Peaks can be extracted from a time series by setting minimum width and height – i.e. the threshold – criteria. The identification of peaks followed a compromise between maximising the size of the statistical population while ensuring their independence. This was sought by means of analytical procedures aided by visual inspection on an iterative process, by adjusting the minimum peak height and width.

The independence between values is a key pre-requisite for the estimation of a probability distribution, and is generally satisfied in the case of annual maxima Cunnane (1989). In the case of the POT method, several different approaches have been adopted in order to meet this criterion (Cunnane, 1989).

Minimum width

The autocorrelation function of the discharge time series provides an indication of the minimum peak width criterion to be adopted in order to ensure independence, and is illustrated in Figure 44. A maximum autocorrelation value of 0.50 was initially adopted and later adjusted to 0.54 by visual inspection. The selected value corresponds to a lag time of 38 days, which was adopted as the peak width.

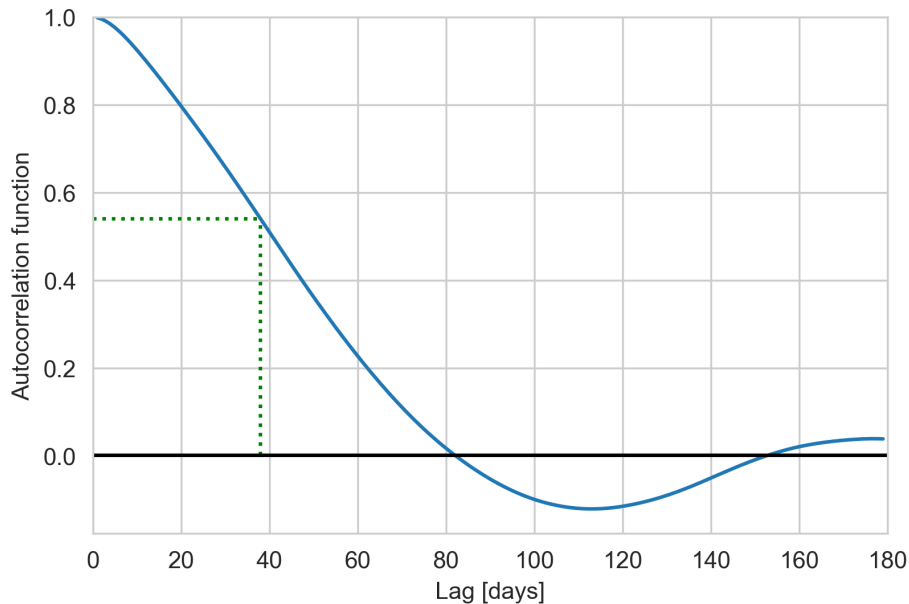


Figure 44: Autocorrelation function for simulated discharges at the Kanzenze station, and selected maximum correlation and corresponding lag time value, adopted as minimum peak width

The large peak width value required to ensure independence among peaks in the retrieved sample meant that the analysed population consisted, in its majority, of annual maxima. Considering that the distribution-fitting procedure is the same for both POT and AM approaches (Goda, 2010), this did not require any methodological adaptations. However, it is likely to have significantly affected the performance of different extreme value distributions.

Threshold selection

The selected threshold value has a direct impact on the performance of different distributions (Cunnane, 1989).

Following the adoption of the peak width, a minimum height (threshold) of $157.5 \text{ m}^2\text{s}^{-1}$ was selected by visual inspection. The selection of a threshold involves a compromise between bias (for an exceedingly low threshold) and variance (for an exceedingly high value) (Coles, 2001). In general, the threshold should be set as low as possible as long as the model provides an acceptable fit.

The adoption of these criteria resulted in the selection of 39 events (N_T), which are illustrated in Figure 45, where the annual maxima are plotted for comparison. It can be observed that, due to the strong seasonality in the rainfall pattern of Rwanda (see section 2.2), a relatively large peak width has to be adopted in order to ensure independence between peaks. As a result, most of the peaks selected through the POT criterion coincided with the annual maxima of the respective years.

The period spanned by the total discharge time series (K) ranges from 09/01/1981 to 31/08/2018, and hence $K = 37.7$ years. The mean rate of extreme events (λ) is hence:

$$\lambda = \frac{N_T}{K} \cong 1.04 \text{ events/year} \quad (35)$$

4.2.2 Estimation of return periods

The return period can be defined as the average of the periods of time separating successive flood peaks (Cunnane, 1989). Once a cumulative distribution function $F(x)$ and parametrisation have been selected, they can be used to estimate the exceedance probability of any given value (within the domain for which the function is valid), and hence its return period $R(x)$. In the case of the peaks-over-threshold approach, the return period of a given value is estimated as (Cunnane, 1989):

$$R(x) = \frac{1}{\lambda(1 - F(x))} \quad (36)$$

Hence, the associated return period for a given value x is:

$$F(x) = 1 - \frac{1}{\lambda \cdot R(x)} \quad (37)$$

and

$$x = F^{-1} \left(1 - \frac{1}{\lambda \cdot R(x)} \right) \quad (38)$$

Where F^{-1} is the inverse cdf or ppt function and λ is given by equation 35. It is highlighted that, as shown in Figure 45, in the current context the peaks-over-threshold largely coincide with the annual maxima and $\lambda \cong 1$. In this case, equation 36 (and hence equations 37 and 38) approaches the equivalent formulations for the annual maxima approach.

In line with equation 38, the first step for the estimation of return periods consists of the identification of a suitable function $F(x)$ to describe the probability distribution of seasonal peak discharges. Several formulas have been developed and adopted for this purpose (please refer to Cunnane (1989) for a discussion). Theoretical arguments alone are not able to select the most appropriate distribution function for floods, and its relevance is often secondary to that of empirical suitability (Cunnane, 1989). Hence, several candidate distribution functions were tested in the current study:

- a. Generalised Extreme Value distribution
 - a. Type I (i.e. Gumbel)
 - b. Type II (i.e. Fréchet)
 - c. Type III (i.e. Weibull maxima)
- b. Pearson Type III (i.e. 3-parameter gamma distribution)
- c. Generalised Gamma distribution
- d. Generalised Logistic distribution
- e. Generalised Pareto distribution

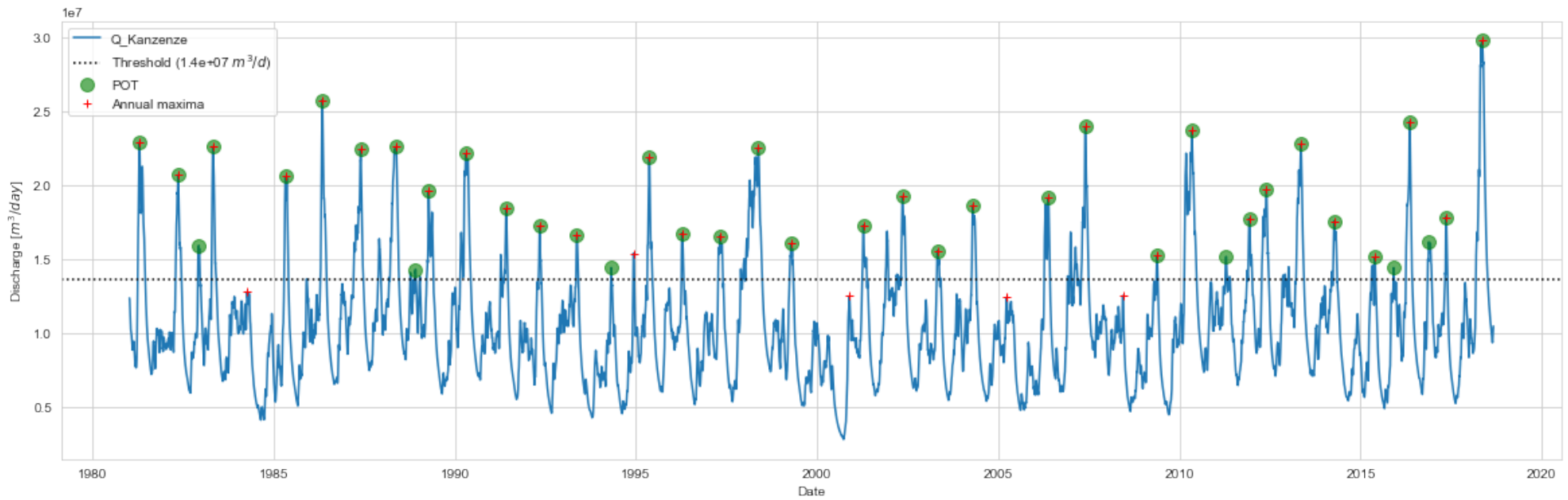


Figure 45: Simulated discharge time series and identified peaks over threshold (POT) for the no-reservoir scenario. Annual maxima plotted for comparison.

For every scenario, the optimal values for the parameters of each distribution were estimated by the method of maximum likelihood estimation (MLE), which is considered to yield a relatively low sampling variance (Cunnane, 1989). Adopting these parameters, the goodness-of-fit of each candidate function was assessed by the sum of squared residuals (SSR) between the theoretical cumulative distribution estimated by the fitted function and the empirical probabilities of non-exceedance of the original points. The performances of all tested distribution functions to the simulated peaks in all scenarios are summarised in Figure 46.

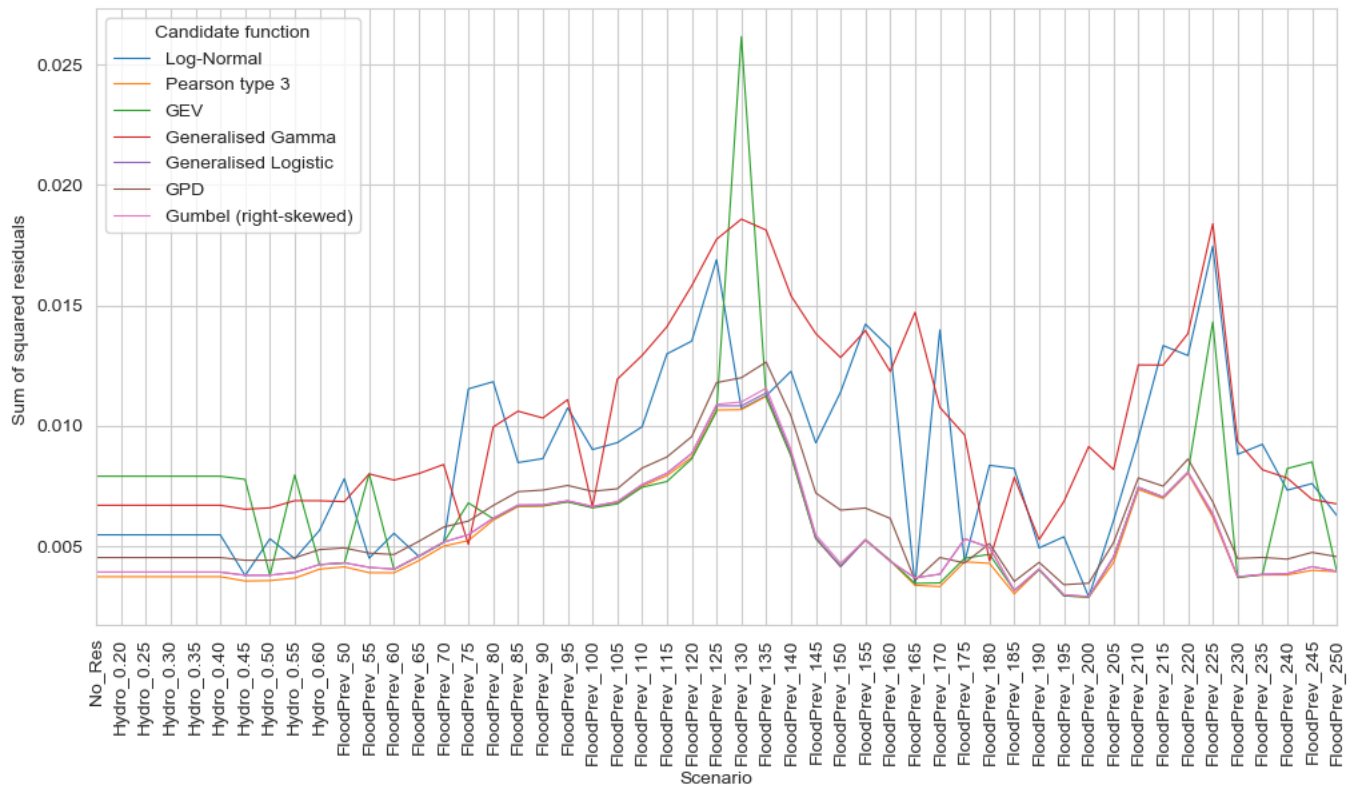


Figure 46: Sum of squared residuals for candidate extreme value distribution functions for all simulated scenarios. No_Res: no-reservoir scenario. “Hydro” and “FloodPrev” labels correspond to hydropower and flood mitigation scenarios, followed by the assumed capacity factor and target maximum downstream releases, respectively.

All distributions with an SSR value within 0.001 of the SSR value of the best-performing function were considered feasible distributions for the peaks of a given scenario. However, eventual Pearson type III fits with a negative skew coefficient – resulting in decreasing discharge estimates for increasing return periods – were excluded regardless of goodness-of-fit performance. The match between observations and the distribution function that aims to explain them can be illustrated in diagnostic plots (Coles, 2001). These are illustrated for the case of the Gumbel distribution fitted to the peaks simulated in the no-reservoir scenario in Figure 47.

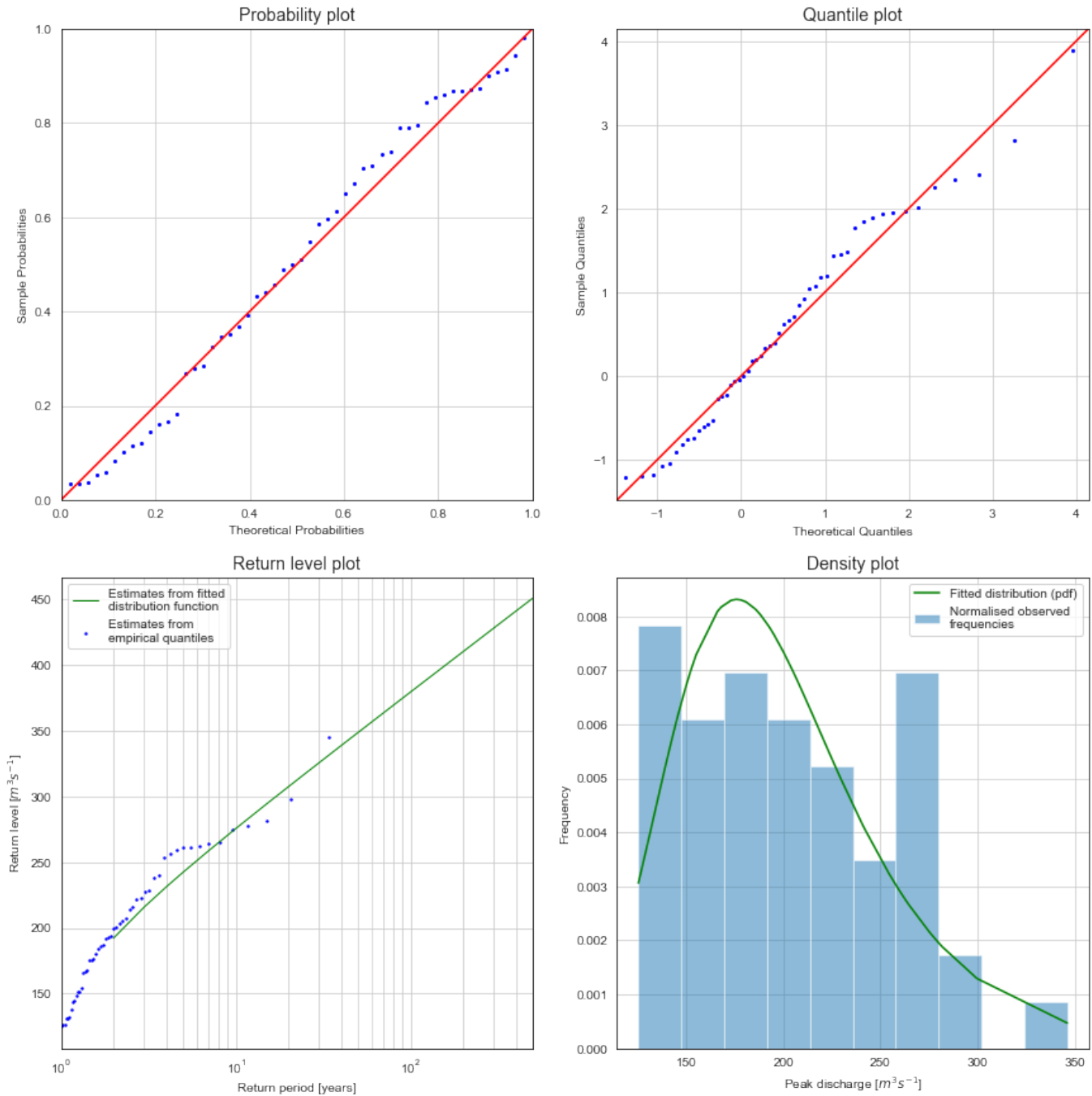


Figure 47: Diagnostic plots for Gumbel distribution fitted to the selected peaks of the simulated time series for the no-reservoir scenario.

In the POT method, extreme values are generally fitted to a Generalised Pareto Distribution (GPD) (Kang and Song, 2017). However, in the present study other distributions yielded consistently higher goodness-of-fit performances, as illustrated in Figure 46. This may be related to the fact that the reference population consisted largely of annual maxima, for which the GEV distribution is generally adopted (Kang and Song, 2017). In particular, the Gumbel distribution (i.e. GEV Type I) is commonly adopted for extreme values of river discharges (Vrijling and Van Gelder, 2002), and had good performances in this case too. This can be theoretically related to the fact that the entire populations of discharges were Gumbel-distributed for most scenarios, and hence their population of annual maxima may also be expected to follow this distribution (see demonstration in Vrijling and Van Gelder (2002)) – an illustration is provided in Figure 48.

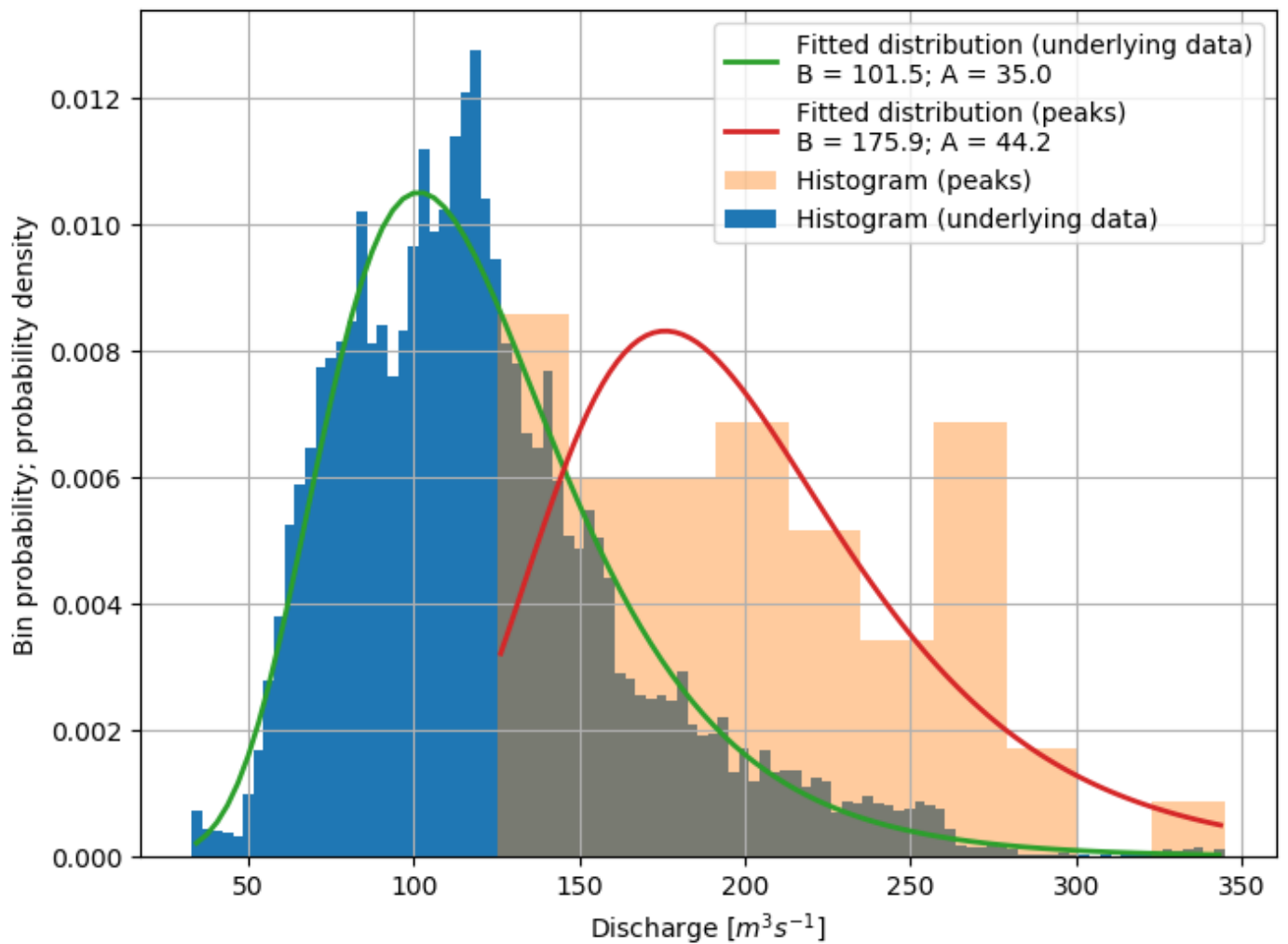


Figure 48 Density plot for entire discharge time series and annual peaks (no-reservoir scenario). A and B correspond to the values of the location and scale parameters of the Gumbel distribution that was fitted to both samples.

Estimation of confidence intervals for parametrisation and distribution type uncertainty

The determination of the parameters of an extreme value distribution involves uncertainty to some degree, even if the MLE approach tends to perform relatively better than others on this regard. In order to quantify, to some degree, this uncertainty, a pragmatic bootstrapping approach was adopted as described below.

- i. Retrieve the peaks for the no-reservoir scenario
- ii. Generate 10^5 samples with substitution
- iii. For each generated sample, estimate the location and scale parameters of the Gumbel distribution
- iv. Estimate the two-sided 95% confidence interval (i.e. 0.025 and 0.975 percentiles) of the distributions of the 10^5 values of the location and scale parameters (Figure 49)
- v. Estimate the confidence interval in estimated discharges for varying return periods by varying each parameter individually (Figure 50)
- vi. Estimate the confidence interval generated by the superposition of the confidence intervals of both shape and location parameters (Figure 51).

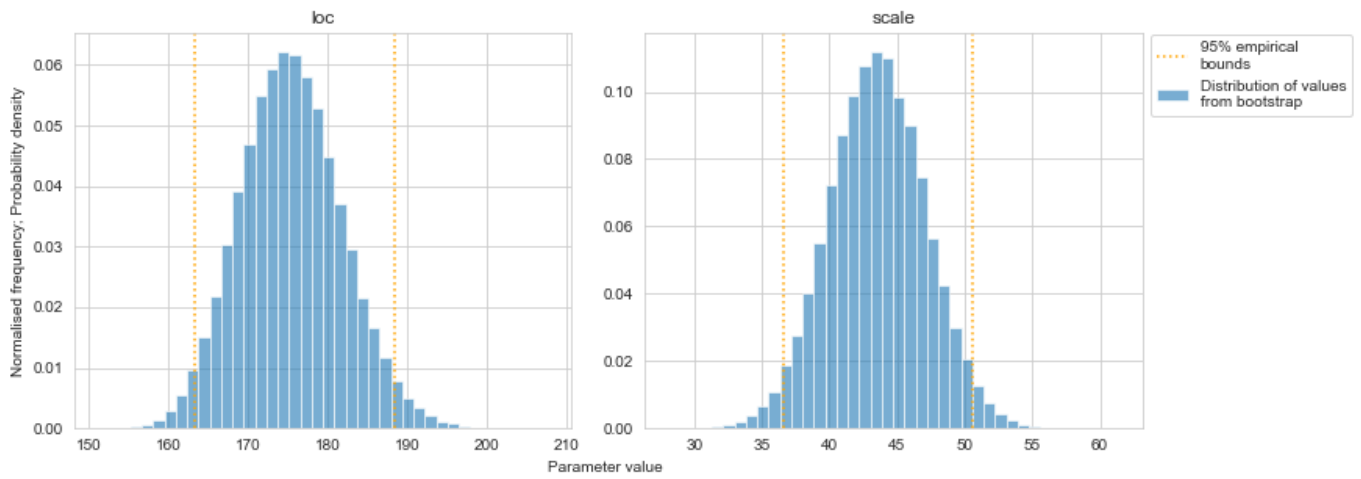


Figure 49: Distribution of MLE estimates for Gumbel parameters in 10^5 bootstrap samples of peak discharges for the no-reservoir scenario.

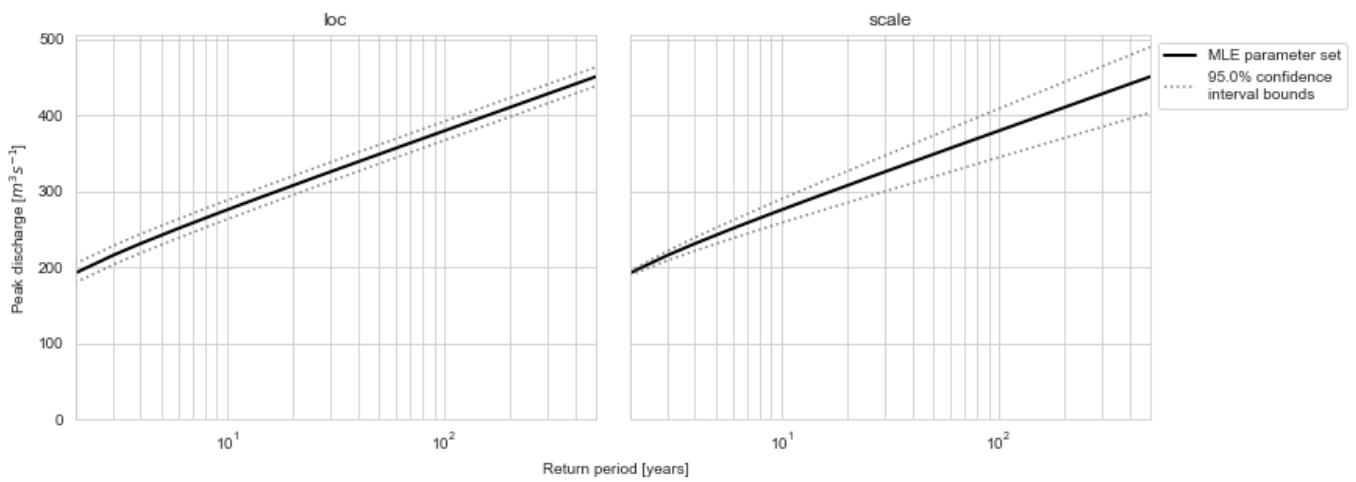


Figure 50: Return level plots with the respective 95% confidence interval of each parameter of Gumbel distribution. Plots share the same horizontal and vertical axes scales.

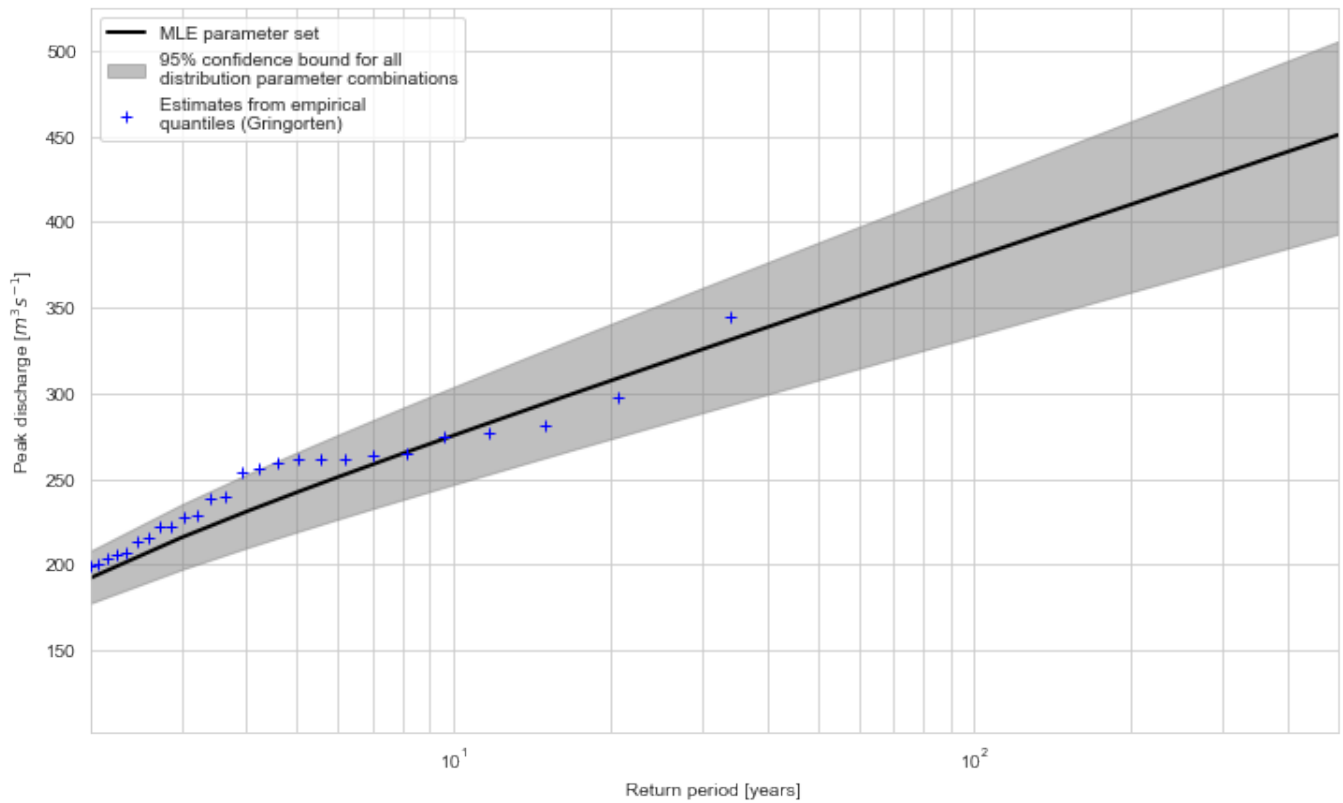


Figure 51: Return level plot for peak discharges generated in the no-reservoir scenario. Confidence bound indicates the range of estimates obtained with the parametrisation of the Gumbel function with 95% confidence for the scale and location parameters.

It is also known that different distribution families have remarkably distinct behaviours as return periods increase (Cunnane, 1989). For the no-reservoir scenario, the effect of adopting different potential distributions on estimated peak discharges for large return periods is illustrated in Figure 52.

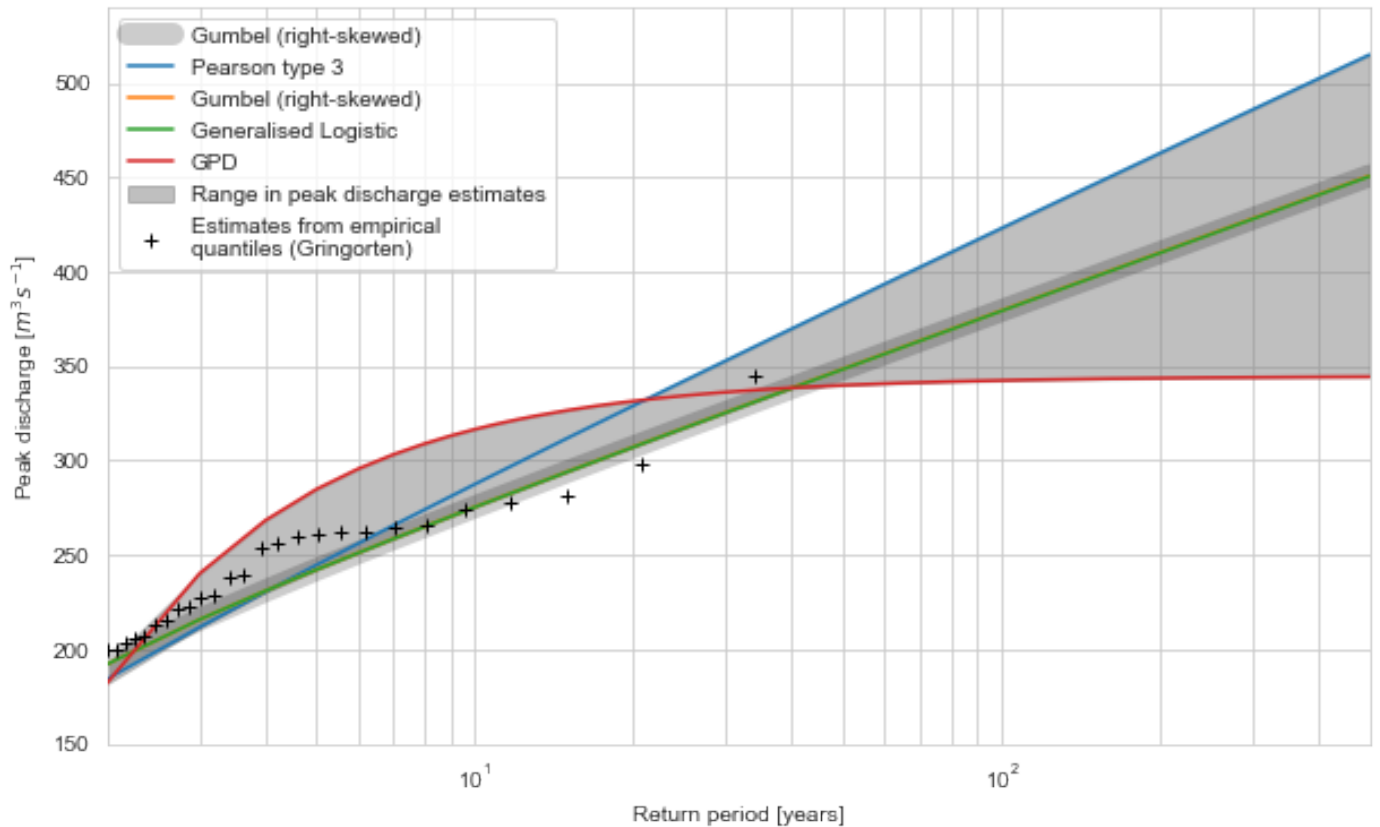


Figure 52: Return level plot for peak discharges generated in the no-reservoir scenario. Area illustrates the range in predicted peak discharges by different distribution functions fitted to the reference data. The exceedance probabilities estimated by the fitted generalised logistic distribution largely coincides with those of the Gumbel distribution, which was therefore highlighted.

4.3 Estimation of flood durations

Each of the simulated scenarios resulted in a time series of estimated daily discharges. For the purpose of estimating the periods of time with discharge corresponding to bankfull conditions and higher, a threshold of $127.5 \text{ m}^3\text{s}^{-1}$ or $1.102 \times 10^7 \text{ m}^3\text{day}^{-1}$ was adopted, as previously described. Flood durations were implemented as the period of time between the first day at which the bankfull discharge was exceeded and the day before the value returned to in-bank flow. Such flood durations were estimated for the time series of each scenario, and the highest value of each year in each series was retrieved. Flood events encompassing two years were allocated to the year when the discharge peak occurred.

5 Results and discussion

Figure 53 provides a comparison between the simulated discharges for the calibrated semi-distributed model on the no-reservoir scenario and reference discharges at the Kanzenze station. NSE and logNSE calibration values of 0.94 and 0.87 were obtained, respectively. Considering (a) the primary interest in seasonal hydrographs and (b) uncertainties in the reference data – particularly peak discharges – the obtained performance can be considered satisfactory.

Similar time series have been generated for each of the reservoir operating scenarios, as will be discussed in the coming sections. A differentiation is made between the discharge components originating from the Akanyaru river and those from the Nyabarongo river (refer to Figure 17 for the representation of these areas).

5.1 The relative contribution of the Akanyaru catchment to flooding and the potential for reservoir regulation

Hypothesis A referred to the relative influence of discharges from the Akanyaru river on flood occurrence in the Masaka wetland. For the analysis of this proposition, Figure 54 illustrates the simulated hydrographs for both discharge components on the same vertical axis scale. In spite of the spatial heterogeneity in precipitation and potential evaporation reported in section 2.2.1 and the different parametrisation of the calibrated models (see Table 5), the catchments have a remarkably similar seasonal pattern. This is justified by the strong seasonal signal in rainfall, which exists for both catchments in spite of differences over shorter time scales.

However, at a finer level of detail differences in the response of each catchment are visible. Figure 55 provides a representation of the proportion of the total simulated discharge originating from each catchment for the entire simulation period. Over most of the time, this the Akanyaru river discharge is smaller than what would be expected based on the fraction of the Kanzenze station catchment that it comprises. However, this contribution ranges from 7.6% to 43.1% of the total.

The variability in this proportion appears to follow, to some extent, a seasonal pattern, as illustrated in Figure 56. As seen in the left plot, periods of the year with higher total discharge tend to have a contribution from the Akanyaru catchment above the long-term mean. The right plot illustrates the simulated daily discharges during the months of March, April and May, when the most severe floods tend to occur. It is visible that most points plot to the right of the long-term ratio, indicating a relatively higher contribution of the Akanyaru catchment.

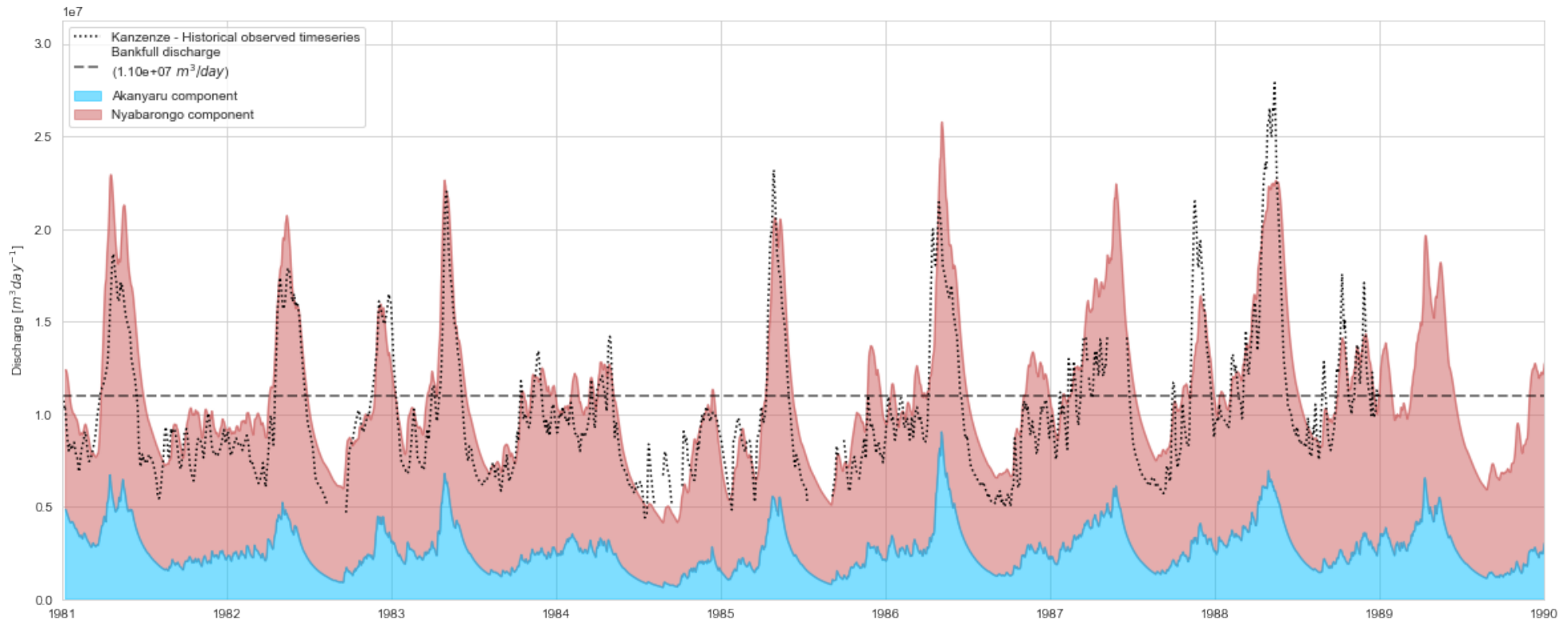


Figure 53: Output of semi-distributed model discretised by discharge components from the Nyabarongo and Akanyaru rivers for the 1981-1990 period. Reference discharge records at the Kanzeze station are plotted for comparison.

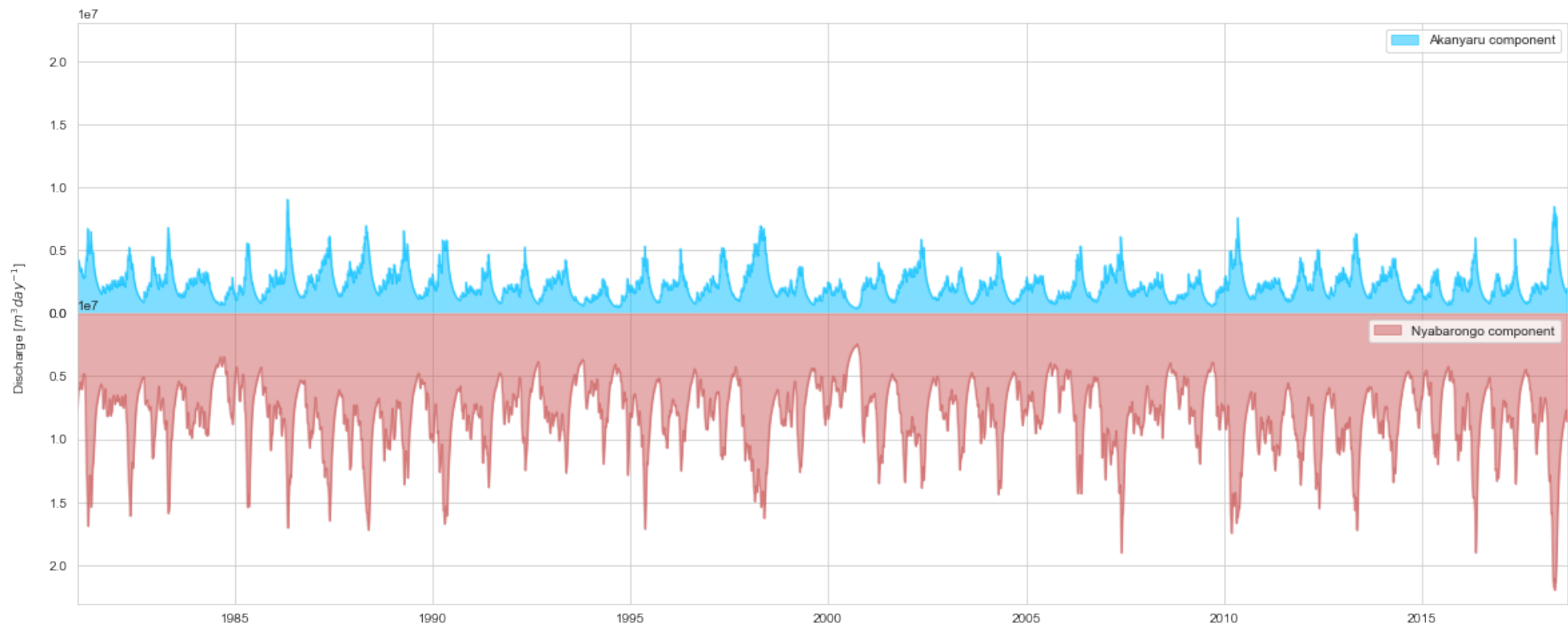


Figure 54: Contributions to total discharge at the Kanzenze station from the Nyabarongo river (above) and Akanyaru river (below) for the entire simulation period.

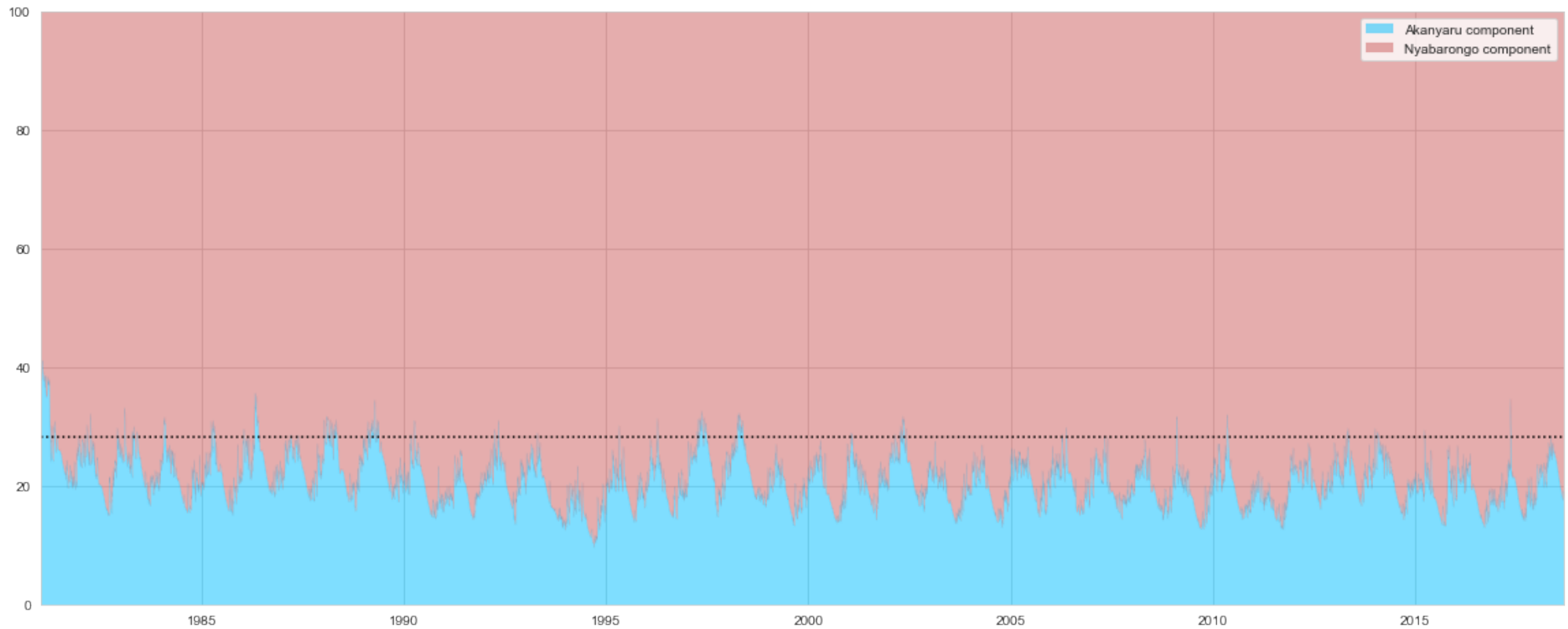


Figure 55: Relative (percentual) contributions to total discharge at the Kanzenze station from the Nyabarongo and Akanyaru rivers for the entire simulation period. The dotted line indicates the expected proportion in discharges based on the relative catchment sizes.

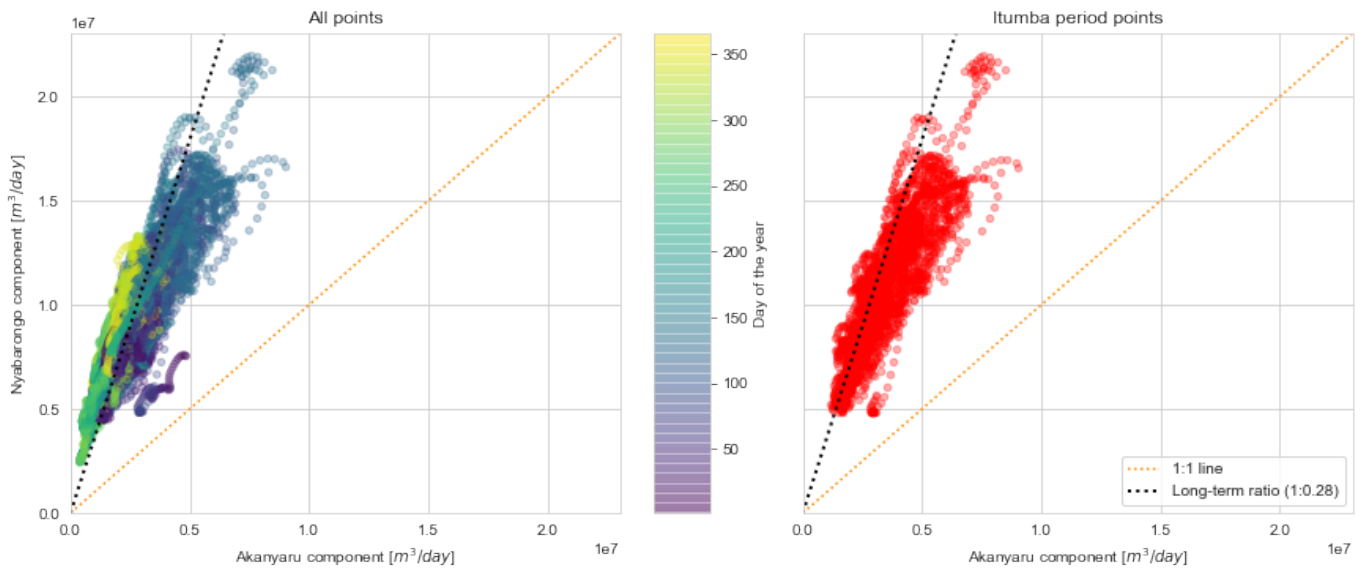


Figure 56: Comparison of contributions from the Akanyaru and Nyabarongo rivers to simulated daily discharges in the no-reservoir scenario, for the entire simulated period (left) and during the Itumba season (right).

Figure 57 illustrates, in blue, the cross-correlation function between the daily forcing precipitation data of the Nyabarongo (i.e. Ruliba station) and Akanyaru river catchments. It is visible that considerable correlation exists for precipitation in the different catchments on a given day (i.e. no shift), with a step decrease in correlation for varying shift values. In contrast, the peak in correlation of simulated discharges (shown in red) corresponds to a shift in three days on the simulations for the Akanyaru river discharge component. This can be at least partly associated with buffering caused by the linear reservoir through which discharges from the Nyabarongo river are routed in the model (see Figure 17 and accompanying description).

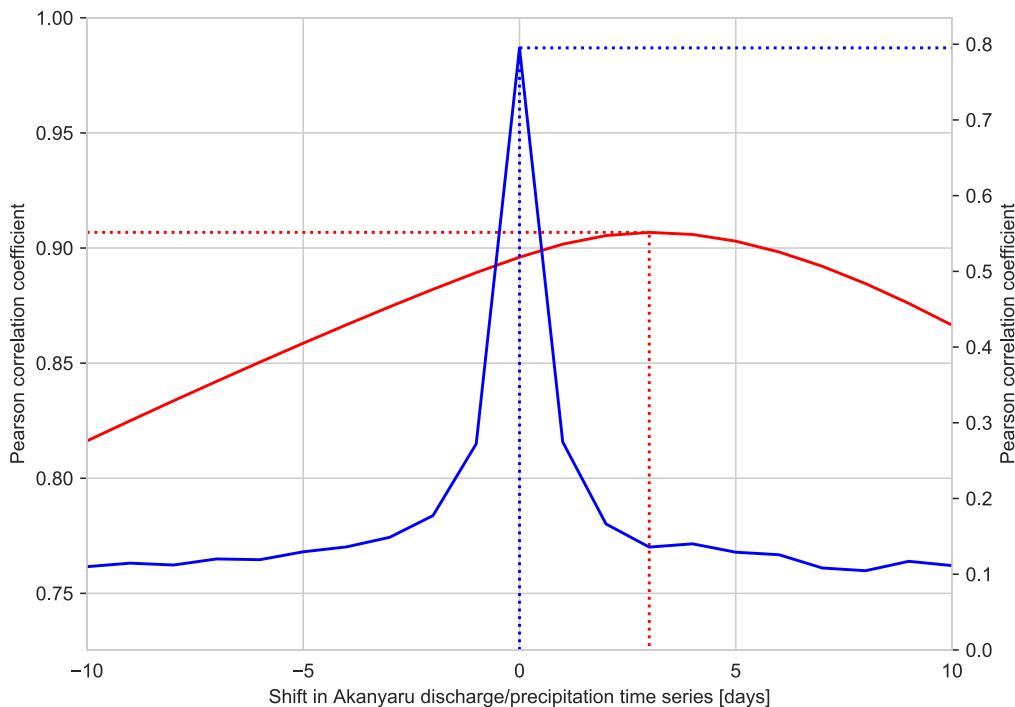


Figure 57: Cross correlation between area-aggregated rainfall time series (red; left vertical axis) and simulated discharge components (blue; right vertical axis) of the Nyabarongo and Akanyaru rivers for the no-reservoir scenario.

Considering the scope of this research and knowing the approximate mean long-term discharges of the Akanyaru and Nyabarongo rivers, it is relevant to investigate the maximum theoretical potential for reservoir regulation of each of them to influence flooding in the Masaka wetland. Figure 58 illustrates boundary cases in this respect: the total regulation of each of the two subcatchments individually, and the total regulation of both catchments. For demonstration purposes, the total regulation of each river is assumed to result in a constant discharge equivalent to its respective long-term mean. All plots are overlaid, for comparison, with the simulated discharge time series assuming negligible reservoir regulation; i.e. the current scenario.

The top plot indicates that a theoretical total regulation of the Akanyaru river would have a very limited effect on the seasonal discharge behaviour at the Kanzenze station, which is expectable due to its relatively limited contribution. In contrast, the regulation of the Nyabarongo river has the potential to significantly reduce the range of oscillation in discharges at the Masaka wetland; i.e.: to concentrate discharges in the vicinities of the mean value, as discussed in section 1.1.2.

However, in the present case regulation may reduce peak discharges but does not necessarily imply a decrease in flooding duration, as shall be illustrated in the next section. This is related to the relatively low banks at the Masaka wetland, which cause the bankfull discharge (estimated at $1.102 \times 10^7 \text{ m}^3 \text{ day}^{-1}$; see 2.1) to be close to the long-term mean discharge: $1.055 \times 10^7 \text{ m}^3 \text{ day}^{-1}$, as illustrated in the bottom plot. Considering the previously mentioned practical limitations for reservoir commissioning in both catchments, the degree of discharge regulation required to completely prevent flooding in the Masaka wetland – all other factors being constant – is unfeasible.

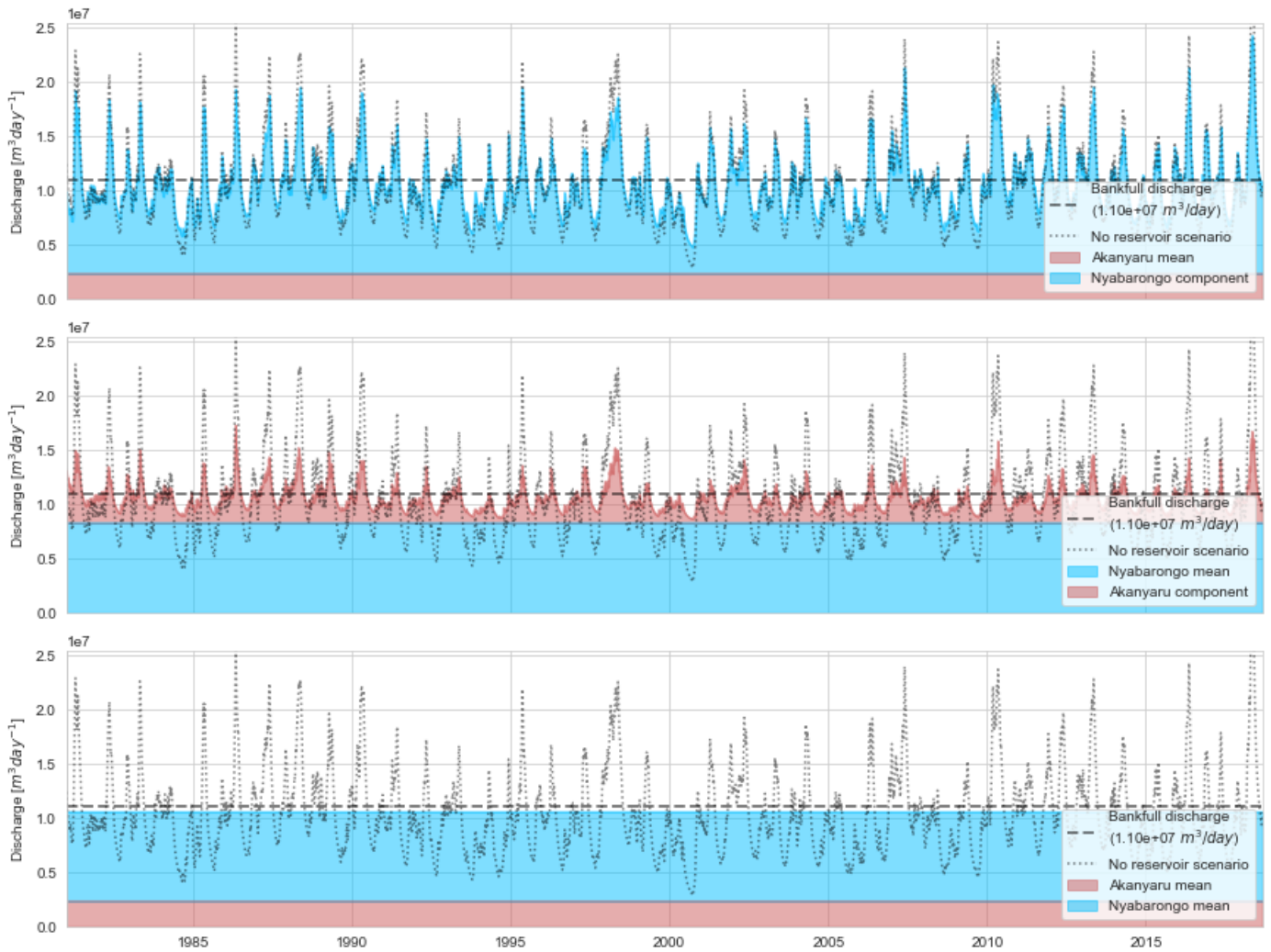


Figure 58: Hypothetical boundary scenarios for discharge regulation in the two main subcatchments of the Ruliba station catchment, from top to bottom: total regulation of the Akanyaru river, total regulation of the Nyabarongo river, total regulation of both rivers. Total regulation in this context is implemented by replacing simulated daily discharges by their long-term means.

5.2 A seasonal hydrograph example: the flood of 2018

In order to assist the interpretation of results illustrated in the coming section, one seasonal hydrograph is hereby described for different simulated scenarios. As mentioned in section 1.1, in 2018 several locations in Rwanda experienced floods described to have far exceeded the expected seasonal magnitudes. However, extensive routing through floodplains and the lack of a reliable and up-to-date rating curve at the Kanzenze station provide severe limitations to the estimation of the discharges in this period based on field observations. In this context, the hydrological model developed in the current study can provide an indication of the magnitude of the event at this location, as shown in Figure 59. Given that the Shyorongi dam has not yet been commissioned, this estimate corresponds to the simulation of the pre-reservoir scenario, which is shown as a thick black line in the plot.

This event provides an illustration of the range in seasonal hydrographs that could be expected had the Shyorongi reservoir already been commissioned, which reflect its potential future influence once in operation. The reservoir operation with the aim of flood mitigation provides varying levels of attenuation of the peak discharge, according to the imposed maximum downstream release value.

An apparent paradox is observed in that scenarios where a lower boundary was set for this value displayed higher peaks. This is explained by the limited storage capacity of the reservoir: lower release caps imply

that the reservoir reaches full capacity (and loses its regulation capability) earlier in the season. If this occurs before the peak of the inflow hydrograph, the reservoir effectively provides no peak attenuation.

The moment when the reservoir reaches full capacity is also visible for the hydropower scenarios as sudden increases in discharge occur and the hydrographs approach that of the no-reservoir scenario. Depending on the specified capacity factor and associated discharge for electricity generation, the reservoir may never (on an extreme case) reach full storage capacity. In contrast, when the required discharge is relatively small, the implemented SOP implies a fast filling and subsequent spilling of the reservoir.

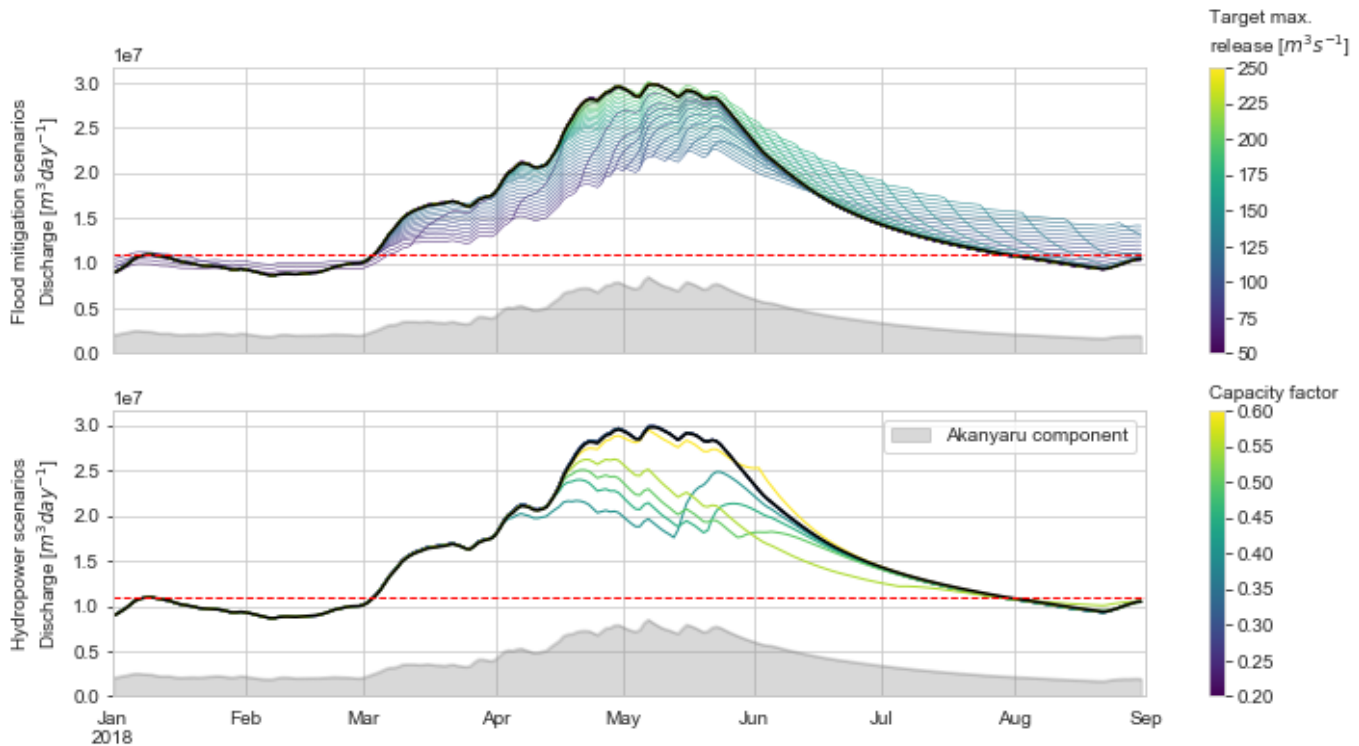


Figure 59: Simulated 2018 seasonal hydrograph for all flood mitigation and hydropower scenarios (top and bottom, respectively). The baseline scenario is overlaid on both plots for comparison. The Akanyaru river discharge component is constant for all scenarios. The discharges from the Nyabarongo river catchment for each scenario are given by the distance between the grey area and the respective lines.

It is, however, highlighted that the performance of different policies for both hydropower and flood mitigation scenarios is directly tied to the areas of the incoming hydrographs. Figure 59 and Figure 60 illustrate this phenomenon by comparing the hydrograph of 2018 with the relatively runoff volume of 2017 for flood mitigation and hydropower scenarios, respectively. In Figure 59, it is visible that a given target release policy ($120 \text{ m}^3\text{s}^{-1}$) results in a considerable reduction in the flood peak for the 2018 scenario. In this case, the reservoir approaches the conceptualised behaviour of a control reservoir shown in Figure 3, reaching full capacity at the end of the rainy season and gradually emptying over the ensuing months. In contrast, the very same policy has a negligible effect when the inflow hydrograph of 2017 is considered. Since during this year reservoir inflows were below $120 \text{ m}^3\text{s}^{-1}$ for nearly the entire period, the reservoir released all inflows and remained virtually empty over the rainy season.

Figure 61 provides a visual aid to the interpretation of the variability of performance in flood peak reduction for different scenarios over different years, and particularly in understanding the optimal performance of the $120 \text{ m}^3\text{s}^{-1}$ scenario in 2018. The bottom-right plot illustrates that, for a maximum release of $125 \text{ m}^3\text{s}^{-1}$, the reservoir is able to buffer all discharges in excess of this value that occur in the months of April and May. The stored volume at the end of the wet season corresponds to the integration of the difference in inflows and releases over this period; i.e. the area between the green line (inflows) and the top of the blue area (releases). This stored volume is lower than the active storage capacity of the reservoir, indicating a sub-utilisation of its buffering potential.

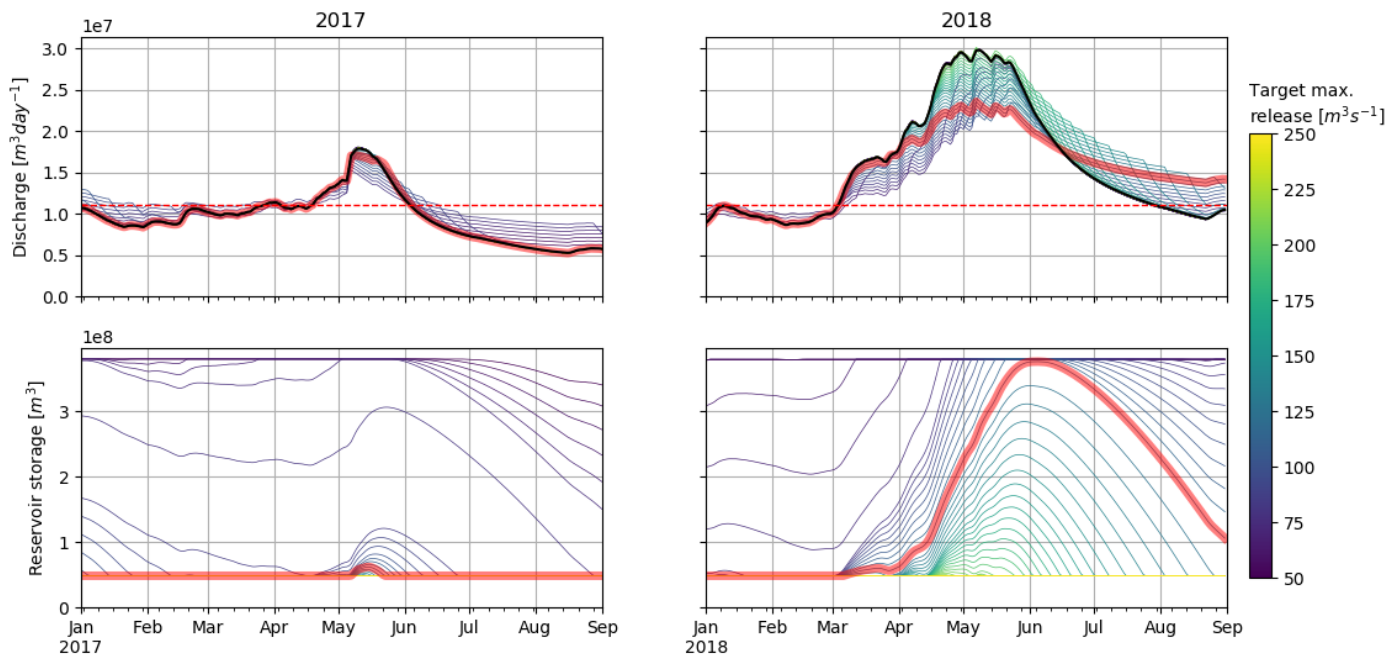


Figure 60: Comparison of simulated seasonal hydrographs at the Kanzenze station (top) and respective reservoir storage evolution (bottom) for flood mitigation scenarios in 2017 and 2018. The curves highlighted in red correspond to a policy with a target maximum downstream release of $120 \text{ m}^3 \text{ s}^{-1}$. The black curve indicates the baseline (no reservoir) scenario. For the year 2017, scenarios with high target maximum releases coincide with this curve.

The centre-right plot provides a similar illustration for a maximum release of $120 \text{ m}^3 \text{ s}^{-1}$. This scenario presents an improvement in that the maximum release over the entire period is limited to this value. A further reduction in the prescribed maximum release is illustrated on the top-right plot, which corresponds to a target release of $115 \text{ m}^3 \text{ s}^{-1}$. The difference in inflows and releases is such that the reservoir is filled before the end of the rainy season – in this particular year and scenario, in mid-May. At this point in time, the reservoir begins to spill (orange area), so that outflows equal inflows, and the buffering capacity is effectively lost. It is highlighted that, for the range of scenarios where the storage capacity of the reservoir is not exceeded, the peak seasonal discharges correspond to the respective maximum reservoir releases; hence gradually increasing from scenario to scenario. However, an abrupt step in the maximum seasonal peak discharge at Masaka as one shifts to a scenario where the storage capacity is exceeded – in the case of 2018, a discharge of $115 \text{ m}^3 \text{ s}^{-1}$. This observation will assist the interpretation of the results presented in section 5.3.

Based on these plots and associated descriptions, a generalisation can be made for the flood mitigation scenarios: the prescribed maximum release should be such that the reservoir storage capacity is efficiently used, while preventing spills from occurring. In terms of Figure 61, this corresponds to setting the horizontal line to a value so that the area encompassed by the green line and this line over the rainy season corresponds to the active storage capacity of the reservoir – not less and not more. While this area (i.e. the reservoir storage volume) is considered constant for any given year, there are considerable differences on the inflow hydrographs (i.e. green lines) for each year, which require the horizontal line to be adjusted accordingly.

An illustration of this difference is presented on the left column of Figure 61, which illustrates the corresponding plots for the same scenarios in 2017. Being a considerably drier year, the threshold discharge of $120 \text{ m}^3 \text{ s}^{-1}$ – which yielded optimal results in 2018 – would have resulted in a gross underutilisation of the reservoir's storage capacity.

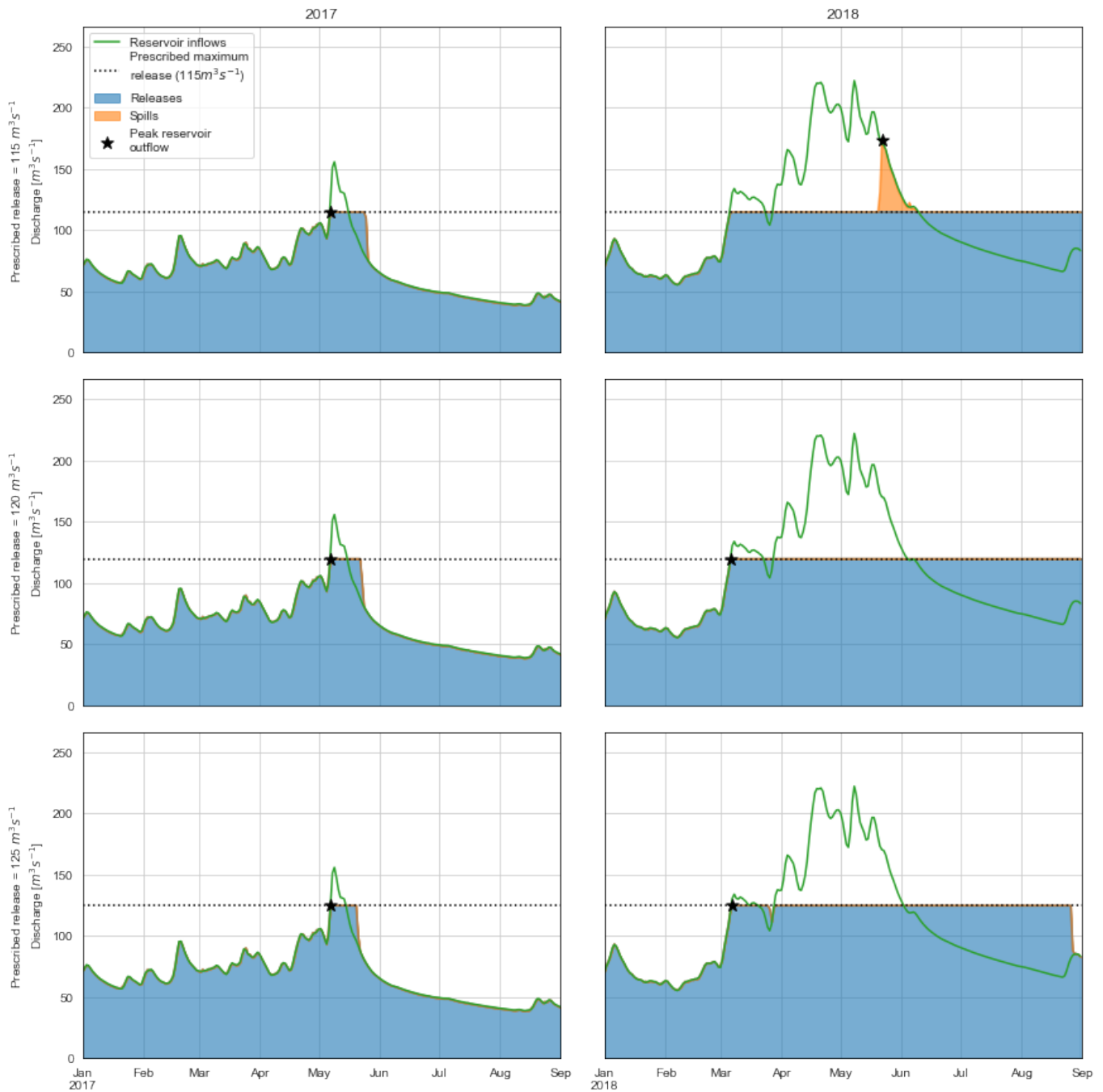


Figure 61: Comparison of simulated reservoir behaviour for the hydropower scenario for different prescribed maximum reservoir releases in 2017 and 2018. Releases and spills are the two components of total reservoir outflows.

As previously mentioned, the hydropower scenarios – in opposition to the flood mitigation scenarios – aimed at maximising storage at any given moment. In Figure 62, the scenario with an assumed capacity factor of 0.40 is highlighted for demonstration purposes. This value corresponds to a target electricity output of 17.40 MW (see equations 33 and 34). Considering the assumptions made with regards to the reservoir characteristics (i.e. the elevation of the reservoir outlet conversion efficiency), this electricity target is met by means of reservoir releases between approximately $56 \text{ m}^3\text{s}^{-1}$ and $170 \text{ m}^3\text{s}^{-1}$ for full reservoir (highest head) and empty reservoir (lowest head) conditions.

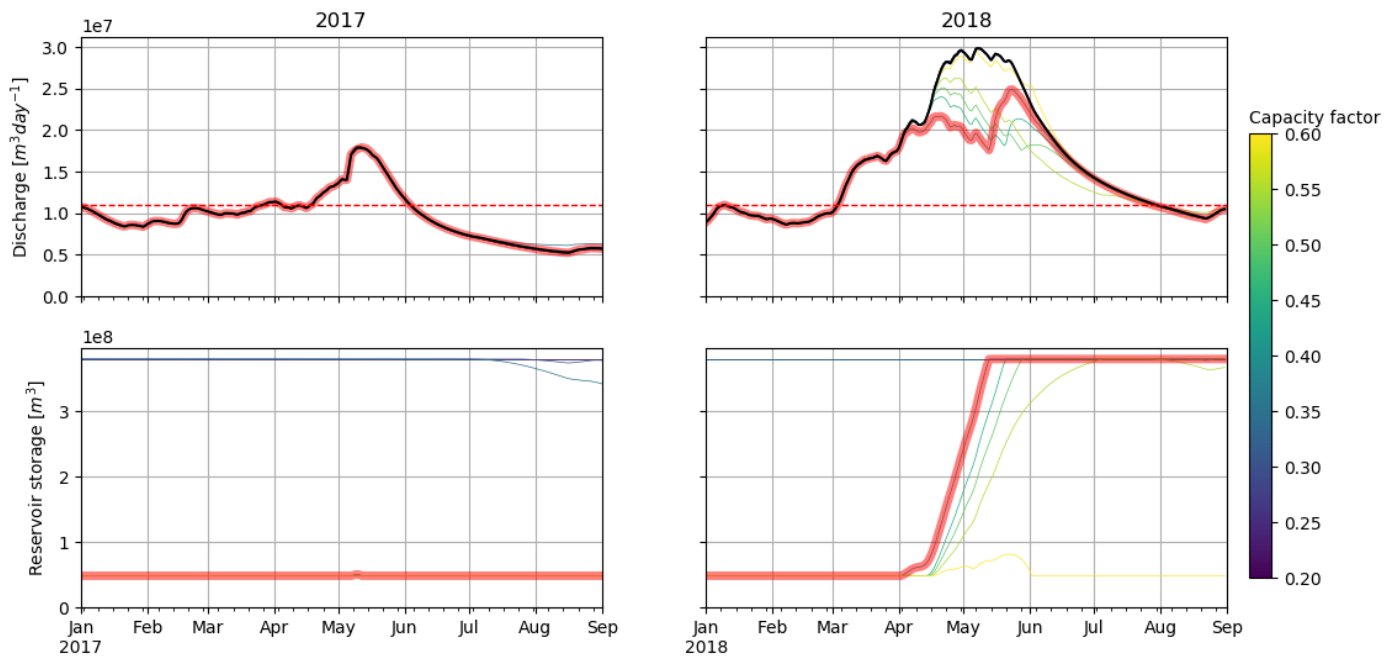


Figure 62: Comparison of simulated seasonal hydrographs at the Kanzenze station and respective reservoir storage evolution for hydropower scenarios in 2017 and 2018. The black curve indicates the baseline (no reservoir) scenario. The curves highlighted in red correspond to a policy with an assumed capacity factor of 0.40.

Figure 63 provides further detail on the behaviour of the reservoir in the two compared years (the top plots correspond to the same capacity factor adopted in Figure 60 and Figure 62). In 2017, reservoir inflows were below $170 \text{ m}^3\text{s}^{-1}$ and the active storage of the reservoir remained virtually empty throughout the wet season. Therefore, the electricity generation target was not met on most time steps and the reservoir released the maximum possible volume at each time step (which corresponds to the inflows) in order to maximise the generated electricity. Hence, it had virtually no effect on the seasonal hydrograph.

In contrast, in 2018 the reservoir inflows begin to consistently exceed $170 \text{ m}^3\text{s}^{-1}$ in mid-April. As a result, storage increases and the required releases for the target electricity generation decrease due to a higher head (see conceptualisation in Figure 42). This activates a positive feedback loop where higher storage volumes lead to lower releases, which in turn tend to increase in storage. As a result, the reservoir fills within a relatively short period of time (between early April and mid-May). Once the reservoir is full, its releases are limited to the amount necessary to generate the target electricity on that storage level. However, since inflows exceed this amount over the ensuing months, the additional discharge is spilled, and the total reservoir releases match the inflows – i.e. the reservoir ceases to regulate discharges. It is highlighted that the step in reservoir releases shown in Figure 63 is not visible in Figure 62 due to the attenuation expected to occur between the Ruliba station and the Masaka wetland, which in this study has been conceptualised by a linear reservoir (refer to Figure 17).

The interpretation of the provided plots leads to the observation that reservoir operation for hydropower has the potential to attenuate peak discharges. However, this potential is dependent on the target electricity output (and associated required releases) in relation to the inflow hydrographs. Higher target electricity outputs (i.e. in the present case higher assumed capacity factors) mean that the reservoir will release a higher discharge for a given stored volume and fill up later in the rainy season – see right plots on Figure 63. With an increasing cf value, the reservoir release at the moment it is exceeded by the inflow (i.e. the moment where the blue area diverges from the green line) is higher than the total reservoir release after it reaches full capacity (i.e. highest point above orange area). In summary, a target electricity output that minimises the seasonal flood peak is in theory one that minimises the two aforementioned points. Based on Figure 63, it is observed that, for the seasonal hydrograph of 2018, this would correspond to a cf just above 0.45. However, for the 2017 wet season, none of the plotted cf values brought significant reductions in the peak discharge.

This illustrates that the optimum electricity output in terms of peak discharge reduction is dependent on the seasonal hydrograph. In practice, this information is unknown in advance, not allowing for the previous determination of the reservoir release policy. Hence, the importance of seasonal forecasts of discharges is highlighted.

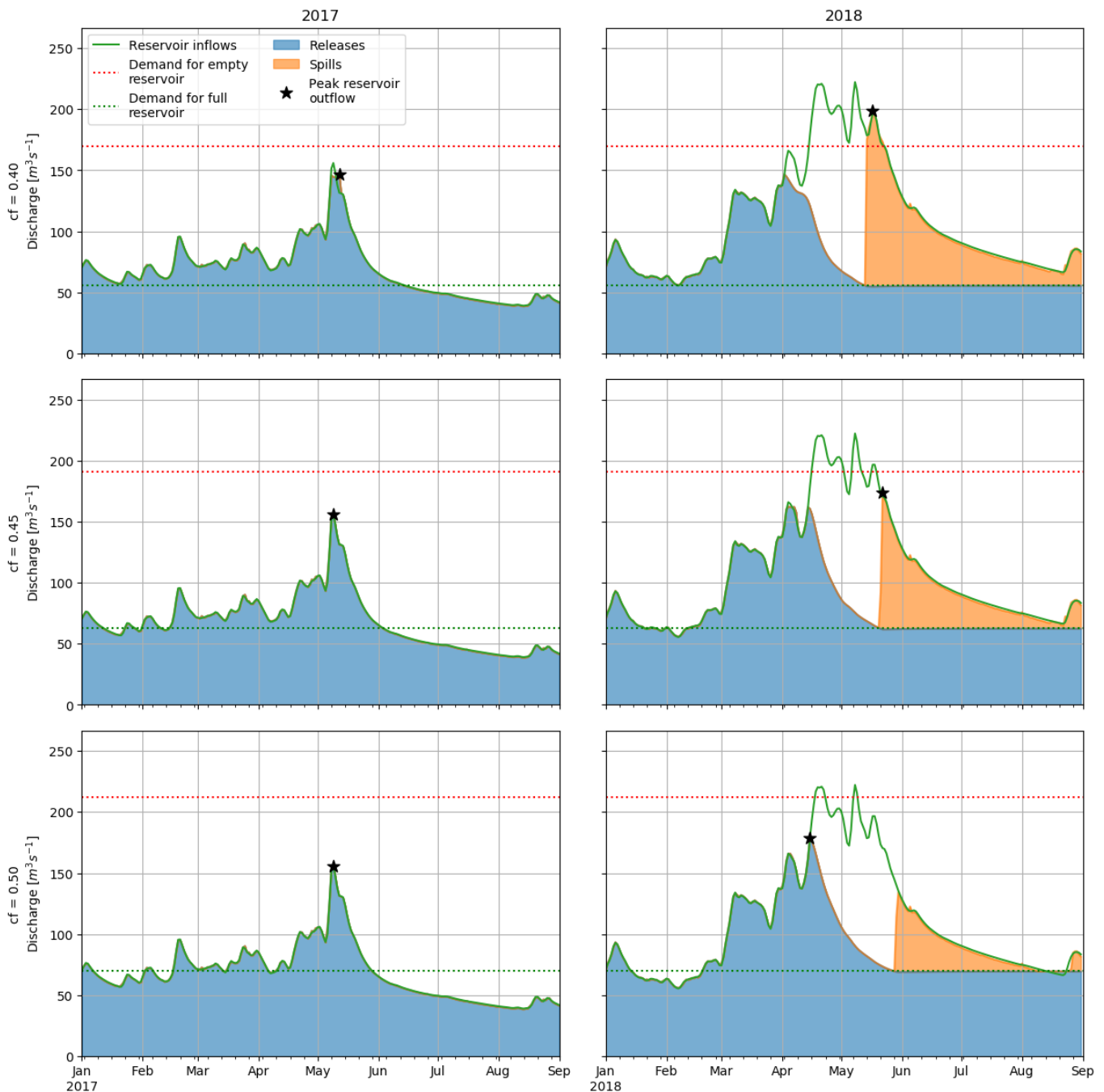


Figure 63: Comparison of simulated reservoir behaviour for the hydropower scenario for different assumed capacity factors in 2017 and 2018. Releases and spills are the two components of total reservoir outflows.

5.3 Peak discharges

The behaviour described in the previous section assists the interpretation of the variability in the flood peak attenuation performance of different operational rules in different years. Figure 65 and Figure 66 illustrate the relative reductions in flood peak magnitudes for each scenario over all simulated years. For any given year, the optimal flood mitigation policy consisted of the one that prescribed a downstream release that is

small enough to result in temporary storage of large discharges and at the same time prevents the reservoir storage from being prematurely exceeded. For any given year, a sudden drop on the flood peak reduction performance is observed between the scenario with the highest performance and the scenario to its left, whose prescribed release discharge corresponds to the upper boundary of the range of scenarios for which spilling occurs – as explained in the previous section. The location of this boundary – and hence the optimal target – varied according to the different inflow hydrographs in each simulated year.

In contrast, the simulated policies with an emphasis on hydropower generation yielded less uniform results. This behaviour is explained by the storage-maximising operation described in previous sections. On years where relatively high inflow hydrograph volumes occur, the target electricity generation (and associated releases) are such that the reservoir fills over the Itumba season, hence providing a buffer during peak discharges. This is the case, for example, for the scenarios with capacity factors ranging from 0.4, 0.45 and 0.5 in 2018. On the bottom-left plot of Figure 66, it is visible that the cf value of 0.45 provided the highest reduction in peak discharges on this particular year. The interpretation of this result is given on the right column of Figure 63, where it is visible that this operation policy provided the best compromise between limiting downstream releases and delaying the moment when the reservoir reaches full capacity and ceases to buffer inflows.

However, on years such as 2017, simulated reservoir inflows were below the minimum required discharge for the target power output even for the lowest assumed capacity factors. Hence, the reservoir operated with the goal of maximising power output and released all inflows, remaining empty throughout the rainy season and providing no attenuation in peak discharges. Due to the positive feedback loop between stored volume, head and discharge retention, initial conditions on each rainy season may also partially explain the uneven observed behaviour. If, on a given year, the reservoir was near full capacity at the start of the rainy season, the required releases for hydropower generation would be lower and hence the reservoir would have lower downstream releases until the moment full capacity was reached.

It should be highlighted, however, that the peak discharge reductions hereby presented are the result of an operation policy aiming to maximise electricity output on each time step individually. In contrast to the behaviour of decreasing releases with an increasing stored volume, it is likely that in practice releases will be limited during periods of low stored volume and increased when storage is high. As a result, the positive feedback loop that led to accelerating filling and emptying of the reservoir would instead be a self-balancing cycle where the goal is to prevent storage from reaching extreme values.

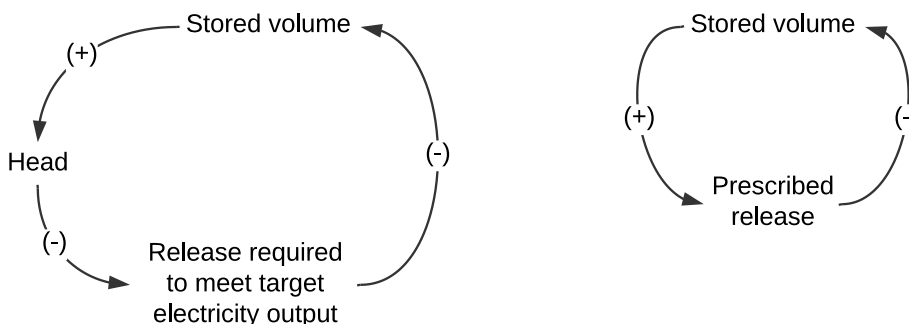


Figure 64: Simplified illustration of implemented policy for hydropower reservoir operation (left) and likely practical operation (right). The implemented policy triggers a positive feedback loop where increased storage leads to higher heads, which drive lower releases and hence further increases in storage (and vice-versa for decreasing storage). In contrast, practical reservoir operation can be expected to involve, to some extent, of a negative feedback loop with a self-balancing component with the goal of preventing fast filling or depletion of storage.

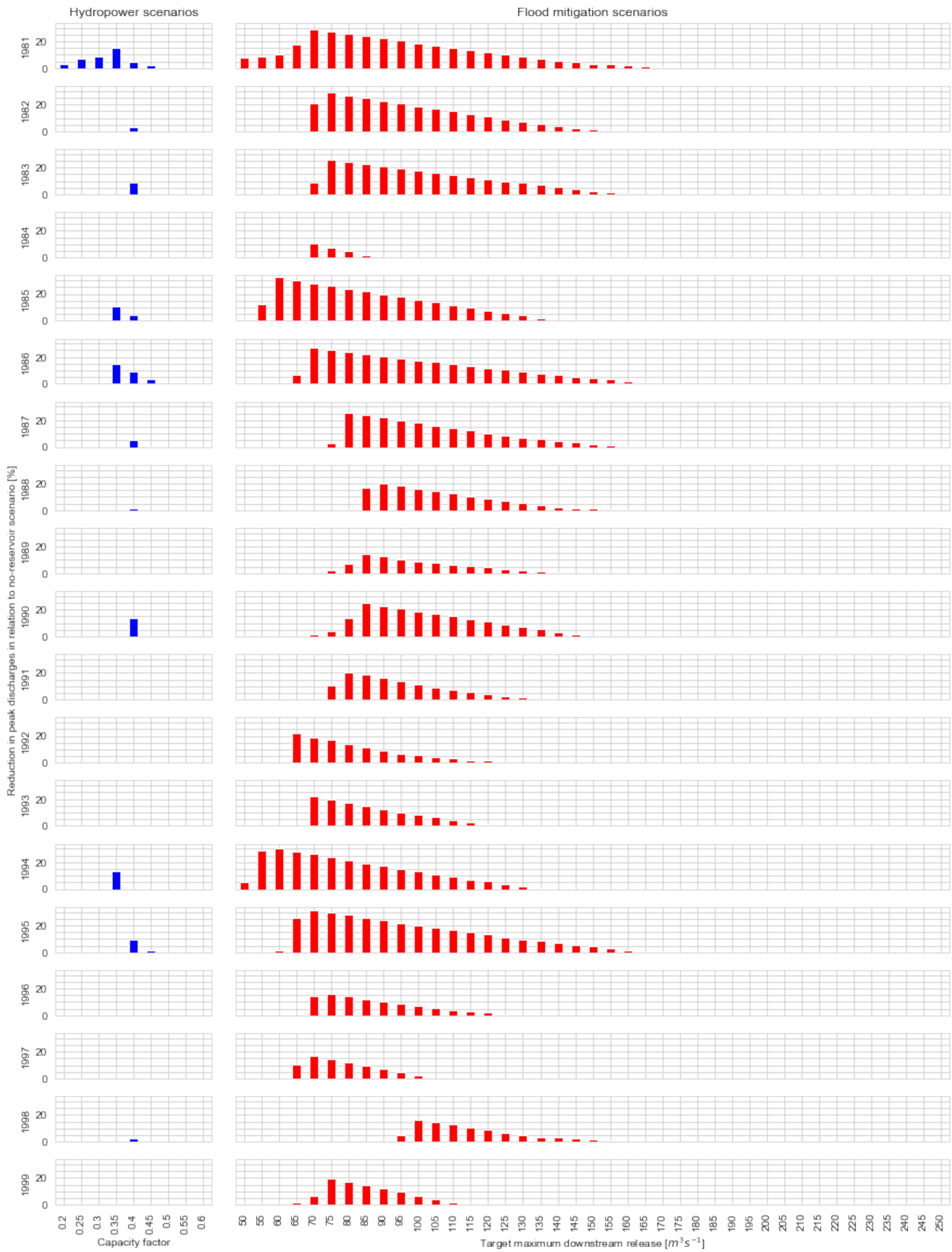


Figure 65: Estimated percentage reductions in the maximum seasonal peak discharge magnitudes (in relation to the no-reservoir scenario) for all simulated scenarios, for the years 1981 to 1999.

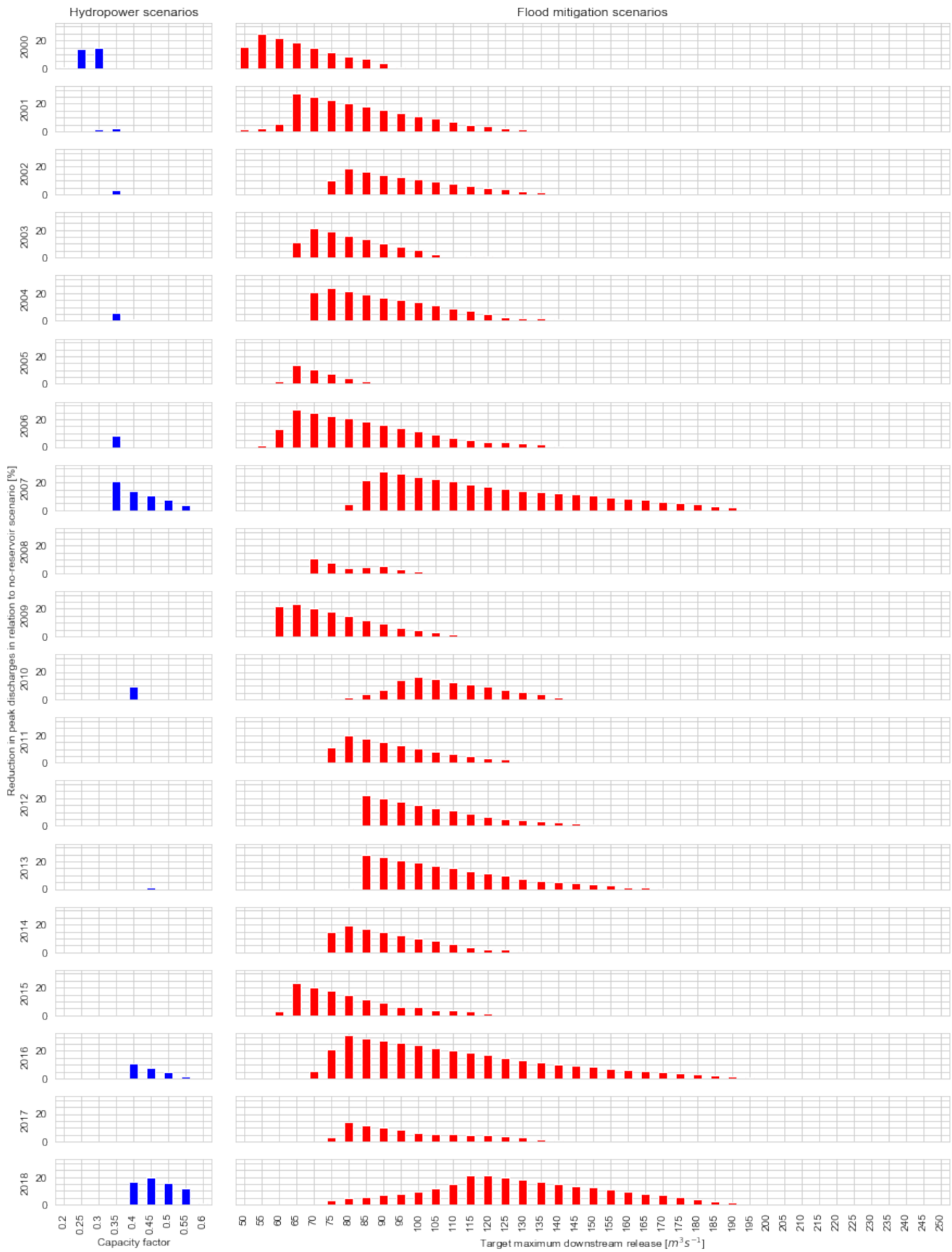


Figure 66: Estimated percentage reductions in the maximum seasonal peak discharge magnitudes (in relation to the no-reservoir scenario) for all simulated scenarios, for the years 1999 to 2018.

The peaks simulated for each scenario were fit to the Gumbel distribution. The fitted functions are illustrated in the form of probability density function and cumulative distribution function in Figure 67 and Figure 68, respectively. It is visible that the different assumed capacity factors for the hydropower scenario family have had a very limited effect on the distribution of peak discharge values. In contrast, operation centred at flood peak reductions achieved sensible results in the distribution of peak discharges, with a qualitative behaviour meeting what can be expected for reservoir regulation (see Figure 4). However, such shift was mostly constrained to peaks above the bankfull discharge threshold. This implies that reservoir regulation has had a limited impact on the probability of exceedance of the bankfull discharge on a given seasonal flood (i.e. the probability that flood will occur).

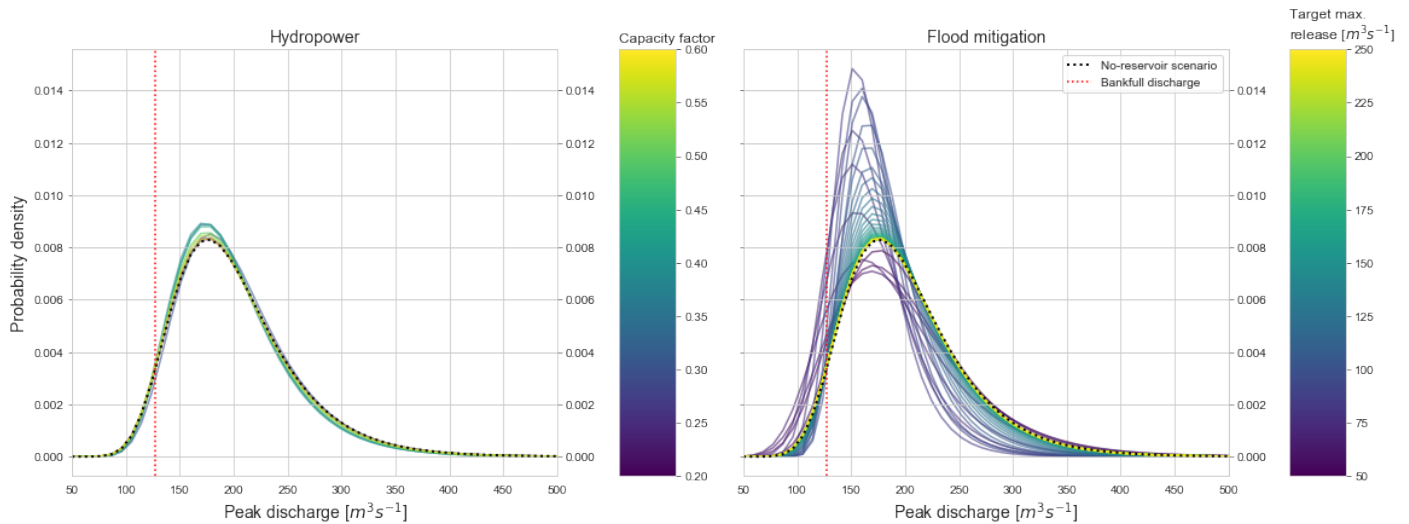


Figure 67: Gumbel probability density function fitted to the peak discharges simulated for each scenario.

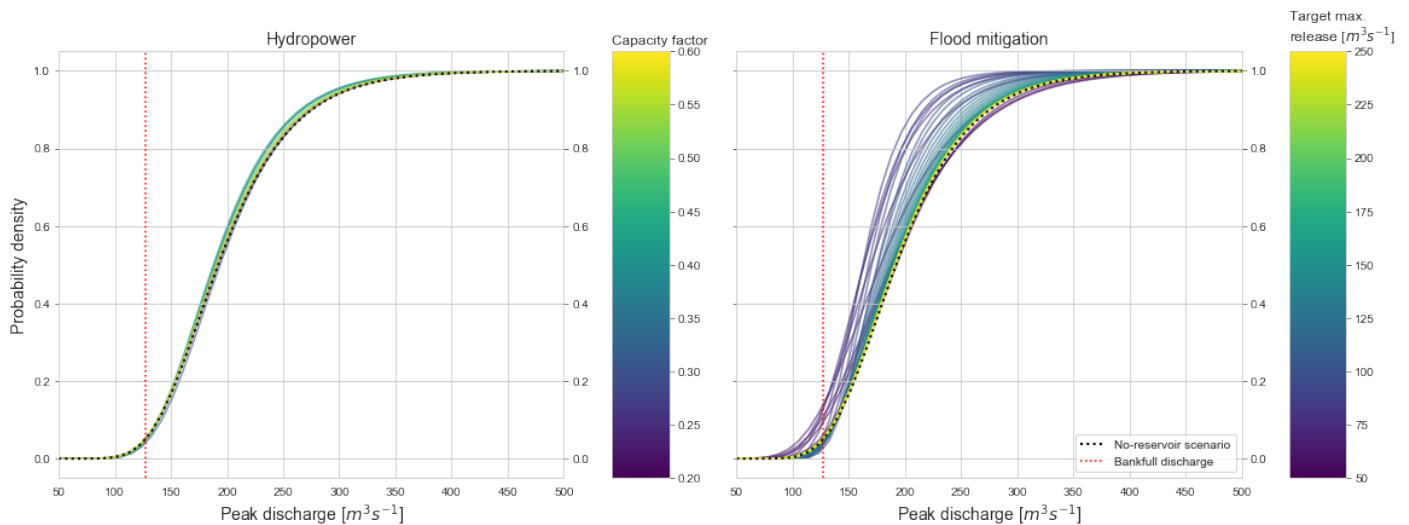


Figure 68: Gumbel cumulative distribution function fitted to the peak discharges simulated for each scenario.

Further insight is gained by plotting the values of the two parameters of the Gumbel distribution fitted to the peaks of each scenario. The limited effect of the hydropower scenario family is once again made evident by the small deviations in comparison with the baseline scenario. For the flood mitigation scenario family, it is visible that different target maximum releases have had different effects on the probability distribution of both quantitative and qualitative natures. A first observation is that all scenarios in this family have yielded a general shift in the distribution towards lower peaks, which is visible in the lower values of the location parameters. However, the magnitude of this shift varies considerably according to the simulated target maximum release, with the largest change corresponding to a value of $75 \text{ m}^3\text{s}^{-1}$.

Significant differences are also observed in the scale parameter, for which higher values imply heavier tails in the Gumbel probability density function. Relatively low target reservoir releases are observed to increase the value of this parameter – the corresponding probability density functions are identifiable in Figure 67 as having lower peaks than that of the no-reservoir scenario. However, an accentuated drop is observed between values of 65 and 85 m^3s^{-1} , the latter corresponding to the lowest scale value, and hence the greatest concentration in the frequency distribution of peak discharges at the Masaka wetland.

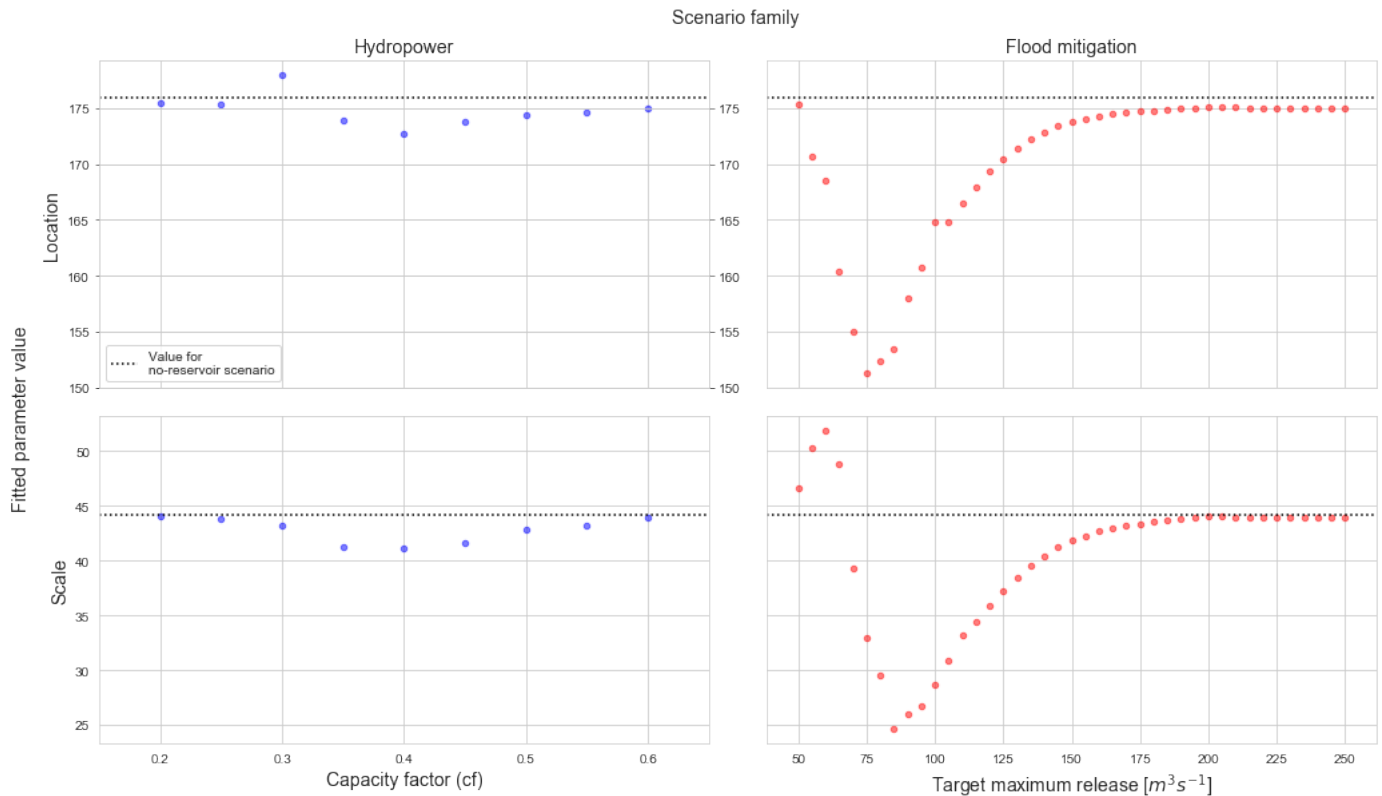


Figure 69: Values of the location and scale parameters of the Gumbel distribution fitted to the peaks simulated for all scenarios.

Following the procedure described in section 4.2, return periods were estimated for extreme discharges based on the fitted distribution functions. The results are summarised in Figure 70. It is visible that nearly all scenarios tend to reduce the probability of exceedance of given peak discharge values for most return periods. As expected, the scenarios where flood mitigation is the operational priority present the greatest potential for shifting the return level plot. In contrast, all scenarios where hydropower generation was emphasised resulted in negligible effects on peak discharges, particularly if uncertainties are considered.

Hypotheses B and C involved the quantification of the potential decrease in the expected frequency for flood peaks that are currently associated with a 2-year return period (indicated by the lower dotted line on the plots of Figure 70) in operation scenarios for hydropower and flood mitigation, respectively. It is visible from the plots that some flood mitigation policies allow for the discharge with a 2-year return period in the baseline scenario to be shifted to up to a maximum 5-year return period. Therefore, both hypotheses are false based on the results of this study. It should, however, be remarked that optimised reservoir operation would likely enable further shifts on the return periods for given discharges to an extent that potentially could cause hypothesis C not to be rejected. However, the estimation of the magnitude of such changes would require appropriate simulation of more complex operating rules.

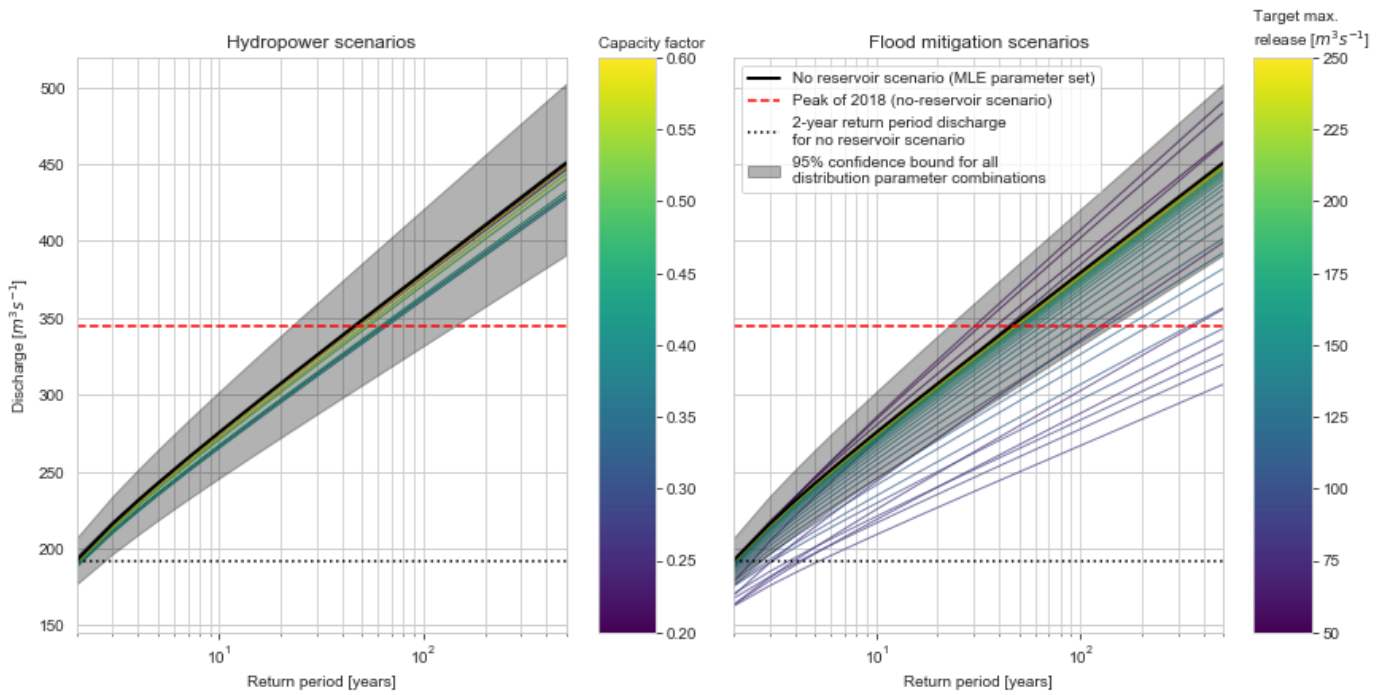


Figure 70: Return level plots of peak discharges at the Kanzenze station for all simulated scenarios. For consistency purposes, all curves correspond to the estimates associated with the Gumbel distribution fitted to each scenario. Please refer to Figure 76 for an illustration of the range in return levels estimated by different functions fitted to each scenario.

5.4 Flood durations

Flood duration is a critical factor for the development of certain crops, and therefore this study aimed to investigate the hypothesis that reservoir operation will have significant effects on it. Figure 71 illustrates the envelope of flood durations estimated for the hydropower and flood mitigation scenario families. The distribution of flood durations did not follow any particular shape, and therefore fitting to a probability distribution and subsequent analyses were not carried out. Instead, the effects of different reservoir operation regimes are visually compared. The scenarios focussed on hydropower generation show little alteration with respect to the no-reservoir scenario. In contrast, the operation of the reservoir with the goal of limiting downstream peak discharges shows the potential for increasing and reducing flood durations.

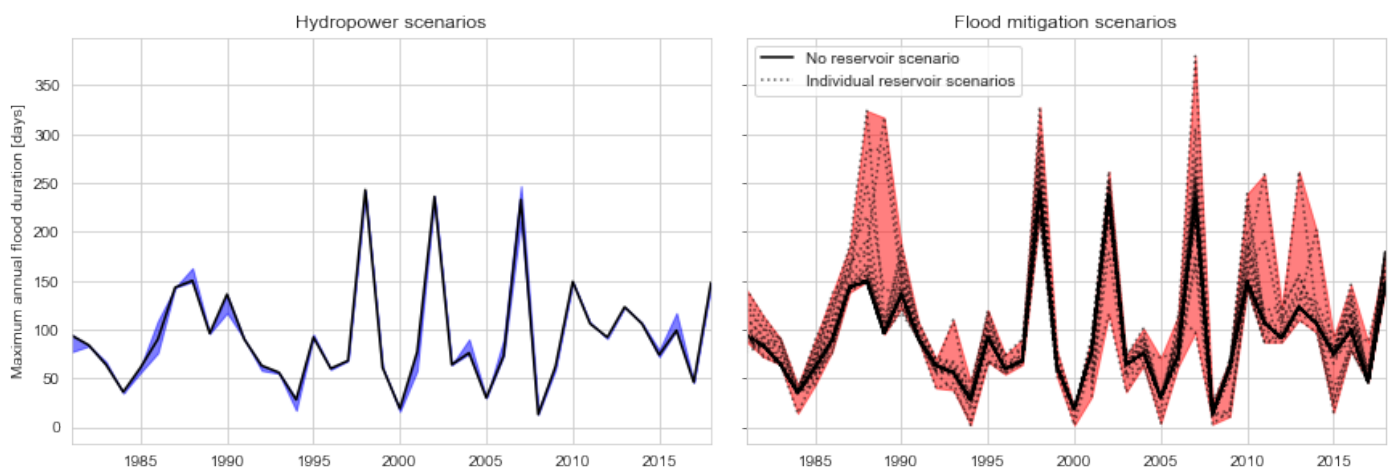


Figure 71: Range of maximum annual flood durations per scenario type: no-reservoir (baseline) scenario shown in black.

This effect can be explained by the limited storage capacity of the reservoir relatively to the seasonal discharge volumes. As a result, the reservoir tends to fill at some moment along the Itumba period (depending on the specified release quota) and afterwards loses its attenuation function, as previously explained. When inflows reduce, the emptying of the reservoir causes downstream releases to be higher than they would otherwise be. When added to the contributions of the unregulated catchments, this causes the discharge at Masaka to exceed the bankfull value. This effect is visible for the flood of 2018 illustrated in Figure 59, where flood mitigation policies reduced – to a greater or lesser extent – the peak discharge but simultaneously extended the period during which bankfull conditions were exceeded.

Figure 72 and Figure 73 illustrate the relative changes in the maximum flood duration of each year for all simulated scenarios, in comparison to the baseline scenario. For the flood mitigation scenarios, it is generally observed that, on a given year, there is a threshold in target release below which regulation results in increased flood durations, and above which some degree of reduction in flood duration is achieved. Similarly to the observations for flood peaks, this threshold value varies per year according to the inflow hydrographs. It should be noted, however, that the presentation of results normalised by the baseline flood duration on each year implies that even small absolute decreases in flood duration may result in large percentage reductions on years where the baseline flood duration is low. For the majority of hydropower scenarios, the simulated changes in flood duration are negligible.

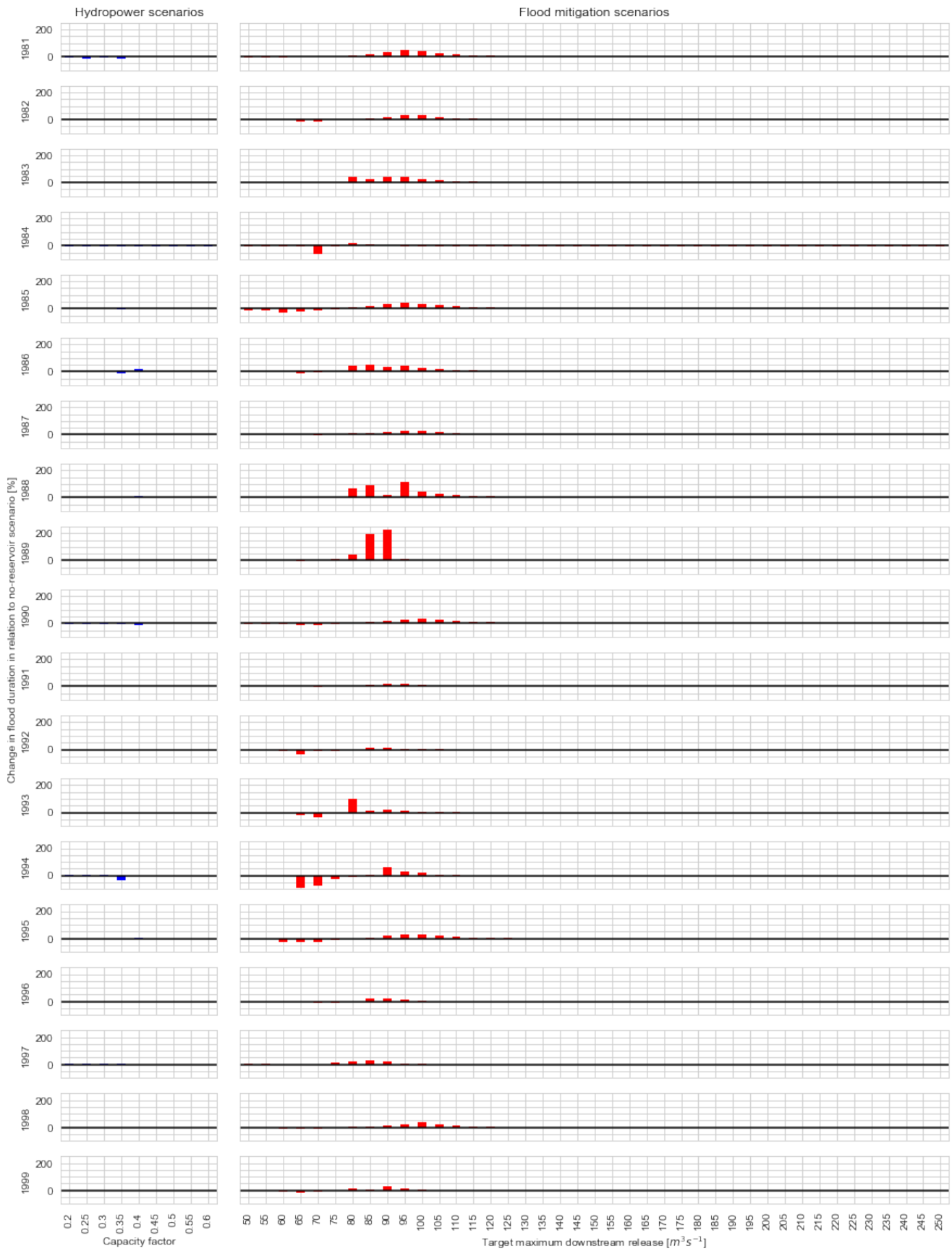


Figure 72: Estimated percentage changes in the maximum yearly flood durations (in relation to the no-reservoir scenario) for all simulated scenarios, for the years 1981 to 1999.

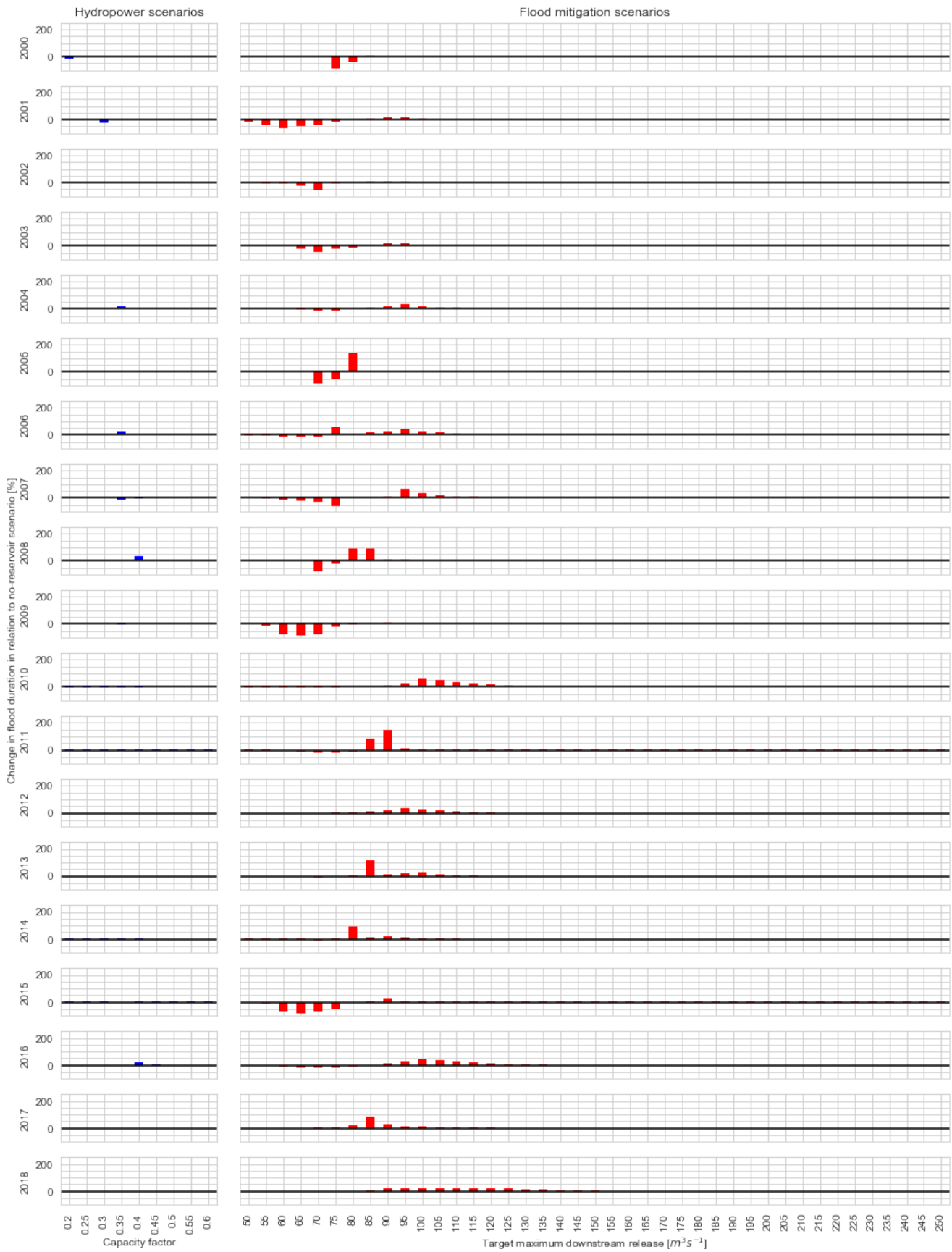


Figure 73: Estimated percentage changes in the maximum yearly flood durations (in relation to the no-reservoir scenario) for all simulated scenarios, for the years 1999 to 2018.

Figure 74 provides an overview of the combined effects on flood peaks and durations simulated in all scenarios for each year. The proximity of each scenario to the origin indicates its effectiveness in the reduction of flood peaks and/or durations. The considerable potential for flood mitigation policies to reduce flood peaks (shown in Figure 65 and Figure 66) is visible in the horizontal scatter of the red markers on each year. In spite of the interannual variability in the simulation results, a general pattern is observed for several years: starting at the baseline scenario, flood mitigation policies that enable increasing reductions in flood peaks are also associated with increases in flood durations. However, a discontinuity exists beyond which reductions in flood peaks and flood durations occur simultaneously, up to a point where a considerable reduction in flood peaks is met by a flood duration approximately equal to that of the baseline scenario. This behaviour is observed, for example, on the years 1981, 1982, 1983, 1987, 1990, 2012, 2013 and 2016. This leads to the observation that – even for an extremely simplified reservoir operation policy – the careful selection of a target release may enable reductions in flood peaks with no compromise for flood durations. However, this is typically achieved on years with relatively low discharges, when the additional flow caused by the emptying of the reservoir at the tail of the seasonal hydrograph is not large enough to cause flooding (i.e. the top scenario in Figure 5).

In contrast, on wetter years such as 1988 and 1998, the regulated behaviour approaches that of the bottom plot in Figure 5, where the buffering of hydrograph peaks is accompanied by a lengthening of the period over which bankfull discharge is exceeded. It is remarked, that Figure 5 illustrates the effect of different bankfull discharge values for a given hydrograph attenuation, while here the comparison is among different hydrograph attenuation for a fixed bankfull discharge threshold. However, the emphasis is on the hydrograph shape in relation to the bankfull discharge value. As such, higher hydrograph discharges or a lower bankfull discharge value are equivalent in the sense that they both cause a lengthening of flood durations.

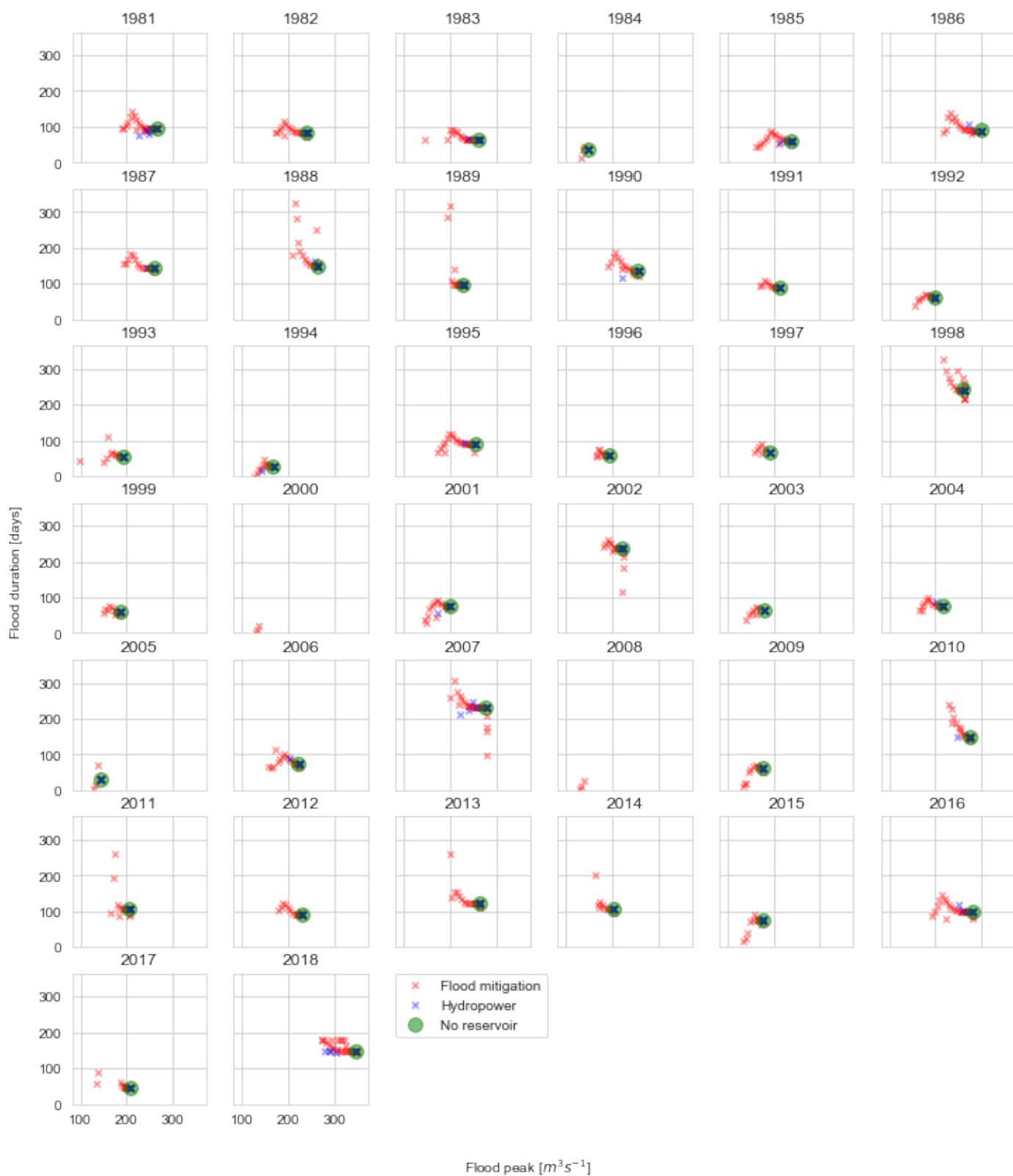


Figure 74: Maximum flood durations and respective peak discharges per year, per simulated scenario. For certain scenarios in certain years, no peaks over threshold were identified and hence no corresponding points exist. Flood durations for the year 2018 have been trimmed to the end of the simulation period and may be underestimated for certain scenarios where flooding would have exceeded this date (see top plot of Figure 59).

5.5 Considerations on uncertainty propagation and key assumptions

The data and methods adopted in the current study have resulted in the propagation of a significant amount of uncertainty in the results hereby presented, which is illustrated in Figure 75. The quantification of such uncertainty has been limited to the step of selection, fitting and extrapolation of extreme value distributions to the generated peak discharges, described in section 4.2. However, such values have been generated by a process that involved numerous assumptions concerning the behaviour of the catchment and of the reservoir.

As detailed in sections 3.1 and 3.4.2, the reference discharge time series adopted for the calibration of the hydrological models were derived from gauge height and rating curves that, although subject to previous inspection, possess known limitations, particularly for high flows. In the case of the Akanyaru river catchment, the uncertainties in discharge estimates for the Kanzenze and for the Ruliba stations were compounded to each other and to the limited knowledge on the flow routing between them.

As with any hydrological modelling exercise, additional sources of error include possible biases in the adopted forcing data and the limited ability of a conceptual model as the one implemented to properly reproduce all relevant mechanisms involved in the rainfall-runoff process (which come for the benefit of reduced potential for equifinality). For example, the estimated peak discharge for 2018 is higher than any observed peaks in the reference series adopted at the model calibration step. Hence it is in principle not known to which extent additional runoff mechanisms might be active on extreme scenarios which may require adaptations in the conceptualisation. As discussed and illustrated in section 4.1.1.4, in spite of the acceptable performance of the model in terms of the adopted metrics (NSE and logNSE), the limited capacity of the model to reproduce observed discharges introduces a significant error in their frequency distribution (see Figure 41).

Additionally, adopting a rainfall-runoff model calibrated against data observed between 40 and 30 years ago in order to generate recent discharge time series carries the implicit assumption that the overall catchment behaviour has not changed. However, as seen in section 2, Rwanda has undergone considerable changes in land use over the past 30 years. This means that, even without the commissioning of reservoirs in the catchment, other factors may have on their own caused changes in the discharge behaviour at the Masaka wetland – although this was outside the scope of this study.

Uncertainty also exists in the discharge assumed to correspond to bankfull conditions, which is a key information for the estimation of flood durations. This value is only known to an approximate extent and has been estimated by an empirical extrapolation as described in section 2.1. Additionally, a seemingly obvious assumption that flood periods end when river discharges fall below the bankfull threshold (described in 4.3). However, this is known not to fully apply to the particular context of the Masaka wetland, where low elevations and limited natural drainage cause extended periods of stagnation even after the Nyabarongo river has receded. Obtaining a better understanding of the nexus between discharges at the Nyabarongo river and flooding in the Masaka wetland will be possible once a hydraulic model of the area is devised, which was outside the scope of this study.

As discussed and illustrated in 4.2.2, both the selection of a function and the fitting of parameters for the probability distribution of peak discharges are subject to uncertainties. Even among distributions with a high goodness-of-fit to a given sample, the estimation of peak discharges with high return periods involves a large range of possible values due to different behaviours of probability distribution functions for high quantiles (Cunnane, 1989). Hence, while in this study the Gumbel distribution has been adopted for its reasonable performance across all scenarios, the selection of equally or better-performing functions to describe peaks in different scenarios would have resulted in significantly different estimates, as illustrated in Figure 76.

Hence, it can be expected that eventually accounting for the other sources of error such as those described above will result in significantly wider confidence bounds. The reader is requested to account for this potentially large uncertainty propagation when interpreting the results of this study.

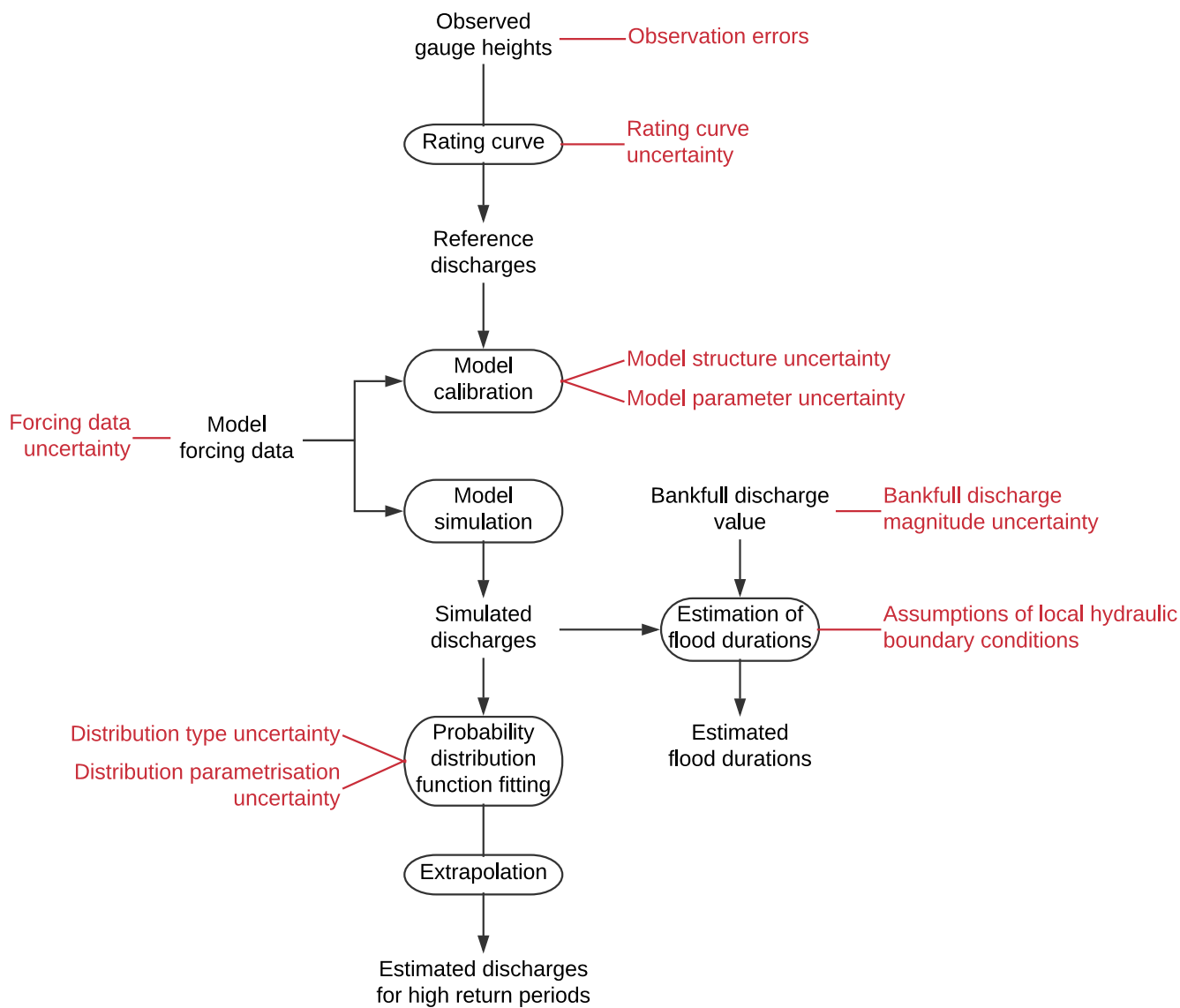


Figure 75: Non-exhaustive illustration of sources of uncertainty in the data and methods adopted in the current study.

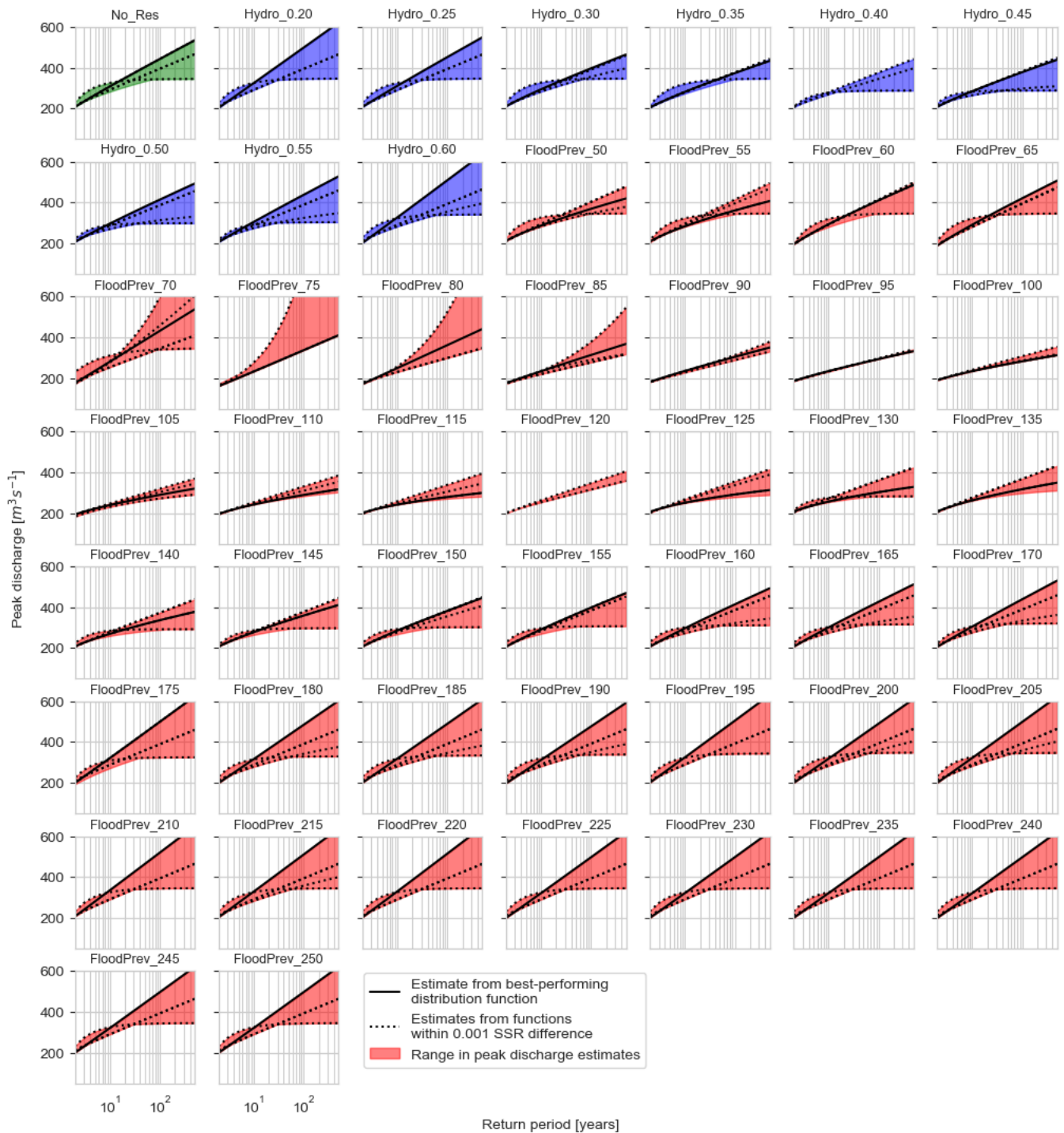


Figure 76: Illustration of range in predicted return levels for alternative distribution functions fitted to peak discharges simulated in each scenario. Plotted range includes functions with a difference in performance measured by SSR of less than 0.001. Areas are coloured by scenario family: No reservoir (green), hydropower (blue) and flood mitigation (red). Values on the title of subplots correspond to the assumed capacity factor (for hydropower scenarios) or target maximum release in m^3s^{-1} (for flood mitigation scenarios).

6 Conclusions

This study aimed to quantify, to the maximum possible extent, the range of behaviours that can be expected for discharges in the Nyabarongo river and associated seasonal flooding in the Masaka wetland after the commissioning of the Shyorongi dam – with all other factors remaining equal. This estimation was made by generating discharge time series at key locations in the Masaka wetland catchment and, where appropriate, routing the discharges through a reservoir model with different operational scenarios.

Hypothesis A concerned the extent to which contributions from the Akanyaru river influence flooding in the Masaka wetland. Since the outlet of this river is located downstream of the planned Shyorongi dam site, a large contribution from this tributary would imply a lower potential for the reservoir to regulate flooding at this location. As illustrated in section 5.1, at most times the Akanyaru river contributes to 15 to 30% of total discharges of the Nyabarongo river in the vicinities of the Masaka wetland. It has been shown that even the hypothetical total regulation of the Akanyaru river catchment would have limited implications on discharge behaviour at the Masaka wetland. Therefore, this hypothesis is discarded based on the results hereby presented.

Hypotheses B and C stated – for scenarios focussed on hydropower generation and flood peak mitigation, respectively – that certain operational rules for the Shyorongi reservoir may entail significant shifts in the probability distribution of peak seasonal discharges. It was hypothesised that, in these cases, the flows associated with a 2-year return period in a no-reservoir scenario would assume a return period of 10 years or more with reservoir regulation. Hypothesis D involved the potential increase in flood durations at the Masaka wetland caused by reservoir regulation. Table 6 provides an overview of the conclusions drawn regarding such hypotheses, based on the results and interpretation presented in previous sections.

Table 6: Overview of estimated Shyorongi reservoir influences on riverine flooding at the Masaka wetland according to scenario family and criterion of assessment

		Scenario family	
		Hydropower	Flood mitigation
Criterion	Flood peaks	Reduction of individual peaks on selected years; limited influence on frequency distributions	Potential for reductions of 20~30% on most years, with variability on best-performing scenario.
	Flood durations	Negligible influence	Considerable potential for increasing or decreasing flood durations depending on the relative magnitude of seasonal inflow hydrographs

Reservoir operation emphasising hydropower generation demonstrated some potential to reduce individual flood peaks. However, this effect was limited to specific capacity factors on isolated years, due to variable inflow hydrograph timing and volumes. Hence, eventual shifts in exceedance probabilities of peak discharges were largely irrelevant, particularly if uncertainties are considered.

In contrast, considerable potential for flood peak reduction was observed in scenarios where this was the primary goal of reservoir operation. On most years, flood peak reductions between 20% and 30% were achieved for the flood mitigation scenario family. However, similarly to the hydropower scenario family, interannual variability in inflows meant that prescribed maximum releases performed inconsistently over different years. Over most wet seasons, the target maximum release associated with the highest reduction in peak discharges was in the range between 70 and 100 m³s⁻¹. Hence, scenarios in this range of release presented the best performance over the entire simulated period, which was reflected in the greatest shifts in the distribution of the probabilities of exceedance. However, none of the simulated operational scenarios

yielded the hypothesised shift in exceedance probability, causing hypotheses B and C to be rejected based on the results of this study.

With regards to flood durations, operation for hydropower generally had negligible effects. In contrast, operation for flood mitigation focussed on minimising storage, and therefore beginning to empty the reservoir as soon as inflows were smaller than the target maximum release. The difference between inflows and releases was an incremental discharge that caused the lengthening of the seasonal hydrograph.

With the goal of flood peak reductions in a reservoir operated primarily for hydropower generation, the determination of an optimal policy consists of defining a target generation that (a) delays the moment when reservoir reaches full capacity (and hence ceases to attenuate the incoming hydrograph) while (b) avoiding releases that cause downstream flooding. In the case of a policy particularly aimed at the reduction of peak discharges, the adopted release target for a given season should reflect a compromise between (a) having the reservoir release virtually all inflows (for a target release that is too high) and (b) retaining an exceedingly high proportion of inflows and filling up before the peak of inflows. In both cases, an appropriate policy selection depends on the availability of an accurate forecast of seasonal inflows, highlighting the importance of the availability and enhancement of this kind of product in Rwanda.

It is remarked that the standard operation policies implemented in this study have a limited capacity to simulate reservoir operations under real conditions (see section 5.3 for a brief discussion), and hence the associated potential for reductions in flood durations and peaks. However, the results obtained in this study provide solid evidence for the need to adopt a reservoir policy that is flexible and adaptive depending on expected seasonal inflows if optimal reductions in flood peaks and durations are to be achieved. Hence, there is considerable potential for the optimisation of the operation of the Shyorongi reservoir with this goal in sight, and it is recommended that future studies explore possibilities in this regard. As briefly described in section 1.2.1, there is a need for the maintenance of a flow regime that preserves ecological and morphological aspects of the Masaka area. While this aspect was not explicitly assessed in this study, this objective should also be considered in the definition of an operation policy.

The uncertainties and assumptions in the variables such as those summarised in section 5.5 mean that the results obtained in this study should be interpreted mostly on a relative basis: while they allow for scenarios to be compared against each other; the absolute values of peak discharges or flood durations should not necessarily be taken as truthful representations of expected behaviour. A variable that deserves particular attention is the discharge corresponding to overflow of the Nyabarongo river into the Masaka wetland. The sensitivity analysis for this variable would simultaneously (a) assist in quantifying the error in flood durations associated with uncertainty in this value and (b) provide an approximate indication of the possible effects of interventions aimed at increasing this value, such as levees.

Evidently, a greater availability of data with higher resolution and accuracy may allow the generation of results that lend themselves to more refined analyses. Fortunately, this appears to be the case for hydrometric data. If recent efforts in data collection are continued, future research on the topics covered by this study will benefit from the availability of greater quantity and quality of data, and hence reduced uncertainty propagation.

References

- ABIMBOLA, O. P. 2014. *Assessment of Water Resources in Ungauged Catchments in Rwanda*. MSc thesis, IHE Delft.
- ABIMBOLA, O. P., WENNINGER, J., VENNEKER, R. & MITTELSTET, A. R. 2017. The assessment of water resources in ungauged catchments in Rwanda. *Journal of Hydrology: Regional Studies*, 13, 274-289.
- AFDB 2013. Rwanda Energy Sector Review and Action Plan. African Development Bank Group.
- AGRITERRA 2017. Action Oriented Research - Sugar cane as engine for socio-economic development in the Akagera Valley. Agriterra - Centre for Development Innovation.
- ASHOURI, H., HSU, K.-L., SOROOSHIAN, S., BRAITHWAITE, D. K., KNAPP, K. R., CECIL, L. D., NELSON, B. R. & PRAT, O. P. 2015. PERSIANN-CDR: Daily Precipitation Climate Data Record from Multisatellite Observations for Hydrological and Climate Studies. *Bulletin of the American Meteorological Society*, 96, 69-83.
- BAECHER, G. B., PATÉ, M. E. & NEUFVILLE, R. D. 1980. Risk of dam failure in benefit-cost analysis. *Water Resources Research*, 16, 449-456.
- BAYLEY, P. B. 1995. Understanding Large River: Floodplain Ecosystems. *BioScience*, 45, 153-158.
- BECK, H. E., VERGOPOLAN, N., PAN, M., LEVIZZANI, V., VAN DIJK, A. I. J. M., WEEDON, G. P., BROCCA, L., PAPPENBERGER, F., HUFFMAN, G. J. & WOOD, E. F. 2017. Global-scale evaluation of 22 precipitation datasets using gauge observations and hydrological modeling. *Hydrology and Earth System Sciences*, 21, 6201-6217.
- BLÖSCHL, G., SIVAPALAN, M., WAGENER, T., VIGLIONE, A. & SAVENIJE, H. 2013. *Runoff Prediction in Ungauged Basins: Synthesis across Processes, Places and Scales*, Cambridge, Cambridge University Press.
- BUGINGO, D. 2017. *Assessing the potential use of PERSIANN-CDR and African Flood and Drought Monitor based products for precipitation and stream flows in Rwanda*. MSc thesis, IHE Delft.
- CAYAN, D. R., MAURER, E. P., DETTINGER, M. D., TYREE, M. & HAYHOE, K. 2008. Climate change scenarios for the California region. *Climatic Change*, 87, 21-42.
- CITY OF KIGALI 2013. Kigali City Master Plan Report.
- COLES, S. 2001. *An introduction to statistical modeling of extreme values*, Springer.
- CUNNANE, C. 1989. *Statistical distributions for flood frequency analysis*.
- DEANE, J. P., Ó GALLACHÓIR, B. P. & MCKEOGH, E. J. 2010. Techno-economic review of existing and new pumped hydro energy storage plant. *Renewable and Sustainable Energy Reviews*, 14, 1293-1302.
- DEWITTE, O., JONES, A., SPAARGAREN, O., BREUNING-MADSEN, H., BROSSARD, M., DAMPHA, A., DECKERS, J., GALLALI, T., HALLETT, S., JONES, R., KILASARA, M., LE ROUX, P., MICHÉLI, E., MONTANARELLA, L., THIOMBIANO, L., VAN RANST, E., YEMEFACK, M. & ZOUGMORE, R. 2013. Harmonisation of the soil map of Africa at the continental scale. *Geoderma*, 211-212, 138-153.
- DINKU, T., CECCATO, P., GROVER-KOPEC, E., LEMMA, M., CONNOR, S. J. & ROPELEWSKI, C. F. 2007. Validation of satellite rainfall products over East Africa's complex topography. *International Journal of Remote Sensing*, 28, 1503-1526.
- EDCL 2016. Part A: Hydrological Studies. *Feasibility Study For Nyabarongo II Multipurpose Development Project, Rwanda*. Energy Development Corporation Limited.

- EDCL 2018. Baseline study for hydrology of lakes Burera and Ruhondo.
- ENDEV & EDCL 2016. Status of the Hydropower Sector in Rwanda: Achievements and trends by December 2016.
- FAO. 2005. *Main types of dams and reservoirs* [Online]. Available: <http://www.fao.org/docrep/005/AC675E/AC675E04.htm> [Accessed 07/08/2018].
- FUNK, C., PETERSON, P., LANDSFELD, M., PEDREROS, D., VERDIN, J., SHUKLA, S., HUSAK, G., ROWLAND, J., HARRISON, L., HOELL, A. & MICHAELSEN, J. 2015. The climate hazards infrared precipitation with stations--a new environmental record for monitoring extremes. *Sci Data*, 2, 150066.
- FUNK, C. C., PETERSON, P. J., LANDSFELD, M. F., PEDREROS, D. H., VERDIN, J. P., ROWLAND, J. D., ROMERO, B. E., HUSAK, G. J., MICHAELSEN, J. C. & VERDIN, A. P. 2014. A quasi-global precipitation time series for drought monitoring.
- FUTUREWATER & ELEAF 2017. Water Balance and Allocation Modelling in Rwanda. *In*: DROOGERS, P., KRUISHEER, M., BOER, F. D., TERINK, W., ANDRIESSEN, M. & PELGRUM, H. (eds.). FutureWater.
- GODA, Y. 2010. *Random seas and design of maritime structures*, World Scientific Publishing Company.
- GOR & WATER4GROWTH 2017. Catchment Plan Upper Nyabarongo 2017-2023.
- GORELICK, N., HANCHER, M., DIXON, M., ILYUSHCHENKO, S., THAU, D. & MOORE, R. 2017. Google Earth Engine: Planetary-scale geospatial analysis for everyone. *Remote Sensing of Environment*, 202, 18-27.
- GRDC 2018. The Global Runoff Data Centre. 56068 Koblenz, Germany.
- GROEVE, T. D., BRAKENRIDGE, R. G. & PARIS, S. 2015. Global Flood Detection System: Data Product Specifications. European Commission - Joint Research Centre.
- HIDAKA, T. & KARIM, M. A. 2007. Flooding tolerance of sugarcane in relation to growth, physiology and root structure. *South Pacific studies*, 28, 9-22.
- HRACHOWITZ, M., SAVENIJE, H. H. G., BLÖSCHL, G., MCDONNELL, J. J., SIVAPALAN, M., POMEROY, J. W., ARHEIMER, B., BLUME, T., CLARK, M. P., EHRET, U., FENICIA, F., FREER, J. E., GELFAN, A., GUPTA, H. V., HUGHES, D. A., HUT, R. W., MONTANARI, A., PANDE, S., TETZLAFF, D., TROCH, P. A., UHLENBROOK, S., WAGENER, T., WINSEMIUS, H. C., WOODS, R. A., ZEHE, E. & CUDENNEC, C. 2013. A decade of Predictions in Ungauged Basins (PUB)—a review. *Hydrological Sciences Journal*, 58, 1198-1255.
- HUNTER, J. D. 2007. Matplotlib: A 2D graphics environment. *Computing in science & engineering*, 9, 90-95.
- ICOLD, C. 2018. *Twenty-Sixth International Congress on Large Dams/Vingt-Sixième Congrès International des Grands Barrages: 4th-6th July 2018, Vienna, Austria*, CRC Press.
- ILUNGA, L. & MUHIRE, I. 2010. Comparaison des fluctuations des précipitations moyennes annuelles au Rwanda avec les épisodes EL-NINO/LA NINA et les cycles des taches solaires. *Geo-Eco-Trop*, 34, 75-86.
- JONES, E., OLIPHANT, T. & PETERSON, P. 2001. SciPy: Open source scientific tools for Python. <http://www.scipy.org/>.
- KABALISA, V. D. P. 2016. Status of Water Resources in Rwanda.
- KANAMUGIRE, J. 2018. *Raging floods destroy costly infrastructure in East Africa* [Online]. The EastAfrican. Available: <http://www.theeastafrican.co.ke/business/Raging-floods-destroy-costly-infrastructure-East-Africa/2560-4570392-jf9cpsz/index.html> [Accessed 11/09/2018].

- KANG, S. & SONG, J. 2017. Parameter and quantile estimation for the generalized Pareto distribution in peaks over threshold framework. *Journal of the Korean Statistical Society*, 46, 487-501.
- KARAMAGE, F., ZHANG, C., FANG, X., LIU, T., NDAYISABA, F., NAHAYO, L., KAYIRANGA, A. & NSENGIYUMVA, J. 2017. Modeling Rainfall-Runoff Response to Land Use and Land Cover Change in Rwanda (1990–2016). *Water*, 9.
- KOICA 2008. Feasibility Study of Water Resources Development in Nyabarongo River in Rwanda, Final Report. Korea International Cooperation Agency, Korea Water Resources Corporation.
- LE COZ, C. 2018. Comparison of rainfall products over sub-Saharan Africa (Draft).
- LEENAARS, J. G. B., CLAESSENS, L., HEUVELINK, G. B. M., HENGL, T., RUIPEREZ GONZALEZ, M., VAN BUSSEL, L. G. J., GUILPART, N., YANG, H. & CASSMAN, K. G. 2018. Mapping rootable depth and root zone plant-available water holding capacity of the soil of sub-Saharan Africa. *Geoderma*, 324, 18-36.
- LEHNER, B. & DÖLL, P. 2004. Development and validation of a global database of lakes, reservoirs and wetlands. *Journal of Hydrology*, 296, 1-22.
- LEHNER, B., VERDIN, K. & JARVIS, A. 2011. New Global Hydrography Derived From Spaceborne Elevation Data. *Eos, Transactions American Geophysical Union*, 89, 93-94.
- LI, H., SHEFFIELD, J. & WOOD, E. F. 2010. Bias correction of monthly precipitation and temperature fields from Intergovernmental Panel on Climate Change AR4 models using equidistant quantile matching. *Journal of Geophysical Research*, 115.
- LOUCKS, D. P. & VAN BEEK, E. 2017. *Water resource systems planning and management: An introduction to methods, models, and applications*, Springer.
- LTS 2012a. Feasibility Study for an Integrated Watershed Management Programme for the Kagera River Basin.
- LTS 2012b. Feasibility Study for an Integrated Watershed Management Programme for the Kagera River Basin - Annex B: Wetlands Management.
- MANYIFIKA, M. 2015. *Diagnostic Assessment on Urban Floods Using Satellite Data and Hydrologic Models in Kigali, Rwanda*. University of Twente Faculty of Geo-Information and Earth Observation (ITC).
- MAYAUX, P., BARTHOLOMÉ, E., MASSART, M., VAN CUTSEM, C., CABRAL, A., NONGUIERMA, A., DIALLO, O., PRETORIUS, C., THOMPSON, M. & CHERLET, M. 2003. A land cover map of Africa. Carte de l'occupation du sol de l'Afrique.
- MCCUEN, R. H. 1998. *Hydrologic analysis and design*.
- MCKINNEY, W. Data structures for statistical computing in python. 2010.
- MEI, X. 2013. *Probability analysis of floods in catchments with dams*. Doctoral thesis, Delft University of Technology.
- MEI, X., DAI, Z., TANG, Z. & VAN GELDER, P. H. A. J. M. 2018. Impacts of historical records on extreme flood variations over the conterminous United States. *Journal of Flood Risk Management*, 11, S359-S369.
- MEI, X., VAN GELDER, P. H. A. J. M., DAI, Z. & TANG, Z. 2016. Impact of dams on flood occurrence of selected rivers in the United States. *Frontiers of Earth Science*, 11, 268-282.
- MIDIMAR 2015. *The National Risk Atlas of Rwanda*, Ministry of Disaster Management and Refugee Affairs.
- MINAGRI 2010. Rwanda Irrigation Master Plan. In: MAIMBO, M. M., BIAMAH, E. K., CHEROGONY, K., GACHENE, C. K. K., IYAMA, M., MOGO, I. J. B., NYOLEI, D., ODUOR, A. R. & O'NEILL, M. K. (eds.). Nairobi, Kenya: World Agroforestry Centre (ICRAF);
- MINAGRI;

Ebony Enterprises Ltd.

MININFRA 2015. Energy Sector Strategic Plan. Ministry of Infrastructure.

MININFRA. 2018. *Hydro Power in Rwanda* [Online]. Available: <http://www.mininfra.gov.rw/index.php?id=79> [Accessed 04/10/2018].

MININFRA, WSA & RDB 2012. Energy - The Opportunity in Rwanda.

MINIRENA & RNRA 2015. Rwanda National Water Resources Master Plan.

MUHIRE, I. & AHMED, F. 2014. Spatio-temporal trend analysis of precipitation data over Rwanda. *South African Geographical Journal*, 97, 50-68.

MUNYANEZA, O. 2014. *Space-time variation of hydrological processes and water resources in Rwanda: focus on the Migina catchment*. PhD dissertation, UNESCO-IHE

TU Delft.

MUNYANEZA, O., MUKUBWA, A., MASKEY, S., UHLENBROOK, S. & WENNINGER, J. 2014. Assessment of surface water resources availability using catchment modelling and the results of tracer studies in the mesoscale Migina Catchment, Rwanda. *Hydrology and Earth System Sciences*, 18, 5289-5301.

MUNYANEZA, O., NDAYISABA, C., WALI, U., MULUNGU, M. & DULO, O. 2011a. Integrated flood and drought management for sustainable development in the Kagera River basin. *Nile Water Sci. Eng. J*, 4, 60-70.

MUNYANEZA, O., UHLENBROOK, S., WENNINGER, J., VAN DEN BERG, H., BOLT, H. R., WALI, G. & MASKEY, S. 2010. Setup of a Hydrological Instrumentation Network in a Meso-Scale Catchment—the case of the Migina Catchment, Southern Rwanda, *Nile Water Sci. Eng. J*, 3, 61-70.

MUNYANEZA, O., WALI, U. G., UFITEYEZU, F. & UHLENBROOK, S. 2011b. A simple Method to Predict River Flows in the Agricultural Migina Catchment in Rwanda.

MUNYANEZA, O., WENNINGER, J. & UHLENBROOK, S. 2012. Identification of runoff generation processes using hydrometric and tracer methods in a meso-scale catchment in Rwanda. *Hydrology and Earth System Sciences*, 16, 1991-2004.

MUSHUTI, A. & NARCISSE, J. Rwanda Country Report. Seminar on Water Resources Management & Small Hydropower Development for Countries along the Belt and Road, 14/06/2018 2018 Hangzhou, China.

MUSONI, J. P. 2009. *Development of runoff coefficient in the Nyabugogo Catchment*. MSc, National University of Rwanda.

NAHAYO, A., NKURUNZIZA, D. & NSABIMANA, F. Comparative study between Global Positioning System (GPS) surveying methods and Geographic Information Systems (GIS)-based flood volume for reservoir capacity determination in Makera marshland, Muhanga district, Rwanda.

NBI 2012. Assessment of the Irrigation Potential in Burundi, Eastern DRC, Kenya, Rwanda, Southern Sudan, Tanzania and Uganda.

NBI 2016. Nile Basin Water Resources Atlas.

NCEA 2015. Quick Scan (Review) of the National Water Resources Master Plan for Rwanda. The Netherlands Commission for Environmental Assessment.

NDEKEZI, F.-X. 2010. *Hydrological modelling of Nyabarongo River basin in Rwanda using combinations of precipitation input from meteorological models, remote sensing, and ground station measurements*. Master's Degree, UNESCO-IHE.

NHAPI, I., WALI, U., UWONKUNDA, B., NSENGIMANA, H., BANADDA, N. & KIMWAGA, R. 2011. Assessment of water pollution levels in the Nyabugogo Catchment, Rwanda. *Open Environmental Engineering Journal*, 4, 40-53.

- NIELSEN, S. A. & HANSEN, E. 1973. Numerical simulation of the rainfall-runoff process on a daily basis. *Hydrology Research*, 4, 171-190.
- NKURUNZIZA, D. 2018. Stormwater runoff management challenges for city of Kigali.
- OBERRAUCH, F. 2017. Hydropower design under uncertainties. EPFL-LCH.
- OKIROR, S. 2018. *Lethal flash floods hit east African countries already in dire need* [Online]. The Guardian. Available: <https://www.theguardian.com/global-development/2018/may/08/deadly-flash-floods-east-africa-dire-need-kenya-rwanda-somalia> [Accessed 07/07/2018].
- OLIPHANT, T. E. 2006. *A guide to NumPy*, Trelgol Publishing USA.
- PANAGOS, P., VAN LIEDEKERKE, M., JONES, A. & MONTANARELLA, L. 2012. European Soil Data Centre: Response to European policy support and public data requirements. *Land Use Policy*, 29, 329-338.
- PANDEY, M. 2014. *Water Resources Assessment of Rwanda*. MSc thesis, IHE Delft.
- PANOFISKY, H. A., BRIER, G. W. & BEST, W. H. 1958. Some application of statistics to meteorology.
- PHAM, L. 2018. *Should I use GLDAS Version 2.0 (GLDAS-2.0) or GLDAS Version 2.1 (GLDAS-2.1)?* [Online]. Available: <https://disc.gsfc.nasa.gov/information/faqs/58bdd6050413344259516c9b/should-i-use-gldas-version-2-0-gldas-2-0-or-gldas-version-2-1-gldas-2-1> [Accessed 10/08/2018 2018].
- QUACKENBUSH, C. 2018. *200 People Have Been Killed in Landslides Across Rwanda This Year* [Online]. Time. Available: <http://time.com/5268983/rwanda-landslides/> [Accessed 07/08/2018].
- RDB. 2018. *Energy: Overview* [Online]. Rwanda Development Board. Available: <http://www.rdb.rw/rdb/energy.html> [Accessed 12/02/2018 2018].
- REG. 2018. *Hydro Power in Rwanda* [Online]. Rwanda Energy Group. Available: <http://www.reg.rw/index.php/projects/generation/169-hydro-power> [Accessed 12/02/2018 2018].
- REMA 2009. State of Environment and Outlook Report 2009. Kigali, Rwanda: Rwanda Environment Management Authority.
- REMA 2013. The Assessment of Economic Impacts of the 2012 Wet Season Flooding in Rwanda. Kigali, Rwanda: Rwanda Environment Management Authority.
- REMA 2015. State of Environment and Outlook Report 2015. Kigali, Rwanda: Rwanda Environment Management Authority.
- REMA. 2018. *Wetlands: Natual and Irrigated* [Online]. Available: <https://waterportal.rwfa.rw/toolbox/465> [Accessed 16/03/2018].
- RHDHV 2017a. Water management Masaka Wetlands: Pre-feasibility Study. Royal HaskoningDHV.
- RHDHV 2017b. Water Management survey Nyabarongo River. *Field campaign SWIAVI - Rwanda*. Royal HaskoningDHV.
- RIWSP 2012a. Assessment of Available Water Resources Data and Information from Selected Hydrometric Stations in Rwanda. In: VENNEKER, R. & WENNINGER, J. (eds.). Rwanda Integrated Water Security Program (RIWSP).
- RIWSP 2012b. Review of the National Hydrological Service in Rwanda. In: VENNEKER, R. & WENNINGER, J. (eds.). Kigali, Rwanda.
- RIWSP 2012c. RNRA hydrometric archive - Data conversion and recovery report, Version 2. In: VENNEKER, R. & WENNINGER, J. (eds.). Kigali, Rwanda: Rwanda Integrated Water Security Program.
- RIWSP 2012d. RNRA Hydrometric Observing Network - Observing Station Details, Version 2. In: VENNEKER, R. & WENNINGER, J. (eds.). Kigali, Rwanda: Rwanda Integrated Water Security Program.

- RIWSP 2012e. RWRIS Hydroscape, Version 2. *In*: VENNEKER, R. & WENNINGER, J. (eds.). Kigali, Rwanda: Rwanda Integrated Water Security Program.
- RNRA 2016. Assessment of Water Storage per Capita in Rwanda. Senior Construction Company Ltd.
- RODELL, M., HOUSER, P. R., JAMBOR, U., GOTTSCHALCK, J., MITCHELL, K., MENG, C. J., ARSENAULT, K., COSGROVE, B., RADA KOVICH, J., BOSILOVICH, M., ENTIN, J. K., WALKER, J. P., LOHMANN, D. & TOLL, D. 2004. The Global Land Data Assimilation System. *Bulletin of the American Meteorological Society*, 85, 381-394.
- RUKUNDO, E. & DOGAN, A. 2016. Assessment of Climate and Land Use Change Projections and their Impacts on Flooding. *Polish Journal of Environmental Studies*, 25, 2541-2551.
- RWFA 2018. Rwanda Water Portal: Surface Water. Rwanda Water and Forestry Authority.
- SAVENIJE, H. H. G. 2010. Topography driven conceptual modelling (FLEX-Topo). *Hydrology and Earth System Sciences*, 14, 2681-2692.
- SENDAMA, M. I. 2015. *Assessment of Meteorological Remote Sensing Products for Stream Flow Modelling Using HBV-light in Nyabarongo Basin, Rwanda*. University of Twente Faculty of Geo-Information and Earth Observation (ITC).
- SHER INGÉNIEURS-CONSEILS S.A. 2014. Consultancy services for development of Rwanda National Water Resources Master Plan - Master Plan Report - Annexes. Rwanda Natural Resources Authority.
- SUTCLIFFE, J. V. & PARKS, Y. P. 1999. *The hydrology of the Nile*, Wallingford, IAHS Press.
- THIEMIG, V. 2014. *The development of pan-African food forecasting and the exploration of satellite-based precipitation estimates*. Utrecht University.
- U.S. NRC. 2018. *Capacity factor (net)* [Online]. Available: <https://www.nrc.gov/reading-rm/basic-ref/glossary/capacity-factor-net.html> [Accessed 04/09/2018].
- UMUTONI, M., MASIH, I., MOHAMED, Y. A. & VAN DER ZAAG, P. 2016. Improving rainfall estimates for Rwanda using remotely sensed data. *17th WaterNet/WARFSA/GWPSA Symposium*. Gaborone, Botswana.
- UN DESA. 2018. *World Population Prospects 2017* [Online]. Available: <https://esa.un.org/unpd/wpp/> [Accessed 05/03/2018].
- VAN DEN BERG, H. & BOLT, R. 2010. *Catchment analysis in the Migina marshlands, southern Rwanda*. MSc thesis, Vrije University (VU) Amsterdam, Amsterdam, the Netherlands.
- VAN GRIENSVEN, A., XUAN, Y., HAGUMA, D. & NIYONZIMA, W. 2008. *Understanding riverine wetland-catchment processes using remote sensing data and modelling*. International Environmental Modelling and Software Society.
- VOTRUBA, L. & BROŽA, V. 1989. *Water management in reservoirs*, Elsevier.
- VRIJLING, J. K. & VAN GELDER, P. H. A. J. M. 2002. Probabilistic Design in Hydraulic Engineering - Temporary Issue. Delft, the Netherlands: Delft University of Technology.
- WAGESHO, N. & CLAIRE, M. 2016. Analysis of Rainfall Intensity-Duration-Frequency Relationship for Rwanda. *Journal of Water Resource and Protection*, 8, 706.
- WANG, L. & CHEN, W. 2014. Equiratio cumulative distribution function matching as an improvement to the equidistant approach in bias correction of precipitation. *Atmospheric Science Letters*, 15, 1-6.
- WATER4GROWTH & MINIRENA 2018. Terms of Reference - Assessing flood risk and its potential control and management in Masaka wetland, Rwanda. Water for Growth Rwanda, Ministry of Environment.

- WECA LTD. 2014. A baseline assessment of hydrological observing network, database management and information system - Final Report.
- WMO 2010a. *Manual on Stream Gauging*, Geneva, Switzerland, World Meteorological Organization.
- WMO 2010b. *Manual on Stream Gauging*, Geneva, Switzerland, World Meteorological Organization.
- WURBS RALPH, A. 1993. Reservoir-System Simulation and Optimization Models. *Journal of Water Resources Planning and Management*, 119, 455-472.
- YU, T. R. 1997. *Chemistry of variable charge soils*, Oxford University Press.
- ZHAO, T., ZHAO, J., LUND JAY, R. & YANG, D. 2014. Optimal Hedging Rules for Reservoir Flood Operation from Forecast Uncertainties. *Journal of Water Resources Planning and Management*, 140, 04014041.